

UNCLASSIFIED

AD NUMBER
ADB261561
NEW LIMITATION CHANGE
TO Approved for public release, distribution unlimited
FROM Distribution authorized to U.S. Gov't. agencies only; Proprietary Info.; Oct 2000. Other requests shall be referred to US Army Medical Reserch and Materiel Command, Fort Detrick, MD 21702-5012.
AUTHORITY
USAMRMC ltr, 1 Jun 2001.

THIS PAGE IS UNCLASSIFIED

AD \_\_\_\_\_

Award Number: DAMD17-95-C-5078

TITLE: A Spine Loading Model of Women in the Military

PRINCIPAL INVESTIGATOR: William S. Marras, Ph.D.

CONTRACTING ORGANIZATION: The Ohio State University  
Columbus, Ohio 43210-1063

REPORT DATE: October 2000

TYPE OF REPORT: Final

PREPARED FOR: U.S. Army Medical Research and Materiel Command  
Fort Detrick, Maryland 21702-5012

DISTRIBUTION STATEMENT: Distribution authorized to U.S. Government agencies only (proprietary information, Oct 00). Other requests for this document shall be referred to U.S. Army Medical Research and Materiel Command, 504 Scott Street, Fort Detrick, Maryland 21702-5012.

The views, opinions and/or findings contained in this report are those of the author(s) and should not be construed as an official Department of the Army position, policy or decision unless so designated by other documentation.

DTIC QUALITY INSPECTED 3

20010108 141

## NOTICE

USING GOVERNMENT DRAWINGS, SPECIFICATIONS, OR OTHER DATA INCLUDED IN THIS DOCUMENT FOR ANY PURPOSE OTHER THAN GOVERNMENT PROCUREMENT DOES NOT IN ANY WAY OBLIGATE THE U.S. GOVERNMENT. THE FACT THAT THE GOVERNMENT FORMULATED OR SUPPLIED THE DRAWINGS, SPECIFICATIONS, OR OTHER DATA DOES NOT LICENSE THE HOLDER OR ANY OTHER PERSON OR CORPORATION; OR CONVEY ANY RIGHTS OR PERMISSION TO MANUFACTURE, USE, OR SELL ANY PATENTED INVENTION THAT MAY RELATE TO THEM.

### LIMITED RIGHTS LEGEND

Award Number: DAMD17-95-C-5078  
Organization: The Ohio State University  
Location of Limited Rights Data (Pages):

Those portions of the technical data contained in this report marked as limited rights data shall not, without the written permission of the above contractor, be (a) released or disclosed outside the government, (b) used by the Government for manufacture or, in the case of computer software documentation, for preparing the same or similar computer software, or (c) used by a party other than the Government, except that the Government may release or disclose technical data to persons outside the Government, or permit the use of technical data by such persons, if (i) such release, disclosure, or use is necessary for emergency repair or overhaul or (ii) is a release or disclosure of technical data (other than detailed manufacturing or process data) to, or use of such data by, a foreign government that is in the interest of the Government and is required for evaluational or informational purposes, provided in either case that such release, disclosure or use is made subject to a prohibition that the person to whom the data is released or disclosed may not further use, release or disclose such data, and the contractor or subcontractor or subcontractor asserting the restriction is notified of such release, disclosure or use. This legend, together with the indications of the portions of this data which are subject to such limitations, shall be included on any reproduction hereof which includes any part of the portions subject to such limitations.

THIS TECHNICAL REPORT HAS BEEN REVIEWED AND IS APPROVED FOR PUBLICATION.

---

---

---

---

# REPORT DOCUMENTATION PAGE

OMB No. 074-0188

Public reporting burden for this collection of information is estimated to average 1 hour per response, including the time for reviewing instructions, searching existing data sources, gathering and maintaining the data needed, and completing and reviewing this collection of information. Send comments regarding this burden estimate or any other aspect of this collection of information, including suggestions for reducing this burden to Washington Headquarters Services, Directorate for Information Operations and Reports, 1215 Jefferson Davis Highway, Suite 1204, Arlington, VA 22202-4302, and to the Office of Management and Budget, Paperwork Reduction Project (0704-0188), Washington, DC 20503

<b>1. AGENCY USE ONLY (Leave blank)</b>		<b>2. REPORT DATE</b> October 2000	<b>3. REPORT TYPE AND DATES COVERED</b> Final (25 Sep 95 - 24 Sep 00)	
<b>4. TITLE AND SUBTITLE</b> A Spine Loading Model of Women in the Military			<b>5. FUNDING NUMBERS</b> DAMD17-95-C-5078	
<b>6. AUTHOR(S)</b> William S. Marras, Ph.D.				
<b>7. PERFORMING ORGANIZATION NAME(S) AND ADDRESS(ES)</b> The Ohio State University Columbus, Ohio 43210-1063  <b>E-MAIL:</b> marras.1@osu.edu			<b>8. PERFORMING ORGANIZATION REPORT NUMBER</b>	
<b>9. SPONSORING / MONITORING AGENCY NAME(S) AND ADDRESS(ES)</b> U.S. Army Medical Research and Materiel Command Fort Detrick, Maryland 21702-5012			<b>10. SPONSORING / MONITORING AGENCY REPORT NUMBER</b>	
<b>11. SUPPLEMENTARY NOTES</b>				
<b>12a. DISTRIBUTION / AVAILABILITY STATEMENT</b> Distribution authorized to U.S. Government agencies only (proprietary information, Oct 00). Other requests for this document shall be referred to U.S. Army Medical Research and Materiel Command, 504 Scott Street, Fort Detrick, Maryland 21702-5012.				<b>12b. DISTRIBUTION CODE</b>
<b>13. ABSTRACT (Maximum 200 Words)</b> <p>The risk of low-back disorders (LBD) may be particularly great for women in the military, influencing training, costs and military readiness. The goal of this research is to quantify musculoskeletal loads on the spine of women performing manual materials handling tasks. This will permit assessment of risk factors for military women, and the potential to evaluate tasks and training methods for female military personnel.</p> <p>This goal of this research was accomplished by quantifying trunk geometry via MRI and incorporating muscle fiber orientation, investigating the muscle length-strength and force-velocity relationships during lifting trials, and developing and validating the female biomechanical model utilizing these findings as inputs.</p> <p>Females exhibited smaller muscle physiological cross-sectional areas, moment-arms, and different characteristics for the length-strength and force-velocity modulation factors. Thus, biomechanical torso models need gender specific inputs for predicting spinal loading.</p> <p>Evaluation of spinal loading for a simulated military manual materials handling task indicated that females and males experienced similar magnitudes of spinal loading (e.g., compression force and shear forces) for many of the same tasks. However, since females tend to exhibit lower intervertebral disc compression force tolerance than males, they may be at an elevated risk for low back injury when performing the same tasks.</p>				
<b>14. SUBJECT TERMS</b> Women's Health, biomechanical modeling, spinal loading, manual materials handling, gender differences, low back disorders			<b>15. NUMBER OF PAGES</b> 195	
			<b>16. PRICE CODE</b>	
<b>17. SECURITY CLASSIFICATION OF REPORT</b> Unclassified	<b>18. SECURITY CLASSIFICATION OF THIS PAGE</b> Unclassified	<b>19. SECURITY CLASSIFICATION OF ABSTRACT</b> Unclassified	<b>20. LIMITATION OF ABSTRACT</b> Unlimited	

NSN 7540-01-280-5500

Standard Form 298 (Rev. 2-89)  
Prescribed by ANSI Std. Z39-18  
298-102

# TABLE OF CONTENTS

<b>TABLE OF CONTENTS .....</b>	<b>1</b>
<b>LIST OF FIGURES .....</b>	<b>3</b>
<b>LIST OF TABLES .....</b>	<b>5</b>
<b>INTRODUCTION .....</b>	<b>10</b>
<b>PART 1: ANTHROPOMETRIC MRI MEASUREMENT OF FEMALE MUSCULOSKELETAL TORSO .....</b>	<b>11</b>
Introduction.....	11
Background and Objectives .....	13
Administrative Note.....	13
Methods.....	14
Results.....	21
Discussion.....	30
<b>PART 2: PHYSIOLOGICAL MEASUREMENT OF THE IN-VIVO MUSCULAR LENGTH- STRENGTH AND FORCE-VELOCITY RELATIONSHIPS IN THE FEMALE TRUNK TORSO. 113</b>	
Introduction.....	113
Background and Objectives .....	113
Administrative Note.....	114
Methods.....	114
Results.....	129
Discussion.....	146
Conclusions.....	148
<b>PART 3: IMPLEMENTATION AND VALIDATION OF THE EMG-ASSISTED MODEL FOR FEMALE SUBJECTS. ....</b>	<b>149</b>
Introduction.....	149
Background and Objectives .....	149
Administrative Note.....	149
Methods.....	150
Results.....	154
Discussion.....	161
Conclusions.....	162
<b>PART 4: ASSESS BIOMECHANICAL LOADS ON THE FEMALE SPINE DURING MILITARY MMH .....</b>	<b>163</b>
Introduction.....	163
Background and Objectives .....	163

Methods.....	164
Results.....	166
Discussion.....	171
Conclusions.....	172
<b>PART 5: EVALUATE HIGH RISK MILITARY MMH TASKS .....</b>	<b>173</b>
Introduction.....	173
Background and Objectives .....	173
Methods.....	174
Results.....	177
Discussion.....	183
Conclusions.....	185
<b>KEY RESEARCH ACCOMPLISHMENTS .....</b>	<b>186</b>
<b>REPORTABLE OUTCOMES.....</b>	<b>187</b>
<b>CONCLUSION .....</b>	<b>188</b>
<b>REFERENCES .....</b>	<b>189</b>

## LIST OF FIGURES

Figure 2.1.	Experimental equipment for the free-dynamic lifting conditions.....	117
Figure 2.2.	Experimental equipment for the lifting trials using the pelvic support structure.....	118
Figure 2.3.	Distribution of the $r^2$ s for the performance of Female Model 10, resulting from lifting trials in the pelvic support structure.....	136
Figure 2.4.	Distribution of the estimated muscle gains for the performance of Female Model 10, resulting from lifting trials in the pelvic support structure.....	137
Figure 2.5.	Distribution of the $r^2$ s for the performance of Female Model 10, when the length-strength and force-velocity modulation factors derived from trials in the Pelvic Support Structure were applied to the lifting trials in the free-dynamic conditions.....	137
Figure 2.6.	Distribution of the estimated muscle gains for the performance of Female Model 10, when the length-strength and force-velocity modulation factors derived from trials in the Pelvic Support Structure were applied to the lifting trials performed in the free-dynamic conditions.....	138
Figure 2.7.	Distribution of the $r^2$ s for the performance of Male Model 10, resulting from lifting trials in the pelvic support structure.....	139
Figure 2.8.	Distribution of the estimated muscle gains for the performance of Male Model 10, resulting from lifting trials in the pelvic support structure.....	140
Figure 2.9.	Distribution of the $r^2$ s for the performance of Male Model 10, when the length-strength and force-velocity modulation factors derived from trials in the Pelvic Support Structure were applied to the lifting trials in the free-dynamic conditions.....	140
Figure 2.10.	Distribution of the estimated muscle gains for the performance of Male Model 10, when the length-strength and force-velocity modulation factors derived from trials in the Pelvic Support Structure were applied to the lifting trials performed in the free-dynamic conditions.....	141
Figure 2.11.	Female Model 10 length-strength versus Male Model 10 length-strength modulation factor comparison.....	145
Figure 2.12.	Female Model 10 force-velocity versus Male Model 10 force-velocity modulation factor comparison.....	146
Figure 3.1.	Mean muscle gain as a function of gender and weight.....	155
Figure 3.2.	Mean muscle gain as a function of gender and lift condition.....	155
Figure 3.3.	Squared correlation ( $r^2$ ) as a function of gender and weight.....	155
Figure 4.1.	Mean anterior/posterior shear force (N) on the L <sub>5</sub> /S <sub>1</sub> intervertebral disc as a function of gender and lifting condition.....	168
Figure 4.2.	Compression force tolerance ratio for the L <sub>5</sub> /S <sub>1</sub> intervertebral disc as a function of gender.....	170
Figure 5.1.	Predicted mean L5/S1 lateral shear force as a function of gender and lift condition for one-person lifts.....	180
Figure 5.2.	Predicted mean L5/S1 anterior/posterior (A/P) shear force as a function of gender and lift condition for one-person lifts.....	180
Figure 5.3.	Predicted mean L5/S1 lateral shear force as a function of gender and lift condition for two-person lifts.....	181

Figure 5.4.	Predicted mean L5/S1 anterior/posterior (A/P) shear force as a function of gender and lift condition for two-person lifts .....	181
Figure 5.5.	Predicted mean L5/S1 compression force as a function of gender and lift condition for one-person lifts.....	182
Figure 5.6.	Predicted mean L5/S1 compression force tolerance ratio as a function of gender and lift condition for one-person lifts .....	182
Figure 5.7.	Predicted mean L5/S1 compression force as a function of gender and lift condition for two-person lifts.....	183
Figure 5.8.	Predicted mean L5/S1 compression force tolerance ratio as a function of gender and lift condition for two-person lifts .....	183

## LIST OF TABLES

Table 1.1.	Fiber angle cosine adjustments for correction of raw cross-sectional areas into estimated physiological cross-sectional areas.....	17
Table 1.2.	Linear regression independent variables and descriptions for the prediction of the physiological cross-sectional areas.....	20
Table 1.3.	Linear regression independent variables and descriptions for the prediction of the trunk muscle moment-arms.....	21
Table 1.4.	Female and male subject mean (s.d.) anthropometric measurements.....	37
Table 1.5.	Right latissimus dorsi anatomical cross-sectional areas.....	38
Table 1.6.	Left latissimus dorsi anatomical cross-sectional areas.....	39
Table 1.7.	Right erector spinae anatomical cross-sectional areas.....	40
Table 1.8.	Left erector spinae anatomical cross-sectional areas.....	41
Table 1.9.	Right rectus abdominis anatomical cross-sectional areas.....	42
Table 1.10.	Left rectus abdominis anatomical cross-sectional areas.....	43
Table 1.11.	Right external oblique anatomical cross-sectional areas.....	44
Table 1.12.	Left external oblique anatomical cross-sectional areas.....	45
Table 1.13.	Right internal oblique anatomical cross-sectional areas.....	46
Table 1.14.	Left internal oblique anatomical cross-sectional areas.....	47
Table 1.15.	Right psoas major anatomical cross-sectional areas.....	48
Table 1.16.	Left psoas major anatomical cross-sectional areas.....	49
Table 1.17.	Right quadratus lumborum anatomical cross-sectional areas.....	50
Table 1.18.	Left quadratus lumborum anatomical cross-sectional areas.....	51
Table 1.19.	Vertebral body cross-sectional areas.....	52
Table 1.20.	Trunk cross-sectional areas.....	53
Table 1.21.	Right latissimus dorsi coronal plane moment-arms.....	54
Table 1.22.	Left latissimus dorsi coronal plane moment-arms.....	55
Table 1.23.	Right erector spinae coronal plane moment-arms.....	56
Table 1.24.	Left erector spinae coronal plane moment-arms.....	57
Table 1.25.	Right rectus abdominis coronal plane moment-arms.....	58
Table 1.26.	Left rectus abdominis coronal plane moment-arms.....	59
Table 1.27.	Right external oblique coronal plane moment-arms.....	60
Table 1.28.	Left external oblique coronal plane moment-arms.....	61
Table 1.29.	Right internal oblique coronal plane moment-arms.....	62
Table 1.30.	Left internal oblique coronal plane moment-arms.....	63
Table 1.31.	Right psoas major coronal plane moment-arms.....	64
Table 1.32.	Left psoas major coronal plane moment-arms.....	65
Table 1.33.	Right quadratus lumborum coronal plane moment-arms.....	66
Table 1.34.	Left quadratus lumborum coronal plane moment-arms.....	67
Table 1.35.	Right latissimus dorsi sagittal plane moment-arms.....	68
Table 1.36.	Left latissimus dorsi sagittal plane moment-arms.....	69
Table 1.37.	Right erector spinae sagittal plane moment-arms.....	70
Table 1.38.	Left erector spinae sagittal plane moment-arms.....	71
Table 1.39.	Right rectus abdominis sagittal plane moment-arms.....	72
Table 1.40.	Left rectus abdominis sagittal plane moment-arms.....	73
Table 1.41.	Right external oblique sagittal plane moment-arms.....	74

Table 1.42.	Left External Oblique sagittal plane moment-arms .....	75
Table 1.43.	Right Internal Oblique sagittal plane moment-arms .....	76
Table 1.44.	Left Internal Oblique sagittal plane moment-arms .....	77
Table 1.45.	Right Psoas Major sagittal plane moment-arms .....	78
Table 1.46.	Left Psoas Major sagittal plane moment-arms.....	79
Table 1.47.	Right Quadratus Lumborum sagittal plane moment-arms.....	80
Table 1.48.	Left Quadratus Lumborum sagittal plane moment-arms .....	81
Table 1.49.	Significant regression equations predicting average of right and left female PCSAs from external anthropometric measures .....	82
Table 1.50.	Significant regression equations predicting female trunk muscle PCSA from external anthropometric measures .....	82
Table 1.51.	Significant regression equations predicting average of right and left male PCSAs from external anthropometric measures .....	83
Table 1.52.	Significant regression equations predicting male trunk muscle PCSA from external anthropometric measures .....	83
Table 1.53.	Regression equations predicting PCSAs for female and male Latissimus Dorsi.....	84
Table 1.54.	Regression equations predicting PCSAs for female and male erector spinae .....	85
Table 1.55.	Regression equations predicting PCSAs for female and male rectus abdominis.....	86
Table 1.56.	Regression equations predicting PCSAs for female and male external obliques.....	87
Table 1.57.	Regression equations predicting PCSAs for female and male internal obliques.....	88
Table 1.58.	Regression equations predicting PCSAs for female and male psoas major .....	89
Table 1.59.	Regression equations predicting PCSAs for female and male quadratus lumborum.....	90
Table 1.60.	p-values for regression equations predicting female coronal plane moment-arms at the origin.....	91
Table 1.61.	p-values for regression equations predicting female sagittal plane moment-arms at the origin.....	91
Table 1.62.	p-values for regression equations predicting female coronal plane moment-arms at the insertion.....	92
Table 1.63.	p-values for regression equations predicting female sagittal plane moment-arms at the insertion.....	92
Table 1.64.	p-values for regression equations predicting male coronal plane moment-arms at the origin.....	93
Table 1.65.	p-values for regression equations predicting male sagittal plane moment-arms at the origin.....	93
Table 1.66.	p-values for regression equations predicting male coronal plane moment-arms at the insertion.....	94
Table 1.67.	p-values for regression equations predicting male sagittal plane moment-arms at the insertion.....	94
Table 1.68.	Regression equations predicting right latissimus dorsi moment-arms for males and females .....	95

Table 1.69.	Regression equations predicting left latissimus dorsi moment-arms for males and females .....	96
Table 1.70.	Regression equations predicting right erector spinae moment-arms for males and females .....	97
Table 1.71.	Regression equations predicting left erector spinae moment-arms for males and females .....	98
Table 1.72.	Regression equations predicting right rectus abdominis moment-arms for males and females .....	99
Table 1.73.	Regression equations predicting left rectus abdominis moment-arms for males and females .....	100
Table 1.74.	Regression equations predicting right external obliques moment-arms for males and females .....	101
Table 1.75.	Regression equations predicting left external obliques moment-arms for males and females .....	102
Table 1.76.	Regression equations predicting right internal obliques moment-arms for males and females .....	103
Table 1.77.	Regression equations predicting left internal obliques moment-arms for males and females .....	104
Table 1.78.	Mean (s.d.) PCSA (cm <sup>2</sup> ) for each muscle and gender .....	105
Table 1.79.	ANOVA p-values for vertebral level × side interaction for ACSAs .....	105
Table 1.80.	Post-hoc results of analysis of variance of right versus left side ACSA. ....	106
Table 1.81.	Difference (cm <sup>2</sup> and percent difference) between female right and left side ACSA for each muscle group .....	107
Table 1.82.	Difference (cm <sup>2</sup> and percent difference) between male right and left side ACSA for each muscle group .....	108
Table 1.83.	Female and male muscle vector locations for the muscle insertions relative to the L <sub>5</sub> /S <sub>1</sub> spine location, in the coronal and sagittal plane, as a function of anthropometric measurements at the xyphoid process and the iliac crest .....	109
Table 1.84.	Female and male muscle vector locations for the muscle origins, in the coronal and sagittal plane, as a function of anthropometric measurements at the xyphoid process and the iliac crest .....	109
Table 1.85.	Female and male muscle vector locations for the muscle insertions relative to the L <sub>5</sub> /S <sub>1</sub> spine location, in the coronal and sagittal plane, as a function of anthropometric measurements at the xyphoid process and the iliac crest. External and internal obliques are projected from L4 through insertion level at 135 and 45 degree angle in sagittal plane, respectively.....	110
Table 1.86.	Female and male muscle vector locations for the muscle insertions, as a function of anthropometric measurements at the xyphoid process and the iliac crest. External and internal obliques are projected from L4 through insertion level at 135 and 45 degree angle in sagittal plane, respectively .....	110
Table 1.87.	Female and male muscle vector locations for the muscle insertions relative to the L <sub>5</sub> /S <sub>1</sub> spine location, in the coronal and sagittal plane, as a function of anthropometric measurements at the xyphoid process and the iliac crest. Muscle vectors are reflective of muscle fiber orientations.....	111
Table 1.88.	Female and male muscle vector locations for the muscle origins, in the coronal and sagittal plane, as a function of anthropometric measurements at the xyphoid	

	process and the iliac crest. Muscle vectors are reflective of muscle fiber orientations.....	111
Table 1.89.	Percent of subjects with physiological cross-sectional area present at a specific vertebral level, by gender and muscle.....	112
Table 2.1.	Anthropometric data (mean and s.d.) from the subjects for the lifting trials in the pelvic support structure.....	115
Table 2.2.	Anthropometric data (mean and s.d.) from the subjects for the free-dynamic lifting trials.....	115
Table 2.3.	Female biomechanical model inputs.....	122
Table 2.4.	Regression equations predicting the female physiological cross-sectional areas from anthropometric measures .....	123
Table 2.5.	Male biomechanical model inputs .....	127
Table 2.6.	Regression equations predicting the male physiological cross-sectional areas from anthropometric measures .....	128
Table 2.7.	Descriptive results for the mean (s.d.) normalized female muscle activity (percent of maximum muscle activity) occurring at the maximum moment, and the maximum sagittal moment as a function of velocity and weight, for lifting trials performed in the pelvic support structure .....	131
Table 2.8.	Descriptive results for the mean (s.d.) normalized female muscle activity (percent of maximum muscle activity) occurring at the maximum moment, and the maximum sagittal moment as a function of velocity and weight, for lifting trials performed in the free-dynamic mode.....	132
Table 2.9.	MANOVA and ANOVA p-values for normalized EMG for female lifting trials in the Pelvic Support Structure and the Free Dynamic mode .....	132
Table 2.10.	Descriptive results for the mean (s.d.) normalized male muscle activity (percent of maximum muscle activity) occurring at the maximum moment, and the maximum sagittal moment as a function of velocity and weight, for lifting trials performed in the pelvic support structure.....	133
Table 2.11.	Descriptive results for the mean (s.d.) normalized male muscle activity (percent of maximum muscle activity) occurring at the maximum moment, and the maximum sagittal moment as a function of velocity and weight, for lifting trials performed in the free-dynamic mode .....	134
Table 2.12.	MANOVA and ANOVA p-values for normalized EMG for female lifting trials in the Pelvic Support Structure and the Free Dynamic mode .....	134
Table 2.13.	Female model results for lifting trials in the pelvic support structure and free dynamic lifting trials as a function of each of the ten models, with different combinations of inputs for the cross-sectional areas, length-strength and force-velocity modulation factors, and vector locations. ....	143
Table 2.14.	Male model results for lifting trials in the pelvic support structure and free dynamic lifting trials as a function of each of the ten models, with different combinations of inputs for the cross-sectional areas, length-strength and force-velocity modulation factors, and vector locations. ....	144
Table 2.15.	Female model performance results from Female Model 10, compared to the model performance results when applied to trials from the free-dynamic lifting exertions.....	144

Table 2.16.	Male model performance results from Male Model 10, compared to the model performance results when applied to trials from the free-dynamic lifting exertions.....	145
Table 3.1.	Anthropometric measurements (mean and s.d.) from male and female subjects.....	151
Table 3.2.	Analysis of Variance p-values on the EMG biomechanical model performance parameters as a function of the independent variables for both males and females.....	156
Table 3.3.	Overall biomechanical model performance parameters for males and females, collapsed across all experimental conditions .....	157
Table 3.4.	Descriptive statistics (mean and s.d.) for the muscle gain, $r^2$ and AAE (as a percent of measured moment) model performance parameters for the female biomechanical model .....	158
Table 3.5.	Descriptive statistics (mean and s.d.) for the muscle gain, $r^2$ and AAE (as a percent of measured moment) model performance parameters for the male biomechanical model .....	158
Table 3.6.	Model $r^2$ descriptive statistics for male and female biomechanical models as a function of the experimental conditions .....	159
Table 3.7.	Model muscle gain descriptive statistics for male and female biomechanical models as a function of the experimental conditions .....	160
Table 4.1	Descriptive statistics (mean and s.d.) for spinal loading as a function of gender and the experimental conditions .....	169
Table 4.2.	Analysis of Variance p-value results on spinal loading as a function of the experimental conditions.....	167
Table 4.3.	Compression tolerance ratio for females and males, as a function of the experimental conditions.....	170
Table 4.4.	Analysis of Variance p-value results for spinal compression tolerance ratio as a function of gender and the experimental conditions.....	171
Table 5.1	Anthropometric measurements (mean and s.d.) from female and male subjects.....	174
Table 5.2.	Predicted spinal loading for one-person lifts for male female and male subjects as a function of lift condition.. .....	179
Table 5.3.	Predicted spinal loading for two-person lifts for male female and male subjects as a function of lift condition. ....	179

## INTRODUCTION

Low back injuries in female military personnel can significantly impact training effectiveness, costs and military readiness. Low back injuries accounted for 75% of compensable military injuries in 1988 through 1991 (Army Safety Center, 1992). When one considers that women have significantly higher incidence of lost time injuries during basic training than men (Jones et al., 1988), it is apparent that the risk of work related low back disorders (LBD) may be particularly great for women in the military. Heavy manual materials handling (MMH) that would challenge the injury tolerance of most industrial workers' spines has been shown to be the most physically demanding task in 90% of all military job specialties (Sharp and Vogel, 1992). As these military occupational specialties (MOSs) are becoming increasingly available to women, the risk of LBD to women will have greater consequences as they fill these roles, particularly when considering a downsizing military. Thus, there is a need to reliably assess the risk of military task related LBD to women, and to identify potential features or training that might mitigate that risk.

The goal of this research is to extend the capability of predicting musculoskeletal loads on the trunk and spine to women performing realistic MMH tasks. Current models of musculoskeletal loading on the spine are based upon male biomechanics, and must be enhanced to account for the anatomical geometry and physiology of the female musculoskeletal torso. This will permit accurate evaluation of the spinal loads in women as they perform military MMH activities, and the potential to assess the relative risk of female military personnel performing MMH tasks in comparison to male personnel.

## **PART 1: Anthropometric MRI Measurement of Female Musculoskeletal Torso**

### **Introduction**

The control of women's low-back disorder (LBD) risk should be a priority for the military to mitigate escalating injuries and associated costs, and to maintain military readiness and combat effectiveness. Low back injuries accounted for 75% of compensable military injuries and have cost the Army between 46.9 and 61 million dollars per year from 1988 through 1991 (Army Safety Center, 1992). When one considers that women have significantly higher incidence of lost time injuries during basic training than men (Jones et al., 1988), it is apparent that the risk of work related LBD may be particularly great for women in the military. The cost of LBD risk among military women extends beyond medical care expenditures and long term or permanent compensation for the soldier. There is a great cost associated with lost duty time, training and retraining replacement personnel if a soldier must be discharged because of a LBD. Furthermore, military effectiveness and readiness are compromised if the soldier is not able to perform peacetime or combat related tasks because of a LBD.

Many of the military occupational specialties (MOSs) have recently been made available to military women (Army Times, 1994). As of 1995 there were women filling roles as combat engineers, in field artillery, and land combat MOSs. The number of women in these combat related MOSs is expected to increase. As women fill an expanded role in the modern military, the risk of lost female personnel due to LBD will have greater consequences upon military readiness and combat effectiveness than ever before. With military downsizing, the importance of each military woman, and the repercussions of LBD will become critical.

Many of the MOSs now being filled by women requires heavy manual material handling and would be expected to challenge the tolerance of most industrial workers' spines. Sharp and Vogel (1992) have shown that "heavy MMH is the most physically demanding task in 90% of all military job specialties." Yet these activities have never been quantitatively evaluated with military women. Thus, there is a need for a biomechanical model that can accurately and reliably assess and evaluate the risk of LBD to women as well as what features or training might mitigate that risk.

The Ohio State University EMG-assisted biomechanical model can be developed to provide a tool to assess and evaluate the risk of LBD to women performing military MMH tasks as part of their MOSs. Our previous efforts have demonstrated that we have been able to build a three-dimensional model of the trunk that is capable of accurately assessing spine loads during free-dynamic trunk motion which accounts for muscle co-contraction (Granata and Marras, 1993; Marras and Granata, 1995; Marras and Sommerich, 1991a,b). However, the modeling efforts to date have been successful in modeling the trunk geometry and subsequent loading imposed upon the spine of only males performing manual materials handling activities.

The geometry of the female trunk is vastly different from that of the male. Women tend to possess greater hip breadth and narrower abdominal depth than men (Pheasant, 1988). The sacroiliac joint is positioned several centimeters anteriorly in the female changing the moment arm associated with the external load as well as affecting the internal moment arm distances between the muscles and the point of rotation of the spine (Tischauer, 1978). In addition, it is suspected that the muscle attachment locations are significantly different between males and females. These changes will dramatically affect the force-length and force-velocity relationships that are vital for the determination of muscle force. In addition, one must understand the differences in the muscle lines of action (attachments) so that the trunk mechanics representation accurately reflects loading of the female trunk.

The ultimate goal of this research is to extend the capability of predicting musculoskeletal loads to that of women performing realistic MMH tasks. This model will be employed to assess the relative risk for musculoskeletal injury due to a MMH task for women relative to men, and to evaluate the proposed changes to those tasks to quantify the change in LBD risk. This EMG-driven biomechanical model will then be available as a tool to assess the risk associated with specific MMH tasks performed as part of MOSs that have recently been made available to military women. In this manner it will be possible to: a) assess risk for a given task, b) evaluate the physical attributes of a potential recruit that would place her at an increased risk of LBD, and c) determine how training or workplace procedures might be changed to minimize risk of LBDs to women (and men) performing the military MMH task.

In order to accomplish these objectives, it will be necessary to accomplish five specific aims. 1.) Quantitatively describe the internal geometry of the female trunk musculoskeletal system so that the model can accurately represent internal trunk mechanics and lines of muscle

action. Magnetic Resonance Imaging (MRI) will be used to collect this information in a safe and accurate manner. 2.) Determine the force-velocity relationship and length-strength relationships that are unique to the female trunk musculature. 3.) Implement female trunk geometry and muscle relationships into the existing OSU EMG-assisted biomechanical model. 4.) Test and validate the model under laboratory conditions. 5.) Use the model to evaluate military MMH tasks of physically demanding MOSs performed by both males and females.

### **Background and Objectives**

The objective of Part 1 was to generate descriptive statistics to describe the relative anthropometric values of muscle cross-sectional areas, origins, and lines of action in the female torso. The EMG-assisted biomechanical model currently accepts regression equations to predict muscle anthropometry of male subjects (Granata and Marras, 1993; Marras and Granata, 1995; Marras and Sommerich, 1991a,b). This is critical for scaling modeled muscle force amplitudes, dynamic behavior and to predict musculoskeletal loads. In order to generate accurate assessments of spinal loading and associated LBD risk of females performing military MMH tasks, it is necessary to generate a biomechanical geometry that accurately describes military age women. Although measures of soft tissue have been reported on elderly females (Chaffin et al., 1990; Kumar, 1988), there have been no studies designed to measure the trunk muscle area and geometry of young active women.

### **Administrative Note**

In the accepted research proposal, the "Statement of Work Addendum" included the collection of anthropometric data describing relative trunk muscle sizes and biomechanical lines of action on 20 women from existing MRI scans. Thus, we were to find torso imaging data of women who had required medical diagnosis of disabilities. The originally proposed "Statement of Work" suggested MRI analyses be performed by scanning 20 healthy women. However, due to budget limitations imposed by USARMC prior to approving the research, it was necessary to revise this part of the research to meet the financial constraints with the "Statement of Work Addendum" as described above.

We have managed to supplement the experimental design of the MRI with alternative funding that will improve the validity and specificity of the research for the purposes of the research goals and objectives. This was achieved by finding the opportunity to support data

collection of healthy military age women, a population which more realistically represents active military women. A local hospital with a state-of-the-art MRI facility agreed to participate in this effort, allowing us the opportunity to scan 20 healthy women and 10 healthy men. This will improve the validity of the data by providing MRI scans of healthy women instead of scans from disabled women, avoiding confounding of musculoskeletal factors.

The alternative funding opportunity also allowed us to collect data for direct comparison of male versus female relative muscle areas, attachment points, and lines of action. To date, there have been no such published analyses of muscular mechanical geometry. This data will allow a direct comparison of the biomechanical loads generated by female versus male soldiers during MMH activities. The comparison will also permit a more valid assessment of LBD risk of women as compared to men, and the influence of task design upon gender related LBD risk.

## **Methods**

### ***Experimental Design***

The subjects were placed in the MRI chamber at the Riverside Methodist Hospital, Columbus, OH, where cross-sectional images of the trunk were collected. A Philips 1.5 T GyroScan MRI was set to a spin echo sequence of TR=240 and TE=12, generating T1 weighted slices of 10 mm in thickness. Subjects were placed in a neutral position (supine postures with knees extended and hands lying across their abdomen) on the MRI gantry. The gantry moved the subjects into the center bore of the MRI magnet, aligning the subjects such that the scans could be performed on the desired region of the torso. A sagittal scout view was first collected to permit vertical quantification of individual transverse planes, and to ensure the cross-sectional scans would be captured in the field-of-view. A single set of 11 torso musculature scans was next performed, which were perpendicular to the gantry table at transverse levels through approximate centers of the vertebral bodies in the lumbar/sacrum and lower thoracic regions of the spine. Specifically, this included transverse scans of the torso through the T<sub>8</sub> through S<sub>1</sub> vertebral levels.

### ***Subjects***

Twenty females subjects of military age were recruited from the local community. In order to directly compare the female results with relative male anthropometry, MRI data were

also collected on 10 male subjects of military age, also recruited from the local community. None of the subjects had a history of chronic activity limiting chronic back or leg injuries, nor were any experiencing any low back pain at the time of the MRI scan. Upon arrival, anthropometric data were collected from each subject including the age, height and weight, the trunk width and depth measured at the trochanter, iliac crest, and xyphoid process, trunk circumference about the iliac crest, and right and left trochanter height from the floor.

### ***Data Extraction***

The MRI scans for each subject were transferred onto a Philips GyroView, where muscle cross-sectional areas could be estimated, as well as muscle centroids located relative to the spinal vertebral body centroid (McGill et al., 1993). The GyroView allows the user to inscribe an object of interest with a computer mouse, which then provides descriptive statistical data including the area of the enclosed region and the three-dimensional location of the area centroids relative to the scan set origin. In this manner, each of the muscles of interest were identified, outlined, and quantified where present for each of the 11 scan levels. The quantified muscles included the right and left pairs of the erector spinae group, quadratus lumborum, latissimus dorsi, internal obliques, external obliques, rectus abdominis, and psoas major. The cross-sectional areas and centroids were also quantified for each vertebral body and the torso at each of the 11 scan levels.

To determine the muscle, vertebral body, and trunk cross-sectional areas and centroids at each scan level, each were inscribed several times, with the average of the observation used as the representative values. The coefficient of variation (C.V.) was calculated for the first 15 female subjects, which showed that using three observations resulted in average C.V.'s of 9% or less for each muscle, with most C.V.'s less than 5%. Likewise, the coronal plane and sagittal plane moment-arms for each muscle were determined by averaging the three observed distances between the muscle centroid and vertebral centroid.

Since the scan planes were perpendicular to the scan table, the raw CSAs derived directly from MRI scans will be overestimates of the true CSA as the direction of most muscles will not be perpendicular to the scan plane. Thus, similar to the approach used by McGill et al. (1993), corrections to the raw muscle CSAs were performed by taking the dot product of the unit vectors using muscle fiber angles determined from different literature sources, and multiplying the

correction factor by the raw cross-sectional area. The correction factors are shown in Table 1.1. Fiber angles for the latissimus dorsi, rectus abdominis, external oblique, internal oblique and quadratus lumborum were obtained from Dumas et al. (1991), data from Macintosh and Bogduk (1991) were used for the lumbar erector spinae, orientations described by Dumas et al. (1991) were used for the thoracic portions of the erector spinae, and fiber orientations reported in McGill et al. (1993) were used for the psoas major. The resulting corrected cross-sectional areas at each vertebral level corresponds to the anatomical cross-sectional area (ACSA) (Narici 1999). The PCSA, which is necessary to estimate the force producing capability of the muscle, is defined as the cross-sectional area that “cuts” all fibers at right angles (Narici 1999). For parallel-fibered muscles, the PCSA corresponds to the ACSA, typically measured at the site of the maximum circumference (Narici 1999). Thus, the largest ACSA for each muscle will be defined as the estimate of the PCSA.

The moment-arms of the muscles at each level were determined by calculating the absolute difference between the muscle centroid and the vertebral body centroid, in both the sagittal plane and the coronal plane. Sign designations were given to the moment-arms, such that positive and negative values for the sagittal moment-arms represented anterior and posterior to the vertebral body centroid, respectively.

Table 1.1. Fiber angle cosine adjustments for adjustment of raw cross-sectional areas into estimated physiological cross-sectional areas. The raw cross-sectional area from the MRI scan is multiplied by the superior/inferior cosine to correct the ACSA for muscle fiber angle.

Muscle/Study	Level	Anterior/Posterior	Superior/Inferior	Lateral
Latissimus Dorsi Dumas et al. (1991)	T <sub>8</sub> - L <sub>3</sub>	0.204	0.911	0.357
Erector Spinae (Thoracic region from longissimus) Macintosh and Bogduk (1991)	T <sub>8</sub> - T <sub>12</sub>	-0.003	0.997	0.061
Erector Spinae (combined iliocostalis and longissimus fibers in lumbar region) Macintosh and Bogduk (1991)	L <sub>1</sub>	0.203	0.977	0.061
	L <sub>2</sub>	0.287	0.954	0.087
	L <sub>3</sub>	0.452	0.876	0.165
	L <sub>4</sub>	0.647	0.720	0.250
	L <sub>5</sub>	0.849	0.270	0.454
Rectus Abdominis Dumas et al. (1991)	T <sub>12</sub> - S <sub>1</sub>	0.078	0.993	0.070
External Oblique Dumas et al. (1991)	L <sub>3</sub>	-0.374	0.859	0.155
	L <sub>4</sub>	-0.495	0.905	0.209
Internal Oblique Dumas et al. (1991)	L <sub>3</sub>	0.299	0.785	0.328
	L <sub>4</sub>	0.188	0.949	0.231
Psoas Major McGill et al. (1993)	L <sub>1</sub>	0.135	0.978	0.135
	L <sub>2</sub>	0.229	0.964	0.125
	L <sub>3</sub>	0.086	0.988	0.119
	L <sub>4</sub>	0.084	0.990	0.117
	L <sub>5</sub>	0.079	0.992	0.098
Quadratus Lumborum Dumas et al. (1991)	L <sub>1</sub>	-0.245	0.899	-0.348
	L <sub>2</sub>	-0.259	0.870	-0.393
	L <sub>3</sub>	-0.212	0.805	-0.535
	L <sub>4</sub>	-0.074	0.486	-0.821

### *Descriptive Statistics*

Descriptive statistics (means and standard deviations at each vertebral level) were first generated for the ACSAs, as well as for the cross-sectional areas for the vertebral bodies and trunk cross-sectional areas. Descriptive statistics were also generated for the moment-arms for each muscle, both in the coronal and sagittal planes.

In the current EMG-assisted biomechanical model (Granata and Marras 1993; Marras and Granata 1995; Marras and Sommerich 1991a,b), the muscle vector locations for the muscle origins and insertions are identified as a percentage of the trunk width for the coronal plane location, and the sagittal plane location is calculated as a percentage of the trunk depth, both measured at the iliac crest. The current database of 20 females and 10 males, however, allows other anthropometric measures to be explored; therefore, in addition to the vector locations being

calculated as a function of trunk measurements about the iliac crest, the vector locations as a function of the trunk width and depth measured at the xyphoid process were also calculated.

Finally, since individual differences may dictate where the PCSA exists along the spine, the distribution of the PCSA for each muscle by vertebral level for both males and females were determined.

As a benchmark, the results of the ACSAs and moment-arms in the coronal and sagittal plane were then compared with data from Chaffin et al. (1990) who examined elderly women, and McGill et al. (1993) who examined young males. These comparisons consisted of the magnitude of the difference of similar measures, as well as the percent difference. Difficulty arose when comparing ACSAs from level to level, since in both the Chaffin et al. (1990) and the McGill et al. (1993) study, the scan slices were set through the middle of the intervertebral disc, whereas in the current study, the scan slices were set through the estimated midpoint of the vertebral body. Therefore, the comparisons of ACSAs and moment-arms were off by one-half of a level. To account for the difference in the location of the slices, the area and moment-arm midpoint between adjacent slices of the data in the current study were determined, thus creating a more comparable area value to the Chaffin et al. (1990) and the McGill et al. study (1993). For example, averaging the muscle cross-sectional area at T<sub>8</sub> and T<sub>9</sub> of the current study, would allow a more logical comparison to the muscle cross-sectional areas of the T<sub>8</sub>/T<sub>9</sub> scan slice from McGill et al. (1993).

### *Statistical Analyses*

All prior studies that have attempted to predict trunk muscle cross-sectional areas from external anthropometry have been developed using either uncorrected cross-sectional areas or on cross-sectional areas at vertebral levels which are not the largest cross-sectional area (Schultz and Andersson 1981; Schultz et al. 1982; Chaffin et al. 1990; McGill et a. 1988; Reid et al. 1987; Tracy et al. 1989; Wood et al. 1996). Thus the predicted cross-sectional areas from these studies will either overestimate the PCSA due to the obliquity of the muscle in relation to the direction of the muscle and the scan plane, or underestimated the PCSA if the cross-sectional area used was not at the largest point of the muscle. Therefore, linear regression techniques were used to predict the gender specific PCSA from anthropometric measures for each muscle (both right and left side PCSA, as well as the average of the right and left side PCSA). Regression equations

were restricted to one independent variable, which included subject weight, body mass index ( $\text{kg}/\text{m}^2$ ), the product of subject height and weight ( $\text{kg}\cdot\text{m}$ ), the product of trunk width and trunk depth ( $\text{cm}^2$ ) measured at the xyphoid process and the iliac crest, and the product of trunk width and trunk depth measured at the xyphoid process divided by subject height, and subject height divided by weight and subject weight divided by height (see Table 1.2 for definitions).

Gender differences between the regression equations predicting PCSAs were investigated using a hierarchical multiple linear regression approach, testing the significance of a gender indicator variable (Neter et al. 1985). If there was a significant difference, then the male and female regression equations were statistically different, which indicates that the male regression equation could not be used to predict the female PCSA, and vice versa. Finally, gender differences for the ACSAs at each vertebral level were determined by using *t*-tests with independent observations, with either equal or unequal variances where appropriate, using a significance level of  $\alpha=0.05$ .

Regression equations were also developed to predict the moment-arms of the muscles at the muscle origin and insertion points, for both the sagittal and coronal planes. In the EMG-assisted biomechanical model for males (Granata and Marras, 1993; Marras and Granata, 1995; Marras and Sommerich, 1991a,b), the origin was defined to exist at the  $L_5/S_1$ , where the specific insertion point for each muscle pair was a function of the magnitude of forward sagittal bending. The dependent variable consisted of either the coronal or sagittal plane moment-arm. The independent variables are shown in Table 1.3.

Differences between the right and left side PCSA for each muscle was assessed by using dependent sample *t*-tests, performed independently for each gender. Differences between the right and left side ACSA at each specific vertebral level were assessed by performing an Analysis of Variance (ANOVA). The dependent variable consisted of the muscle PCSA, and the independent variables included the subject, vertebral level, side (right or left), and a vertebral level by side interaction. Since each muscle was not always present at the same level for each subject, the data set was restricted to the levels where complete data existed, and where each subject had the muscle present between the two vertebral level endpoints. Thus, the latissimus dorsi muscle was restricted between  $T_8$  and  $L_3$ , the erector spinae between  $T_8$  and  $L_5$ , the rectus abdominis between  $L_1$  and  $S_1$ , the external obliques between  $L_1$  and  $L_4$ , the internal obliques between and quadratus lumborum between  $L_2$  and  $L_4$ , and the psoas major between  $L_2$  and  $L_5$ .

For subjects who did not have muscle areas present between the vertebral level endpoints listed above, they were excluded from the ANOVA. Post-hoc analyses consisted of Tukey pairwise comparisons on significant effects using a family-wise error rate of  $\alpha = 0.05$ .

Finally, statistical differences between males and females for the ACSAs, PCSAs, and the coronal and sagittal plane moment-arms were determined by using *t*-tests with independent observations, with equal or unequal variances where appropriate, with a significant difference indicated when  $p \leq 0.05$ .

Table 1.2. Linear regression independent variables and descriptions for the prediction of the physiological cross-sectional areas.

Independent Variable	Description
TDTWXP (cm <sup>4</sup> )	Trunk depth (cm) multiplied by trunk width (cm) measured at the level of the xyphoid process.
BMI (kg/m <sup>2</sup> )	Body mass index: subject weight (kg) divided by square of subject height (m <sup>2</sup> ).
HTWT (m·kg)	Height (m) multiplied by weight (kg).
Weight (kg)	Subject weight (kg).
TDTWXP (cm <sup>2</sup> /m)	Trunk depth (cm) multiplied by trunk width (cm) measured at the xyphoid process, divided by subject height (m).
HTDWT (cm/kg)	Subject height (cm) divided by subject weight (kg).
WTDHT (kg/cm)	Subject weight (kg) divided by subject height (cm).

Table 1.3. Linear regression independent variables and descriptions for the prediction of the trunk muscle moment-arms.

Independent Variable	Description
TDXP (cm)	Trunk depth measured at the level of the xyphoid process (cm).
TWXP (cm)	Trunk width measured at the level of the xyphoid process (cm).
TDIC (cm)	Trunk depth measured at the level of the iliac crest (cm).
TWIC (cm)	Trunk width measured at the level of the iliac crest (cm).
TDTR (cm)	Trunk depth measured at the level of the trochanter (cm).
TWTR (cm)	Trunk width measured at the level of the trochanter (cm).
TDICW (cm/kg)	Trunk depth at iliac crest (cm) divided by subject weight (kg).
TWICW (cm/kg)	Trunk width at iliac crest (cm) divided by subject weight (kg).
TDICH (cm/m)	Trunk depth at iliac crest (cm) divided by subject height (m).
TWICH (cm/m)	Trunk width at iliac crest (cm) divided by subject height (m).
TDXPW (cm/kg)	Trunk depth at xyphoid process (cm) divided by subject weight (kg).
TWXPW (cm/kg)	Trunk width at xyphoid process (cm) divided by subject weight (kg).
TDXPH (cm/m)	Trunk depth at xyphoid process (cm) divided by subject height (m).
TWXPW (cm/m)	Trunk width at xyphoid process (cm) divided by subject height (m).
TCIRW (cm/kg)	Trunk circumference about iliac crest (cm) divided by subject weight (kg).
TCIRH (cm/m)	Trunk circumference about iliac crest (cm) divided by subject height (m).
BMI (kg/m <sup>2</sup> )	Body mass index: subject weight (kg) divided by square of subject height (m <sup>2</sup> ).
HTWT (m·kg)	Height (m) multiplied by weight (kg).
Weight (kg)	Subject weight (kg).
HTDWT (cm/kg)	Subject height (cm) divided by subject weight (kg).
WTDHT (kg/cm)	Subject weight (kg) divided by subject height (cm).

## Results

### *Anthropometric Measurements*

The anthropometric data from the males and females are shown in Table 1.4. As expected, the mean value of each variable for the males were statistically greater in magnitude than those of the females, except for age. When compared to other studies, the females in this study were much younger (25.0 vs 49.6 yrs), slightly taller (165.5 vs 163.1 cm), and lighter (57.9 vs 67.6 kg) than those females in the study by Chaffin et al. (1990). The males in this study were slightly older (26.4 vs 25.3 yrs), were virtually the same height (175.9 vs 176.1 cm), and slightly lighter (79.8 vs 81.5 kg) than the males in the study by McGill et al. (1993).

### ***Anatomical Cross-Sectional Muscle Areas***

The ACSAs for each of the muscles are shown in Tables 1.5 through 1.18. These tables list the mean and standard deviation of the ACSA for each muscle, by vertebral level. Also included in these tables are comparisons between the female ACSA from this study and the data from the females in Chaffin et al. (1990), comparisons between the male ACSAs of this study and the data from the males in McGill et al. (1993), as well as comparisons between the female and male ACSAs of this study. The comparison between the different data sets consist of the magnitude of the difference, as well as the percent difference, where the shaded cells represent significant differences between the male and female ACSA.

As expected, the ACSAs of the females were smaller than those of the males, however, this difference differed as a function of the muscle of interest. The female latissimus dorsi areas (Tables 1.5 and 1.6) ranged from 38% to 51% smaller than that of the males, with an average of 42.2%, and were all significantly smaller than the male muscle areas. Similarly, the female erector spinae areas (Tables 1.7 and 1.8) ranged from 37% to 46% smaller than that of the males, with an average of 39.5%, again with the female ACSAs significantly smaller at every level. The female rectus abdominis areas (Tables 1.9 and 1.10) ranged from 24% to 42% smaller than the males, with an average of 31.4%. The female ACSAs at all levels except for T<sub>12</sub> were significantly smaller than the male ACSA. The female external obliques (Tables 1.11 and 1.12) ranged from 23% to 39% smaller than the males external obliques, with an average of 32.0% across all levels. The internal obliques (Tables 1.13 and 1.14) of the females showed a wide range of area in comparison to the males, ranging from 7% to 47% smaller than the males, with the female areas at L<sub>3</sub> and L<sub>4</sub> significantly smaller than the males for both right and left sides. The female psoas major ACSA ranged from 16% to 54% smaller than the males ACSA, averaging 43.6% smaller than the male psoas major ACSA (Tables 1.15 and 1.16). The female psoas major was significantly smaller than the male ACSA at levels L<sub>2</sub> through L<sub>5</sub>. Finally, the female quadratus lumborum (Tables 1.17 and 1.18) ranged from 32% to 59% smaller than the male area, with an average of 42.0% smaller, with the female ACSA significantly smaller than the male ACSA at L<sub>2</sub>, L<sub>3</sub> and L<sub>4</sub>.

The cross-sectional area of the female vertebral body (Table 1.19) was consistently smaller than that of the males, ranging from 20% to 27% smaller, averaging 24.4% smaller than that of the males. The trunk cross-sectional areas for the females (Table 1.20) ranged from 6%

smaller to 34% smaller. The largest difference was at T<sub>8</sub> (34% smaller than the male trunk area), and the difference consistently decreased while descending the spine caudally to the smallest difference (6% smaller) at the S<sub>1</sub> level.

Comparisons between the results of this study and similar studies from the literature are also shown in Tables 1.5 through 1.20. Comparisons between the ACSAs for the males of this study and the male subjects from McGill et al. (1993) after making the one-half vertebral level adjustment to the current dataset indicated the overall ACSAs were 4.6% smaller than the ACSAs reported by McGill et al. (1993).

The study on elderly females by Chaffin et al. (1990) also set the scan slices through the intervertebral disc, at the L<sub>2</sub>/L<sub>3</sub>, L<sub>3</sub>/L<sub>4</sub>, and L<sub>4</sub>/L<sub>5</sub> levels. The ACSAs of the current study were 2.0% larger across all muscles when using the midpoint adjusted area data than the ACSAs found by Chaffin et al. (1990). Generally, the ACSAs for the latissimus dorsi, rectus abdominis, and the external obliques for the current study were larger in comparison to the data from Chaffin et al. (1990), whereas, the ACSAs for the erector spinae, internal obliques, psoas major and quadratus lumborum were smaller than the cross-sectional areas of the females in Chaffin et al. (1990).

### ***Coronal Plane Moment-Arms***

The coronal plane moment-arms for the males and females, as well as those documented in other studies for comparison purposes are shown in Tables 1.21 through 1.34. The male moment-arms were significantly greater than the females at all levels for the latissimus dorsi and left erector spinae, and all but the lower three levels for the right erector spinae. Only the right rectus abdominis resulted in significant differences between males and females, whereas none of the levels were different on the left side. Five of the six levels resulted in significantly larger male moment-arms for the external obliques and the psoas major, and three of the four levels resulted in significantly larger male coronal plane moment-arms for the quadratus lumborum. Three of the four levels for the right internal oblique and two of the for levels for the left internal oblique resulted in larger male moment-arms.

The male coronal plane moment-arms of this study were very consistent with those reported in McGill et al. (1993), with an average absolute difference of 8.0%, which decreased to 5.5% when adjusting for the one-half vertebral level difference. The absolute percent difference

between the coronal plane moment-arms were slightly larger when comparing the female data of the current study to those of the Chaffin et al. (1990) study. Without adjusting for the one-half vertebral level difference, the absolute percent difference was 11.2%, where the difference dropped to 8.6% when adjusting for the vertebral level difference. Generally, the moment-arms were smaller for all muscles except for the erector spinae, which were very similar to those of the elderly female population in the Chaffin et al. (1990) study.

### ***Sagittal Plane Moment-Arms***

The sagittal plane moment-arms for the males and females, as well as those documented in other studies for comparison purposes are shown in Tables 1.35 through 1.48. Compared to the coronal plane moment-arms, there were fewer significant differences between males and females. For the latissimus dorsi, only the moment-arm at L<sub>3</sub> was significantly larger for the males; the remaining levels resulted in no significant differences. The majority of levels, however, for both sides of the erector spinae showed the males to have significantly larger sagittal plane moment-arms than the females. Only the moment-arm at the S<sub>1</sub> level was not significantly different between males and females for both right and left rectus abdominis. The results were mixed for the external and internal obliques as well as the psoas major; the left side of each muscle, however, did result in more significant differences than the right side, with the males exhibiting larger moment-arms than the females, except for the psoas major. Finally, there were no significant difference between the moment-arms for both the right and left quadratus lumborum.

The absolute percent differences between the sagittal plane moment-arms for the males of the current study and those of McGill et al. (1993) were much larger than the differences of the coronal plane moment-arms. Generally, the absolute percent difference between the two studies was 32.8%, which dropped to 23.6% when adjusting the data of the current study for the one-half vertebral level difference. Large percent differences exist for the external obliques and the internal obliques, with the upper levels of the males in the current study having larger moment-arms and the lowest level having smaller moment-arms. Large average percent differences also resulted for the psoas major (75.2% and 52.2% for the right and left side, respectively), with the moment-arms for the males in the current study being smaller at each level (Tables 1.44 and 1.45). Aside from the left latissimus dorsi, (Table 1.35), the rest of the muscles resulted in

absolute percent differences between 6.6% and 11.4% (5.6% and 6.3% when adjusting for the one-half vertebral difference).

The absolute percent difference between the females of the current study and those from Chaffin et al. (1990) was fairly large (32.0%), although this large difference was primarily driven by large percent differences between the psoas major. When accounting for the one-half vertebral difference, the absolute percent difference drops to 16.7%, where the difference between the sagittal plane moment-arms of the external and internal obliques increases the percent difference.

### ***Prediction of the Physiological Cross-sectional Areas***

Summary tables consisting of  $R^2$ 's for significant regression equations predicting the PCSA, by muscle and gender are shown in Tables 1.49 through 1.52. The regression equations predicting PCSAs are shown in Tables 1.53 through 1.59, with each table documenting a separate muscle. For the latissimus dorsi, use of the anthropometric measurements at the xyphoid process resulted in significant regression equations for females, with 34.7% to 39.7% of the variability in the PCSA explained. However, for the males, the xyphoid process resulted in a significant regression equation predicting the left latissimus dorsi PCSA and the average of the largest of the right and left PCSA. Measures of height times weight (HTWT) and subject weight were also significant for both sides of the erector spinae. When comparing the male and female regression equations, there were no significant differences between the male and female regression equations for those gender specific equations which significantly predicted muscle PCSAs.

Measures about the xyphoid process (trunk width times the trunk depth, as well as divided by the height) and measures consisting of either height and/or weight (weight, height times weight, height divided by weight, weight divided by height, body mass index and trunk circumference divided by weight) were all significant predictors of the female erector spinae PCSA, with  $R^2$ 's ranging between 0.36 and 0.72 (Tables 1.49 and 1.50). Similarly, for male erector spinae PCSAs, measures consisting of either height and/or weight also accounted for significant proportions of the erector spinae PCSA variability, with  $R^2$ 's ranging from 0.410 and 0.624 (Tables 1.51 and 1.52). Significant differences existed between the gender specific

regression equations (Table 1.54), indicating that the regression equations cannot be used interchangeably to predict male or female muscle erector spinae PCSA.

For prediction of the rectus abdominis PCSA (Tables 1.49 and 1.50), the use of the BMI and measurements about the xyphoid process resulted in significant regression equations for the females, with  $R^2$ 's ranging from 0.191 to 0.420 using the xyphoid process measurements and 0.237 and 0.255 for the BMI. Measures using height and weight resulted in significant regression equations for predicting male rectus abdominis PCSA, with  $R^2$ 's ranging from 0.446 to 0.634 (Tables 1.49 and 1.50). Investigation of differences between regression equations predicting male and female muscle PCSA resulted in no significant differences between the gender specific equations (Table 1.55).

The use of the measurements about the xyphoid process were consistent predictors of the female external oblique (right, left, and average of right and left) for females (Tables 1.49 and 1.50), where the  $R^2$ 's ranged from 0.221 to 0.286. For the males, only measures about the xyphoid process (width times depth) and the subject height were significant predictors of the left external oblique (Table 1.52). As shown in Table 1.56, male and female regression equations were significantly different from each other when predicting the external oblique PCSA. Thus, the individual regression equations for the males and females are not interchangeable for predicting the largest PCSAs of the external obliques.

Measures about the xyphoid process and combinations of height and weight (body mass index, height divided by weight, weight divided by height) resulted in significant regression equations predicting the PCSA of the right internal obliques for the females (Tables 1.49 and 1.50), with  $R^2$ 's ranging from 0.241 to 0.290 when using the xyphoid process, and ranging from 0.201 to 0.267 when using combinations of height and weight. The xyphoid process measurements (trunk width times depth) resulted in significant regression equations for predicting male internal obliques PCSA ( $R^2$ 's ranging from 0.425 and 0.461), as well as different combinations of height and weight ( $R^2$ 's ranging from 0.469 to 0.584) (Tables 1.51 and 1.52). A significant gender affect was also present (Table 1.57), thus, the gender specific regression equations cannot be used interchangeably to predict PCSA.

As shown in Table 1.50, only the trunk circumference divided by subject weight significantly predicted the psoas major PCSA (right side only,  $R^2 = 0.226$ ), and only the trunk depth by trunk width at the xyphoid process was a significant predictor of male psoas major

PCSA ( $R^2$  from 0.408 to 0.459, Tables 1.51 and 1.52). A significant gender affect was when using the xyphoid process measure (depth times width, Table 1.58), thus, the gender specific regression equations cannot be used interchangeably to predict psoas major PCSA.

The use of measurements about the xyphoid process ( $R^2$ 's from 0.314 to 0.387) and combinations of height and weight ( $R^2$ 's from 0.225 to 0.430) resulted in significant regression equations predicting the PCSA of the female quadratus lumborum (Tables 1.49 and 1.50). Only the left male quadratus lumborum demonstrated significant predictability, which consisted of measures about the xyphoid process and iliac crest ( $R^2$  of 0.411 and 0.607, respectively) and combinations of height and weight ( $R^2$  between 0.401 and 0.439). Finally, the male and female regression equations were significantly different from each other for predicted PCSA predicted (Table 1.59).

### ***Prediction of Muscle Moment-Arms***

Summary statistics (p-values) for the prediction of female moment-arms at the origin and insertion in both the coronal and sagittal plane, from external anthropometric measurements are shown in Table 1.60 to 1.63. Generally, there were no significant prediction equations of the moment-arms at the origin ( $L_5$ ) in the sagittal plane for females, and only the right external oblique was predicted by any external anthropometric measure (trunk width at the xyphoid process). Summary statistics for prediction of male moment-arms at the origin and insertion in both the coronal and sagittal plane, from external anthropometric measurements are shown in Table 1.64 to 1.67. The resulting regression equations for each muscle, plane, and gender are shown in Table 1.68 to 1.77. For the latissimus dorsi (Tables 1.68 and 1.69), the trunk depth and width measures at the iliac crest did not result in any significant associations for females. Generally, the xyphoid process and BMI resulted in significant predictions of the coronal plane moment-arm for both sides for females. The BMI was significant for the coronal plane male moment-arm at the origin of the right latissimus dorsi, and also for the coronal plane moment-arm of the left latissimus dorsi at the insertion. For the erector spinae (Tables 1.70 and 1.71), there were no significant regression equations for moment-arms for either gender for the left erector spinae, and only the sagittal plane moment-arm at the insertion for females and coronal plane moment-arm for males at the insertion resulted in significant predictions. The regression equations predicting coronal and sagittal plane moment-arms for the rectus abdominis (Tables

1.72 and 1.73) resulted in several significant associations. The most consistent predictions occurred for the moment-arms in the sagittal plane at the insertion, for both males and females, for both the right and left side. The trunk depth measured at the xyphoid process and the BMI significant for both sides. Prediction of right and left external oblique moment-arms in the coronal plane at the origin and insertion for males resulted in several significant anthropometric variables, including the trunk depth measured at the xyphoid process and iliac crest, as well as the BMI (Tables 1.74 and 1.75). Essentially, only the coronal plane female moment-arms at the insertion were significant, with the trunk width measured at the xyphoid process and the BMI resulting in significant regression equations (Tables 1.74 and 1.75). Finally, the trunk width and depth measures at the xyphoid process and the BMI were significant predictors of both coronal and sagittal plane moment-arms for the right and left internal obliques for the females at the insertion level (Tables 1.76 and 1.77).

#### ***Differences between Right and Left Muscle Areas***

The mean difference between the right and left muscle PCSAs, for both males and females are shown in Table 1.78. Both males and females exhibited significantly larger right side than left side for the latissimus dorsi. The psoas major and quadratus lumborum exhibited significantly larger left side than right side PCSA for the females. No other significant differences between the sides existed for the males. The Analysis of Variance on the differences between the right and left side ACSAs by vertebral level for both females and males are shown in Table 1.79. Significant differences existed between the right and left latissimus dorsi for both males and females. Post-hoc tests indicated that these differences occurred at the T<sub>8</sub> through T<sub>10</sub> levels for both males and females for the latissimus dorsi, with the right side being larger than the left side (Table 1.80). The magnitude and percent difference between the right and left sides for each muscle group are shown in Table 1.81 for the females, and 1.82 for the males. Significant differences found from the Tukey pairwise comparisons are also shown, which correspond to the significant levels and sides shown in Table 1.82.

#### ***Muscle Vector Locations***

The locations of the components for the female and male muscle vectors in the coronal and sagittal plane at the insertion and origin levels with respect to the L<sub>5</sub>/S<sub>1</sub> joint specified by the EMG-assisted model for each of the five pairs of muscles are shown in Tables 1.83 to 1.88.

Each of the values in these tables represents the coefficient in which the external anthropometric measure (e.g., trunk width at the xyphoid process) is multiplied by to estimate the distance of the muscle vector from the centroid of the L<sub>5</sub>/S<sub>1</sub> intervertebral disc.

The vector locations in Table 1.83 (insertions) and Table 1.84 (origins) were derived directly from the centroids of the muscles observed from the MRI scans. Generally, there were very little differences between male and female vector coefficients, with few exceptions. Males exhibited larger coefficients for the rectus abdominis vector location in the sagittal plane based on the trunk depth at the iliac crest (Table 1.83). Conversely, for the origin insertions, females demonstrated consistently larger coronal vector coefficients than males for the external and internal obliques, and also for sagittal plane vector coefficients for the erector spinae and rectus abdominis, all based on measures about the xyphoid process (Table 1.84).

The vector locations at the origin and insertion for the external and internal obliques were also investigated to correspond with the assumed vector angles indicated by Schultz et al. (1982). The vectors for the external obliques were projected at a 45° anterior/caudal angle from the centroid at L<sub>4</sub>, where the vector coefficients at the insertion are shown in Table 1.85, and for the origin in Table 1.86. Males and females were fairly similar except for moderate differences in the sagittal plane vector coefficients for the external obliques (females larger than males). Similarly, the vectors for the internal obliques were projected 45° posterior/caudal from the centroid at L<sub>4</sub>, where the vector coefficients at the insertion are shown in Table 1.85, and for the origin in Table 1.86.

Finally, utilizing muscle fiber orientation for the erector spinae (Macintosh and Bogduk 1991) and the external and internal oblique (Dumas et al. 1991), vector locations at the insertion are shown in Table 1.87, and for the origin in Table 1.88. These results indicate that females exhibit generally larger relative vector locations with respect to the L<sub>5</sub>/S<sub>1</sub> location for both the external and internal oblique based on measures about the xyphoid process, at both the insertion level and origin level.

### ***Distribution of the Largest Muscle Area***

The distribution of the PCSA for both the right and left pairs of each muscle, as a function of vertebral level are shown in Table 1.89. Although there was some variability between the right and left pairs of each muscle as far as which vertebral levels had the highest

percentage of the PCSAs, as well as which levels had the PCSA present, general trends did exist. For the latissimus dorsi, the PCSA occurred mostly at the T<sub>8</sub> level, with very few at T<sub>9</sub>. The PCSA for the erector spinae were generally split between L<sub>2</sub> and L<sub>3</sub>, with a few located at L<sub>1</sub>. The PCSA location for the rectus abdominis indicated a large variability for both males and females. For the females, the PCSA generally occurred at S<sub>1</sub> for both right and left sides with a few located at other levels. For both male and females, the external oblique PCSA for the right and left sides were generally located at L<sub>2</sub> and L<sub>4</sub>. The internal obliques PCSA generally were located at L<sub>4</sub>, with a few also located at L<sub>2</sub> and L<sub>3</sub>. The PCSA for the quadratus lumborum was typically found at L<sub>3</sub> for females (90%), and split between L<sub>3</sub> and L<sub>4</sub> for males. Finally, the psoas major PCSAs were found between L<sub>4</sub> and L<sub>5</sub>.

## **Discussion**

### ***Female Data***

The database of muscle cross-sectional areas and moment-arms from the vertebral centroid represent the largest and most complete database for the females to date, as well as for male to female comparisons. The female areas for the latissimus dorsi, rectus abdominis and external obliques are larger than those quantified by Chaffin et al. (1990), whereas the areas were smaller for the erector spinae, internal obliques, psoas major and quadratus lumborum were smaller than Chaffin et al. (1990). The scans in Chaffin et al. (1990) were taken by computed tomography (CT), and the separation between muscles or the muscle borders may not have been as clear as when using MRI technology. The female subjects in Chaffin et al (1990) were elderly females, with a mean age of 49 yrs, compared to 25.3 yrs in the current study, which may show up as muscle atrophy in the elderly population for some of the muscles. Additionally, differences may also have been influenced by the subject posture in the imaging device, where the females in Chaffin et al. had their hips and knees flexed, whereas in our study, the hips and knees were fully extended.

Differences also existed for the moment-arms in both planes between the females from Chaffin et al. (1990) and the current study. Generally, all the coronal plane moment-arms in the current study were smaller than from Chaffin et al. (1990), with the one-half level adjustment making better comparisons only for the psoas major and quadratus lumborum. The sagittal plane

moment-arms for the current study showed no apparent patterns. The erector spinae moment-arms of the current study were slightly smaller than those in Chaffin et al. (1990), with the one-half level adjustment not making much difference for comparability, and the rectus abdominis were smaller at the lower two levels of comparison for the current study, again the one-half level adjustment not making much difference. The external and internal obliques, as well as the psoas major were both smaller and larger, depending on the level of comparison, with the one-half level of adjustment decreasing the differences between the two studies. The differences between the moment-arm distances between the two studies may have been influenced by the different scan techniques, with Chaffin et al (1990) using CT technology versus MRI in the current study. The use of MRI technology, again, may increase the clarity of the muscle border and spine border locations, which can affect the resulting distances between the centroids of the objects of interest.

Differences in the moment-arm distances may also exist due to possible age-related differences such as increases in body mass. The females in Chaffin et al. (1990) average 49.6 years compared to 25.0 yrs for the current study, with the elderly females being shorter (163.1 cm vs 165.5 cm) and heavier (67.6 kg vs 57.9 kg) than the females of the current study. This indicates that the elderly females had a higher BMI, or more adipose tissue, which may increase the distance between the spine and certain muscles, depending on the deposit locations of adipose tissue. The larger BMI of the elderly female populations is also consistent with observation that the trunk cross-sectional areas at the three levels of comparison, with the females of the current study averaging 23% less cross-sectional area at the levels of comparison than the older females in the Chaffin et al. (1990) study.

For the prediction of the cross-sectional areas, Chaffin et al.(1990) found that height and weight significantly predicted the erector spinae ACSA ( $R^2=0.26$ ). However, knowledge of female height and weight in our study (weight divided by height) produced significant prediction equations for the erector spinae PCSA accounting for 61% to 72% of the PCSA variability. Chaffin et al. also found that height and weight were significant predictors of the female psoas major ( $R^2=0.18$ ), however, our study revealed no significant predictors of the psoas major PCSA. No other significant prediction equations for comparable muscles to this study were found by Chaffin et al., including the rectus abdominis, internal and external obliques, latissimus dorsi, and the quadratus lumborum. Thus, this is the first study to find significant prediction equations

for female trunk muscle PCSA based upon external anthropometry for the muscles identified above.

### ***Male Data***

The largest database for comparison purposes to the male data in the current study was from McGill et al. (1993), which quantified the muscle cross-sectional areas and moment-arms from T<sub>5</sub>/T<sub>6</sub> through L<sub>5</sub>/S<sub>1</sub>, also with the use of MRI technology. Generally, when correcting for the one-half of a level difference of the location of the scan slices, the cross-sectional areas of similar muscles were fairly consistent between the two studies for the lower levels of the latissimus dorsi, mid to upper levels of the erector spinae, rectus abdominis (Tables 1.5 through 1.10), and the psoas major (Tables 1.15 and 1.16). Larger differences existed between the external and internal obliques (Tables 1.8 through 1.11), as well as the quadratus lumborum (Tables 1.14 and 1.15), between the two studies. These differences may be indicative of differences in the two populations studied, or the inability of the half-level adjustment factor to adequately correct for the different location of the scan levels between the two studies.

Comparisons of the coronal plane moment-arms between the males of the current study and those of McGill et al. (1993) found that the moment-arm distances were all very comparable, with most of the differences ranging from an average of 2.8% difference (left psoas major) to a 6.2% difference (left rectus abdominis). Only the right rectus abdominis and left quadratus lumborum resulted in larger differences between the two studies (15.5% and 9.0%, respectively). The differences between the sagittal plane moment-arms, however, were much higher between similar muscles and scan levels between the males from the current study and those of McGill et al. (1993). The erector spinae and rectus abdominis sagittal moment-arms were very similar between the two studies. However, the left latissimus dorsi (30.8%), the external obliques (14.3% and 25.2%, for right and left, respectively), internal obliques (26.7% and 30%, for right and left, respectively), and the psoas major (81.8% and 53.8%, for right and left, respectively), had fairly large absolute percent differences. The large percent differences between the psoas major can be attributed to the small moment-arms, where slight differences would result in large percent differences.

No prior studies have found significant predictors of cross-sectional areas for the latissimus dorsi (Tracy et al. 1989) or the quadratus lumborum (Tracy et al. 1989; Wood et al.

1996). However, our study found significant predictors of the latissimus dorsi PCSA ( $R^2$  ranging from 0.425 and 0.516) and for the left quadratus lumborum PCSA ( $R^2 = 0.607$ ). Male height divided by weight resulted in the best prediction equations for both the erector spinae PCSA ( $R^2$  of 0.533 and 0.624 for right and left side, respectively) and rectus abdominis PCSA ( $R^2$  of 0.595 and 0.634 for right and left side, respectively). Contrary to other studies which did not find significant anthropometric predictors of erector spinae CSA (McGill et al. 1988; Tracy et al. 1989; Wood et al. 1996), Reid et al. (1987) found significant predictors, however, their model was overspecified, with six independent variables ( $R^2=0.77$ ). Thus, our models performed almost as well for the prediction of the erector spinae PCSA with only one independent variable. Our regression models for the prediction of the rectus abdominis PCSA also performed better than those by Tracey et al.(1989) ( $R^2$  from 0.27 to 0.44) and Reid et al. (1987) ( $R^2=0.40$ ), whereas McGill et al. (1988) did not find a significant relationship between the rectus abdominis CSA at L<sub>4</sub>/L<sub>5</sub> and height and weight measures. Whereas this study found that measures about the xyphoid process ( $R^2$  from 0.375 to 0.466) significantly predicted the external oblique PCSA, and different combinations of height and weight significantly predicted the internal oblique PCSA, previous studies found mixed results. Only McGill et al. (1988) and Wood et al. (1996) found significant relations between anthropometric measures and oblique muscle CSA. Finally, similar to other studies, external anthropometric measures were predictive of the psoas major PCSA (McGill et al. 1988; Reid et al. 1987; Tracy et al. 1989). Overall, the results of this study provide additional prediction equations not previously found for male trunk muscles, as well as better predictive models for those previously found by other researchers.

### ***Females vs. Males***

As expected, the comparisons of the ACSAs, PCSAs and coronal and sagittal plane moment-arms resulted in many significant differences between the two genders. The importance of these differences may, however, be apparent when trying to predict the PCSAs of the males and females based upon external anthropometry, or in other words, normalizing the PCSAs, as well as the moment-arms in both the coronal and sagittal planes, to measurable external anthropometry variables. The current EMG-assisted biomechanical model (Granata and Marras, 1993; Marras and Granata, 1995; Marras and Sommerich, 1991a,b) uses coefficients which are multiplied by the trunk width to estimate the coronal plane moment-arms, and trunk depth to

estimate the sagittal plane moment-arm, where the trunk width and depth are measured at the iliac crest. Additionally, the product of the trunk width and trunk depth measured at the iliac crest is used to predict the cross-sectional areas of the trunk muscles. However, the use of trunk width and trunk measurements at the iliac crest to predict the PCSA of each of the 10 trunk muscles used in the biomechanical model, as well as the average of the right and left muscles for each of the five pairs of muscles resulted in no significant regression equations for females (Tables 1.49 and 1.50), nor for the males (Tables 1.51 and 1.52). Typically, the measures about the xyphoid process and different combinations of subject height and weight did much better at predicting the PCSAs for females, whereas different combinations of subject height and weight did better for predicting the different male PCSAs.

The use of measures about the iliac crest to predict moment-arms in the coronal and sagittal plane showed very poor results for females and males. For the females, only the right external oblique resulted in a significant predicted moment-arm at the origin, which was based on the trunk width in the coronal plane (Table 1.72). The use of trunk depth and width measures about the xyphoid process resulted in more significant prediction equations for moment-arms at the insertion. Both anthropometric measures significantly predicted the moment-arms in the coronal plane for the latissimus dorsi, and external and internal obliques (Table 1.74), and also for the rectus abdominis and internal obliques for the moment-arms in the sagittal plane (Table 1.75). For the males, the measures about the iliac crest and xyphoid process resulted in no significant prediction equations for the right and left pairs of the latissimus dorsi and erector spinae for the sagittal moment-arms at both the origin and insertion levels, as well as no significant regression equations for the internal and external obliques at the insertion levels ( $L_3$  for internal obliques, and  $L_1$  for external obliques). The rest of the muscles showed inconsistent associations or no associations to trunk width or trunk depth measurements either at the iliac crest or the xyphoid process. Therefore, the use of measures about the xyphoid process to predict moment-arms, although not consistent across all muscles, performs better at predicting moment-arms than using measures about the iliac crest, for females as well as males.

Most of the male PCSAs were significantly larger than those of the females. However, when normalizing the PCSAs to external anthropometric measures of the trunk width multiplied by the trunk depth, fewer differences resulted. Specifically, the separate regression equations predicting the PCSAs were significantly different for the erector spinae, external and internal

obliques, and the psoas major and quadratus lumborum, but not for the rectus abdominis or latissimus dorsi muscles. Given that the erector spinae are the major extensor muscles which raise the torso during lifting activities, and that the external and internal obliques are involved during twisting activities, it is necessary that the development of the EMG-assisted biomechanical model for females be developed using the female specific regression equations predicting the PCSAs.

### ***Right and Left Side Symmetry***

Both males and females exhibited significantly larger right side latissimus dorsi muscle area when considering PCSAs (Table 1.78). Additionally, there existed statistically larger right side than left side ACSAs for both males and females for the more superior levels scanned (1.80 and 1.81). The findings of McGill et al. (1993) also support the existence of larger right than left side cross-sectional areas for males, although this difference was not tested statistically. Thus, the influence of the force generating capability of the muscles may be influenced by the direction of the exertion (right or left side), as well as the type of exertion which would have an influence on the muscle groups recruited. This is consistent with the previous research indicating that individuals have demonstrated greater twisting strength and lateral bending strength in one direction versus the other (Marras and Granata 1995, 1997a; McGill and Hoodless 1990).

### ***Muscle Vector Locations***

As shown in Tables 1.83 to 1.88, the muscle vector locations for males and females, as a function of external anthropometric measurements are given for each of the ten muscles used in the EMG-assisted biomechanical model, as a function of external anthropometric measurements. Generally, there were very small differences between the coefficients determined from the iliac crest and from the xyphoid process at the muscle origins ( $L_5/S_1$ ). Differences between the coefficients for males and females were very small, generally in the 1 to 3% range. However, somewhat larger differences existed at the origin for the external and internal obliques in the coronal plane (Tables 1.84 and Table 1.88), with the female vector location lying more lateral than the males vector location when the xyphoid process trunk width measurement was used. This is consistent with the observation of females possessing greater relative hip breadth than men (Brinckmann et al. 1981). Additionally, the female coefficients at the insertion level were smaller than the males for the rectus abdominis in the sagittal plane when using the trunk depth

measured at the iliac crest as a reference (Table 1.83). This is consistent with the findings of Reid and Costigan (1987) who found the females exhibited smaller sagittal plane moment-arm to trunk depth ratios than males, with the trunk depth measured at the L<sub>5</sub> level. Thus, these gender differences in muscle vector location indicates that the loading directions may be different depending on the direction of the exertion (e.g., flexion for the rectus abdominis or twisting or extension for the internal obliques), or as increases in coactivity occur, which would influence the loading on the spine (Granata and Marras 1995).

Table 1.4. Female and Male Subject mean (s.d.) anthropometric measurements.

Gender	Age (yrs)	Height (cm)*	Weight (kg)*	Trunk Depth at Trochanter (cm)*	Trunk Width at Trochanter (cm)*	Trunk Depth at Iliac Crest (cm)*	Trunk Width at Iliac Crest (cm)*	Trunk Depth at Xyphoid Process (cm)*	Trunk Width at Xyphoid Process (cm)*	Trunk Circumference at Iliac Crest (cm)*	Right Trochanter Height (cm)*	Left Trochanter Height (cm)*	Body Mass Index (kg/m <sup>2</sup> )*
Female (N=20)	25.0 (7.2)	165.5 (5.9)	57.9 (6.4)	23.1 (2.1)	33.7 (1.9)	19.8 (2.1)	28.0 (2.4)	18.4 (1.8)	27.0 (1.9)	76.0 (5.7)	85.3 (9.0)	86.7 (5.0)	21.2 (2.5)
Male (N=10)	26.4 (5.5)	175.9 (9.1)	79.8 (13.3)	25.4 (2.1)	34.8 (2.4)	22.3 (2.2)	30.3 (2.2)	22.9 (2.2)	32.4 (2.0)	86.8 (7.5)	89.0 (6.8)	88.8 (6.6)	25.7 (2.3)

\* Significantly different at  $p \leq 0.05$ .

Table 1.5. Mean (s.d.) trunk muscle anatomical cross-sectional area of the Right Latissimus Dorsi. Data collected (OSU) are compared with literature values for males and females. Differences between literature values and the current data are described in terms of area and as a percent of the literature values [ ]. Absolute and percent differences in muscle areas between male and female subjects are also shown.

**Right Latissimus Dorsi - Anatomical Cross-Sectional Area**

Level	OSU Male mean <sup>A</sup> (s.d.)	McGill et al., (1993) mean <sup>A</sup> (s.d.)	Difference <sup>A</sup> [% Diff.]	Difference <sup>D</sup> [% Diff.]	OSU Female mean <sup>A</sup> (s.d.)	Chaffin et al., (1990) mean <sup>A</sup> (s.d.)	Difference <sup>A</sup> [% Diff.]	Difference <sup>D</sup> [% Diff.]	Female vs Male <sup>B,C</sup> [% Diff.]
T8	21.68 (4.3)	15.81 (1.6)	5.87 [37]	4.8 [30]	13.15 (4.4)				-8.53 [-39]
T9	19.53 (4.4)	14.58 (2.7)	4.95 [34]	3.49 [24]	11.51 (5.1)				-8.02 [-41]
T10	16.61 (5.0)	13.68 (3.3)	2.93 [21]	1.68 [12]	9.77 (5.1)				-6.84 [-41]
T11	14.10 (4.2)	12.54 (2.8)	1.56 [12]	0.53 [4]	8.45 (0.5)				-5.65 [-40]
T12	12.03 (3.7)	10.14 (2.6)	1.89 [19]	0.36 [4]	7.34 (4.4)				-4.69 [-39]
L1	8.96 (2.5)	7.17 (2.6)	1.79 [25]	0.42 [6]	5.39 (3.1)				-3.57 [-40]
L2	6.22 (2.0)	4.29 (2.0)	1.93 [45]	0.18 [4]	3.44 (1.8)	1.20 (0.4)	2.24 [188]	1.25 [104]	-2.78 [-45]
L3	2.71 (1.4)	2.32 (1.9)	0.39 [17]		1.45 (0.6)	1.30 (0.4)	0.15 [12]		-1.26 [-46]
L4						1.30 (0.5)			
L5									
S1									

A: Square cm;

B: Female minus Male (Square cm);

C: Shaded cells represent significant difference between females and males ( $p \leq 0.05$ );

D: Comparisons based on data adjusted one-half of a vertebral level.

Table 1.6. Mean (s.d.) trunk muscle anatomical cross-sectional area of the Left Latissimus Dorsi. Data collected (OSU) are compared with literature values for males and females. Differences between literature values and the current data are described in terms of area and as a percent of the literature values [ ]. Absolute and percent differences in muscle areas between male and female subjects are also shown.

**Left Latissimus Dorsi - Anatomical Cross-Sectional Area**

Level	OSU Male mean <sup>A</sup> (s.d.)	McGill et al., (1993) mean <sup>A</sup> (s.d.)	Difference <sup>A</sup> [% Diff.]	Difference <sup>D</sup> [% Diff.]	OSU Female mean <sup>A</sup> (s.d.)	Chaffin et al., (1990) mean <sup>A</sup> (s.d.)	Difference <sup>A</sup> [% Diff.]	Difference <sup>D</sup> [% Diff.]	Female vs Male <sup>B,C</sup> [%Diff.]
T8	19.36 (5.2)	15.82 (2.8)	3.54 [24]	2.74 [17]	12.01 (4.7)				-7.35 [-38]
T9	17.76 (4.4)	14.17 (2.9)	3.59 [25]	2.25 [16]	10.56 (4.9)				-7.20 [-41]
T10	15.08 (4.9)	12.39 (2.6)	2.69 [22]	1.97 [16]	8.12 (4.8)				-6.96 [-46]
T11	13.63 (4.6)	11.02 (3.2)	2.61 [24]	1.33 [12]	6.88 (4.3)				-6.75 [-50]
T12	11.07 (4.0)	9.60 (3.1)	1.47 [15]	0.25 [3]	5.46 (3.0)				-5.61 [-51]
L1	8.62 (2.8)	6.82 (2.6)	1.8 [26]	0.46 [7]	5.46 (3.0)				-3.16 [-37]
L2	5.93 (2.3)	3.72 (1.6)	2.21 [59]	0.62 [17]	3.51 (2.4)	1.40 (0.6)	2.11 [150]	1.17 [84]	-2.42 [-41]
L3	2.74 (1.5)	2.56 (2.2)	0.18 [7]		1.63 (0.7)	1.30 (0.5)	0.33 [25]		-1.11 [-41]
L4						1.50 (0.6)			
L5									
S1									

A: Square cm

B: Female minus Male (Square cm);

C: Shaded cells represent significant difference between females and males ( $p \leq 0.05$ );

D: Comparisons based on data adjusted one-half of a vertebral level.

Table 1.7. Mean (s.d.) trunk muscle anatomical cross-sectional area of the Right Erector Spinae. Data collected (OSU) are compared with literature values for males and females. Differences between literature values and the current data are described in terms of area and as a percent of the literature values [ ]. Absolute and percent differences in muscle areas between male and female subjects are also shown.

**Right Erector Spinae - Anatomical Cross-Sectional Area**

Level	OSU Male mean <sup>A</sup> (s.d.)	McGill et al., (1993) mean <sup>A</sup> (s.d.)	Difference <sup>A</sup> [% Diff.]	Difference <sup>D</sup> [% Diff.]	OSU Female mean <sup>A</sup> (s.d.)	Chaffin et al., (1990) mean <sup>A</sup> (s.d.)	Difference <sup>A</sup> [% Diff.]	Difference <sup>D</sup> [% Diff.]	Female vs Male <sup>B,C</sup> [%Diff.]
T8	12.96 (2.1)	10.49 (2.0)	2.47 [24]	2.85 [28]	7.63 (1.7)				-5.33 [-41]
T9	13.91 (2.5)	14.13 (3.0)	-0.22 [-2]	0.52 [4]	8.38 (1.7)				-5.53 [-40]
T10	15.38 (2.9)	16.90 (2.1)	-1.52 [-9]	-0.57 [-3]	9.56 (1.9)				-5.82 [-38]
T11	17.28 (2.8)	18.32 (2.8)	-1.04 [-6]	-0.15 [0]	10.92 (2.5)				-6.36 [-37]
T12	19.65 (3.0)	26.14 (5.8)	-6.49 [-25]	-5.07 [-19]	11.69 (2.5)				-7.96 [-41]
L1	22.49 (3.7)	26.15 (4.1)	-3.66 [-14]	-2.11 [-8]	13.67 (3.3)				-8.82 [-39]
L2	25.60 (4.2)	28.54 (5.5)	-2.94 [-10]	-3.2 [-11]	15.68 (3.6)	18.20 (2.7)	-2.52 [-14]	-2.65 [-15]	-9.92 [-39]
L3	25.03 (3.7)	28.31 (4.6)	-3.28 [-12]	-5.76 [-20]	15.43 (3.6)	18.50 (3.0)	-3.07 [-17]	-4.6 [-25]	-9.60 [-38]
L4	20.08 (2.3)	21.51 (5.4)	-1.43 [-7]	-8.99 [-42]	12.37 (2.5)	17.40 (3.0)	-5.03 [-29]	-5.81 [-56]	-7.71 [-38]
L5	4.95 (1.8)	9.05 (3.3)	-4.1 [-45]		2.81 (1.1)				-2.14 [-43]
S1									

A: Square cm;

B: Female minus Male (Square cm);

C: Shaded cells represent significant difference between females and males (p≤0.05);

D: Comparisons based on data adjusted one-half of a vertebral level.

Table 1.8. Mean (s.d.) trunk muscle anatomical cross-sectional area of the Left Erector Spinae. Data collected (OSU) are compared with literature values for males and females. Differences between literature values and the current data are described in terms of area and as a percent of the literature values [ ]. Absolute and percent differences in muscle areas between male and female subjects are also shown.

**Left Erector Spinae – Anatomical Cross-Sectional Area**

Level	OSU Male mean <sup>A</sup> (s.d.)	McGill et al., (1993) mean <sup>A</sup> (s.d.)	Difference <sup>A</sup> [% Diff.]	Difference <sup>D</sup> [% Diff.]	OSU Female mean <sup>A</sup> (s.d.)	Chaffin et al., (1990) mean <sup>A</sup> (s.d.)	Difference <sup>A</sup> [% Diff.]	Difference <sup>D</sup> [% Diff.]	Female vs Male <sup>B,C</sup> [%Diff.]
T8	13.09 (2.2)	11.29 (1.0)	1.8 [16]	2.24 [20]	7.81 (1.6)				-5.28 [-40]
T9	13.97 (2.4)	14.71 (3.5)	-0.74 [-5]	0.25 [2]	8.42 (1.9)				-5.55 [-40]
T10	15.94 (3.1)	17.22 (2.8)	-1.28 [-7]	-0.29 [-2]	9.69 (2.3)				-6.25 [-39]
T11	17.92 (3.5)	20.41 (2.9)	-2.48 [-12]	-1.53 [-7]	10.95 (2.5)				-6.97 [-39]
T12	19.84 (3.5)	26.01 (5.6)	-6.17 [-24]	-4.83 [-19]	11.94 (2.7)				-7.90 [-40]
L1	22.53 (3.7)	27.23 (4.3)	-4.7 [-17]	-3.2 [-12]	13.84 (3.0)				-8.69 [-39]
L2	25.41 (4.2)	28.33 (4.6)	-2.92 [-10]	-3.02 [-11]	15.64 (3.5)	17.90 (3.1)	-2.26 [-13]	-2.29 [-13]	-9.77 [-38]
L3	25.21 (4.1)	29.33 (3.8)	-4.12 [-14]	-6.65 [-23]	15.58 (3.2)	18.50 (3.0)	-2.92 [-16]	-4.34 [-23]	-9.63 [-38]
L4	20.15 (2.7)	22.34 (4.8)	2.19 [-10]	-9.68 [-43]	12.74 (2.4)	17.30 (3.0)	-4.56 [-26]	-9.53 [-55]	-7.41 [-37]
L5	5.17 (1.7)	9.86 (3.4)	-4.69 [-48]		2.80 (1.1)				-2.37 [-46]
S1									

A: Square cm;

B: Female minus Male (Square cm);

C: Shaded cells represent significant difference between females and males ( $p \leq 0.05$ );

D: Comparisons based on data adjusted one-half of a vertebral level.

Table 1.9. Mean (s.d.) trunk muscle anatomical cross-sectional area of the Right Rectus Abdominis. Data collected (OSU) are compared with literature values for males and females. Differences between literature values and the current data are described in terms of area and as a percent of the literature values [ ]. Absolute and percent differences in muscle areas between male and female subjects are also shown.

**Right Rectus Abdominis - Anatomical Cross-Sectional Area**

Level	OSU Male mean <sup>A</sup> (s.d.)	McGill et al., (1993) mean <sup>A</sup> (s.d.)	Difference <sup>A</sup> [% Diff.]	Difference <sup>D</sup> [% Diff.]	OSU Female mean <sup>A</sup> (s.d.)	Chaffin et al., (1990) mean <sup>A</sup> (s.d.)	Difference <sup>A</sup> [% Diff.]	Difference <sup>D</sup> [% Diff.]	Female vs Male <sup>B,C</sup> [%Diff.]
T8									
T9									
T10									
T11									
T12	5.80 (1.9)				4.25 (0.7)				-1.55 [-27]
L1	6.39 (1.7)	5.76 (1.5)	0.63 [11]	0.45 [8]	4.85 (1)				-1.54 [-24]
L2	6.02 (1.2)	7.12 (2.4)	-1.1 [-15]	-0.45 [-6]	4.23 (1.2)	3.30 (1.6)	0.93 [28]	1.04 [31]	-1.79 [-28]
L3	7.32 (2.9)	6.70 (1.3)	0.62 [9]	0.49 [7]	4.44 (1.3)	3.70 (1.1)	0.74 [20]	0.96 [26]	-2.88 [-39]
L4	7.05 (2.2)	7.50 (2.1)	-0.46 [-6]	0.29 [4]	4.88 (1.8)	4.00 (1.0)	0.88 [22]	1.11 [28]	-2.17 [-31]
L5	8.53 (2.2)	7.87 (2.5)	0.66 [8]	0.83 [10]	5.33 (1.5)				-3.20 [-38]
S1	8.86 (2.3)				6.01 (2.2)				-2.85 [-32]

A: Square cm;

B: Female minus Male (Square cm);

C: Shaded cells represent significant difference between females and males ( $p \leq 0.05$ );

D: Comparisons based on data adjusted one-half of spine level.

Table 1.10. Mean (s.d.) trunk muscle anatomical cross-sectional area of the Left Rectus Abdominis. Data collected (OSU) are compared with literature values for males and females. Differences between literature values and the current data are described in terms of area and as a percent of the literature values [ ]. Absolute and percent differences in muscle areas between male and female subjects are also shown.

**Left Rectus Abdominis - Anatomical Cross-Sectional Area**

Level	OSU Male mean <sup>A</sup> (s.d.)	McGill et al., (1993) mean <sup>A</sup> (s.d.)	Difference <sup>A</sup> [% Diff.]	Difference <sup>D</sup> [% Diff.]	OSU Female mean <sup>A</sup> (s.d.)	Chaffin et al., (1990) mean <sup>A</sup> (s.d.)	Difference <sup>A</sup> [% Diff.]	Difference <sup>D</sup> [% Diff.]	Female vs Male <sup>B,C</sup> [%Diff.]
T8									
T9									
T10									
T11									
T12	6.13 (1.9)				4.54 (0.9)				-1.59 [-26]
L1	6.67 (2.1)	5.14 (1)	1.53 [30]	1.31 [25]	4.89 (1.1)				-1.78 [-27]
L2	6.22 (1.4)	7.48 (2.4)	-1.26 [-17]	-0.49 [-6]	4.43 (1.3)	3.40 (1.2)	1.03 [30]	1.07 [31]	-1.79 [-29]
L3	7.77 (2.7)	6.93 (1.8)	0.84 [12]	0.42 [6]	4.51 (1.3)	3.70 (1.2)	0.81 [22]	1.08 [29]	-3.26 [-42]
L4	6.92 (2.4)	7.46 (1.8)	-0.54 [-7]	0.35 [5]	5.04 (2.3)	4.10 (1.2)	0.94 [23]	1.13 [27]	-1.88 [-27]
L5	8.69 (2.4)	8.02 (2.5)	0.67 [8]	0.77 [10]	5.41 (1.3)				-3.28 [-38]
S1	8.88 (2.4)				6.14 (2.4)				-2.74 [-31]

A: Square cm;

B: Female minus Male (Square cm);

C: Shaded cells represent significant difference between females and males ( $p \leq 0.05$ );

D: Comparisons based on data adjusted one-half of spine level.

Table 1.11. Mean (s.d.) trunk muscle anatomical cross-sectional area of the Right External Obliques. Data collected (OSU) are compared with literature values for males and females. Differences between literature values and the current data are described in terms of area and as a percent of the literature values [ ]. Absolute and percent differences in muscle areas between male and female subjects are also shown.

**Right External Obliques - Anatomical Cross-Sectional Area**

Level	OSU Male mean <sup>A</sup> (s.d.)	McGill et al., (1993) mean <sup>A,E</sup> (s.d.)	Difference <sup>A</sup> [% Diff.]	Difference <sup>D</sup> [% Diff.]	OSU Female mean <sup>A</sup> (s.d.)	Chaffin et al., (1990) mean <sup>A</sup> (s.d.)	Difference <sup>A</sup> [% Diff.]	Difference <sup>D</sup> [% Diff.]	Female vs Male <sup>B,C</sup> [%Diff.]
T8									
T9									
T10									
T11									
T12	6.54 (1.5)				5.0 (1.1)				-1.54 [-23]
L1	8.63 (1.9)				5.68 (1.2)				-2.95 [-34]
L2	9.33 (1.9)	11.58 (2.2)	-2.25 [-19]	-2.43 [-21]	6.45 (1.3)	3.70 (1.2)	2.75 [74]	2.6 [70]	-2.88 [-31]
L3	8.97 (1.8)	11.21	-2.2 [-20]	-1.62 [-14]	6.15 (0.9)	4.40 (1.4)	1.75 [40]	1.98 [45]	-2.82 [-31]
L4	10.21 (2.0)	9.15 (2.0)	1.06 [12]		6.60 (1.0)	4.60 (1.4)	2.0 [43]		-3.61 [-35]
L5									
S1									

A: Square cm;

B: Female minus Male (Square cm);

C: Shaded cells represent significant difference between females and males (p≤0.05);

D: Comparisons based on data adjusted one-half of spine level.

E: Cross-sectional area at L3/L4 (shown as L3 in the table) corrected for muscle fiber direction.

Table 1.12. Mean (s.d.) trunk muscle anatomical cross-sectional area of the Left External Obliques. Data collected (OSU) are compared with literature values for males and females. Differences between literature values and the current data are described in terms of area and as a percent of the literature values [ ]. Absolute and percent differences in muscle areas between male and female subjects are also shown.

**Left External Obliques - Anatomical Cross-Sectional Area**

Level	OSU Male mean <sup>A</sup> (s.d.)	McGill et al., (1993) mean <sup>A,E</sup> (s.d.)	Difference <sup>A</sup> [% Diff.]	Difference <sup>D</sup> [% Diff.]	OSU Female mean <sup>A</sup> (s.d.)	Chaffin et al., (1990) mean <sup>A</sup> (s.d.)	Difference <sup>A</sup> [% Diff.]	Difference <sup>D</sup> [% Diff.]	Female vs Male <sup>B,C</sup> [%Diff.]
T8									
T9									
T10									
T11									
T12	6.35 (1.6)				4.58 (0.7)				-1.77 [-28]
L1	8.17 (1.8)				5.46 (1.1)				-2.71 [-33]
L2	9.31 (2.1)	13.51 (2.8)	-4.2 [-31]	-4.28 [-32]	6.47 (1.3)	5.50 (1.6)	0.97 [18]	0.71 [13]	-2.84 [-31]
L3	9.16 (2.1)	11.21	-2.05 [-18]	-1.45 [-13]	5.94 (1.1)	6.00 (1.4)	-0.06 [-1]	0.13 [2]	-3.22 [-35]
L4	10.36 (2.0)	9.92 (2.8)	0.44 [4]		6.31 (1.0)	6.00 (1.6)	0.31 [5]		-4.05 [-39]
L5									
S1									

A: Square cm;

B: Female minus Male (Square cm);

C: Shaded cells represent significant difference between females and males ( $p \leq 0.05$ );

D: Comparisons based on data adjusted one-half of spine level.

E: Cross-sectional area at L3/L4 (shown as L3 in the table) corrected for muscle fiber direction.

Table 1.13. Mean (s.d.) trunk muscle anatomical cross-sectional area of the Right Internal Obliques. Data collected (OSU) are compared with literature values for males and females. Differences between literature values and the current data are described in terms of area and as a percent of the literature values [ ]. Absolute and percent differences in muscle areas between male and female subjects are also shown.

**Right Internal Obliques - Anatomical Cross-Sectional Area**

Level	OSU Male mean <sup>A</sup> (s.d.)	McGill et al., (1993) mean <sup>A,E</sup> (s.d.)	Difference <sup>A</sup> [% Diff.]	Difference <sup>D</sup> [% Diff.]	OSU Female mean <sup>A</sup> (s.d.)	Chaffin et al., (1990) mean <sup>A</sup> (s.d.)	Difference <sup>A</sup> [% Diff.]	Difference <sup>D</sup> [% Diff.]	Female vs Male <sup>B,C</sup> [%Diff.]
T8									
T9									
T10									
T11									
T12									
L1									
L2	3.79 (1.6)	10.55 (1.7)	-6.76 [-64]	-5.47 [-52]	3.51 (1.6)	4.00 (1.4)	-0.49 [-12]	-0.38 [-10]	-0.28 [-7]
L3	6.38 (2.4)	11.54	-5.16 [-48]	-3.37 [-29]	3.73 (1.4)	5.30 (1.3)	-1.57 [-30]	-0.35 [-7]	-2.65 [-42]
L4	9.96 (2.4)	9.03 (0.8)	0.93 [10]		6.17 (1.4)	5.30 (1.8)	0.87 [16]		-3.79 [-38]
L5									
S1									

A: Square cm;

B: Female minus Male (Square cm);

C: Shaded cells represent significant difference between females and males ( $p \leq 0.05$ );

D: Comparisons based on data adjusted one-half of spine level.

E: Cross-sectional area at L3/L4 (shown as L3 in the table) corrected for muscle fiber direction.

Table 1.14. Mean (s.d.) trunk muscle anatomical cross-sectional area of the Left Internal Obliques. Data collected (OSU) are compared with literature values for males and females. Differences between literature values and the current data are described in terms of area and as a percent of the literature values [ ]. Absolute and percent differences in muscle areas between male and female subjects are also shown.

**Left Internal Obliques - Anatomical Cross-Sectional Area**

Level	OSU Male mean <sup>A</sup> (s.d.)	McGill et al., (1993) mean <sup>A,E</sup> (s.d.)	Difference <sup>A</sup> [% Diff.]	Difference <sup>D</sup> [% Diff.]	OSU Female mean <sup>A</sup> (s.d.)	Chaffin et al., (1990) mean <sup>A</sup> (s.d.)	Difference <sup>A</sup> [% Diff.]	Difference <sup>D</sup> [% Diff.]	Female vs Male <sup>B,C</sup> [%Diff.]
T8									
T9									
T10									
T11									
T12									
L1									
L2	4.28 (1.8)	10.27 (3.4)	-5.99 [-58]	-4.95 [-48]	3.31 (1.8)	4.30 (1.5)	-0.99 [-23]	-0.88 [-20]	-0.97 [-23]
L3	6.37 (2.3)	11.54	-5.17 [-49]	-3.23 [-28]	3.54 (1.4)	5.80 (1.5)	-2.26 [-40]	-0.83 [-14]	-2.83 [-44]
L4	10.25 (2.5)	9.00 (1.2)	1.25 [14]		6.41 (1.1)	5.20 (1.5)	1.21 [23]		-3.84 [-37]
L5									
S1									

A: Square cm;

B: Female minus Male (Square cm);

C: Shaded cells represent significant difference between females and males ( $p \leq 0.05$ );

D: Comparisons based on data adjusted one-half of spine level.

E: Cross-sectional area at L3/L4 (shown as L3 in the table) corrected for muscle fiber direction.

Table 1.15. Mean (s.d.) trunk muscle anatomical cross-sectional area of the Right Psoas Major. Data collected (OSU) are compared with literature values for males and females. Differences between literature values and the current data are described in terms of area and as a percent of the literature values [ ]. Absolute and percent differences in muscle areas between male and female subjects are also shown.

**Right Psoas Major - Anatomical Cross-Sectional Area**

Level	OSU Male mean <sup>A</sup> (s.d.)	McGill et al., (1993) mean <sup>A</sup> (s.d.)	Difference <sup>A</sup> [% Diff.]	Difference <sup>D</sup> [% Diff.]	OSU Female mean <sup>A</sup> (s.d.)	Chaffin et al., (1990) mean <sup>A</sup> (s.d.)	Difference <sup>A</sup> [% Diff.]	Difference <sup>D</sup> [% Diff.]	Female vs Male <sup>B,C</sup> [%Diff.]
T8									
T9									
T10									
T11									
T12		3.30 (2.1)							
L1	2.58 (--)	5.13 (3.3)	-2.55 [-50]	-0.4 [8]	2.17 (1.2)				-0.41 [-16]
L2	6.88 (2.3)	11.77 (2.9)	-4.89 [-42]	-1.67 [-14]	3.30 (0.9)	5.80 (1.5)	-2.5 [-43]	-0.81 [-14]	-3.58 [-52]
L3	13.32 (3.1)	15.94 (3.7)	-2.62 [-16]	-0.12 [0]	6.69 (1.8)	8.30 (1.9)	-1.61 [-19]	-0.13 [-2]	-6.63 [-50]
L4	18.32 (3.6)	18.61 (3.5)	-0.29 [-2]	0.0 [0]	9.65 (1.7)	9.80 (2.0)	-0.15 [-2]	0.09 [0]	-8.67 [-47]
L5	18.90 (3.8)	16.06 (2.0)	2.84 [18]		10.13 (1.7)				-8.77 [-46]
S1									

A: Square cm;

B: Female minus Male (Square cm);

C: Shaded cells represent significant difference between females and males ( $p \leq 0.05$ );

D: Comparisons based on data adjusted one-half of spine level.

Table 1.16. Mean (s.d.) trunk muscle anatomical cross-sectional area of the Left Psoas Major. Data collected (OSU) are compared with literature values for males and females. Differences between literature values and the current data are described in terms of area and as a percent of the literature values [ ]. Absolute and percent differences in muscle areas between male and female subjects are also shown.

**Left Psoas Major - Anatomical Cross-Sectional Area**

Level	OSU Male mean <sup>A</sup> (s.d.)	McGill et al., (1993) mean <sup>A</sup> (s.d.)	Difference <sup>A</sup> [% Diff.]	Difference <sup>D</sup> [% Diff.]	OSU Female mean <sup>A</sup> (s.d.)	Chaffin et al., (1990) mean <sup>A</sup> (s.d.)	Difference <sup>A</sup> [% Diff.]	Difference <sup>D</sup> [% Diff.]	Female vs Male <sup>B,C</sup> [%Diff.]
T8									
T9									
T10									
T11									
T12		4.62 (1.9)							
L1	3.23 (1.4)	4.88 (2.5)	-1.65 [-34]	0.64 [13]	2.24 (0.4)				-0.99 [-31]
L2	7.81 (2.5)	12.11 (3.0)	-4.3 [-36]	-1.37 [-11]	3.56 (0.9)	5.90 (1.7)	-2.34 [-40]	-0.73 [-12]	-4.25 [-54]
L3	13.68 (2.7)	15.93 (2.9)	-2.25 [-14]	0.25 [2]	6.79 (1.7)	8.30 (1.9)	-1.51 [-18]	0.06 [0]	-6.89 [-50]
L4	18.68 (3.1)	18.20 (2.7)	0.48 [3]	0.64 [4]	9.93 (1.8)	9.80 (2.2)	0.13 [1]	0.54 [6]	-8.75 [-47]
L5	19.00 (2.9)	15.90 (2.4)	3.1 [19]		10.75 (1.8)				-8.25 [-43]
S1									

A: Square cm;

B: Female minus Male (Square cm);

C: Shaded cells represent significant difference between females and males ( $p \leq 0.05$ );

D: Comparisons based on data adjusted one-half of spine level.

Table 1.17. Mean (s.d.) trunk muscle anatomical cross-sectional area of the Right Quadratus Lumborum. Data collected (OSU) are compared with literature values for males and females. Differences between literature values and the current data are described in terms of area and as a percent of the literature values [ ]. Absolute and percent differences in muscle areas between male and female subjects are also shown.

**Right Quadratus Lumborum - Anatomical Cross-Sectional Area**

Level	OSU Male mean <sup>A</sup> (s.d.)	McGill et al., (1993) mean <sup>A,E</sup> (s.d.)	Difference <sup>A</sup> [% Diff.]	Difference <sup>D</sup> [% Diff.]	OSU Female mean <sup>A</sup> (s.d.)	Chaffin et al., (1990) mean <sup>A</sup> (s.d.)	Difference <sup>A</sup> [% Diff.]	Difference <sup>D</sup> [% Diff.]	Female vs Male <sup>B,C</sup> [%Diff.]
T8									
T9									
T10									
T11									
T12		3.20 (2.0)							
L1	2.50 (--)	3.58	-1.08 [-30]	-0.81 [-23]	1.71 (0.6)				-0.79 [-32]
L2	3.04 (1.2)	5.07	-2.03 [-40]	-0.95 [-19]	1.88 (0.5)	3.00 (0.7)	-1.12 [-37]	-1.01 [-34]	-1.16 [-38]
L3	5.20 (1.7)	5.82	-0.62 [-11]	-1.44 [-25]	2.11 (0.5)	4.10 (1.2)	-1.99 [-49]	-2.06 [-50]	-3.09 [-59]
L4	3.56 (1.1)	3.28	0.28 [9]		1.97 (0.3)	4.60 (1.0)	2.62 [-57]		-1.59 [-45]
L5									
S1									

A: Square cm;

B: Female minus Male (Square cm);

C: Shaded cells represent significant difference between females and males ( $p \leq 0.05$ );

D: Comparisons based on data adjusted one-half of spine level.

E: Cross-sectional area between L1/L2 and L4/L5 (shown as L1 through L4 in the table) are corrected for muscle fiber direction.

Table 1.18. Mean (s.d.) trunk muscle anatomical cross-sectional area of the Left Quadratus Lumborum. Data collected (OSU) are compared with literature values for males and females. Differences between literature values and the current data are described in terms of area and as a percent of the literature values [ ]. Absolute and percent differences in muscle areas between male and female subjects are also shown.

**Left Quadratus Lumborum - Anatomical Cross-Sectional Area**

Level	OSU Male mean <sup>A</sup> (s.d.)	McGill et al., (1993) mean <sup>A,E</sup> (s.d.)	Difference <sup>A</sup> [% Diff.]	Difference <sup>D</sup> [% Diff.]	OSU Female mean <sup>A</sup> (s.d.)	Chaffin et al., (1990) mean <sup>A</sup> (s.d.)	Difference <sup>A</sup> [% Diff.]	Difference <sup>D</sup> [% Diff.]	Female vs Male <sup>B,C</sup> [%Diff.]
T8									
T9									
T10									
T11									
T12		3.26 (0.1)							
L1	2.71 (1.3)	3.58	-0.87 [-24]	-0.71 [-20]	1.71 (0.4)				-1.0 [-37]
L2	3.03 (1.1)	5.07	-2.04 [-40]	-0.87 [-17]	1.91 (0.5)	3.30 (1.6)	-1.39 [-42]	-1.15 [-35]	-1.12 [-37]
L3	5.38 (1.9)	5.82	-0.44 [-8]	-1.34 [-23]	2.39 (0.7)	4.50 (1.4)	-2.11 [-47]	-2.17 [-48]	-2.99 [-56]
L4	3.59 (1.0)	3.28	0.31 [9]		2.28 (0.4)	4.50 (1.3)	-2.22 [-49]		-1.31 [-36]
L5									
S1									

A: Square cm;

B: Female minus Male (Square cm);

C: Shaded cells represent significant difference between females and males ( $p \leq 0.05$ );

D: Comparisons based on data adjusted one-half of spine level.

E: Cross-sectional area between L1/L2 and L4/L5 (shown as L1 through L4 in the table) are corrected for muscle fiber direction.

Table 1.19. Vertebral body mean (s.d.) cross-sectional area. Data collected (OSU) are compared with literature values for males and females. Differences between literature values and the current data are described in terms of area and as a percent of the literature values [ ]. Absolute and percent differences in muscle areas between male and female subjects are also shown.

**Vertebral Body - Cross-Sectional Area**

Level	OSU Male mean <sup>A</sup> (s.d.)	McGill et al., (1993) mean <sup>A</sup> (s.d.)	Difference <sup>A</sup> [% Diff.]	OSU Female mean <sup>A</sup> (s.d.)	Chaffin et al., (1990) mean <sup>A</sup> (s.d.)	Difference <sup>A</sup> [% Diff.]	Female vs Male <sup>B</sup> [% Diff.]
T8	9.83 (1.8)	7.98 (0.9)	1.85 [23]	7.28 (1.1)			-2.55 [-26]
T9	10.41 (2.1)	9.33 (1.1)	1.08 [12]	7.80 (0.9)			-2.61 [-25]
T10	10.87 (1.7)	10.15 (1.3)	0.72 [7]	8.43 (0.8)			-2.44 [-22]
T11	12.25 (1.8)	11.33 (1.2)	0.92 [8]	8.93 (1.0)			-3.32 [-27]
T12	12.87 (1.9)	12.41 (1.7)	0.46 [4]	9.37 (1.2)			-3.50 [-27]
L1	12.49 (2.1)	13.34 (2.9)	-0.85 [-6]	9.49 (1.0)			-3.00 [-24]
L2	13.11 (2.4)	13.32 (2.9)	-0.21 [-2]	10.11 (1.2)	14.20 (2.4)	-4.09 [-29]	-3.00 [-23]
L3	14.13 (2.0)	14.15 (2.5)	-0.02 [0]	10.89 (1.1)	15.20 (2.3)	-4.31 [-28]	-3.24 [-23]
L4	14.78 (2.4)	14.59 (2.7)	0.19 [1]	11.25 (1.2)	15.30 (2.2)	-4.05 [-26]	-3.53 [-24]
L5	14.66 (2.2)	13.60 (2.8)	1.06 [8]	11.80 (2.2)			-2.86 [-20]
S1	17.42 (2.6)			12.75 (2.5)			-4.68 [-27]

A: Square cm;

B: Female minus Male (Square cm).

Table 1.20. Trunk mass mean (s.d.) cross-sectional area. Data collected (OSU) are compared with literature values for males and females. Differences between literature values and the current data are described in terms of area and as a percent of the literature values [ ]. Absolute and percent differences in muscle areas between male and female subjects are also shown.

**Trunk - Cross-Sectional Area**

Level	OSU Male mean <sup>A</sup> (s.d.)	McGill et al., (1993) mean <sup>A</sup> (s.d.)	Difference <sup>A</sup> [% Diff.]	OSU Female mean <sup>A</sup> (s.d.)	Chaffin et al., (1990) mean <sup>A</sup> (s.d.)	Difference <sup>A</sup> [% Diff.]	Female vs Male <sup>B</sup> [% Diff.]
T8	733.38 (110.8)	657.94 (52.5)	75.44 [11]	482.30 (65.7)			-251.08 [-34]
T9	688.31 (90.2)	617.32 (69.6)	70.99 [11]	466.05 (63.3)			-222.26 [-32]
T10	645.59 (82.6)	610.51 (75.7)	35.08 [6]	444.05 (61.2)			-201.54 [-31]
T11	616.48 (85.5)	592.49 (72.7)	23.99 [4]	430.92 (59.9)			-185.56 [-30]
T12	594.41 (84.6)	632.87 (91.5)	-38.46 [-6]	425.51 (60.0)			-168.90 [-28]
L1	574.78 (79.3)	590.91 (69.0)	-16.13 [-3]	415.98 (61.6)			-158.80 [-28]
L2	544.35 (81.1)	558.34 (81.1)	-13.99 [-3]	399.13 (61.4)	443.00 (122.0)	-43.87 [-10]	-145.22 [-27]
L3	525.43 (87.7)	542.86 (87.0)	-17.43 [-3]	377.56 (57.9)	509.00 (168.0)	-131.46 [-26]	-147.89 [-28]
L4	514.32 (101.8)	518.13 (98.5)	-3.82 [-1]	388.82 (71.7)	576.00 (159.0)	-187.18 [-33]	-125.50 [-24]
L5	524.81 (88.2)	529.12 (91.23)	-4.31 [-1]	471.66 (77.7)			-53.15 [-10]
.S1	565.47 (77.0)			533.20 (79.6)			-32.77 [-6]

A: Square cm;

B: Female minus Male (Square cm).

Table 1.21. Right Latissimus Dorsi mean (s.d.) coronal plane moment-arm distance from the center of the vertebral body to the area centroid of the muscle cross-sectional area. Data collected (OSU) are compared with literature values for males and females. Differences between literature values and the current data are described in terms of the magnitude (cm) and as a percent of the literature values [ ]. Magnitude and percent difference in coronal plane moment-arms between male and female subjects are also shown.

**Right Latissimus Dorsi – Coronal Plane Moment Arms**

Level	OSU Male mean <sup>A</sup> (s.d.)	McGill et al., (1993) mean <sup>A</sup> (s.d.)	Difference <sup>A</sup> [% Diff.]	OSU Female mean <sup>A</sup> (s.d.)	Chaffin et al., (1990) mean <sup>A</sup> (s.d.)	Difference <sup>A</sup> [% Diff.]	Female vs Male <sup>B,C</sup> [% Diff.]
T8	15.3 (1.0)	14.5 (0.7)	8 [4]	13.2 (1.0)			-2.1 [-14]
T9	14.5 (0.9)	14.1 (0.8)	4 [3]	12.4 (0.9)			-2.1 [-14]
T10	13.5 (1.0)	14.0 (0.9)	-5 [-4]	11.4 (0.9)			-2.1 [-16]
T11	12.8 (0.9)	12.9 (0.9)	-1 [-1]	10.9 (0.9)			-1.9 [-15]
T12	12.2 (0.8)	12.9 (1.0)	-7 [-5]	10.4 (0.9)			-1.8 [-15]
L1	11.6 (0.6)	12.2 (1.2)	-6 [-5]	9.9 (0.9)			-1.7 [-15]
L2	10.9 (0.7)	10.8 (0.8)	1 [1]	9.3 (1.0)	10.0 (1.1)	-7 [-7]	-1.6 [-15]
L3	10.3 (0.8)	10.2 (0.8)	1 [1]	9.0 (1.1)	10.6 (1.6)	-16 [-15]	-1.3 [-13]
L4					11.9 (1.1)		
L5							
S1							

A = centimeters (cm)

B = Female minus Male (cm)

C = Shaded cells represent significant difference between females and males ( $p \leq 0.05$ ).

Table 1.22. Left Latissimus Dorsi mean (s.d.) coronal plane moment-arm distance from the center of the vertebral body to the area centroid of the muscle cross-sectional area. Data collected (OSU) are compared with literature values for males and females. Differences between literature values and the current data are described in terms of the magnitude (cm) and as a percent of the literature values [ ]. Magnitude and percent difference in coronal plane moment-arms between male and female subjects are also shown.

**Left Latissimus Dorsi – Coronal Plane Moment Arms**

Level	OSU Male mean <sup>A</sup> (s. d.)	McGill et al., (1993) mean <sup>A</sup> (s.d.)	Difference <sup>A</sup> [% Diff.]	OSU Female mean <sup>A</sup> (s.d.)	Chaffin et al., (1990) mean <sup>A</sup> (s.d.)	Difference <sup>A</sup> [% Diff.]	Female vs Male <sup>B,C</sup> [% Diff.]
T8	15.0 (0.7)	14.3 (0.6)	7 [5]	13.1 (0.9)			-1.9 [-13]
T9	14.0 (0.8)	13.9 (0.8)	1 [1]	12.2 (0.9)			-1.8 [-13]
T10	13.2 (0.9)	13.7 (0.9)	-5 [-4]	11.4 (1.0)			-1.8 [-14]
T11	12.6 (0.9)	12.9 (1.0)	-3 [-2]	10.8 (1.0)			-1.8 [-14]
T12	12.1 (0.9)	12.8 (0.7)	-7 [-5]	10.4 (0.9)			-1.7 [-14]
L1	11.6 (0.9)	11.7 (1.1)	-1 [-1]	10.1 (0.9)			-1.5 [-13]
L2	11.0 (0.7)	10.7 (0.9)	3 [3]	9.4 (1.1)	9.9 (1.2)	-5 [-5]	-1.6 [-15]
L3	10.5 (0.8)	10.4 (1.5)	1 [1]	9.2 (1.1)	10.7 (1.4)	-15 [-14]	-1.3 [-12]
L4					11.8 (1.5)		
L5							
S1							

A = centimeters (cm)

B = Female minus Male (cm)

C = Shaded cells represent significant difference between females and males ( $p \leq 0.05$ ).

Table 1.23. Right Erector Spinae mean (s.d.) coronal plane moment-arm distance from the center of the vertebral body to the area centroid of the muscle cross-sectional area. Data collected (OSU) are compared with literature values for males and females. Differences between literature values and the current data are described in terms of the magnitude (cm) and as a percent of the literature values [ ]. Magnitude and percent difference in coronal plane moment-arms between male and female subjects are also shown.

**Right Erector Spinae – Coronal Plane Moment Arms**

Level	OSU Male mean <sup>A</sup> (s.d.)	McGill et al., (1993) mean <sup>A</sup> (s.d.)	Difference <sup>A</sup> [% Diff.]	OSU Female mean <sup>A</sup> (s.d.)	Chaffin et al., (1990) mean <sup>A</sup> (s.d.)	Difference <sup>A</sup> [% Diff.]	Female vs Male <sup>B,C</sup> [% Diff.]
T8	3.1 (0.2)	3.1 (0.7)	0 [0]	2.6 (0.3)			-0.5 [-16]
T9	3.2 (0.3)	3.2 (0.4)	0 [0]	2.8 (0.3)			-0.4 [-13]
T10	3.4 (0.3)	3.4 (0.4)	0 [0]	2.9 (0.3)			-0.5 [-15]
T11	3.6 (0.3)	3.4 (0.4)	2 [6]	3.1 (0.3)			-0.5 [-14]
T12	3.6 (0.3)	4.2 (0.3)	-6 [-14]	3.2 (0.3)			-0.4 [-11]
L1	4.0 (0.4)	4.4 (0.5)	-4 [-9]	3.4 (0.3)			-0.6 [-15]
L2	4.1 (0.3)	4.2 (0.4)	-1 [-2]	3.5 (0.3)	3.4 (0.4)	1 [3]	-0.6 [-15]
L3	3.8 (0.3)	4.0 (0.4)	-2 [-5]	3.4 (0.3)	3.4 (0.4)	0 [0]	-0.4 [-11]
L4	3.6 (0.3)	3.4 (0.7)	2 [6]	3.4 (0.3)	3.5 (0.4)	-1 [3]	-0.2 [-6]
L5	3.0 (0.7)	2.2 (0.6)	8 [36]	2.6 (0.6)			-0.4 [-13]
S1	1.9 (0.3)			1.9 (0.3)			-0.0 [-0]

A = centimeters (cm)

B = Female minus Male (cm)

C = Shaded cells represent significant difference between females and males ( $p \leq 0.05$ ).

Table 1.24. Left Erector Spinae mean (s.d.) coronal plane moment-arm distance from the center of the vertebral body to the area centroid of the muscle cross-sectional area. Data collected (OSU) are compared with literature values for males and females. Differences between literature values and the current data are described in terms of the magnitude (cm) and as a percent of the literature values [ ]. Magnitude and percent difference in coronal plane moment-arms between male and female subjects are also shown.

**Left Erector Spinae – Coronal Plane Moment Arms**

Level	OSU Male mean <sup>A</sup> (s.d.)	McGill et al., (1993) mean <sup>A</sup> (s.d.)	Difference <sup>A</sup> [% Diff.]	OSU Female mean <sup>A</sup> (s.d.)	Chaffin et al., (1990) mean <sup>A</sup> (s.d.)	Difference <sup>A</sup> [% Diff.]	Female vs Male <sup>B,C</sup> [% Diff.]
T8	3.3 (0.4)	3.3 (0.6)	0 [0]	2.7 (0.4)			-0.6 [-18]
T9	3.4 (0.4)	3.5 (0.4)	-1 [-3]	2.8 (0.3)			-0.06 [-18]
T10	3.6 (0.3)	3.6 (0.3)	0 [0]	3.1 (0.2)			-0.5 [-14]
T11	3.8 (0.3)	4.0 (0.3)	-2 [-5]	3.2 (0.3)			-0.6 [-16]
T12	3.8 (0.3)	4.0 (0.4)	-2 [-5]	3.4 (0.4)			-0.4 [-11]
L1	4.2 (0.3)	4.1 (0.7)	1 [2]	3.5 (0.3)			-0.7 [-17]
L2	4.3 (0.4)	4.1 (0.6)	2 [5]	3.5 (0.3)	3.3 (0.4)	2 [6]	-0.8 [-19]
L3	4.0 (0.2)	3.8 (0.5)	2 [5]	3.5 (0.3)	3.4 (0.4)	1 [3]	-0.5 [-13]
L4	3.8 (0.3)	3.3 (0.6)	5 [15]	3.5 (0.3)	3.5 (0.4)	0 [0]	-0.3 [-8]
L5	3.2 (0.5)	2.1 (0.5)	11 [52]	2.7 (0.5)			-0.5 [-16]
S1	2.2 (0.2)			1.9 (0.2)			-0.3 [-14]

A = centimeters (cm)

B = Female minus Male (cm)

C = Shaded cells represent significant difference between females and males ( $p \leq 0.05$ ).

Table 1.25. Right Rectus Abdominis mean (s.d.) coronal plane moment-arm distance from the center of the vertebral body to the area centroid of the muscle cross-sectional area. Data collected (OSU) are compared with literature values for males and females. Differences between literature values and the current data are described in terms of the magnitude (cm) and as a percent of the literature values [ ]. Magnitude and percent difference in coronal plane moment-arms between male and female subjects are also shown.

**Right Rectus Abdominis – Coronal Plane Moment Arms**

Level	OSU Male mean <sup>A</sup> (s.d.)	McGill et al., (1993) mean <sup>A</sup> (s.d.)	Difference <sup>A</sup> [% Diff.]	OSU Female mean <sup>A</sup> (s.d.)	Chaffin et al., (1990) mean <sup>A</sup> (s.d.)	Difference <sup>A</sup> [% Diff.]	Female vs Male <sup>B,C</sup> [% Diff.]
T8							
T9							
T10							
T11							
T12	3.9 (0.6)			2.9 (0.8)			-1.0 [-26]
L1	4.6 (1.1)	3.7 (0.8)	9 [24]	3.4 (0.9)			-1.2 [-26]
L2	4.9 (1.1)	4.6 (0.8)	3 [7]	3.6 (0.8)	4.4 (1.2)	-8 [-18]	-1.3 [-27]
L3	4.7 (0.7)	4.3 (0.7)	4 [9]	3.9 (0.8)	4.3 (1.1)	-4 [-9]	-0.8 [-17]
L4	4.6 (0.5)	3.8 (0.7)	8 [21]	4.0 (0.8)	4.2 (1.1)	-2 [-5]	-0.6 [-13]
L5	4.1 (0.5)	3.2 (0.5)	9 [28]	3.8 (0.9)			-0.3 [-7]
S1	3.8 (0.5)			3.3 (0.7)			-0.5 [-13]

A = centimeters (cm)

B = Female minus Male (cm)

C = Shaded cells represent significant difference between females and males ( $p \leq 0.05$ ).

Table 1.26. Left Rectus Abdominis mean (s.d.) coronal plane moment-arm distance from the center of the vertebral body to the area centroid of the muscle cross-sectional area. Data collected (OSU) are compared with literature values for males and females. Differences between literature values and the current data are described in terms of the magnitude (cm) and as a percent of the literature values [ ]. Magnitude and percent difference in coronal plane moment-arms between male and female subjects are also shown.

**Left Rectus Abdominis – Coronal Plane Moment Arms**

Level	OSU Male mean <sup>A</sup> (s.d.)	McGill et al., (1993) mean <sup>A</sup> (s.d.)	Difference <sup>A</sup> [% Diff.]	OSU Female mean <sup>A</sup> (s.d.)	Chaffin et al., (1990) mean <sup>A</sup> (s.d.)	Difference <sup>A</sup> [% Diff.]	Female vs Male <sup>B,C</sup> [% Diff.]
T8							
T9							
T10							
T11							
T12	3.5 (0.7)			3.5 (0.5)			0.0 [0]
L1	4.1 (0.8)	3.5 (1.7)	6 [17]	3.7 (0.7)			-0.4 [-10]
L2	3.9 (0.8)	4.3 (0.7)	-4 [-9]	3.4 (0.8)	4.2 (1.0)	-8 [-19]	-0.5 [-13]
L3	4.0 (0.7)	3.8 (0.8)	2 [5]	3.3 (0.9)	4.3 (1.2)	-10 [-23]	-0.7 [-18]
L4	3.6 (0.8)	3.6 (0.7)	0 [0]	3.5 (0.8)	4.1 (1.1)	-6 [-15]	-0.1 [-3]
L5	3.3 (0.8)	3.3 (0.5)	0 [0]	3.2 (0.8)			-0.1 [-3]
S1	2.9 (0.5)			3.3 (0.6)			0.4 [14]

A = centimeters (cm)

B = Female minus Male (cm)

C = Shaded cells represent significant difference between females and males ( $p \leq 0.05$ ).

Table 1.27. Right External Obliques mean (s.d.) coronal plane moment-arm distance from the center of the vertebral body to the area centroid of the muscle cross-sectional area. Data collected (OSU) are compared with literature values for males and females. Differences between literature values and the current data are described in terms of the magnitude (cm) and as a percent of the literature values [ ]. Magnitude and percent difference in coronal plane moment-arms between male and female subjects are also shown.

**Right External Obliques – Coronal Plane Moment Arms**

Level	OSU Male mean <sup>A</sup> (s.d.)	McGill et al., (1993) mean <sup>A</sup> (s.d.)	Difference <sup>A</sup> [% Diff.]	OSU Female mean <sup>A</sup> (s.d.)	Chaffin et al., (1990) mean <sup>A</sup> (s.d.)	Difference <sup>A</sup> [% Diff.]	Female vs Male <sup>B,C</sup> [% Diff.]
T8							
T9							
T10							
T11							
T12	12.9 (1.0)			10.8 (0.8)			-2.1 [-16]
L1	13.0 (1.2)			10.9 (1.0)			-2.1 [-16]
L2	13.2 (1.0)	14.0 (0.5)	-8 [-6]	10.9 (0.8)	11.7 (1.5)	-8 [-7]	-2.1 [-16]
L3	12.8 (0.7)	13.0 (1.0)	-2 [-2]	10.8 (0.7)	12.0 (1.6)	-12 [-10]	-2.0 [-16]
L4	12.8 (0.7)	12.5 (1.3)	3 [2]	11.2 (0.8)	12.1 (1.4)	-9 [-7]	-1.6 [-13]
L5	12.6 (0.6)			11.6 (0.3)			-1.0 [-8]
S1							

A = centimeters (cm)

B = Female minus Male (cm)

C = Shaded cells represent significant difference between females and males ( $p \leq 0.05$ ).

Table 1.28. Left External Obliques mean (s.d.) coronal plane moment-arm distance from the center of the vertebral body to the area centroid of the muscle cross-sectional area. Data collected (OSU) are compared with literature values for males and females. Differences between literature values and the current data are described in terms of the magnitude (cm) and as a percent of the literature values [ ]. Magnitude and percent difference in coronal plane moment-arms between male and female subjects are also shown.

**Left External Obliques – Coronal Plane Moment Arms**

Level	OSU Male mean <sup>A</sup> (s.d.)	McGill et al., (1993) mean <sup>A</sup> (s.d.)	Difference <sup>A</sup> [% Diff.]	OSU Female mean <sup>A</sup> (s.d.)	Chaffin et al., (1990) mean <sup>A</sup> (s.d.)	Difference <sup>A</sup> [% Diff.]	Female vs Male <sup>B,C</sup> [% Diff.]
T8							
T9							
T10							
T11							
T12	12.4 (0.9)			11.2 (1.0)			-1.2 [-10]
L1	12.6 (0.9)			11.0 (0.9)			-1.6 [-13]
L2	12.4 (1.1)	13.3 (0.7)	-9 [-7]	10.8 (1.0)	11.7 (1.4)	-9 [-8]	-1.6 [-13]
L3	12.4 (1.0)	12.5 (0.9)	-1 [-1]	10.6 (0.9)	12.2 (1.6)	-16 [-13]	-1.8 [-15]
L4	12.2 (0.9)	12.0 (0.9)	2 [2]	10.8 (0.9)	12.3 (2.0)	-15 [-12]	-1.4 [-11]
L5	12.5 (1.1)			11.3 (1.1)			-1.2 [-10]
S1							

A = centimeters (cm)

B = Female minus Male (cm)

C = Shaded cells represent significant difference between females and males (p≤0.05).

Table 1.29. Right Internal Obliques mean (s.d.) coronal plane moment-arm distance from the center of the vertebral body to the area centroid of the muscle cross-sectional area. Data collected (OSU) are compared with literature values for males and females. Differences between literature values and the current data are described in terms of the magnitude (cm) and as a percent of the literature values [ ]. Magnitude and percent difference in coronal plane moment-arms between male and female subjects are also shown.

**Right Internal Obliques – Coronal Plane Moment Arms**

Level	OSU Male mean <sup>A</sup> (s.d.)	McGill et al., (1993) mean <sup>A</sup> (s.d.)	Difference <sup>A</sup> [% Diff.]	OSU Female mean <sup>A</sup> (s.d.)	Chaffin et al., (1990) mean <sup>A</sup> (s.d.)	Difference <sup>A</sup> [% Diff.]	Female vs Male <sup>B,C</sup> [% Diff.]
T8							
T9							
T10							
T11							
T12							
L1				8.3 (-)			
L2	11.4 (1.6)	12.3 (0.9)	-9 [-2]	9.9 (1.4)	10.9 (1.5)	-10 [-9]	-1.5 [-13]
L3	11.5 (0.8)	11.6 (0.8)	-1 [-1]	9.7 (1.1)	11.3 (1.6)	-16 [-14]	-1.8 [-16]
L4	11.4 (0.6)	10.9 (1.1)	5 [5]	10.1 (0.8)	11.5 (2.0)	-14 [-12]	-1.3 [-11]
L5	10.9 (0.3)			10.4 (0.3)			-0.5 [-5]
S1				9.2 (-)			

A = centimeters (cm)

B = Female minus Male (cm)

C = Shaded cells represent significant difference between females and males ( $p \leq 0.05$ ).

Table 1.30. Left Internal Obliques mean (s.d.) coronal plane moment-arm distance from the center of the vertebral body to the area centroid of the muscle cross-sectional area. Data collected (OSU) are compared with literature values for males and females. Differences between literature values and the current data are described in terms of the magnitude (cm) and as a percent of the literature values [ ]. Magnitude and percent difference in coronal plane moment-arms between male and female subjects are also shown.

**Left Internal Obliques – Coronal Plane Moment Arms**

Level	OSU Male mean <sup>A</sup> (s.d.)	McGill et al., (1993) mean <sup>A</sup> (s.d.)	Difference <sup>A</sup> [% Diff.]	OSU Female mean <sup>A</sup> (s.d.)	Chaffin et al., (1990) mean <sup>A</sup> (s.d.)	Difference <sup>A</sup> [% Diff.]	Female vs Male <sup>B,C</sup> [% Diff.]
T8							
T9							
T10							
T11							
T12							
L1				9.3 (-)			
L2	10.7 (1.3)	12.1 (1.1)	-14 [-12]	10.2 (1.5)	10.9 (1.5)	-7 [-6]	-0.5 [-5]
L3	11.1 (1.4)	11.2 (0.8)	-1 [-1]	9.4 (1.4)	11.4 (1.6)	-20 [-18]	-1.7 [-15]
L4	10.7 (0.8)	10.3 (0.9)	4 [4]	9.8 (0.8)	11.4 (2.0)	-16 [-14]	-0.9 [-8]
L5	10.6 (0.9)			10.3 (1.0)			-0.3 [-3]
S1				9.4 (-)			

A = centimeters (cm)

B = Female minus Male (cm)

C = Shaded cells represent significant difference between females and males ( $p \leq 0.05$ ).

Table 1.31. Right Psoas Major mean (s.d.) coronal plane moment-arm distance from the center of the vertebral body to the area centroid of the muscle cross-sectional area. Data collected (OSU) are compared with literature values for males and females. Differences between literature values and the current data are described in terms of the magnitude (cm) and as a percent of the literature values [ ]. Magnitude and percent difference in coronal plane moment-arms between male and female subjects are also shown.

**Right Psoas Major – Coronal Plane Moment Arms**

Level	OSU Male mean <sup>A</sup> (s.d.)	McGill et al., (1993) mean <sup>A</sup> (s.d.)	Difference <sup>A</sup> [% Diff.]	OSU Female mean <sup>A</sup> (s.d.)	Chaffin et al., (1990) mean <sup>A</sup> (s.d.)	Difference <sup>A</sup> [% Diff.]	Female vs Male <sup>B,C</sup> [% Diff.]
T8							
T9							
T10							
T11							
T12		3.2 (0.3)					
L1	2.6 (-)	3.2 (0.3)	-6 [-19]	2.3 (0.2)			-0.3 [-12]
L2	3.3 (0.3)	3.9 (0.2)	-6 [-15]	2.7 (0.2)	3.3 (0.4)	-6 [-18]	-0.6 [-18]
L3	3.9 (0.3)	4.4 (0.3)	-5 [-11]	3.3 (0.2)	3.7 (0.4)	-4 [-11]	-0.6 [-15]
L4	4.7 (0.3)	5.0 (0.3)	-3 [-6]	4.0 (0.3)	4.4 (0.4)	-4 [-9]	-0.7 [-15]
L5	5.3 (0.3)	5.4 (0.4)	-1 [-2]	4.7 (0.4)			-0.6 [-11]
S1	5.6 (0.4)			5.0 (0.4)			-0.6 [-11]

A = centimeters (cm)

B = Female minus Male (cm)

C = Shaded cells represent significant difference between females and males ( $p \leq 0.05$ ).

Table 1.32. Left Psoas Major mean (s.d.) coronal plane moment-arm distance from the center of the vertebral body to the area centroid of the muscle cross-sectional area. Data collected (OSU) are compared with literature values for males and females. Differences between literature values and the current data are described in terms of the magnitude (cm) and as a percent of the literature values [ ]. Magnitude and percent difference in coronal plane moment-arms between male and female subjects are also shown.

**Left Psoas Major – Coronal Plane Moment Arms**

Level	OSU Male mean <sup>A</sup> (s.d.)	McGill et al., (1993) mean <sup>A</sup> (s.d.)	Difference <sup>A</sup> [% Diff.]	OSU Female mean <sup>A</sup> (s.d.)	Chaffin et al., (1990) mean <sup>A</sup> (s.d.)	Difference <sup>A</sup> [% Diff.]	Female vs Male <sup>B,C</sup> [% Diff.]
T8							
T9							
T10							
T11							
T12		3.2 (0.2)					
L1	2.8 (0.2)	3.1 (0.3)	-3 [-10]	2.3 (0.1)			-0.5 [-18]
L2	3.3 (0.3)	3.8 (0.3)	-5 [-13]	2.7 (0.1)	3.2 (0.4)	-5 [-16]	-0.6 [-18]
L3	3.9 (0.3)	4.2 (0.3)	-3 [-7]	3.2 (0.2)	3.8 (0.4)	-5 [-13]	-0.7 [-18]
L4	4.4 (0.4)	4.8 (0.4)	-4 [-8]	3.8 (0.3)	4.3 (0.4)	-5 [-12]	-0.6 [-14]
L5	5.0 (0.5)	5.4 (0.5)	-4 [-7]	4.5 (0.3)			-0.5 [-10]
S1	5.4 (0.5)			5.1 (0.3)			-0.3 [-6]

A = centimeters (cm)

B = Female minus Male (cm)

C = Shaded cells represent significant difference between females and males ( $p \leq 0.05$ ).

Table 1.33. Right Quadratus Lumborum mean (s.d.) coronal plane moment-arm distance from the center of the vertebral body to the area centroid of the muscle cross-sectional area. Data collected (OSU) are compared with literature values for males and females. Differences between literature values and the current data are described in terms of the magnitude (cm) and as a percent of the literature values [ ]. Magnitude and percent difference in coronal plane moment-arms between male and female subjects are also shown.

**Right Quadratus Lumborum – Coronal Plane Moment Arms**

Level	OSU Male mean <sup>A</sup> (s.d.)	McGill et al., (1993) mean <sup>A</sup> (s.d.)	Difference <sup>A</sup> [% Diff.]	OSU Female mean <sup>A</sup> (s.d.)	Chaffin et al., (1990) mean <sup>A</sup> (s.d.)	Difference <sup>A</sup> [% Diff.]	Female vs Male <sup>B,C</sup> [% Diff.]
T8							
T9							
T10							
T11							
T12		4.6 (1.1)					
L1	3.8 (-)	4.6 (0.6)	-8 [-17]	3.8 (0.6)			0.0 [0]
L2	5.0 (0.6)	6.3 (0.5)	-13 [-21]	4.1 (0.4)	5.6 (0.8)	-15 [-27]	-0.9 [-18]
L3	6.4 (0.6)	7.5 (0.6)	-11 [-15]	5.5 (0.7)	6.5 (0.7)	-10 [-15]	-0.9 [-14]
L4	7.5 (0.5)	8.1 (0.5)	-6 [-7]	6.8 (0.5)	7.4 (0.8)	-6 [-8]	-0.7 [-9]
L5				7.4 (-)			
S1							

A = centimeters (cm)

B = Female minus Male (cm)

C = Shaded cells represent significant difference between females and males ( $p \leq 0.05$ ).

Table 1.34. Left Quadratus Lumborum mean (s.d.) coronal plane moment-arm distance from the center of the vertebral body to the area centroid of the muscle cross-sectional area. Data collected (OSU) are compared with literature values for males and females. Differences between literature values and the current data are described in terms of the magnitude (cm) and as a percent of the literature values [ ]. Magnitude and percent difference in coronal plane moment-arms between male and female subjects are also shown.

**Left Quadratus Lumborum – Coronal Plane Moment Arms**

Level	OSU Male mean <sup>A</sup> (s.d.)	McGill et al., (1993) mean <sup>A</sup> (s.d.)	Difference <sup>A</sup> [% Diff.]	OSU Female mean <sup>A</sup> (s.d.)	Chaffin et al., (1990) mean <sup>A</sup> (s.d.)	Difference <sup>A</sup> [% Diff.]	Female vs Male <sup>B,C</sup> [% Diff.]
T8							
T9							
T10							
T11							
T12		4.7 (0.5)					
L1	4.4 (0.4)	5.0 (0.6)	-6 [-12]	3.7 (0.3)			-0.7 [-16]
L2	4.7 (1.0)	6.4 (0.5)	-17 [-27]	4.2 (0.3)	5.5 (0.7)	-13 [-24]	-0.5 [-11]
L3	6.5 (0.7)	7.3 (0.4)	-8 [-11]	5.7 (0.7)	6.5 (0.7)	-8 [-12]	-0.8 [-12]
L4	7.3 (0.6)	7.8 (1.2)	-5 [-6]	6.8 (0.7)	7.5 (1.0)	-7 [-9]	-0.5 [-7]
L5				7.9 (-)			
S1							

A = centimeters (cm)

B = Female minus Male (cm)

C = Shaded cells represent significant difference between females and males ( $p \leq 0.05$ ).

Table 1.35. Right Latissimus Dorsi mean (s.d.) sagittal plane moment-arm distance from the center of the vertebral body to the area centroid of the muscle cross-sectional area. Negative values represent posterior and positive represent anterior to L5 centroid. Data collected (OSU) are compared with literature values for males and females. Differences between literature values and the current data are described in terms of the magnitude (cm) and as a percent of the literature values [ ]. Magnitude and percent difference in sagittal plane moment-arms between male and female subjects are also shown.

**Right Latissimus Dorsi – Sagittal Plane Moment Arms**

Level	OSU Male mean <sup>A</sup> (s.d.)	McGill et al., (1993) mean <sup>A</sup> (s.d.)	Difference <sup>A</sup> [% Diff.]	OSU Female mean <sup>A</sup> (s.d.)	Chaffin et al., (1990) mean <sup>A</sup> (s.d.)	Difference <sup>A</sup> [% Diff.]	Female vs Male <sup>B,C</sup> [% Diff.]
T8	-1.8 (0.9)	-1.8 (0.9)	0 [0]	-1.6 (1.2)			-0.2 [-11]
T9	-2.2 (1.0)	-2.2 (0.7)	0 [0]	-1.9 (1.1)			-0.3 [-14]
T10	-2.4 (0.9)	-2.4 (0.7)	0 [0]	-2.3 (0.9)			-0.1 [-4]
T11	-2.7 (0.8)	-3.2 (0.7)	-5 [-16]	-2.6 (0.8)			-0.1 [-4]
T12	-2.9 (0.7)	-3.9 (0.8)	-10 [-26]	-2.9 (0.8)			0.0 [0]
L1	-3.8 (0.9)	-4.7 (1.0)	-9 [-19]	-3.2 (1.0)			-0.6 [-16]
L2	-4.1 (0.7)	-4.7 (1.2)	-6 [-13]	-3.4 (1.1)	-3.6 (0.9)	-2 [-6]	-0.7 [-17]
L3	-4.2 (0.8)	-4.5 (1.6)	-3 [-7]	-3.1 (1.2)	-3.0 (1.0)	1 [3]	-1.1 [-26]
L4	-4.0 (1.3)				-1.7 (1.1)		
L5							
S1							

A = centimeters (cm)

B = Female minus Male (cm)

C = Shaded cells represent significant difference between females and males ( $p \leq 0.05$ ).

Table 1.36. Left Latissimus Dorsi mean (s.d.) sagittal plane moment-arm distance from the center of the vertebral body to the area centroid of the muscle cross-sectional area. Negative values represent posterior and positive represent anterior to L5 centroid. Data collected (OSU) are compared with literature values for males and females. Differences between literature values and the current data are described in terms of the magnitude (cm) and as a percent of the literature values [ ]. Magnitude and percent difference in sagittal plane moment-arms between male and female subjects are also shown.

**Left Latissimus Dorsi – Sagittal Plane Moment Arms**

Level	OSU Male mean <sup>A</sup> (s.d.)	McGill et al., (1993) mean <sup>A</sup> (s.d.)	Difference <sup>A</sup> [% Diff.]	OSU Female mean <sup>A</sup> (s.d.)	Chaffin et al., (1990) mean <sup>A</sup> (s.d.)	Difference <sup>A</sup> [% Diff.]	Female vs Male <sup>B,C</sup> [% Diff.]
T8	-0.7 (1.1)	-1.7 (0.7)	-10 [-59]	-0.7 (1.0)			0.0 [0]
T9	-.9 (1.1)	-1.9 (0.7)	-10 [-53]	-1.1 (0.9)			0.2 [22]
T10	-1.3 (1.1)	-2.3 (0.7)	-10 [-43]	-1.6 (0.9)			0.3 [23]
T11	-1.6 (1.0)	-2.8 (0.9)	-12 [-43]	-2.0 (0.8)			0.4 [25]
T12	-2.2 (1.0)	-3.7 (0.8)	-15 [-41]	-2.6 (0.8)			0.4 [18]
L1	-3.0 (1.2)	-4.6 (0.7)	-16 [-35]	-3.1 (1.0)			0.1 [3]
L2	-4.0 (1.1)	-4.6 (1.0)	-6 [-13]	-3.9 (1.1)	-3.4 (1.1)	5 [15]	-0.1 [-3]
L3	-3.9 (1.1)	-4.3 (1.7)	-4 [-9]	-4.0 (1.2)	-3.0 (1.0)	10 [33]	0.1 [3]
L4	-3.7 (1.1)				-1.4 (1.3)		
L5							
S1							

A = centimeters (cm)

B = Female minus Male (cm)

C = Shaded cells represent significant difference between females and males ( $p \leq 0.05$ ).

Table 1.37. Right Erector Spinae mean (s.d.) sagittal plane moment-arm distance from the center of the vertebral body to the area centroid of the muscle cross-sectional area. Negative values represent posterior and positive represent anterior to L5 centroid. Data collected (OSU) are compared with literature values for males and females. Differences between literature values and the current data are described in terms of the magnitude (cm) and as a percent of the literature values [ ]. Magnitude and percent difference in sagittal plane moment-arms between male and female subjects are also shown.

**Right Erector Spinae – Sagittal Plane Moment Arms**

Level	OSU Male mean <sup>A</sup> (s.d.)	McGill et al., (1993) mean <sup>A</sup> (s.d.)	Difference <sup>A</sup> [% Diff.]	OSU Female mean <sup>A</sup> (s.d.)	Chaffin et al., (1990) mean <sup>A</sup> (s.d.)	Difference <sup>A</sup> [% Diff.]	Female vs Male <sup>B,C</sup> [% Diff.]
T8	-5.2 (0.4)	-5.2 (0.3)	0 [0]	-4.4 (0.3)			-0.8 [-15]
T9	-5.3 (0.4)	-5.2 (0.4)	1 [2]	-4.5 (0.4)			-0.8 [-15]
T10	-5.2 (0.4)	-5.4 (0.4)	-2 [-4]	-4.4 (0.4)			-0.8 [-15]
T11	-5.1 (0.4)	-5.4 (0.4)	-3 [-6]	-4.4 (0.4)			-0.7 [-14]
T12	-5.0 (0.4)	-5.6 (0.5)	-6 [-11]	-4.4 (0.4)			-0.6 [-12]
L1	-5.2 (0.5)	-5.9 (0.5)	-7 [-12]	-4.7 (0.5)			-0.5 [-10]
L2	-5.4 (0.7)	-6.1 (0.5)	-7 [-11]	-4.8 (0.4)	-5.4 (0.4)	-6 [-11]	-0.6 [-11]
L3	-5.7 (0.7)	-6.1 (0.5)	-4 [-7]	-5.0 (0.5)	-5.2 (0.4)	-2 [-4]	-0.7 [-12]
L4	-5.6 (0.6)	-6.1 (0.5)	-5 [-8]	-4.9 (0.4)	-5.2 (0.3)	-3 [-6]	-0.7 [-13]
L5	-6.1 (0.7)	-6.4 (0.6)	-3 [-5]	-5.4 (0.5)			-0.7 [-11]
S1	-6.2 (0.7)			-5.4 (0.5)			-0.8 [-13]

A = centimeters (cm)

B = Female minus Male (cm)

C = Shaded cells represent significant difference between females and males ( $p \leq 0.05$ ).

Table 1.38. Left Erector Spinae mean (s.d.) sagittal plane moment-arm distance from the center of the vertebral body to the area centroid of the muscle cross-sectional area. Negative values represent posterior and positive represent anterior to L5 centroid. Data collected (OSU) are compared with literature values for males and females. Differences between literature values and the current data are described in terms of the magnitude (cm) and as a percent of the literature values [ ]. Magnitude and percent difference in sagittal plane moment-arms between male and female subjects are also shown.

**Left Erector Spinae – Sagittal Plane Moment Arms**

Level	OSU Male mean <sup>A</sup> (s.d.)	McGill et al., (1993) mean <sup>A</sup> (s.d.)	Difference <sup>A</sup> [% Diff.]	OSU Female mean <sup>A</sup> (s.d.)	Chaffin et al., (1990) mean <sup>A</sup> (s.d.)	Difference <sup>A</sup> [% Diff.]	Female vs Male <sup>B,C</sup> [% Diff.]
T8	-4.9 (0.5)	-5.1 (0.3)	-2 [-4]	-4.2 (0.3)			-0.7 [-14]
T9	-4.9 (0.6)	-5.1 (0.4)	-2 [-4]	-4.3 (0.3)			-0.6 [-12]
T10	-4.8 (0.5)	-5.2 (0.4)	-4 [-8]	-4.2 (0.3)			-0.6 [-13]
T11	-4.7 (0.5)	-5.2 (0.4)	-5 [-10]	-4.2 (0.4)			-0.5 [-11]
T12	-4.8 (0.5)	-5.7 (0.5)	-9 [-16]	-4.3 (0.4)			-0.5 [-10]
L1	-5.0 (0.6)	-6.0 (0.4)	-10 [-17]	-4.7 (0.5)			-0.3 [-6]
L2	-5.4 (0.6)	-6.2 (0.5)	-8 [-13]	-5.1 (0.6)	-5.4 (0.4)	-3 [-6]	-0.3 [-6]
L3	-5.6 (0.6)	-6.1 (0.5)	-5 [-8]	-5.3 (0.6)	-5.3 (0.2)	0 [0]	-0.3 [-5]
L4	-5.7 (0.5)	-6.1 (0.5)	-4 [-7]	-5.3 (0.5)	-5.4 (0.4)	-1 [-2]	-0.4 [-7]
L5	-6.1 (0.7)	-6.3 (0.5)	-2 [-3]	-5.7 (0.6)			-0.4 [-7]
S1	-6.3 (0.8)			-5.6 (0.5)			-0.7 [-11]

A = centimeters (cm)

B = Female minus Male (cm)

C = Shaded cells represent significant difference between females and males ( $p \leq 0.05$ ).

Table 1.39. Right Rectus Abdominis mean (s.d.) sagittal plane moment-arm distance from the center of the vertebral body to the area centroid of the muscle cross-sectional area. Negative values represent posterior and positive represent anterior to L5 centroid. Data collected (OSU) are compared with literature values for males and females. Differences between literature values and the current data are described in terms of the magnitude (cm) and as a percent of the literature values [ ]. Magnitude and percent difference in sagittal plane moment-arms between male and female subjects are also shown.

**Right Rectus Abdominis – Sagittal Plane Moment Arms**

Level	OSU Male mean <sup>A</sup> (s.d.)	McGill et al., (1993) mean <sup>A</sup> (s.d.)	Difference <sup>A</sup> [% Diff.]	OSU Female mean <sup>A</sup> (s.d.)	Chaffin et al., (1990) mean <sup>A</sup> (s.d.)	Difference <sup>A</sup> [% Diff.]	Female vs. Male <sup>B,C</sup> [% Diff.]
T8							
T9							
T10							
T11							
T12	13.5 (1.7)			10.4 (0.9)			-3.1 [-23]
L1	12.4 (1.2)	10.9 (0.8)	15 [14]	9.6 (1.0)			-2.8 [-23]
L2	10.7 (1.2)	9.0 (1.4)	17 [19]	8.5 (0.9)	7.0 (1.5)	15 [21]	-2.4 [-22]
L3	8.9 (1.3)	7.9 (1.3)	10 [13]	7.0 (0.9)	7.0 (1.9)	0 [0]	-1.9 [-21]
L4	7.7 (1.5)	7.3 (1.4)	4 [5]	6.1 (0.9)	6.9 (2.0)	-8 [-12]	-1.6 [-21]
L5	7.6 (1.4)	8.1 (1.6)	-5 [-6]	6.5 (1.0)			-1.1 [-14]
S1	8.4 (1.2)			7.5 (1.3)			-0.9 [-11]

A = centimeters (cm)

B = Female minus Male (cm)

C = Shaded cells represent significant difference between females and males ( $p \leq 0.05$ ).

Table 1.40. Left Rectus Abdominis mean (s.d.) sagittal plane moment-arm distance from the center of the vertebral body to the area centroid of the muscle cross-sectional area. Negative values represent posterior and positive represent anterior to L5 centroid. Data collected (OSU) are compared with literature values for males and females. Differences between literature values and the current data are described in terms of the magnitude (cm) and as a percent of the literature values [ ]. Magnitude and percent difference in sagittal plane moment-arms between male and female subjects are also shown.

**Left Rectus Abdominis – Sagittal Plane Moment Arms**

Level	OSU Male mean <sup>A</sup> (s.d.)	McGill et al., (1993) mean <sup>A</sup> (s.d.)	Difference <sup>A</sup> [% Diff.]	OSU Female mean <sup>A</sup> (s.d.)	Chaffin et al., (1990) mean <sup>A</sup> (s.d.)	Difference <sup>A</sup> [% Diff.]	Female vs. Male <sup>B,C</sup> [% Diff]
T8							
T9							
T10							
T11							
T12	13.7 (1.7)			10.5 (1.0)			-3.2 [-23]
L1	12.7 (1.1)	11.2 (0.6)	15 [13]	9.7 (1.1)			-3.0 [-24]
L2	10.8 (1.3)	9.2 (1.4)	16 [17]	8.5 (1.1)	7.2 (1.6)	13 [18]	-2.3 [-21]
L3	9.2 (1.3)	8.0 (1.4)	12 [15]	6.9 (1.1)	7.2 (1.9)	-3 [-4]	-2.3 [-25]
L4	7.8 (1.4)	7.3 (1.4)	5 [7]	6.0 (0.9)	7.0 (2.0)	-10 [-14]	-1.8 [-23]
L5	7.6 (1.5)	8.0 (1.5)	-4 [-5]	6.1 (1.0)			-15 [-20]
S1	8.2 (1.2)			7.3 (1.2)			-0.9 [-11]

A = centimeters (cm)

B = Female minus Male (cm)

C = Shaded cells represent significant difference between females and males ( $p \leq 0.05$ ).

Table 1.41. Right External Obliques mean (s.d.) sagittal plane moment-arm distance from the center of the vertebral body to the area centroid of the muscle cross-sectional area. Negative values represent posterior and positive represent anterior to L5 centroid. Data collected (OSU) are compared with literature values for males and females. Differences between literature values and the current data are described in terms of the magnitude (cm) and as a percent of the literature values [ ]. Magnitude and percent difference in sagittal plane moment-arms between male and female subjects are also shown.

**Right External Obliques – Sagittal Plane Moment Arms**

Level	OSU Male mean <sup>A</sup> (s.d.)	McGill et al., (1993) mean <sup>A</sup> (s.d.)	Difference <sup>A</sup> [% Diff.]	OSU Female mean <sup>A</sup> (s.d.)	Chaffin et al., (1990) mean <sup>A</sup> (s.d.)	Difference <sup>A</sup> [% Diff.]	Female vs Male <sup>B,C</sup> [% Diff.]
T8							
T9							
T10							
T11							
T12	8.5 (1.2)			6.8 (0.7)			-1.7 [-20]
L1	6.7 (1.0)			5.6 (1.2)			-1.1 [-16]
L2	4.6 (0.6)	2.8 (1.2)	18 [64]	4.0 (1.1)	2.2 (1.3)	18 [82]	-0.6 [-13]
L3	2.2 (1.0)	2.0 (1.4)	2 [10]	2.4 (1.2)	2.3 (1.2)	1 [4]	0.2 [9]
L4	2.1 (0.8)	3.5 (1.0)	-14 [-40]	2.2 (1.2)	3.0 (1.3)	-8 [-27]	0.1 [5]
L5	3.9 (1.2)			3.2 (2.0)			-0.7 [-18]
S1				6.6 (-)			

A = centimeters (cm)

B = Female minus Male (cm)

C = Shaded cells represent significant difference between females and males ( $p \leq 0.05$ ).

Table 1.42. Left External Obliques mean (s.d.) sagittal plane moment-arm distance from the center of the vertebral body to the area centroid of the muscle cross-sectional area. Negative values represent posterior and positive represent anterior to L5 centroid. Data collected (OSU) are compared with literature values for males and females. Differences between literature values and the current data are described in terms of the magnitude (cm) and as a percent of the literature values [ ]. Magnitude and percent difference in sagittal plane moment-arms between male and female subjects are also shown.

**Left External Obliques – Sagittal Plane Moment Arms**

Level	OSU Male mean <sup>A</sup> (s.d.)	McGill et al., (1993) mean <sup>A</sup> (s.d.)	Difference <sup>A</sup> [% Diff.]	OSU Female mean <sup>A</sup> (s.d.)	Chaffin et al., (1990) mean <sup>A</sup> (s.d.)	Difference <sup>A</sup> [% Diff.]	Female vs Male <sup>B,C</sup> [% Diff.]
T8							
T9							
T10							
T11							
T12	9.2 (1.4)			6.6 (1.2)			-2.6 [-28]
L1	7.4 (1.3)			5.7 (1.3)			-1.7 [-23]
L2	5.0 (1.4)	2.8 (1.1)	22 [79]	3.7 (1.2)	2.0 (1.1)	17 [85]	-1.3 [-26]
L3	2.7 (1.4)	1.9 (1.1)	8 [42]	1.5 (1.3)	2.0 (1.1)	-5 [-25]	-1.2 [-44]
L4	2.0 (1.1)	3.2 (1.8)	-12 [-38]	1.2 (1.3)	3.0 (1.2)	-18 [-60]	-0.8 [-40]
L5	3.5 (1.2)			2.5 (0.9)			-1.0 [-29]
S1				4.6 (-)			

A = centimeters (cm)

B = Female minus Male (cm)

C = Shaded cells represent significant difference between females and males ( $p \leq 0.05$ ).

Table 1.43. Right Internal Obliques mean (s.d.) sagittal plane moment-arm distance from the center of the vertebral body to the area centroid of the muscle cross-sectional area. Negative values represent posterior and positive represent anterior to L5 centroid. Data collected (OSU) are compared with literature values for males and females. Differences between literature values and the current data are described in terms of the magnitude (cm) and as a percent of the literature values [ ]. Magnitude and percent difference in sagittal plane moment-arms between male and female subjects are also shown.

**Right Internal Obliques – Sagittal Plane Moment Arms**

Level	OSU Male mean <sup>A</sup> (s.d.)	McGill et al., (1993) mean <sup>A</sup> (s.d.)	Difference <sup>A</sup> [% Diff.]	OSU Female mean <sup>A</sup> (s.d.)	Chaffin et al., (1990) mean <sup>A</sup> (s.d.)	Difference <sup>A</sup> [% Diff.]	Female vs Male <sup>B,C</sup> [% Diff.]
T8							
T9							
T10							
T11							
T12							
L1				9.3 (-)			
L2	7.2 (1.7)	3.6 (1.7)	36 [100]	5.5 (1.5)	2.4 (1.4)	31 [129]	-1.7 [-24]
L3	3.4 (1.3)	2.5 (0.9)	9 [36]	3.3 (1.2)	2.1 (1.1)	12 [57]	-0.1 [-3]
L4	2.5 (1.1)	4.1 (1.2)	-16 [-39]	2.1 (1.1)	3.0 (1.5)	-9 [-30]	-0.4 [-16]
L5	4.5 (1.0)			3.6 (1.5)			-0.9 [-20]
S1				6.3 (-)			

A = centimeters (cm)

B = Female minus Male (cm)

C = Shaded cells represent significant difference between females and males ( $p \leq 0.05$ ).

Table 1.44. Left Internal Obliques mean (s.d.) sagittal plane moment-arm distance from the center of the vertebral body to the area centroid of the muscle cross-sectional area. Negative values represent posterior and positive represent anterior to L5 centroid. Data collected (OSU) are compared with literature values for males and females. Differences between literature values and the current data are described in terms of the magnitude (cm) and as a percent of the literature values [ ]. Magnitude and percent difference in sagittal plane moment-arms between male and female subjects are also shown.

**Left Internal Obliques – Coronal Plane Moment Arms**

Level	OSU Male mean <sup>A</sup> (s.d.)	McGill et al., (1993) mean <sup>A</sup> (s.d.)	Difference <sup>A</sup> [% Diff.]	OSU Female mean <sup>A</sup> (s.d.)	Chaffin et al., (1990) mean <sup>A</sup> (s.d.)	Difference <sup>A</sup> [% Diff.]	Female vs Male <sup>B,C</sup> [% Diff.]
T8							
T9							
T10							
T11							
T12							
L1				7.8 (-)			
L2	7.7 (1.6)	4.0 (1.6)	37 [93]	5.0 (1.9)	2.5 (1.6)	25 [100]	-2.7 [-35]
L3	4.3 (1.5)	2.6 (1.2)	17 [65]	3.0 (1.5)	2.0 (1.0)	10 [50]	-1.3 [-30]
L4	2.7 (1.0)	4.1 (1.7)	-14 [-34]	1.6 (1.0)	2.8 (1.3)	-12 [-43]	-1.1 [-41]
L5	4.5 (1.3)			3.0 (1.5)			-1.5 [-33]
S1				4.4 (-)			

A = centimeters (cm)

B = Female minus Male (cm)

C = Shaded cells represent significant difference between females and males (p≤0.05).

Table 1.45. Right Psoas Major mean (s.d.) sagittal plane moment-arm distance from the center of the vertebral body to the area centroid of the muscle cross-sectional area. Negative values represent posterior and positive represent anterior to L5 centroid. Data collected (OSU) are compared with literature values for males and females. Differences between literature values and the current data are described in terms of the magnitude (cm) and as a percent of the literature values [ ]. Magnitude and percent difference in sagittal plane moment-arms between male and female subjects are also shown.

**Right Psoas Major – Sagittal Plane Moment Arms**

Level	OSU Male mean <sup>A</sup> (s.d.)	McGill et al., (1993) mean <sup>A</sup> (s.d.)	Difference <sup>A</sup> [% Diff.]	OSU Female mean <sup>A</sup> (s.d.)	Chaffin et al., (1990) mean <sup>A</sup> (s.d.)	Difference <sup>A</sup> [% Diff.]	Female vs Male <sup>B,C</sup> [% Diff.]
T8							
T9							
T10							
T11							
T12		-1.4 (0.2)					
L1	-0.5 (-)	-1.1 (0.6)	-6 [-55]	-0.7 (0.9)			0.2 [40]
L2	-0.7 (0.5)	-0.9 (0.5)	-2 [-22]	-0.9 (0.3)	-1.1 (0.3)	-2 [-18]	0.2 [29]
L3	-0.4 (0.4)	-0.7 (0.5)	-3 [-43]	-0.8 (0.4)	-0.8 (.4)	0 [0]	0.4 [100]
L4	-0.1 (0.3)	0.1 (0.5)	-2 [-200]	-0.4 (0.5)	-2 (0.5)	2 [100]	0.3 [300]
L5	0.8 (0.5)	1.8 (0.9)	-10 [-56]	0.7 (0.7)			-0.1 [-13]
S1	2.4 (0.7)			2.3 (1.0)			-0.1 [-4]

A = centimeters (cm)

B = Female minus Male (cm)

C = Shaded cells represent significant difference between females and males ( $p \leq 0.05$ ).

Table 1.46. Left Psoas Major mean (s.d.) sagittal plane moment-arm distance from the center of the vertebral body to the area centroid of the muscle cross-sectional area. Negative values represent posterior and positive represent anterior to L5 centroid. Data collected (OSU) are compared with literature values for males and females. Differences between literature values and the current data are described in terms of the magnitude (cm) and as a percent of the literature values [ ]. Magnitude and percent difference in sagittal plane moment-arms between male and female subjects are also shown.

**Left Psoas Major – Sagittal Plane Moment Arms**

Level	OSU Male mean <sup>A</sup> (s.d.)	McGill et al., (1993) mean <sup>A</sup> (s.d.)	Difference <sup>A</sup> [% Diff.]	OSU Female mean <sup>A</sup> (s.d.)	Chaffin et al., (1990) mean <sup>A</sup> (s.d.)	Difference <sup>A</sup> [% Diff.]	Female vs Male <sup>B,C</sup> [% Diff.]
T8							
T9							
T10							
T11							
T12		-1.1 (0.1)					
L1	-0.9 (0.5)	-1.1 (0.4)	-2 [-18]	-0.2 (0.7)			-0.7 [-22]
L2	-0.6 (0.5)	-0.8 (0.2)	-2 [-25]	-1.0 (0.4)	-1.1 (0.4)	-1 [-9]	0.4 [67]
L3	-0.3 (0.4)	-0.6 (0.4)	-3 [-50]	-1.0 (0.5)	-0.8 (0.5)	2 [25]	0.7 [233]
L4	-0.02 (0.5)	0.2 (0.4)	-2.2 [-110]	-0.7 (0.5)	-0.2 (0.4)	5 [250]	.72 [3600]
L5	0.8 (0.6)	1.9 (0.8)	-11 [-58]	0.2 (0.6)			-0.6 [-75]
S1	2.4 (0.7)			2.0 (0.8)			-0.4 [-17]

A = centimeters (cm)

B = Female minus Male (cm)

C = Shaded cells represent significant difference between females and males ( $p \leq 0.05$ ).

Table 1.47. Right Quadratus Lumborum mean (s.d.) sagittal plane moment-arm distance from the center of the vertebral body to the area centroid of the muscle cross-sectional area. Negative values represent posterior and positive represent anterior to L5 centroid. Data collected (OSU) are compared with literature values for males and females. Differences between literature values and the current data are described in terms of the magnitude (cm) and as a percent of the literature values [ ]. Magnitude and percent difference in sagittal plane moment-arms between male and female subjects are also shown.

**Right Quadratus Lumborum – Sagittal Plane Moment Arms**

Level	OSU Male mean <sup>A</sup> (s.d.)	McGill et al., (1993) mean <sup>A</sup> (s.d.)	Difference <sup>A</sup> [% Diff.]	OSU Female mean <sup>A</sup> (s.d.)	Chaffin et al., (1990) mean <sup>A</sup> (s.d.)	Difference <sup>A</sup> [% Diff.]	Female vs Male <sup>B,C</sup> [% Diff.]
T8							
T9							
T10							
T11							
T12		-3.1 (0.6)					
L1	-2.7 (-)	-3.5 (0.4)	-8 [-23]	-2.9 (0.4)			0.2 [7]
L2	-3.1 (0.6)	-3.7 (0.6)	-6 [-16]	-3.0 (0.4)	-3.6 (0.4)	-6 [-17]	-0.1 [-3]
L3	-3.1 (0.7)	-3.7 (0.6)	-6 [-16]	-3.1 (0.7)	-3.2 (0.7)	-1 [-3]	0.0 [0]
L4	-3.0 (0.6)	-3.6 (0.9)	-6 [-17]	-2.6 (0.8)	-2.8 (0.7)	-2 [-7]	-0.4 [-13]
L5				-1.8 (-)			
S1							

A = centimeters (cm)

B = Female minus Male (cm)

C = Shaded cells represent significant difference between females and males ( $p \leq 0.05$ ).

Table 1.48. Left Quadratus Lumborum mean (s.d.) sagittal plane moment-arm distance from the center of the vertebral body to the area centroid of the muscle cross-sectional area. Negative values represent posterior and positive represent anterior to L5 centroid. Data collected (OSU) are compared with literature values for males and females. Differences between literature values and the current data are described in terms of the magnitude (cm) and as a percent of the literature values [ ]. Magnitude and percent difference in sagittal plane moment-arms between male and female subjects are also shown.

**Left Quadratus Lumborum – Sagittal Plane Moment Arms**

Level	OSU Male mean <sup>A</sup> (s.d.)	McGill et al., (1993) mean <sup>A</sup> (s.d.)	Difference <sup>A</sup> [% Diff.]	OSU Female mean <sup>A</sup> (s.d.)	Chaffin et al., (1990) mean <sup>A</sup> (s.d.)	Difference <sup>A</sup> [% Diff.]	Female vs Male <sup>B,C</sup> [% Diff.]
T8							
T9							
T10							
T11							
T12		-3.1 (0.6)					
L1	-3.0 (0.4)	-3.5 (0.4)	-5 [-14]	-2.6 (0.3)			-0.4 [-13]
L2	-3.1 (0.6)	-3.7 (0.6)	-6 [-16]	-3.2 (0.6)	-3.6 (0.4)	-4 [-11]	0.1 [3]
L3	-3.1 (0.7)	-3.7 (0.6)	-6 [-16]	-3.6 (1.0)	-3.2 (0.7)	4 [13]	0.5 [16]
L4	-3.1 (0.7)	-3.6 (0.9)	-5 [-14]	-3.2 (1.0)	-2.8 (0.7)	4 [14]	0.1 [3]
L5				-2.9 (-)			
S1							

A = centimeters (cm)

B = Female minus Male (cm)

C = Shaded cells represent significant difference between females and males ( $p \leq 0.05$ ).

Table 1.49. Summary of significant R<sup>2</sup> values for regression equations predicting the *female* PCSA based on external anthropometric measures. Each muscle is the average of the right and left side PCSA.

Measure Location	Average of Right and Left PCSA									
	Lattissimus Dorsi	Erector Spinae	Rectus Abdominis	External Obliques	Internal Obliques	Psoas Major	Quad. Lumborum			
TDTWXP	0.379	0.487	0.376	0.281	0.232		0.430			
TDTWXXPH	0.351	0.411	0.423	0.272	0.261		0.400			
Weight		0.662					0.294			
HTWT		0.536					0.207			
HTDWT		0.605					0.286			
WTDHT		0.678					0.349			
BMI		0.552	0.251				0.331			

Table 1.50. Summary of significant R<sup>2</sup> values for regression equations predicting the *female* PCSA based on external anthropometric measures.

Measure Location	Right or Left PCSA															
	RLAT	LLAT	RES	LES	RABD	LABD	REOB	LEOB	RIOB	LIOB	RPSS	LPSS	RQLM	LQLM		
TDTWXP	0.397	0.347	0.509	0.448	0.383	0.358	0.286	0.221	0.241				0.316	0.387		
TDTWXXPH	0.365	0.324	0.439	0.368	0.420	0.412	0.265	0.225	0.290				0.314	0.344		
TDTWXPW		0.184			0.203	0.191										
Weight			0.688	0.612			0.210						0.341			
HTWT			0.546	0.507									0.225			
HTDWT			0.648	0.539			0.243		0.211				0.376			
WTDHT	0.191		0.720	0.610			0.252		0.201				0.429	0.204		
BMI			0.600	0.483	0.237	0.255	0.235		0.267				0.430			
TCIRW			0.434	0.360							0.226					
TCIRH															0.347	

Table 1.51. Summary of significant R<sup>2</sup> values for regression equations predicting the *male* PCSA based on external anthropometric measures. Each muscle is the average of the right and left side PCSA.

Measure Location	Average of Right and Left PCSA							
	Lattissimus Dorsi	Erector Spinae	Rectus Abdominis	External Obliques	Internal Obliques	Psoas Major	Quad. Lumborum	
TDTWXP	0.449				0.504	0.448		
TDTWXP				0.435				
Weight	0.485	0.535	0.609		0.617			
HTWT	0.489	0.511	0.592		0.608			
HTDWT	0.414	0.588	0.621		0.569			
WTDHT	0.451	0.551	0.608		0.611			
BMI		0.472	0.484		0.492			

Table 1.52. Summary of significant R<sup>2</sup> values for regression equations predicting the *male* PCSA based on external anthropometric measures.

Measure Location	Right or Left PCSA													
	RLAT	LLAT	RES	LES	RABD	LABD	REOB	LEOB	RIOB	LIOB	RPSS	LPSS	RQLM	LQLM
TDTWXP		0.480						0.466	0.425	0.461	0.459	0.408		0.411
TDTWIC														0.607
Height				0.410		0.446		0.446						0.428
Weight	0.516	0.413	0.471	0.582	0.577	0.628			0.505	0.579				0.421
HTWT	0.508	0.425	0.444	0.562	0.560	0.612			0.503	0.564				0.439
HTDWT	0.458		0.533	0.624	0.595	0.634			0.469	0.530				0.401
WTDHT	0.502		0.499	0.587	0.579	0.624			0.489	0.584				
BMI			0.451	0.478	0.467	0.491				0.491				

Table 1.53 Regression equations predicting the physiological cross-sectional area (cm<sup>2</sup>) of the Latissimus Dorsi for females and males from various anthropometric measures. Significant regression equations are indicated by shaded rows (p≤0.05).

Muscle	p-value male vs female regression equation	Females			Males		
		Regression Equation	R <sup>2</sup>	p-value	Regression Equation	R <sup>2</sup>	p-value
Average of Right and Left Latissimus Dorsi	0.4402	<b>-7.647 + 0.041TDTWXP</b>	<b>0.379</b>	<b>0.0039</b>	<b>-0.174 + 0.028TDTWXP</b>	<b>0.449</b>	<b>0.0339</b>
	0.2734	1.587 + 0.115HTWT	0.084	0.2152	<b>5.565 + 0.106HTWT</b>	<b>0.489</b>	<b>0.0245</b>
	0.3265	-2.79 + 0.267Weight	0.129	0.1201	<b>1.588 + 0.238Weight</b>	<b>0.485</b>	<b>0.0254</b>
	0.6084	<b>-5.42 + 5.98TDTWXPH</b>	<b>0.351</b>	<b>0.0059</b>	<b>-1.14 + 5.15TDTWXPH</b>	<b>0.310</b>	<b>0.0949</b>
	0.0900	27.8 - 5.24HTDWT	0.125	0.1267	<b>45.1 - 10.93HTDWT</b>	<b>0.414</b>	<b>0.0449</b>
0.3033	-5.01 + 55.48WTDHT	0.160	0.0808	<b>-4.12 + 54.68WTDHT</b>	<b>0.451</b>	<b>0.0334</b>	
R. Latissimus Dorsi	0.2509	<b>-8.24 + 0.043TDTWXP</b>	<b>0.397</b>	<b>0.0029</b>	<b>4.3 + 0.023TDTWXP</b>	<b>0.363</b>	<b>0.0651</b>
	0.1731	0.404 + 0.134HTWT	0.106	0.1613	<b>7.43 + 0.101HTWT</b>	<b>0.508</b>	<b>0.0206</b>
	0.2372	-4.2 + 0.31Weight	0.158	0.0830	<b>3.44 + 0.229Weight</b>	<b>0.516</b>	<b>0.0194</b>
	0.3464	<b>-5.82 + 6.32TDTWXPH</b>	<b>0.365</b>	<b>0.0048</b>	<b>4.19 + 4.16TDTWXPH</b>	<b>0.232</b>	<b>0.1590</b>
	0.0905	30.66 - 6.01HTDWT	0.153	0.0884	<b>45.82 - 10.74HTDWT</b>	<b>0.458</b>	<b>0.0316</b>
0.2604	-6.71 + 57.12WTDHT	0.191	0.0544	<b>-2.59 + 53.84WTDHT</b>	<b>0.502</b>	<b>0.0219</b>	
L. Latissimus Dorsi	0.5708	<b>-7.05 + 0.038TDTWXP</b>	<b>0.347</b>	<b>0.0062</b>	<b>-4.65 + 0.032TDTWXP</b>	<b>0.480</b>	<b>0.0265</b>
	0.3391	2.769 + 0.0965HTWT	0.061	0.2942	<b>3.7 + 0.111HTWT</b>	<b>0.425</b>	<b>0.0410</b>
	0.4199	-1.16 + 0.227Weight	0.097	0.1803	<b>-0.265 + 0.247Weight</b>	<b>0.413</b>	<b>0.0450</b>
	0.8092	<b>-5.02 + 5.64TDTWXPH</b>	<b>0.324</b>	<b>0.0088</b>	<b>-6.46 + 6.13TDTWXPH</b>	<b>0.349</b>	<b>0.0723</b>

Table 1.54. Regression equations predicting the physiological cross-sectional area (cm<sup>2</sup>) of the Erector Spinae for females and males from various anthropometric measures. Significant regression equations are indicated by shaded rows (p≤0.05).

Muscle	p-value male vs female regression equation	Females			Males		
		Regression Equation	R <sup>2</sup>	p-value	Regression Equation	R <sup>2</sup>	p-value
Average of Right and Left Erector Spinae	0.0799	-0.995 + 0.034TDTWXP	0.487	0.0006	9.6 + 0.022TDTWXP	0.347	0.0730
	0.0016	-6.3 + 1.059BMI	0.552	0.0002	-5.52 + 1.228BMI	0.472	0.0282
	0.0030	-4.672 + 0.217HTWT	0.536	0.0002	12.2 + 0.097HTWT	0.511	0.0202
	0.0041	-9.92 + 0.45Weight	0.662	0.0008	8.07 + 0.225Weight	0.535	0.0162
	0.0294	1.58 + 4.81TDTWXP	0.411	0.0023	9.0 + 4.02TDTWXP	0.235	0.1557
	0.0075	40.97 - 8.59HTDWT	0.605	0.0001	52.18 - 11.69HTDWT	0.588	0.0097
R. Erector Spinae	0.0162	-10.95 + 77.4WTDHT	0.678	0.001	1.47 + 54.22WTDHT	0.551	0.0139
	0.0941	-2.617 + 0.0381TDTWXP	0.509	0.0004	9.37 + 0.022TDTWXP	0.362	0.0659
	0.0037	-8.92 + 1.184BMI	0.600	0.0001	-4.59 + 1.191BMI	0.451	0.0336
	0.0024	-6.36 + 0.235HTWT	0.546	0.0002	13.21 + 0.09HTWT	0.444	0.0354
	0.0025	-12.34 + 0.492Weight	0.688	0.0001	9.27 + 0.209Weight	0.471	0.0283
	0.0569	0.035 + 5.334TDTWXP	0.439	0.0015	7.66 + 4.33TDTWXP	0.277	0.1182
L. Erector Spinae	0.0221	43.72 - 9.54HTDWT	0.648	0.0001	50.7 - 11.04HTDWT	0.533	0.0166
	0.0139	-13.78 + 85.55WTDHT	0.720	0.0001	2.83 + 51.16WTDHT	0.499	0.0225
	0.0664	-0.627 + 0.031TDTWXP	0.448	0.0013	9.827 + 0.022TDTWXP	0.323	0.0867
	0.0008	-3.68 + 0.934BMI	0.483	0.0007	-6.456 + 1.265BMI	0.478	0.0269
	0.0050	-2.98 + 0.2HTWT	0.507	0.0004	11.19 + 0.105HTWT	0.562	0.0125
	0.0077	-7.51 + 0.408Weight	0.612	0.0001	6.86 + 0.24Weight	0.582	0.0103
	0.0164	3.13 + 4.3TDTWXP	0.368	0.0046	10.33 + 3.71TDTWXP	0.191	0.2071
	0.0027	38.21 - 7.65HTDWT	0.539	0.0002	53.65 - 12.34HTDWT	0.624	0.0065
	0.0171	-8.12 + 69.25WTDHT	0.610	0.0001	0.106 + 57.28WTDHT	0.587	0.0098

Table 1.55. Regression equations predicting the physiological cross-sectional area (cm<sup>2</sup>) of the Rectus Abdominis for females and males from various anthropometric measures. Significant regression equations are indicated by shaded rows (p≤0.05).

Muscle	p-value male vs female regression equation	Females			Males		
		Regression Equation	R <sup>2</sup>	p-value	Regression Equation	R <sup>2</sup>	p-value
Average of Right and Left Rectus Abdominis	0.2729	-2.676 + 0.018TDTWXP	0.376	0.0040	0.092 + 0.012TDTWXP	0.331	0.0821
	0.3525	-2.716 + 0.429BMI	0.251	0.0245	-8.326 + 0.697BMI	0.484	0.0256
	0.4911	3.43 + 0.031HTWT	0.030	0.4687	0.735 + 0.059HTWT	0.592	0.0093
	0.6904	0.472 + 0.102Weight	0.094	0.1887	-1.662 + 0.134Weight	0.609	0.0078
	0.4734	-2.5 + 2.935TDTWXPH	0.423	0.0019	0.492 + 2.03TDTWXPH	0.190	0.2028
	0.1334	14.02 - 2.65HTDWT	0.159	0.0814	24.14 - 6.73HTDWT	0.621	0.0068
R. Rectus Abdominis	0.6113	-2.14 + 24.3WTDHT	0.185	0.0581	-5.37 + 31.9WTDHT	0.608	0.0079
	0.3244	-2.5 + 0.018TDTWXP	0.383	0.0036	0.019 + 0.012TDTWXP	0.335	0.0795
	0.2729	-2.56 + 0.412BMI	0.237	0.0295	-8.53 + 0.685BMI	0.467	0.0294
	0.4716	3.27 + 0.031HTWT	0.034	0.4401	0.953 + 0.057HTWT	0.560	0.0128
	0.6864	0.54 + 0.1Weight	0.096	0.1831	-1.392 + 0.131Weight	0.577	0.0108
	0.5809	-2.225 + 2.81TDTWXPH	0.420	0.0020	0.165 + 2.1TDTWXPH	0.204	0.1900
L. Rectus Abdominis	0.1165	13.65 - 2.55HTDWT	0.160	0.0804	23.84 + 6.6HTDWT	0.595	0.0090
	0.6059	-1.8 + 23.07WTDHT	0.181	0.0617	-5.04 + 31.18WTDHT	0.578	0.0106
	0.2404	-2.85 + 0.019TDTWXP	0.358	0.0053	0.166 + 0.012TDTWXP	0.319	0.0889
	0.4377	-3.22 + 0.457BMI	0.255	0.0231	-9.12 + 0.708BMI	0.491	0.0241
	0.5039	3.6 + 0.03HTWT	0.025	0.5035	0.517 + 0.06HTWT	0.612	0.0075
	0.6829	0.41 + 0.1Weight	0.089	0.2021	-1.93 + 0.137Weight	0.628	0.0063
	0.3841	-2.784 + 3.06TDTWXPH	0.412	0.0023	0.82 + 1.95TDTWXPH	0.172	0.2329
	0.1514	14.39 - 2.74HTDWT	0.153	0.0882	24.44 - 6.87HTDWT	0.634	0.0058
	0.5739	-2.48 + 25.55WTDHT	0.183	0.0596	-5.7 + 32.62WTDHT	0.624	0.0066

Table 1.56. Regression equations predicting the physiological cross-sectional area (cm<sup>2</sup>) of the External Obliques for females and males from various anthropometric measures. Significant regression equations are indicated by shaded rows (p≤0.05).

Muscle	p-value male vs female regression equation	Females			Males		
		Regression Equation	R <sup>2</sup>	p-value	Regression Equation	R <sup>2</sup>	p-value
Average of Right and Left External Oblique	0.1393	3.158 + 0.008TDTWXP	0.281	0.0162	1.2 + 0.013TDTWXP	0.435	0.0380
	0.0272	3.51 + 1.18TDTWXPH	0.272	0.0183	0.64 + 2.36TDTWXPH	0.307	0.0963
R. External Oblique	0.2251	3.1 + 0.008TDTWXP	0.286	0.0151	2.32 + 0.011TDTWXP	0.375	0.0600
	0.0043	2.62 + 0.218BMI	0.235	0.0301	1.27 + 0.36BMI	0.175	0.2286
	0.0608	2.62 + 0.08Weight	0.210	0.0423	3.85 + 0.084Weight	0.320	0.0886
	0.0505	3.554 + 1.217TDTWXPH	0.265	0.0202	1.6 + 2.116TDTWXPH	0.279	0.1166
	0.0090	12.19 + 1.716HTDWT	0.243	0.0272	19.18 - 3.85HTDWT	0.274	0.1203
	0.0414	2.03 + 14.87WTDHT	0.252	0.0241	2.02 + 18.84WTDHT	0.286	0.1116
L. External Oblique	0.1069	3.22 + 0.007TDTWXP	0.221	0.0365	0.315 + 0.014TDTWXP	0.466	0.0297
	0.0247	3.462 + 1.144TDTWXPH	0.225	0.0345	-0.006 + 2.51TDTWXPH	0.312	0.0936

Table 1.57. Regression equations predicting the physiological cross-sectional area (cm<sup>2</sup>) of the Internal Oblique for females and males from various anthropometric measures. Significant regression equations are indicated by shaded rows (p≤0.05).

Muscle	p-value male vs female regression equation	Females			Males		
		Regression Equation	R <sup>2</sup>	p-value	Regression Equation	R <sup>2</sup>	p-value
Average of Right and Left Internal Oblique	0.0396	2.586 + 0.007TDTWXP	0.232	0.0316	0.129 + 0.014TDTWXP	0.504	0.0214
	0.0001	2.355 + 0.186BMI	0.173	0.0683	-6.341 + 0.653BMI	0.492	0.0238
	0.0032	4.96 + 0.014HTWT	0.023	0.5257	2.574 + 0.055HTWT	0.608	0.0078
	0.0048	3.66 + 0.046Weight	0.069	0.2640	0.387 + 0.125Weight	0.617	0.0071
	0.0069	2.65 + 1.21TDTWXPH	0.261	0.0213	-0.58 + 2.6TDTWXPH	0.362	0.0656
	0.0001	10.02 - 1.29HTDWT	0.137	0.1081	23.82 - 5.98HTDWT	0.569	0.0118
R. Internal Oblique	0.0017	2.55 + 10.72WTDHT	0.131	0.1164	-3.03 + 29.72WTDHT	0.611	0.0075
	0.1169	1.662 + 0.009TDTWXP	0.241	0.0278	0.629 + 0.013TDTWXP	0.425	0.0411
	0.0013	0.337 + 0.276BMI	0.267	0.0197	-4.64 + 0.58BMI	0.373	0.0606
	0.0127	4.17 + 0.021HTWT	0.036	0.4253	2.986 + 0.052HTWT	0.503	0.0215
	0.0245	2.29 + 0.067Weight	0.105	0.1630	1.01 + 0.116Weight	0.505	0.0212
	0.0297	1.6 + 1.514TDTWXPH	0.290	0.0144	0.073 + 2.41TDTWXPH	0.299	0.1019
L. Internal Oblique	0.0017	11.67 - 1.9HTDWT	0.211	0.0416	22.71 - 5.55HTDWT	0.469	0.0289
	0.0172	0.657 + 15.77WTDHT	0.201	0.0475	-2.02 + 27.16WTDHT	0.489	0.0244
	0.0304	3.51 + 0.006TDTWXP	0.146	0.0967	-0.371 + 0.015TDTWXP	0.461	0.0309
	0.0001	4.37 + 0.097BMI	0.048	0.3545	-8.04 + 0.7251BMI	0.491	0.0240
	0.0039	5.745 + 0.007HTWT	0.006	0.7450	2.162 + 0.059HTWT	0.564	0.0122
	0.0037	5.04 + 0.024Weight	0.020	0.5566	-0.233 + 0.135Weight	0.579	0.0103
	0.0001	8.38 - 0.674HTDWT	0.038	0.4088	24.93 - 6.41HTDWT	0.530	0.0170
	0.0009	4.45 + 5.66WTDHT	0.037	0.4146	-4.05 + 32.29WTDHT	0.584	0.0100

Table 1.58. Regression equations predicting the physiological cross-sectional area (cm<sup>2</sup>) of the Psoas Major for females and males from various anthropometric measures. Significant regression equations are indicated by shaded rows (p≤0.05).

Muscle	p-value male vs female regression equation	Females			Males		
		Regression Equation	R <sup>2</sup>	p-value	Regression Equation	R <sup>2</sup>	p-value
Average of Right and Left Psoas Major	0.0001	9.47 + 0.002TDTWXP	0.014	0.6186	5.36 + 0.019TDTWXP	0.448	0.0344
R. Psoas Major	0.0001	9.17 + 0.002TDTWXP	0.016	0.5967	3.07 + 0.022TDTWXP	0.459	0.0313
L. Psoas Major	0.0001	9.77 + 0.002TDTWXP	0.011	0.6678	7.65 + 0.016TDTWXP	0.408	0.0468

Table 1.59. Regression equations predicting the physiological cross-sectional area (cm<sup>2</sup>) of the Quadratus Lumborum for females and males from various anthropometric measures. Significant regression equations are indicated by shaded rows (p≤0.05).

Muscle	p-value male vs female regression equation	Females			Males		
		Regression Equation	R <sup>2</sup>	p-value	Regression Equation	R <sup>2</sup>	p-value
Average of Right and Left Quadratus Lumborum	0.0164	0.328 + 0.004TDIWXXP	0.430	0.0017	-1.91 + 0.01TDIWXXP	0.389	0.0538
	0.0001	0.16 + 0.108BMI	0.331	0.0080	-2.43 + 0.303BMI	0.164	0.2453
	0.0045	0.74 + 0.018HTWT	0.207	0.0436	0.345 + 0.035HTWT	0.384	0.0561
	0.0054	0.16 + 0.039Weight	0.294	0.0135	-0.824 + 0.08Weight	0.362	0.0656
	0.0023	0.555 + 0.623TDIWXXP	0.406	0.0028	-2.1 + 1.76TDIWXXP	0.258	0.1339
R. Quadratus Lumborum	0.0001	4.68 - 0.774HTDWT	0.286	0.0152	13.59 - 3.68HTDWT	0.333	0.0807
	0.0019	-0.11 + 7.28WTDHT	0.349	0.0061	-2.32 + 16.95WTDHT	0.308	0.0960
	0.0053	0.561 + 0.003TDIWXXP	0.316	0.0099	-1.14 + 0.009TDIWXXP	0.326	0.0848
	0.0001	-0.168 + 0.114BMI	0.430	0.0017	-0.58 + 0.228BMI	0.100	0.3745
	0.0013	0.6 + 0.017HTWT	0.225	0.0347	1.076 + 0.03HTWT	0.289	0.1091
L. Quadratus Lumborum	0.0016	-0.034 + 0.069Weight	0.341	0.0069	0.154 + 0.064Weight	0.267	0.1263
	0.0007	0.693 + 0.511TDIWXXP	0.314	0.0102	-1.35 + 1.57TDIWXXP	0.219	0.1729
	0.0001	4.62 - 0.82HTDWT	0.376	0.0041	11.92 - 2.97HTDWT	0.233	0.1581
	0.0009	-0.38 + 7.483WTDHT	0.429	0.0017	-0.937 + 13.72WTDHT	0.216	0.1756
	0.0657	0.095 + 0.005TDIWXXP	0.387	0.0034	-2.68 + 0.01TDIWXXP	0.411	0.0457
Average of Right and Left Quadratus Lumborum	0.0240	0.88 + 0.018HTWT	0.138	0.1074	-0.387 + 0.04HTWT	0.439	0.0369
	0.0237	0.354 + 0.039Weight	0.183	0.0598	-1.8 + 0.09Weight	0.421	0.0425
	0.0130	0.418TDIWXXP	0.344	0.0066	-2.85 + 1.96TDIWXXP	0.270	0.1240
	0.0003	4.73 - 0.726HTDWT	0.155	0.0854	15.26 - 4.39HTDWT	0.401	0.0392
	0.0077	0.162 + 7.07WTDHT	0.204	0.0457	-3.7 + 20.18WTDHT	0.370	0.0623

Table 1.60. p-values for regression equations predicting the *female* coronal plane moment-arms at the origin (L<sub>5</sub>) from anthropometric measures. Significant equations are represented by shaded cells (p≤0.05). The lastissimus dorsi was projected from L<sub>2</sub> through L<sub>5</sub>, the erector spinae and rectus abdominis were present at L<sub>5</sub>, and the external obliques and internal obliques were projected from L<sub>4</sub> through L<sub>5</sub>.

Measure Location	Female Coronal Plane Moment Arm - Origin									
	RLAT	LLAT	RES	LES	RABD	LABD	REOB	LEOB	RIOB	LIOB <sup>#</sup>
XP	0.1591	0.0761	0.9639	0.6501	0.9948	0.6575	0.0237	0.1022	0.6403	0.4988
IC	0.9404	0.6884	0.7683	0.5711	0.8456	0.2227	0.3191	0.4509	0.7317	0.3876
BMI	0.2576	0.1302	0.9681	0.5396	0.5339	0.6294	0.1215	0.1420	0.6566	0.6569

XP = Xyphoid Process;

IC = Iliac Crest;

BMI = Body Mass Index.

Table 1.61. p-values for regression equations predicting the *female* sagittal plane moment-arms at the origin (L<sub>5</sub>) from anthropometric measures. Significant equations are represented by shaded cells (p≤0.05). The lastissimus dorsi was projected from L<sub>2</sub> through L<sub>5</sub>, the erector spinae and rectus abdominis were present at L<sub>5</sub>, and the external obliques and internal obliques were projected from L<sub>4</sub> through L<sub>5</sub>.

Measure Location	Female Sagittal Plane Moment Arm - Origin									
	RLAT	LLAT	RES	LES	RABD	LABD	REOB*	LEOB*	RIOB <sup>#</sup>	LIOB <sup>#</sup>
XP	0.5245	0.6120	0.7970	0.8053	0.2195	0.1314	0.7067	0.4536	0.9447	0.9779
IC	0.0838	0.7810	0.8998	0.6109	0.3749	0.1767	0.2846	0.0902	0.3192	0.4064
BMI	0.2049	0.6559	0.3636	0.3047	0.5038	0.3767	0.7404	0.5514	0.4968	0.3614

XP = Xyphoid Process;

IC = Iliac Crest;

BMI = Body Mass Index.

\* The right and left external obliques were projected from L<sub>4</sub> to L<sub>5</sub> at a 45 degree anterior/caudal angle.

# The right and left internal obliques were projected from L<sub>4</sub> to L<sub>5</sub> at a 45 degree posterior/caudal angle.

Table 1.62. p-values for regression equations predicting the *female* coronal plane moment-arms at the insertion from anthropometric measures. Significant equations are represented by shaded cells ( $p \leq 0.05$ ). The insertions levels were based on the method of Marras and Granata (1995), with the erector spinae, internal oblique and latissimus dorsi lying between L<sub>3</sub> and L<sub>4</sub>, and the external obliques and rectus abdominis lying between L<sub>1</sub> and L<sub>2</sub>.

Measure Location	Female Coronal Plane Moment Arm - Insertion										
	RLAT	LLAT	RES	LES	RABD	LABD	REOB	LEOB	RIOB	LJOB	
XP	0.0274	0.0375	0.1559	0.4041	0.6207	0.0845	0.0012	0.0004	0.0013	0.0111	
IC	0.1120	0.1370	0.9598	0.5798	0.6819	0.1147	0.8786	0.9901	0.5317	0.6767	
BMI	0.0082	0.0146	0.2822	0.6670	0.4046	0.1249	0.0002	0.0009	0.0001	0.0012	

XP = Xyphoid Process;

IC = Iliac Crest;

BMI = Body Mass Index.

Table 1.63. p-values for regression equations predicting the *female* sagittal plane moment-arms at the insertion from anthropometric measures. Significant equations are represented by shaded cells ( $p \leq 0.05$ ). The insertions levels were based on the method of Marras and Granata (1995), with the erector spinae, internal oblique and latissimus dorsi lying between L<sub>3</sub> and L<sub>4</sub>, and the external obliques and rectus abdominis lying between L<sub>1</sub> and L<sub>2</sub>.

Measure Location	Female Sagittal Plane Moment Arm - Insertion										
	RLAT	LLAT	RES	LES	RABD	LABD	REOB	LEOB	RIOB	LJOB	
XP	0.5850	0.3973	0.5200	0.9996	0.0086	0.0162	0.8373	0.2577	0.0088	0.1475	
IC	0.9560	0.0567	0.0226	0.9475	0.0346	0.0075	0.9341	0.0605	0.3200	0.5417	
BMI	0.3774	0.1436	0.1307	0.5720	0.0281	0.0441	0.8706	0.5831	0.0289	0.0436	

XP = Xyphoid Process;

IC = Iliac Crest;

BMI = Body Mass Index.

Table 1.64. p-values for regression equations predicting the *male* coronal plane moment-arms at the origin (L<sub>5</sub>) from anthropometric measures. Significant equations are represented by shaded cells (p≤0.05). The lastissimus dorsi was projected from L<sub>2</sub> through L<sub>5</sub>, the erector spinae and rectus abdominis were present at L<sub>5</sub>, and the external obliques and internal obliques were projected from L<sub>4</sub> through L<sub>5</sub>.

Measure Location	Male Coronal Plane Moment Arm - Origin									
	RLAT	LLAT	RES	LES	RABD	LABD	REOB	LEOB	RIOB	LIOB <sup>#</sup>
XP	0.7833	0.6112	0.3283	0.1623	0.9432	0.0772	0.0300	0.0238	0.3817	0.0804
IC	0.7165	0.4304	0.6098	0.4655	0.2891	0.2600	0.0020	0.0001	0.1140	0.2406
BMI	0.0233	0.1266	0.9363	0.7607	0.3099	0.0218	0.0588	0.0067	0.6902	0.1129

XP = Xyphoid Process;

IC = Iliac Crest;

BMI = Body Mass Index.

Table 1.65. p-values for regression equations predicting the *male* sagittal plane moment-arms at the origin (L<sub>5</sub>) from anthropometric measures. Significant equations are represented by shaded cells (p≤0.05). The lastissimus dorsi was projected from L<sub>2</sub> through L<sub>5</sub>, the erector spinae and rectus abdominis were present at L<sub>5</sub>, and the external obliques and internal obliques were projected from L<sub>4</sub> through L<sub>5</sub>.

Measure Location	Male Sagittal Plane Moment Arm - Origin									
	RLAT	LLAT	RES	LES	RABD	LABD	REOB*	LEOB*	RIOB <sup>#</sup>	LIOB <sup>#</sup>
XP	0.4177	0.8218	0.2861	0.7691	0.0578	0.0283	0.2041	0.0280	0.1168	0.0966
IC	0.5400	0.3467	0.4416	0.2508	0.0628	0.1068	0.0403	0.3414	0.0880	0.6164
BMI	0.1476	0.8703	0.3977	0.9381	0.1118	0.0794	0.4619	0.0807	0.5312	0.4493

XP = Xyphoid Process;

IC = Iliac Crest;

BMI = Body Mass Index.

\* The right and left external obliques were projected from L<sub>4</sub> to L<sub>5</sub> at a 45 degree anterior/caudal angle.

# The right and left internal obliques were projected from L<sub>4</sub> to L<sub>5</sub> at a 45 degree posterior/caudal angle.

Table 1.66. p-values for regression equations predicting the *male* coronal plane moment-arms at the insertion from anthropometric measures. Significant equations are represented by shaded cells ( $p \leq 0.05$ ). The insertions levels were based on the method of Marras and Granata (1995), with the erector spinae, internal oblique and latissimus dorsi lying between L<sub>3</sub> and L<sub>4</sub>, and the external obliques and rectus abdominis lying between L<sub>1</sub> and L<sub>2</sub>.

Measure Location	Male Coronal Plane Moment Arm - Insertion									
	RLAT	LLAT	RES	LES	RABD	LABD	REOB	LEOB	RIOB	LIOB
XP	0.2056	<b>0.0592</b>	0.1232	0.3866	0.3222	0.1669	0.1348	<b>0.0073</b>	0.2736	0.3126
IC	0.2303	<b>0.0316</b>	0.1576	0.1919	0.1344	0.3637	<b>0.0307</b>	<b>0.0346</b>	0.0345	0.1478
BMI	0.2227	<b>0.0196</b>	<b>0.0344</b>	<b>0.0527</b>	0.5509	<b>0.0145</b>	0.2507	<b>0.0014</b>	0.2949	<b>0.0435</b>

XP = Xyphoid Process;

IC = Iliac Crest;

BMI = Body Mass Index.

Table 1.67. p-values for regression equations predicting the *male* sagittal plane moment-arms at the insertion from anthropometric measures. Significant equations are represented by shaded cells ( $p \leq 0.05$ ). The insertions levels were based on the method of Marras and Granata (1995), with the erector spinae, internal oblique and latissimus dorsi lying between L<sub>3</sub> and L<sub>4</sub>, and the external obliques and rectus abdominis lying between L<sub>1</sub> and L<sub>2</sub>.

Measure Location	Male Sagittal Plane Moment Arm - Insertion									
	RLAT	LLAT	RES	LES	RABD	LABD	REOB	LEOB	RIOB	LIOB
XP	0.7655	0.3841	0.1876	0.6351	<b>0.0028</b>	<b>0.0006</b>	0.3819	0.2742	0.3907	0.1404
IC	0.7255	<b>0.7275</b>	0.4896	0.2042	<b>0.0194</b>	0.0892	0.2467	0.7771	0.7803	0.7938
BMI	0.3930	0.5523	0.1923	0.7417	<b>0.0023</b>	<b>0.0004</b>	0.5299	0.1305	0.8619	0.2036

XP = Xyphoid Process;

IC = Iliac Crest;

BMI = Body Mass Index.

Table 1.68. Regression equations predicting the coronal and sagittal plane moment arm (cm) of the muscle centroid of the right Latissimus Dorsi to the centroid of the vertebral body for Females and Males from various anthropometric measures. Significant regression equations are indicated by shaded rows when  $p \leq 0.05$ .

Plane/Location	Females			Males		
	Regression Equation	R <sup>2</sup>	p-value	Regression Equation	R <sup>2</sup>	p-value
Coronal/Origin (L <sub>5</sub> )	0.008 - 0.252TWXP	0.107	0.1591	-6.56 - 0.054TWXP	0.010	0.7833
	-7.1 + 0.011TWIC	0.000	0.9404	-6.35 - 0.064TWIC	0.017	0.7165
	-3.54 - 0.154BMI	0.071	0.2576	<b>0.272 - 0.334BMI</b>	<b>0.494</b>	<b>0.0233</b>
Sagittal/Origin (L <sub>5</sub> )	-2.53 - 0.083TDXP	0.023	0.5245	-0.666 - 0.153TDXP	0.084	0.4177
	-0.51 - 0.179TDIC	0.157	0.0838	-1.63 - 0.114TDIC	0.049	0.5400
	-1.64 - 0.114BMI	0.088	0.2049	2.23 - 0.25BMI	0.243	0.1476
Coronal/Insertion (L <sub>3</sub> /L <sub>4</sub> )	<b>-0.393 - 0.324TWXP</b>	<b>0.285</b>	<b>0.0274</b>	-4.11 - 0.188TWXP	0.192	0.2056
	-3.94 - 0.181TWIC	0.160	0.1120	-5.27 - 0.163TWIC	0.174	0.2303
	<b>-3.4 - 0.27BMI</b>	<b>0.382</b>	<b>0.0082</b>	-6.07 - 0.16BMI	0.179	0.2227
Sagittal/Insertion (L <sub>3</sub> /L <sub>4</sub> )	-4.81 + 0.095TDXP	0.020	0.5850	-3.22 - 0.042TDXP	0.012	0.7655
	-3.23 + 0.008TDIC	0.000	0.9560	-5.27 - 0.049TDIC	0.016	0.7255
	-5.35 + 0.11BMI	0.052	0.3774	-1.28 - 0.113BMI	0.093	0.3930

TDXP = Trunk Depth measured at the Xyphoid Process (cm);  
 TDIC = Trunk Depth measured at the Iliac Crest (cm);  
 TWXP = Trunk Depth measured at the Xyphoid Process (cm);  
 TWIC = Trunk Width measured at the Iliac Crest (cm);  
 BMI = Body Mass Index (kg/m<sup>2</sup>).

Table 1.69. Regression equations predicting the coronal and sagittal plane moment arm (cm) of the muscle centroid of the left Latissimus Dorsi to the centroid of the vertebral body for Females and Males from various anthropometric measures. Significant regression equations are indicated by shaded rows when  $p \leq 0.05$ .

Plane/Location	Females			Males		
	Regression Equation	R <sup>2</sup>	p-value	Regression Equation	R <sup>2</sup>	p-value
Coronal Origin (L <sub>5</sub> )	-1.56 + 0.32TWXP	0.164	0.0761	5.87 + 0.075TWXP	0.034	0.6112
	8.75 - 0.06TWIC	0.009	0.6884	5.12 + 0.105TWIC	0.080	0.4304
	2.68 + 0.21BMI	0.123	0.1302	3.49 + 0.188BMI	0.267	0.1266
Sagittal Origin (L <sub>5</sub> )	-4.85 - 0.067TDXP	0.015	0.6120	-4.06 + 0.03TDXP	0.007	0.8218
	-3.0 - 0.03TDIC	0.004	0.7810	-0.754 - 0.118TDIC	0.111	0.3467
	-2.72 - 0.04BMI	0.011	0.6559	-2.86 - 0.021BMI	0.004	0.8703
Coronal Insertion (L <sub>3</sub> /L <sub>4</sub> )	0.874 + 0.314TWXP	0.243	0.0375	2.058 + 0.258TWXP	0.376	0.0592
	4.34 + 0.176TWIC	0.133	0.1370	2.57 + 0.26TWIC	0.458	0.0316
	3.83 + 0.26BMI	0.319	0.0146	3.56 + 0.268BMI	0.514	0.0196
Sagittal Insertion (L <sub>3</sub> /L <sub>4</sub> )	-6.74 + 0.151TDXP	0.045	0.3973	-7.65 + 0.164TDXP	0.110	0.3841
	-9.25 + 0.27TDIC	0.209	0.0567	-2.54 - 0.061TDIC	0.016	0.7275
	-7.8 + 0.184BMI	0.129	0.1436	-6.49 + 0.1BMI	0.046	0.5523

TDXP = Trunk Depth measured at the Xyphoid Process (cm);  
 TDIC = Trunk Depth measured at the Iliac Crest (cm);  
 TWXP = Trunk Depth measured at the Xyphoid Process (cm);  
 TWIC = Trunk Width measured at the Iliac Crest (cm);  
 BMI = Body Mass Index (kg/m<sup>2</sup>).

Table 1.70. Regression equations predicting the coronal and sagittal plane moment arm (cm) of the muscle centroid of the right Erector Spinae to the centroid of the vertebral body for Females and Males from various anthropometric measures. Significant regression equations are indicated by shaded rows when  $p \leq 0.05$ .

Plane/Location	Females			Males		
	Regression Equation	R <sup>2</sup>	p-value	Regression Equation	R <sup>2</sup>	p-value
Coronal/Origin (L <sub>5</sub> )	-2.69 - 0.003TWXP -2.14 - 0.016TWIC -2.65 + 0.002BMI	0.000 0.005 0.000	0.9639 0.7683 0.9681	-6.58 + 0.112TWXP -4.6 + 0.054TWIC -2.74 - 0.008BMI	0.119 0.034 0.001	0.3283 0.6098 0.9363
Sagittal/Origin (L <sub>5</sub> )	-5.11 - 0.017TDXP -5.28 - 0.007TDIC -6.29 + 0.041BMI	0.004 0.001 0.046	0.7970 0.8998 0.3636	-3.43 - 0.116TDXP -4.23 - 0.083TDIC -3.80 - 0.089BMI	0.140 0.076 0.091	0.2861 0.4416 0.3977
Coronal/Insertion (L <sub>3</sub> /L <sub>4</sub> )	-1.8 - 0.059TWXP -3.42 + 0.002TWIC -2.66 - 0.033BMI	0.109 0.000 0.064	0.1559 0.9598 0.2822	-1.68 - 0.065TWXP -2.12 - 0.055TWIC <b>-1.88 - 0.074BMI</b>	0.271 0.233 <b>0.448</b>	0.1232 0.1576 <b>0.0344</b>
Sagittal/Insertion (L <sub>3</sub> /L <sub>4</sub> )	-4.16 - 0.043TDXP <b>-2.646 - 0.116TDIC</b> -3.49 - 0.068BMI	0.023 <b>0.257</b> 0.122	0.5200 <b>0.0226</b> 0.1307	-2.6 - 0.134TDXP -4.06 - 0.071TDIC -2.41 - 0.126BMI	0.206 0.062 0.202	0.1876 0.4896 0.1923

TDXP = Trunk Depth measured at the Xyphoid Process (cm);  
 TDIC = Trunk Depth measured at the Iliac Crest (cm);  
 TWXP = Trunk Depth measured at the Xyphoid Process (cm);  
 TWIC = Trunk Width measured at the Iliac Crest (cm);  
 BMI = Body Mass Index (kg/m<sup>2</sup>).

Table 1.71. Regression equations predicting the coronal and sagittal plane moment arm (cm) of the muscle centroid of the left Erector Spinae to the centroid of the vertebral body for Females and Males from various anthropometric measures. Significant regression equations are indicated by shaded rows when  $p \leq 0.05$ .

Plane/Location	Females			Males		
	Regression Equation	R <sup>2</sup>	p-value	Regression Equation	R <sup>2</sup>	p-value
Coronal/Origin (L <sub>5</sub> )	1.91 + 0.031TWXP	0.012	0.6501	6.85 - 0.114TWXP	0.229	0.1623
	1.89 + 0.03TWIC	0.018	0.5711	4.87 - 0.057TWIC	0.068	0.4655
	2.08 + 0.031BMI	0.021	0.5396	3.75 - 0.023BMI	0.012	0.7607
Sagittal/Origin (L <sub>5</sub> )	-5.34 - 0.02TDXP	0.004	0.8053	-5.29 - 0.035TDXP	0.011	0.7691
	-6.36 + 0.033TDIC	0.015	0.6109	-3.21 - 0.129TDIC	0.161	0.2508
	-6.9 + 0.057BMI	0.058	0.3047	-5.87 - 0.009BMI	0.001	0.9381
Coronal/Insertion (L <sub>3</sub> /L <sub>4</sub> )	2.711 + 0.03TWXP	0.039	0.4041	2.73 + 0.038TWXP	0.115	0.3386
	3.08 + 0.016TWIC	0.017	0.5798	2.57 + 0.046TWIC	0.203	0.1919
	3.29 + 0.011BMI	0.010	0.6670	2.36 + 0.062BMI	0.392	0.0527
Sagittal/Insertion (L <sub>3</sub> /L <sub>4</sub> )	-5.3 - 0.0TDXP	0.000	0.9996	-4.6 - 0.043TDXP	0.030	0.6351
	-5.52 - 0.004TDIC	0.000	0.9475	-3.19 - 0.107TDIC	0.193	0.2042
	-4.665 - 0.03BMI	0.018	0.5720	-4.85 - 0.029BMI	0.014	0.7417

TDXP = Trunk Depth measured at the Xyphoid Process (cm);  
 TDIC = Trunk Depth measured at the Iliac Crest (cm);  
 TWXP = Trunk Depth measured at the Xyphoid Process (cm);  
 TWIC = Trunk Width measured at the Iliac Crest (cm);  
 BMI = Body Mass Index (kg/m<sup>2</sup>).

Table 1.72. Regression equations predicting the coronal and sagittal plane moment arm (cm) of the muscle centroid of the right Rectus Abdominis to the centroid of the vertebral body for Females and Males from various anthropometric measures. Significant regression equations are indicated by shaded rows when  $p \leq 0.05$ .

Plane/Location	Females			Males		
	Regression Equation	R <sup>2</sup>	p-value	Regression Equation	R <sup>2</sup>	p-value
Coronal/Origin (L <sub>5</sub> )	-3.86 + 0.001TWXP -4.33 + 0.018TWIC -4.97 + 0.053BMI	0.000 0.002 0.022	0.9948 0.8456 0.5339	-4.34 + 0.007TWXP -6.72 + 0.086TWIC -6.18 + 0.08BMI	0.001 0.139 0.128	0.9432 0.2891 0.3099
Sagittal/Origin (L <sub>5</sub> )	3.36 + 0.17TDXP 4.47 + 0.102TDIC 5.1 + 0.066BMI	0.083 0.044 0.025	0.2195 0.3749 0.5038	-1.53 + 0.398TDXP -0.959 + 0.383TDIC -0.871 + 0.329BMI	0.380 0.368 0.285	0.0578 0.0628 0.1118
Coronal/Insertion (L <sub>1</sub> /L <sub>2</sub> )	-2.2 - 0.047TWXP -4.33 - 0.03TWIC -2.07 - 0.066BMI	0.015 0.010 0.041	0.6207 0.6819 0.4046	0.392 - 0.159TWXP 1.6 - 0.21TWIC -2.53 - 0.087BMI	0.122 0.258 0.046	0.3222 0.1344 0.5509
Sagittal/Insertion (L <sub>1</sub> /L <sub>2</sub> )	3.378 + 0.312TDXP 4.744 + 0.22TDIC 4.48 + 0.216BMI	0.342 0.237 0.253	0.0086 0.0346 0.0281	1.93 + 0.423TDXP 3.67 + 0.356TDIC 1.145 + 0.408BMI	0.694 0.515 0.708	0.0029 0.0194 0.0023

TDXP = Trunk Depth measured at the Xyphoid Process (cm);  
 TDIC = Trunk Depth measured at the Iliac Crest (cm);  
 TWXP = Trunk Depth measured at the Xyphoid Process (cm);  
 TWIC = Trunk Width measured at the Iliac Crest (cm);  
 BMI = Body Mass Index (kg/m<sup>2</sup>).

Table 1.73. Regression equations predicting the coronal and sagittal plane moment arm (cm) of the muscle centroid of the left Rectus Abdominis to the centroid of the vertebral body for Females and Males from various anthropometric measures. Significant regression equations are indicated by shaded rows when  $p \leq 0.05$ .

Plane/Location	Females			Males		
	Regression Equation	R <sup>2</sup>	p-value	Regression Equation	R <sup>2</sup>	p-value
Coronal/Origin (L <sub>5</sub> )	2.076 + 0.043TWXP	0.011	0.6575	-4.16 + 0.229TWXP	0.339	0.0772
	5.85 - 0.093TWIC	0.081	0.2227	-1.01 + 0.141TWIC	0.155	0.2600
	2.5 + 0.036BMI	0.013	0.6294	<b>-3.08 + 0.247BMI</b>	<b>0.502</b>	<b>0.0218</b>
Sagittal/Origin (L <sub>5</sub> )	2.35 + 0.205TDXP	0.122	0.1314	<b>-3.03 + 0.464TDXP</b>	<b>0.472</b>	<b>0.0283</b>
	3.12 + 0.151TDIC	0.099	0.1767	-0.359 + 0.356TDIC	0.292	0.1068
	4.3 + 0.086BMI	0.044	0.3767	-1.99 + 0.373BMI	0.335	0.0794
Coronal/Insertion (L <sub>1</sub> /L <sub>2</sub> )	-0.446 + 0.149TWXP	0.165	0.0845	-1.32 + 0.164TWXP	0.224	0.1669
	6.6 - 0.107TWIC	0.140	0.1147	0.913 + 0.102TWIC	0.104	0.3637
	1.21 + 0.111BMI	0.133	0.1249	<b>-1.83 + 0.227BMI</b>	<b>0.547</b>	<b>0.0145</b>
Sagittal/Insertion (L <sub>1</sub> /L <sub>2</sub> )	<b>2.99 + 0.335TDXP</b>	<b>0.295</b>	<b>0.0162</b>	<b>0.807 + 0.479TDXP</b>	<b>0.785</b>	<b>0.0006</b>
	3.0 + 0.31TDIC	0.351	0.0075	5.13 + 0.298TDIC	0.319	0.0892
	<b>4.19 + 0.232BMI</b>	<b>0.218</b>	<b>0.0441</b>	<b>-0.179 + 0.466BMI</b>	<b>0.814</b>	<b>0.0004</b>

TDXP = Trunk Depth measured at the Xyphoid Process (cm);  
 TDIC = Trunk Depth measured at the Iliac Crest (cm);  
 TWXP = Trunk Depth measured at the Xyphoid Process (cm);  
 TWIC = Trunk Width measured at the Iliac Crest (cm);  
 BMI = Body Mass Index (kg/m<sup>2</sup>).

Table 1.74. Regression equations predicting the coronal and sagittal plane moment arm (cm) of the muscle centroid of the right External Obliques to the centroid of the vertebral body for Females and Males from various anthropometric measures. Significant regression equations are indicated by shaded rows when  $p \leq 0.05$ .

Plane/Location	Females			Males		
	Regression Equation	R <sup>2</sup>	p-value	Regression Equation	R <sup>2</sup>	p-value
Coronal/Origin (L <sub>5</sub> )	-4.077 - 0.264TWXP	0.253	0.0237	-5.5 - 0.222TWXP	0.465	0.0300
	-8.477 - 0.098TWIC	0.055	0.3191	-5.1 - 0.252TWIC	0.716	0.0020
	-8.22 - 0.141BMI	0.128	0.1215	-8.14 - 0.178BMI	0.378	0.0588
Sagittal/Origin (L <sub>5</sub> at a 45 degree anterior caudal angle from L <sub>4</sub> )	4.47 + 0.06TWXP	0.008	0.7067	2.04 + 0.167TWXP	0.193	0.2041
	8.38 - 0.141TWIC	0.063	0.2846	0.446 + 0.243TWIC	0.428	0.0403
Coronal/Insertion (L <sub>1</sub> /L <sub>2</sub> )	4.79 + 0.038BMI	0.006	0.7404	3.41 + 0.096BMI	0.069	0.4619
	3.38 - 0.278TWXP	0.452	0.0012	-4.78 - 0.256TWXP	0.257	0.1348
	-10.53 - 0.013TWIC	0.001	0.8786	-3.62 - 0.313TWIC	0.461	0.0307
Sagittal/Insertion (L <sub>1</sub> /L <sub>2</sub> )	-5.67 - 0.246BMI	0.555	0.0002	-8.47 - 0.18BMI	0.161	0.2507
	4.88 + 0.038TDXP	0.002	0.8373	3.17 + 0.11TDXP	0.097	0.3819
	6.44 - 0.044TDIC	0.000	0.9341	2.577 + 0.14TDIC	0.163	0.2467
	5.76 - 0.009BMI	0.002	0.8706	3.73 + 0.076BMI	0.051	0.5299

TDXP = Trunk Depth measured at the Xyphoid Process (cm);  
 TDIC = Trunk Depth measured at the Iliac Crest (cm);  
 TWXP = Trunk Depth measured at the Xyphoid Process (cm);  
 TWIC = Trunk Width measured at the Iliac Crest (cm);  
 BMI = Body Mass Index (kg/m<sup>2</sup>).

Table 1.75. Regression equations predicting the coronal and sagittal plane moment arm (cm) of the muscle centroid of the left External Oblique to the centroid of the vertebral body for Females and Males from various anthropometric measures. Significant regression equations are indicated by shaded rows when  $p \leq 0.05$ .

Plane/Location	Females			Males		
	Regression Equation	R <sup>2</sup>	p-value	Regression Equation	R <sup>2</sup>	p-value
Coronal/Origin (L <sub>5</sub> )	5.457 + 0.2TWXP 8.71 + 0.074TWIC 7.946 + 0.134BMI	0.141 0.032 0.116	0.1022 0.4509 0.1420	1.55 + 0.323TWXP 0.283 + 0.388TWIC 3.75 + 0.322BMI	0.492 0.855 0.622	0.0238 0.0001 0.0067
Sagittal/Origin (L <sub>5</sub> at a 45 degree anterior caudal angle from L <sub>4</sub> )	2.179 + 0.133TWXP -0.106 + 0.239TWIC 3.056 + 0.074BMI	0.032 0.151 0.020	0.4536 0.0902 0.5514	-1.817 + 0.329TWXP 2.21 + 0.158TWIC -1.05 + 0.264BMI	0.473 0.113 0.333	0.0280 0.3414 0.0807
Coronal/Insertion (L <sub>1</sub> /L <sub>2</sub> )	2.11 + 0.325TWXP 10.92 - 0.001TWIC 5.98 + 0.232BMI	0.516 0.000 0.465	0.0004 0.9901 0.0009	0.109 + 0.382TWXP 3.5 + 0.297TWIC 2.94 + 0.372BMI	0.614 0.447 0.740	0.0073 0.0346 0.0014
Sagittal/Insertion (L <sub>1</sub> /L <sub>2</sub> )	1.33 + 0.189TDXP -0.128 + 0.25TDIC 3.44 + 0.065BMI	0.071 0.182 0.017	0.2577 0.0605 0.5831	1.06 + 0.229TDXP 7.65 - 0.06TDIC -1.19 + 0.292BMI	0.147 0.011 0.262	0.2742 0.7771 0.1305

TDXP = Trunk Depth measured at the Xyphoid Process (cm);  
 TDIC = Trunk Depth measured at the Iliac Crest (cm);  
 TWXP = Trunk Depth measured at the Xyphoid Process (cm);  
 TWIC = Trunk Width measured at the Iliac Crest (cm);  
 BMI = Body Mass Index (kg/m<sup>2</sup>).

Table 1.76. Regression equations predicting the coronal and sagittal plane moment arm (cm) of the muscle centroid of the right internal oblique to the centroid of the vertebral body for Females and Males from various anthropometric measures. Significant regression equations are indicated by shaded rows when  $p \leq 0.05$ .

Plane/Location	Females			Males		
	Regression Equation	R <sup>2</sup>	p-value	Regression Equation	R <sup>2</sup>	p-value
Coronal/Origin (L <sub>5</sub> )	-8.61 - 0.072TWXP	0.014	0.6403	-6.38 - 0.151TWXP	0.097	0.3817
	-9.41 - 0.041TWIC	0.008	0.7317	-4.167 - 0.235TWIC	0.282	0.1140
	-11.73 + 0.056BMI	0.013	0.6566	-9.677 - 0.062BMI	0.021	0.6902
Sagittal/Origin (L <sub>5</sub> at a 45 degree posterior caudal angle from L <sub>4</sub> )	-1.505 + 0.011TWXP	0.000	0.9447	-6.83 + 0.243TWXP	0.279	0.1168
	1.28 - 0.13TWIC	0.062	0.3192	-6.94 + 0.255TWIC	0.321	0.0880
	0.468 - 0.084BMI	0.029	0.4968	-3.81 + 0.099BMI	0.051	0.5312
Coronal/Insertion (L <sub>3</sub> /L <sub>4</sub> )	1.88 - 0.431TWXP	0.487	0.0013	-6.775 - 0.146TWXP	0.147	0.2736
	-7.619 - 0.075TWIC	0.025	0.5317	-4.49 - 0.232TWIC	0.447	0.0345
	-0.811 - 0.424BMI	0.695	0.0001	-8.32 - 0.124BMI	0.136	0.2949
Sagittal/Insertion (L <sub>3</sub> /L <sub>4</sub> )	10.7 - 0.404TDXP	0.358	0.0088	-0.55 + 0.167TDXP	0.093	0.3907
	6.02 - 0.139TDIC	0.062	0.3200	2.07 + 0.054TDIC	0.010	0.7803
	8.94 - 0.27BMI	0.265	0.0289	2.43 + 0.033BMI	0.004	0.8619

TDXP = Trunk Depth measured at the Xyphoid Process (cm);  
 TDIC = Trunk Depth measured at the Iliac Crest (cm);  
 TWXP = Trunk Depth measured at the Xyphoid Process (cm);  
 TWIC = Trunk Width measured at the Iliac Crest (cm);  
 BMI = Body Mass Index (kg/m<sup>2</sup>).

Table 1.77. Regression equations predicting the coronal and sagittal plane moment arm (cm) of the muscle centroid of the left Internal Oblique to the centroid of the vertebral body for Females and Males from various anthropometric measures. Significant regression equations are indicated by shaded rows when  $p \leq 0.05$ .

Plane/Location	Females			Males		
	Regression Equation	R <sup>2</sup>	p-value	Regression Equation	R <sup>2</sup>	p-value
Coronal/Origin (L <sub>5</sub> )	8.47 + 0.066TWXP 8.44 + 0.065TWIC 9.5 + 0.036BMI	0.029 0.047 0.013	0.4988 0.3876 0.6569	4.04 + 0.199TWXP 5.05 + 0.178TWIC 6.33 + 0.162BMI	0.374 0.190 0.319	0.0804 0.2406 0.1129
Sagittal/Origin (L <sub>5</sub> at a 45 degree posterior caudal angle from L <sub>4</sub> )	-1.91 + 0.004TWXP -3.86 + 0.102TWIC 0.374 - 0.105BMI	0.000 0.044 0.052	0.9779 0.4064 0.3614	-8.06 + 0.308TWXP -3.147 + 0.098TWIC -4.36 + 0.133BMI	0.345 0.038 0.084	0.0966 0.6164 0.4493
Coronal/Insertion (L <sub>3</sub> /L <sub>4</sub> )	<b>-2.146 + 0.43TWXP</b> 7.74 + 0.06TWIC <b>0.473 + 0.425BMI</b>	<b>0.340</b> 0.011 <b>0.492</b>	<b>0.0111</b> 0.6767 <b>0.0012</b>	3.54 + 0.231TWXP -1.195 + 0.4TWIC <b>1.647 + 0.364BMI</b>	0.145 0.274 <b>0.464</b>	0.3126 0.1478 <b>0.0435</b>
Sagittal/Insertion (L <sub>3</sub> /L <sub>4</sub> )	8.306 - 0.291TDXP 0.889 + 0.104TDIC <b>9.37 - 0.305BMI</b>	0.127 0.024 <b>0.231</b>	0.1475 0.5417 <b>0.0436</b>	-3.906 + 0.346TDXP 5.57 - 0.064TDIC -2.76 + 0.267BMI	0.283 0.010 0.219	0.1404 0.7938 0.2036

TDXP = Trunk Depth measured at the Xyphoid Process (cm);  
 TDIC = Trunk Depth measured at the Iliac Crest (cm);  
 TWXP = Trunk Depth measured at the Xyphoid Process (cm);  
 TWIC = Trunk Width measured at the Iliac Crest (cm);  
 BMI = Body Mass Index (kg/m<sup>2</sup>).

Table 1.78. Mean (s.d.) physiological cross-sectional areas (cm<sup>2</sup>) for each muscle and gender. Shaded cells within each gender indicates a significant difference between right and left physiological cross-sectional area of a specific muscle ( $p \leq 0.05$ ).

Muscle Group	Females	Males
R. Latissimus Dorsi	13.29 (5.0)	21.74 (4.2)
L. Latissimus Dorsi	12.01 (4.7)	19.44 (5.1)
R. Erector Spinae	16.16 (3.8)	25.95 (4.1)
L. Erector Spinae	16.12 (3.4)	26.00 (4.2)
R. Rectus Abdominis	6.28 (2.1)	9.05 (2.3)
L. Rectus Abdominis	6.46 (2.3)	9.04 (2.3)
R. External Oblique	7.24 (1.1)	10.60 (2.0)
L. External Oblique	6.92 (1.1)	10.59 (2.2)
R. Internal Oblique	6.18 (1.3)	10.26 (2.2)
L. Internal Oblique	6.43 (1.1)	10.54 (2.4)
R. Psoas Major	10.39 (1.4)	19.49 (3.6)
L. Psoas Major	10.96 (1.7)	19.76 (2.8)
R. Quadratus Lumborum	2.24 (0.4)	5.26 (1.6)
L. Quadratus Lumborum	2.64 (0.6)	5.42 (1.9)

Table 1.79. Analysis of Variance p-values for vertebral level  $\times$  side interaction. Shaded cells indicates a significant interaction ( $p \leq 0.05$ ).

Muscle	Females	Males
Latissimus Dorsi	0.0001	0.0003
Erector Spinae	0.7175	0.6908
Rectus Abdominis	0.9844	0.6192
External Obliques	0.4532	0.2369
Internal Obliques	0.2281	0.8262
Psoas Major	0.2730	0.1389
Quadratus Lumborum	0.1780	0.6926

Table 1.80. Post-hoc results of Analysis of Variance of right versus left side PCSA (R=right, L=left).

Muscle	Gender	T8	T9	T10	T11	T12	L1	L2	L3	L4	L5	S1
Latissimus Dorsi	Male	R>L	R>L	R>L								
	Female	R>L	R>L	R>L								

Table 1.81. Difference (cm<sup>2</sup>) between *female* right and left side ACSA for each muscle group. Percent difference shown in [ ], calculated as right minus left, divided by the left. Statistically significant differences (p≤0.05) between right and left side ACSAs are indicated by shaded cells.

Muscle	Vertebral Level											
	T <sub>8</sub>	T <sub>9</sub>	T <sub>10</sub>	T <sub>11</sub>	T <sub>12</sub>	L <sub>1</sub>	L <sub>2</sub>	L <sub>3</sub>	L <sub>4</sub>	L <sub>5</sub>	S <sub>1</sub>	
Latissimus Dorsi	1.14 [9.5]	0.94 [8.9]	0.72 [8.0]	0.33 [4.1]	0.45 [6.6]	-0.08 [-1.4]	-0.07 [-1.9]	-0.18 [-10.8]				
Erector Spinae	-0.24 [-3.0]	-4.6 [-0.5]	-12.9 [-1.3]	-0.03 [-0.3]	-0.25 [-2.1]	-0.17 [-1.2]	0.05 [0.3]	-0.15 [-0.9]	-0.38 [-3.0]	0.00 [0.0]		
Rectus Abdominis					-0.29 [-6.4]	-0.04 [-0.8]	-0.20 [-4.5]	-0.07 [-1.6]	-0.16 [-3.2]	-0.08 [-1.7]	-0.13 [-2.0]	
External Obliques					0.42 [9.3]	0.22 [4.0]	-0.02 [-0.3]	0.21 [3.6]	0.29 [4.7]			
Internal Obliques						0.45 [28.1]	0.21 [6.2]	0.18 [5.1]	-0.24 [-3.7]			
Quadratus Lumborum						0.01 [0.6]	-0.02 [-1.1]	-0.28 [-11.8]	-0.31 [-13.6]			
Psoas Major						-0.07 [-3.1]	-0.25 [-7.1]	-0.10 [-1.4]	-0.28 [-2.8]	-0.62 [-5.8]		

Table 1.82. Difference (cm<sup>2</sup>) between *male* right and left side ACSAs for each muscle group. Percent difference shown in [ ], calculated as right minus left, divided by the left. Statistically significant differences (p≤0.05) between right and left side ACSA are indicated by shaded cells.

Muscle	Vertebral Level											
	T <sub>8</sub>	T <sub>9</sub>	T <sub>10</sub>	T <sub>11</sub>	T <sub>12</sub>	L <sub>1</sub>	L <sub>2</sub>	L <sub>3</sub>	L <sub>4</sub>	L <sub>5</sub>	S <sub>1</sub>	
Latissimus Dorsi	2.33 [12.0]	1.77 [1.0]	1.53 [10.2]	0.47 [3.5]	0.97 [8.7]	0.34 [3.9]	0.29 [4.9]	-0.03 [-1.2]				
Erector Spinae	-0.13 [-1.0]	-0.06 [-0.4]	-0.56 [-3.5]	-0.64 [-3.6]	-0.20 [-1.0]	-0.03 [-0.2]	0.19 [0.8]	-0.18 [-0.7]	-0.08 [-0.4]	-0.22 [-4.2]		
Rectus Abdominis					-0.33 [-5.4]	-0.28 [-4.1]	-0.20 [-3.2]	-0.45 [-5.8]	0.13 [1.9]	-0.16 [-1.8]	-0.03 [-0.3]	
External Obliques					0.20 [3.1]	0.46 [5.6]	0.01 [0.2]	-0.20 [-2.1]	-0.15 [-1.5]			
Internal Obliques							-0.50 [-11.6]	0.01 [0.2]	-0.29 [-2.9]			
Quadratus Lumborum						-0.22 [-8.0]	0.01 [0.3]	-0.18 [-3.4]	-0.03 [-0.8]			
Psoas Major						-0.65 [-20.0]	-0.93 [-11.9]	-0.36 [-2.7]	-0.37 [-2.0]	-0.10 [-0.5]		

Table 1.83 Female and male muscle vector locations for the muscle insertions relative to the L<sub>5</sub>/S<sub>1</sub> spine location, in the coronal and sagittal plane, as a function of anthropometric measurements at the xyphoid process and the iliac crest.

Muscle	Coronal Plane				Sagittal Plane			
	Xyphoid Process		Iliac Crest		Xyphoid Process		Iliac Crest	
	Female	Male	Female	Male	Female	Male	Female	Male
RLAT	0.31	0.31	0.30	0.33	-0.21	-0.22	-0.20	-0.23
LLAT	-0.34	-0.32	-0.33	-0.35	-0.25	-0.22	-0.23	-0.23
RES	0.12	0.11	0.11	0.12	-0.24	-0.24	-0.23	-0.25
LES	-0.14	-0.13	-0.14	-0.14	-0.26	-0.24	-0.25	-0.25
RABD	0.12	0.13	0.11	0.14	0.43	0.45	0.40	0.46
LABD	-0.14	-0.12	-0.13	-0.13	0.44	0.46	0.41	0.47
REOB	0.40	0.39	0.39	0.42	0.17	0.13	0.16	0.14
LEOB	-0.41	-0.39	-0.40	-0.41	0.14	0.13	0.13	0.14
RIOB	0.36	0.35	0.35	0.37	0.18	0.13	0.16	0.13
LIOB	-0.36	-0.34	-0.35	-0.36	0.15	0.15	0.14	0.16

Latissimus Dorsi: L<sub>2</sub>/L<sub>3</sub>

Erector Spinae: L<sub>3</sub>/L<sub>4</sub>

Rectus Abdominis: L<sub>1</sub>/L<sub>2</sub> to L<sub>2</sub>/L<sub>3</sub>

External Obliques: L<sub>3</sub>/L<sub>4</sub>

Internal Obliques: L<sub>3</sub>/L<sub>4</sub>

Table 1.84. Female and male muscle vector locations for the muscle origins (L<sub>5</sub>/S<sub>1</sub>), in the coronal and sagittal plane, as a function of anthropometric measurements at the xyphoid process and the iliac crest.

Muscle	Coronal Plane				Sagittal Plane			
	Xyphoid Process		Iliac Crest		Xyphoid Process		Iliac Crest	
	Female	Male	Female	Male	Female	Male	Female	Male
RLAT	0.23	0.24	0.23	0.26	-0.19	-0.22	-0.17	-0.23
LLAT	-0.26	-0.26	-0.26	-0.28	-0.26	-0.24	-0.25	-0.25
RES	0.08	0.07	0.08	0.08	-0.30	-0.27	-0.28	-0.28
LES	-0.09	-0.08	-0.08	-0.09	-0.31	-0.27	-0.29	-0.28
RABD	0.13	0.12	0.13	0.13	0.38	0.35	0.36	0.36
LABD	-0.12	-0.09	-0.12	-0.10	0.37	0.35	0.34	0.36
REOB	0.41	0.39	0.39	0.41	0.12	0.06	0.12	0.06
LEOB	-0.41	-0.38	-0.40	-0.40	0.05	0.03	0.04	0.03
RIOB	0.39	0.34	0.38	0.37	0.09	0.10	0.09	0.10
LIOB	-0.40	-0.33	-0.38	-0.35	0.05	0.08	0.05	0.08

Table 1.85. Female and male muscle vector locations for the muscle insertions relative to the L<sub>5</sub>/S<sub>1</sub> spine location, in the coronal and sagittal plane, as a function of anthropometric measurements at the xyphoid process and the iliac crest. External and internal obliques are projected from L<sub>4</sub> through insertion level at 135 and 45 degree angle in sagittal plane, respectively.

Muscle	Coronal Plane				Sagittal Plane			
	Xyphoid Process		Iliac Crest		Xyphoid Process		Iliac Crest	
	Female	Male	Female	Male	Female	Male	Female	Male
RLAT								
LLAT								
RES								
LES								
RABD								
LABD								
REOB					0.02	0.01	0.02	0.01
LEOB					-0.03	0.00	-0.03	0.00
RIOB					0.25	0.19	0.24	0.20
LIOB					0.22	0.20	0.21	0.21

External Obliques: L<sub>3</sub>/L<sub>4</sub>

Internal Obliques: L<sub>3</sub>/L<sub>4</sub>

Table 1.86. Female and male muscle vector locations for the muscle origins (L<sub>5</sub>/S<sub>1</sub>), in the coronal and sagittal plane, as a function of anthropometric measurements at the xyphoid process and the iliac crest. External and internal obliques are projected from L<sub>4</sub> through L<sub>5</sub>/S<sub>1</sub> at 135 and 45 degree angle in sagittal plane, respectively.

Muscle	Coronal Plane				Sagittal Plane			
	Xyphoid Process		Iliac Crest		Xyphoid Process		Iliac Crest	
	Female	Male	Female	Male	Female	Male	Female	Male
RLAT								
LLAT								
RES								
LES								
RABD								
LABD								
REOB					0.41	0.34	0.39	0.34
LEOB					0.36	0.33	0.34	0.34
RIOB					-0.11	-0.10	-0.10	-0.11
LIOB					-0.13	-0.09	-0.13	-0.10

Table 1.87. Female and male muscle vector locations for the muscle insertions relative to the L<sub>5</sub>/S<sub>1</sub> spine location, in the coronal and sagittal plane, as a function of anthropometric measurements at the xyphoid process and the iliac crest

Muscle	Coronal Plane				Sagittal Plane			
	Xyphoid Process		Iliac Crest		Xyphoid Process		Iliac Crest	
	Female	Male	Female	Male	Female	Male	Female	Male
RLAT								
LLAT								
RES	0.12	0.12	0.12	0.13	-0.29	-0.29	-0.27	-0.30
LES	-0.15	-0.14	-0.14	-0.15	-0.31	-0.29	-0.29	-0.29
RABD								
LABD								
REOB	0.42	0.40	0.41	0.43	0.11	0.07	0.11	0.07
LEOB	-0.43	-0.40	-0.42	-0.43	0.06	0.07	0.05	0.07
RIOB	0.39	0.36	0.37	0.38	0.22	0.17	0.21	0.18
LIOB	-0.39	-0.35	-0.38	-0.37	0.19	0.18	0.18	0.19

\* The erector spinae is projected at a 71.4 degree angle from L<sub>3</sub> in the sagittal plane and a 95.7 degree angle in the coronal plane, through the insertion plate.

\* The external oblique is projected at a 109.3 degree angle from L<sub>4</sub> in the sagittal plane and a 78.0 degree angle from L<sub>4</sub> in the coronal plane, through the insertion plate.

\* The internal oblique is projected at a 55.6 degree angle from L<sub>4</sub> in sagittal plane and a 76.6 degree angle from L<sub>4</sub> in the coronal plane, through the insertion plate.

Table 1.88. Female and male muscle vector locations for the muscle origins (L<sub>5</sub>/S<sub>1</sub>), in the coronal and sagittal plane, as a function of anthropometric measurements at the xyphoid process and the iliac crest.

Muscle	Coronal Plane				Sagittal Plane			
	Xyphoid Process		Iliac Crest		Xyphoid Process		Iliac Crest	
	Female	Male	Female	Male	Female	Male	Female	Male
RLAT								
LLAT								
RES	0.15	0.14	0.14	0.15	-0.41	-0.39	-0.38	-0.40
LES	-0.17	-0.16	-0.17	-0.17	-0.43	-0.38	-0.40	-0.40
RABD								
LABD								
REOB	0.37	0.35	0.36	0.38	0.25	0.19	0.23	0.19
LEOB	-0.37	-0.35	-0.36	-0.37	0.19	0.18	0.18	0.19
RIOB	0.33	0.31	0.32	0.33	-0.02	-0.03	-0.02	-0.03
LIOB	-0.33	-0.30	-0.32	-0.32	-0.05	-0.02	-0.05	-0.02

\* The erector spinae is projected from L<sub>3</sub> through L<sub>5</sub>/S<sub>1</sub> at a 71.4 degree angle in sagittal plane, and from L<sub>3</sub> through L<sub>5</sub>/S<sub>1</sub> at a 95.7 degree angle in the coronal plane.

\* The external oblique is projected from L<sub>4</sub> through L<sub>5</sub>/S<sub>1</sub> at a 109.3 degree angle in sagittal plane and from L<sub>4</sub> through L<sub>5</sub>/S<sub>1</sub> at a 78.0 degree angle in the coronal plane.

\* The internal oblique is projected through L<sub>4</sub> through L<sub>5</sub>/S<sub>1</sub> at a 55.6 degree angle in sagittal plane, and from L<sub>4</sub> through L<sub>5</sub>/S<sub>1</sub> at a 76.6 degree angle in the coronal plane.

Table 1.89. Percent of subjects with physiological cross-sectional area present at a specific vertebral level, by gender and muscle.

Level	Gender	Muscles													
		R Lat Dorsi	L Lat Dorsi	R Er Spinae	L Er Spinae	R Rect Abd	L Rect Abd	R Ext Obliq	L Ext Obliq	R Int Obliq	L Int Obliq	R Psoas Major	L Psoas Major	R Quad Lumb	L Quad Lumb
T <sub>8</sub>	Male	90	90												
	Female	95	95												
T <sub>9</sub>	Male	10	10												
	Female	5	5												
T <sub>10</sub>	Male														
	Female														
T <sub>11</sub>	Male														
	Female														
T <sub>12</sub>	Male														
	Female					5									
L <sub>1</sub>	Male			--	--	--	--	10	--						
	Female			15	5	--	15	5	5						
L <sub>2</sub>	Male			80	80	--	--	30	30	--	--			--	10
	Female			60	65	5	5	40	45	5	5			15	5
L <sub>3</sub>	Male			20	20	20	20	--	--	10	10			90	90
	Female			25	30	--	--	15	10	5	5			40	45
L <sub>4</sub>	Male					--	--	60	70	90	90	40	40	10	--
	Female					15	5	40	40	90	90	30	20	45	50
L <sub>5</sub>	Male					30	30					60	60		
	Female					10	20					70	80		
S <sub>1</sub>	Male					50	50								
	Female					70	50								

## **Part 2: Physiological measurement of the in-vivo muscular length-strength and force-velocity relationships in the female trunk torso.**

### **Introduction**

The estimation of moments and forces about the lower back using the EMG-assisted biomechanical model consists of adding the predicted muscle forces in three dimensions, and then using muscle moment-arm relationships, adding and partitioning the resulting moment in three dimensions. The determination of muscle force, however, is a function of muscle dynamics, which affect the EMG signal and the force output, and the force producing capability of the muscle, which includes the gain and the size of the muscle. The muscle physiological cross-sectional areas and geometry (e.g., location of the vector coordinates for insertion and origins) relationships for females were determined in Part 1. The muscle gains should remain constant in an individual. The force output of a muscle however, depends on the length of the muscle and the velocity of contraction at any point in time during the exertion. These factors also affect the EMG activity elicited from the muscle. Thus, in order to develop a valid dynamic biomechanical EMG-assisted model to estimate spinal loading, the muscle length-strength and force-velocity relationships must be determined.

### **Background and Objectives**

The objective of Part 2 was to develop the empirical muscle length-strength and muscle force-velocity relationships that describe the dynamic muscle behavior of military age females, which then will be incorporated into a female specific dynamic EMG-assisted biomechanical model. Past research has found that the length of the muscle and the velocity of the muscle contraction have an affect on the maximum muscle force capabilities, as well as the electromyographic activity elicited from the muscles (Wilkie, 1950; Bigland and Lippold, 1954; Hill, 1938; Komi, 1973; Granata and Marras, 1993; Raschke and Chaffin, 1996; Davis et al., 1998). Additionally, these relationships have been developed on muscle activities from males. Thus, in order to permit accurate assessments of spinal loading and associated LBD risk of females performing *dynamic* material handling tasks, it is necessary to generate the physiologic description of muscle dynamics that accurately describes military age women.

## **Administrative Note**

The free-dynamic mode of lifting allows the subjects to lift the weights at different controlled isokinetic trunk velocities while their body remained unconstrained, except for their feet. Preliminary analyses from these free-dynamic lifting trials did not result in acceptable model performances, with low  $r^2$ s and high muscle gain values. Thus, it was hypothesized that the subjects were allowing their hips and pelvis's to rotate during the lifting motions, resulting in highly variable length-strength and force-velocity results. Therefore, to remove the potential confounding effect of the rotation of the pelvis and hips, additional subjects were collected in a device called a pelvic support structure (PSS), which restricts movement to the trunk only, and not the pelvis. Thirty-five subjects have been collected in the PSS, and these modulations have enhanced the performance parameters far above those solely on the free-dynamic data. Similarly, when the modulation factors determined from the PSS were applied to the data from the free-dynamic exertions, the biomechanical model performance parameters were again more acceptable than those when the modulation factors were determined solely from the free-dynamic exertions. Thus, the approach used was to determine the muscle length-strength and force-velocity relationships that we know are valid (from the PSS lifting trials), and apply these relationships to the free-dynamic lifting exertions.

## **Methods**

### ***Subjects***

The subjects for the lifting trials in the Pelvic Support Structure consisted of 35 females and 35 males. Their anthropometric measurements are shown in Table 2.1. The subjects for the free-dynamic lifting trials also included 35 females and 35 males, with their anthropometric measurements described in Table 2.2. All subjects were recruited from the local community, and none were experiencing any low back pain at the time of the testing session.

Table 2.1 Anthropometric data (mean and s.d.) from the subjects for the lifting in the Pelvic Support Structure.

Anthropometric Variable	Females	Males
Age (yrs)	23.1 (4.7)	23.9 (4.0)
Standing Height (cm)	166.3 (6.9)	177.5 (7.4)
Weight (kg)	62.1 (9.5)	75.5 (12.7)
Trunk Width at Iliac Crest (cm)	27.2 (2.1)	29.3 (2.6)
Trunk Depth at Iliac Crest (cm)	19.0 (2.1)	20.8 (2.5)
Trunk Width at Xyphoid Process (cm)	26.9 (1.5)	30.3 (2.1)
Trunk Depth at Xyphoid Process (cm)	19.4 (1.7)	21.4 (2.4)
Body Mass Index (kg/m <sup>2</sup> )	22.4 (3.1)	24.0 (3.8)

Table 2.2 Anthropometric data (mean and s.d.) from the subjects for the Free Dynamic lifting trials.

Anthropometric Variable	Females	Males
Age (yrs)	22.2 (3.2)	22.2 (2.6)
Standing Height (cm)	166.3 (5.9)	177.8 (7.3)
Weight (kg)	60.3 (9.4)	80.0 (14.3)
Trunk Width at Iliac Crest (cm)	26.9 (3.5)	30.2 (3.3)
Trunk Depth at Iliac Crest (cm)	19.1 (3.0)	21.7 (2.4)
Trunk Width at Xyphoid Process (cm)	26.4 (1.9)	31.1 (2.4)
Trunk Depth at Xyphoid Process (cm)	19.2 (2.5)	21.9 (2.7)
Body Mass Index (kg/m <sup>2</sup> )	21.7 (2.8)	25.2 (4.0)

### ***Experimental Design***

The experimental design described below applies to the data collected from the free-dynamic mode as well as the lifting with the hips constrained in the PSS. The dependent variable consisted of the normalized electromyographic (EMG) activity from each of ten trunk muscles. The independent variables consisted of the weight of lift (15 lbs or 30 lbs), speed of the lifting motion (15, 30, 45, and 60 degrees per second) through a range of 50 degrees forward flexion to an upright standing position, as well as a static holding position (0 deg/sec) at forward trunk flexion angles of 5, 20, 35, and 50 degrees. The various weight and velocity lifting conditions were presented to each subject in a random order.

### ***Equipment***

A lumbar motion monitor (LMM), which is essentially an exoskeleton of the spine, was used to collect the kinematic trunk variables (Marras et al., 1992). The LMM was placed on the subjects back, and provided feedback via a computer screen as to when the subject reached the starting trunk angle. The LMM also measured and provided feedback on the trunk extension velocity, as the subject viewed the trunk velocity trace and their performance on a computer screen.

Electromyographic (EMG) activity was collected through the use of bipolar silver-silver chloride surface electrodes, spaced approximately 3 cm apart over ten trunk muscles (Mirka and Marras, 1993). The ten trunk muscles included the right and left pairs of the latissimus dorsi, erector spinae, rectus abdominis, external obliques, and the internal obliques. The subjects performed the lifting exertions while standing on a force plate (Bertec 4060A, Worthington, OH), which measured the three dimensional ground reaction moments and forces generated during the lifting exertions.

While the LMM, electromyography, and a force plate were used for both segments of this study (i.e., the lifting performed with the hips constrained and also for the free-dynamic mode), the external structures were different between the two modes. For the free-dynamic conditions, the subjects were not constrained in any way except for the requirement that they keep their feet on the force plate during the lifting exertion. To translate the moments and forces measured from the force plate to the estimated location of the L<sub>5</sub>/S<sub>1</sub> intervertebral disc, the location and orientation of the subjects' lumbosacral joint was monitored by use of a *sacral location*

*orientation monitor* (SLOM) and a *pelvic orientation monitor* (POM, see Figure 2.1), (Fathallah et al., 1997). For lifting trials performed with the hips constrained, the subjects were positioned into a *pelvic support structure* (PSS) that was attached to the force plate. The PSS restrained the subject's pelvis and hips in a fixed position (see Figure 2.2). The position of the L<sub>5</sub>/S<sub>1</sub> relative to the center of the force plate remained constant for all lifting trials, which allowed the forces and moments measured by the force plate to be rotated and translated to the position of the L<sub>5</sub>/S<sub>1</sub> (Granata et al., 1995).

All data signals from the above equipment were collected simultaneously through customized Windows™ based software developed in-house. The signals were collected at 100 Hz and recorded on a 486 computer via an analog-to-digital conversion board and stored for later analysis.

To allow the subjects to control their lifting velocity in an isokinetic manner, an additional computer was used to display the instantaneous velocity recorded by the LMM in real time. The signal was transferred from the LMM to the computer through an analog-to-digital board and converted into velocity by customized software. The subjects were then to control their isokinetic lifting velocity by keeping the trace of the velocity within tolerance lines displayed on the computer.

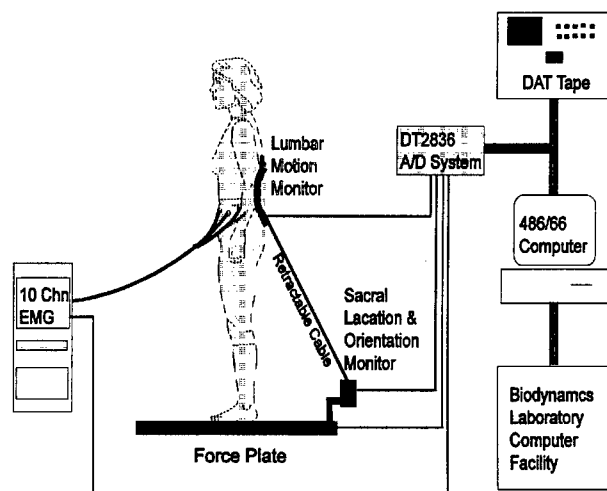


Figure 2.1. Experimental equipment for the Free Dynamic lifting conditions.

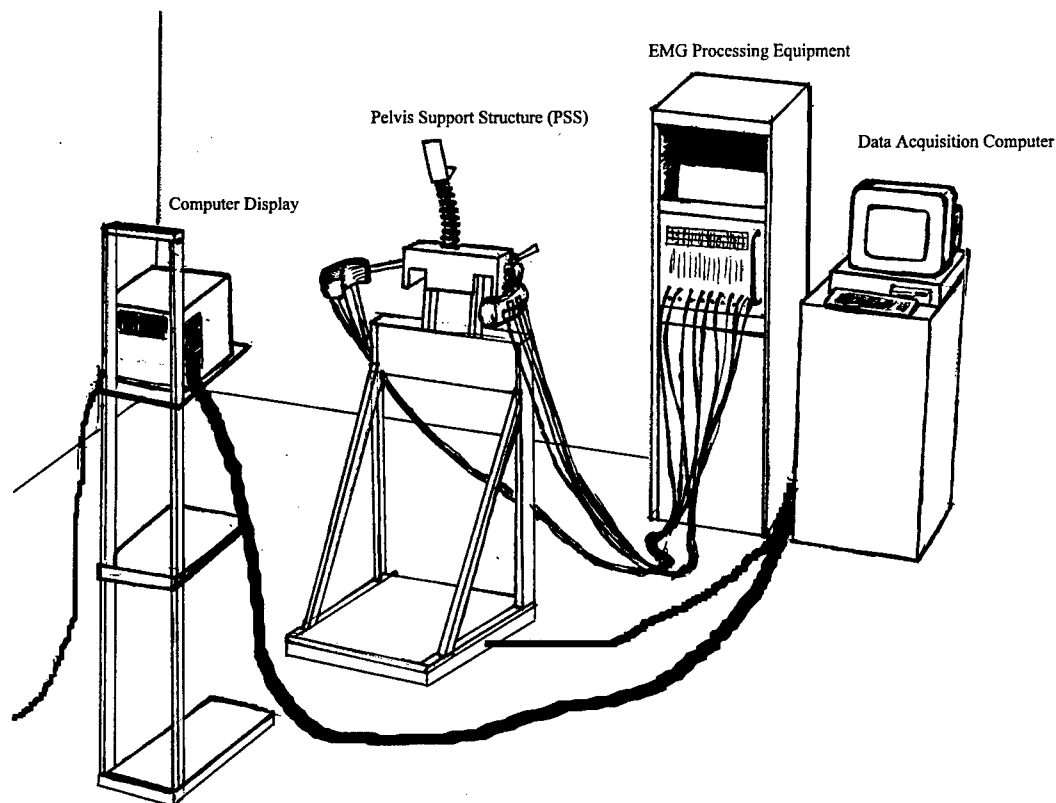


Figure 2.2. Experimental equipment for the lifting trials using the Pelvic Support Structure.

### ***Experimental Procedures***

Upon the subjects' arrival to the testing laboratory, the subjects read and signed a consent form, and took a pregnancy test so as to determine their pregnancy status. Once they were determined not to be pregnant, anthropometric data and demographic information were obtained. The surface electrodes for the EMG were then applied over each of ten trunk muscles, while skin impedance's were kept below 500 k $\Omega$ . Maximum voluntary contractions (MVCs) for each of the trunk muscles were obtained, with the subjects performing MVCs for trunk extension and flexion static exertions, as well as right and left twisting and right and left lateral bending, all against a constant resistance. All resulting trunk muscle EMG data obtained from the experimental trials were then normalized to the maximum EMG activity obtained during these six directional MVCs. Thus, the normalized EMG activity represents the fraction of maximum muscle activity that is applied at any point in time, and also allows relative muscle activity comparisons across subjects as well as within subjects. Following the MVCs, an LMM was placed on the subject's back, and the subject was then allowed to practice the lifting motion to become proficient with

the different controlled trunk velocities. The experimental task required the subject to control and maintain their trunk lifting velocity between tolerance limits (displayed on a computer screen) for each of the different velocity conditions. If the subject failed to maintain the trunk motion within the tolerance limits, the trial was rerun. A three percent tolerance was used by displaying two lines that were 1.5 percent above and below the target velocity.

### ***Modulation Factor Determination***

The determination of the muscle length-strength and force-velocity modulation factors consisted of a biomechanical analysis of the normalized EMG data collected from the subjects in the PSS. This was accomplished by comparing the measured sagittal trunk moment from the force plate with the un-modulated (i.e., without the muscle length-strength and muscle force-velocity relationships) predicted sagittal trunk moment (Granata and Marras, 1995; Granata, 1993). Specifically, this included a systematic analysis procedure incorporating different inputs into an EMG-assisted biomechanical model using the general form of equations 2.1 and 2.2 (Marras and Sommerich, 1991a, 1991b; Granata and Marras, 1993; Marras and Granata, 1995; Granata and Marras, 1995; Marras and Granata, 1997b). This method then minimized the average variation of the ratio of external to internal sagittal moment as a function of muscle length and velocity. Additionally, a simplifying assumption was made that the erector spinae group are the sole muscles that counteract the external moment during the sagittally symmetric lifting exertions. This assumption seemed reasonable as antagonistic muscle activity was shown to be minimal during similar motions of other studies (Granata and Marras, 1995; Davis et al., 1998).

$$\text{Force}_j = \text{Gain} \times (\text{EMG}_t / \text{EMG}_{\text{max}}) \times \text{PCSA}_j \times f(\text{Vel}) \times f(\text{Length}) \quad (\text{Eq 2.1})$$

$$M_{x\text{-pred}} = \sum r_j \times \text{Force}_j \quad (\text{Eq 2.2})$$

where:

Force<sub>j</sub> = tensile force for muscle j;

Gain = physiological muscle stress (N/cm<sup>2</sup>);

EMG<sub>t</sub> = integrated EMG from the lifting exertion;

EMG<sub>max</sub> = integrated EMG from MVCs;

PCSA<sub>j</sub> = physiological cross-sectional area of muscle j;

f(Vel) = the muscle force-velocity modulation factor;

f(Length) = the muscle length-strength modulation factor;

M<sub>x-pred</sub> = predicted sagittal trunk moment during the lifting exertion;

r<sub>j</sub> = moment-arm for muscle j.

Initially, the data for the dynamic lifting exertions were restricted to the range of 0 degrees to 45 degrees sagittal flexion, as the passive structures of the lower back are estimated to begin sharing the loading at increasing rates at sagittal flexion angles greater than 45 degrees (McGill and Norman 1986; Kirking 1997). Thus, restricting the range of dynamic exertion data to less than 45 degrees sagittal flexion ensures that the active structures (e.g., muscles) are fully contributing to the spinal loading. The exertions from each subject were run through the EMG-assisted model without any modulation factors (i.e., without Gain,  $f[Vel]$  and  $f[Length]$ ) to determine the subject specific average gain value. Next, the average gain per subject was input into the biomechanical model, and all the exertions were modeled again using the unmodulated versions of equations 2.1 and 2.2 (i.e.,  $f[Vel]$  and  $f[Length]$  factors equal to 1.0). The measured sagittal moment from the force plate ( $M_{x-meas}$ ) was then compared with the predicted sagittal moment ( $M_{x-pred}$ ) at each point in time, to obtain a vector of the ratio of  $M_{x-meas}$  divided by  $M_{x-pred}$ . This vector of the moment ratio was then used as the dependent variable in a multiple linear regression model to predict the moment ratio as a function of the muscle length for the erector spinae. Specifically, the form of the multiple linear regression model was:

$$Y = \beta_0 + \beta_1(Length) + \beta_2(Length^2) + \beta_3(Length^3) \quad (Eq. 2.3)$$

where:

$Y$  = ratio of measured sagittal moment ( $M_{x-meas}$ ) and predicted sagittal moment ( $M_{x-pred}$ );  
 $Length$  = Muscle length expressed as a ratio of estimated muscle length divided by the resting muscle length.

The resulting regression equation consisting of the  $\beta_0$ ,  $\beta_1$ ,  $\beta_2$  and  $\beta_3$  coefficients for the muscle length factor was then used as the muscle length-strength modulation factor. The length-strength modulation factor was then input into equations 2.1 and 2.2, and the EMG-assisted biomechanical model was then run again with the muscle force-velocity modulation factor [ $f(Vel)$ ] set equal to 1.0 to identify the force-velocity effects. The measured sagittal moment from the force plate was again compared with the predicted sagittal moment at each point in time to obtain a vector of the ratio of  $M_{x-meas}$  divided by  $M_{x-pred}$ . This vector of the moment ratio was then used as the dependent variable in a multiple linear regression model, to predict this moment ratio as a function of the erector spinae muscle velocity. Specifically, the form of the multiple regression model was:

$$Y = \beta_0 + \beta_1(\text{Vel}) \quad (\text{Eq. 2.4})$$

where:

Y = ratio of measured sagittal moment ( $M_{x\text{-meas}}$ ) and predicted sagittal moment ( $M_{x\text{-pred}}$ );  
Vel = Muscle velocity expressed as a ratio  $\leq 1.0$ , where a static condition results in a ratio of 1.0, with increasing velocities having smaller ratios.

The resulting beta coefficients ( $\beta_0$  and  $\beta_1$ ) for the muscle velocity factor was then used as the muscle force-velocity modulation factor in Equation 2.1, which is used to determine the instantaneous muscle force.

### ***Development of the Female Specific Biomechanical Model***

Since the EMG-assisted biomechanical model is an interactive system, a systematic procedure was necessary to determine which combinations of muscle vector locations and physiological cross-sectional areas (PCSAs) result in the best estimates of the modulation factors for the muscle length-strength and muscle force-velocity relationships. A step-by-step approach was used to assess any improvements or decrements in model performance indices as the PCSAs, muscle vector orientations, and length-strength and force-velocity parameters were varied. As shown in Table 2.3, a ten-step model building procedure was performed, varying only one variable at a time.

In order to establish a benchmark against which model performance could be judged, Model 1 was built using the male EMG-assisted biomechanical model, with the regression equations predicting the PCSAs from the body mass index (BMI) (Tables 1.53 to 1.57 from Part 1) as well as the muscle vector locations at the origin and insertion points and the length-strength and force-velocity modulation factors, all based on male data (Granata and Marras 1993; Marras and Granata 1995, 1997b).

Model 2 used the length-strength and force-velocity modulation factors determined from the female lifting exertions performed in the PSS, with all other model parameters based on male data as in Model 1 (i.e., PCSAs and muscle vector locations).

Model 3 was developed using the regression equations for the PCSAs based on the body mass index (Tables 1.53 to 1.57) along with the female length-strength and force-velocity modulations, with the muscle vector locations based on the male biomechanical model (Granata and Marras 1993; Marras and Granata 1995, 1997b).

Table 2.3. Female biomechanical model inputs.

Model Number	Muscle Group	Muscle Vector Locations		PCSA
		Origin	Insertion	
1	Lat Dorsi	Original Male Model	Original Male Model	Original Male Model Male Length/Strength Male Force/Velocity
	Er Sp			
	Rect Abd			
	Ext Obl			
	Int Obl			
2	Lat Dorsi	Original Male Model	Original Male Model	Original Male Model
	Er Sp			
	Rect Abd			
	Ext Obl			
	Int Obl			
3	Lat Dorsi	Original Male Model	Original Male Model	Female BMI Tables 1.53 to 1.57
	Er Sp			
	Rect Abd			
	Ext Obl			
	Int Obl			
4	Lat Dorsi	Original Male Model	Original Male Model	Female Xyphoid Process Tables 1.53 to 1.57
	Er Sp			
	Rect Abd			
	Ext Obl			
	Int Obl			
5	Lat Dorsi	MRI Derived Table 1.84	MRI Derived Table 1.83	Female Xyphoid Process Tables 1.53 to 1.57
	Er Sp			
	Rect Abd			
	Ext Obl			
	Int Obl			
6	Lat Dorsi	MRI Derived Table 1.84	MRI Derived Table 1.83	Female Xyphoid Process Tables 1.53 to 1.57
	Er Sp	MRI Derived Table 1.84	MRI Derived Table 1.83	
	Rect Abd	MRI Derived Table 1.84	MRI Derived Table 1.83	
	Ext Obl	45° Angle Table 1.86	45° Angle Table 1.85	
	Int Obl	-45° Angle Table 1.86	-45° Angle Table 1.85	
7	Lat Dorsi	MRI Derived Table 1.84	MRI Derived Table 1.83	Female Xyphoid Process Tables 1.53 to 1.57
	Er Sp	MRI Derived Table 1.84	MRI Derived Table 1.83	
	Rect Abd	MRI Derived Table 1.84	MRI Derived Table 1.83	
	Ext Obl	MRI Derived Table 1.84	MRI Derived Table 1.83	
	Int Obl	-45° Angle Table 1.86	-45° Angle Table 1.85	
8	Lat Dorsi	MRI Derived Table 1.84	MRI Derived Table 1.83	Fiber Corrected PCSA Table 2.4
	Er Sp	MRI Derived Table 1.84	MRI Derived Table 1.83	
	Rect Abd	MRI Derived Table 1.84	MRI Derived Table 1.83	
	Ext Obl	Fiber Derived Table 1.88	Fiber Derived Table 1.87	
	Int Obl	-45° Angle Table 1.86	-45° Angle Table 1.85	
9	Lat Dorsi	MRI Derived Table 1.84	MRI Derived Table 1.83	Fiber Corrected PCSA Table 2.4
	Er Sp	MRI Derived Table 1.84	MRI Derived Table 1.83	
	Rect Abd	MRI Derived Table 1.84	MRI Derived Table 1.83	
	Ext Obl	Fiber Derived Table 1.88	Fiber Derived Table 1.87	
	Int Obl	Fiber Derived Table 1.88	Fiber Derived Table 1.87	
10	Lat Dorsi	MRI Derived Table 1.84	MRI Derived Table 1.83	Fiber Corrected PCSA Table 2.4
	Er Sp	Fiber Derived Table 1.88	Fiber Derived Table 1.87	
	Rect Abd	MRI Derived Table 1.84	MRI Derived Table 1.83	
	Ext Obl	Fiber Derived Table 1.88	Fiber Derived Table 1.87	
	Int Obl	Fiber Derived Table 1.88	Fiber Derived Table 1.87	

Table 2.4. Regression equations predicting the female physiological cross-sectional area from external anthropometric measures.

Muscle	Independent Variable	Regression Equation	R <sup>2</sup>
R. Lat Dorsi	TDTWXP	$-8.24 + 0.043TDTWXP$	0.397
L. Lat Dorsi	TDTWXP	$-7.05 + 0.038TDTWXP$	0.347
R. Erector Spinae	WTDHT	$-13.78 + 85.55WTDHT$	0.720
L. Erector Spinae	WTDHT	$-8.125 + 69.25WTDHT$	0.610
R. Rectus Abd.	TDTWXP	$-2.225 + 2.812TDTWXP$	0.420
L. Rectus Abd.	TDTWXP	$-2.784 + 3.059TDTWXP$	0.412
R. External Obl.	TDTWXP	$3.1 + 0.008TDTWXP$	0.286
L. External Obl.	TDTWXP	$3.22 + 0.007TDTWXP$	0.221
R. Internal Obl.	TDTWXP	$1.6 + 1.514TDTWXP$	0.290
L. Internal Obl.	TDTWXP	$3.71 + 0.902TDTWXP$	0.148

TDTWXP = trunk depth (cm) × trunk width (cm) measured at the xyphoid process;

TDTWXP<sub>H</sub> = trunk depth (cm) × trunk width (cm) at xyphoid process, divided by stand height (cm);

WTDHT = subject weight (kg) ÷ standing height (cm).

Model 4 was developed using the regression equations predicting the PCSA based on the trunk width multiplied by the trunk depth measured at the xyphoid process (Tables 1.53 to 1.57), the female length-strength and force-velocity modulations, and the vector locations based on the male biomechanical model (Granata and Marras 1993; Marras and Granata 1995, 1997b).

Model 5 consisted of the PCSAs predicted from regression equations used in Model 4 (measures about the xyphoid process, Tables 1.53 to 1.57), the female length-strength and force-velocity modulation factors, and the female vector locations directly from MRI scans (Table 1.83 for insertions and Table 1.84 for the origin).

Model 6 used the PCSAs derived from measures about the xyphoid process (Tables 1.53 to 1.57). The vector locations for the internal oblique and external oblique were projected at a 45 and -45 degree angle in the caudal direction, passing through the L<sub>4</sub> muscle centroid (Table 1.85 for the insertions and Table 1.86 for the origin). The vector locations for the other muscles were derived directly from the MRI scans (Table 1.83 for the insertion, and Table 1.84 for the origin).

Model 7 utilized the PCSAs derived from the measures about the xyphoid process (Tables 1.53 to 1.57), the muscle vector locations derived from the MRI for the latissimus dorsi,

erector spinae, rectus abdominis and external oblique (Table 1.83 for the insertion and Table 1.84 for the origin), and vector locations for the internal oblique projected at a  $-45$  degree angle in the caudal direction, passing through the L<sub>4</sub> centroid (Table 1.85 for the insertion and Table 1.86 for the origin).

Model 8 included the fiber corrected PCSAs determined from the regression equations from Table 2.4, which represent the best predictors for each muscle group, the female length-strength and force-velocity modulation factors, the vector locations derived from the MRI scans for the rectus abdominis, latissimus dorsi and erector spinae (Table 1.83 for the insertions and 1.84 for the origins), the internal obliques projected at a  $-45$  degree angle in the sagittal plane, and the external oblique corrected for the fiber angle passing through the origin and insertion level (Table 1.87 for the insertion and Table 1.88 for the origin).

Model 9 was the same as Model 8, except the vector location for the internal oblique was corrected for the fiber angle of the muscle as it passed through the insertion (Table 1.87) and the origin (Table 1.88).

Finally, for Model 10, the PCSAs were predicted the same as Models 7 and 8 (regression equations in Table 2.4), the vector locations for the rectus abdominis and latissimus dorsi were derived directly from the MRI scans (Table 1.83 for the insertions and Table 1.84 for the origins), and the vector locations for the erector spinae, external and internal oblique were derived from the fiber orientations (Table 1.87 for insertions and Table 1.88 for origins).

Except for Model 1 where the female EMG, kinetic and kinematic data were applied to an existing male biomechanical model with already determined male length-strength and force-velocity modulation factors, the length-strength and force-velocity modulation determination procedures were developed specifically for each of the models based on the varied PCSA and vector orientations locations at the origin and insertion. Thus, in theory, the modulation factors will vary between the different models depending upon the differences in the prediction of the other factors (e.g., gain, PCSA).

### ***Development of the Male Specific Biomechanical Model***

Similar to the development of the female specific biomechanical model, a male specific biomechanical model was also developed using the male data derived from Part 1. Each of the different inputs for the ten different models, which are discussed below, are shown in Table 2.5.

Model 1 consisted of all the original male biomechanical model inputs previously developed in the Biodynamics Laboratory over the past decade (Granata and Marras 1993, 1995; Marras and Granata 1995, 1997a,b).

Model 2 utilized the original inputs from Model 1 except for the prediction of the PCSA, which used the regression equations from Tables 1.53 to 1.57 using either the body mass index (BMI) or measures about the xyphoid process as independent variables.

Model 3 was the same as Model 2 except the vector locations at the origin were derived from the MRI scans for each of the five muscle groups (Table 1.84).

Model 4 consisted of the PCSAs predicted from the BMI and measures about the xyphoid process (Tables 1.53 to 1.57), the insertion vector locations derived from the original male model (as in Model 1). The origin vector locations for the latissimus dorsi, erector spinae and rectus abdominis were derived from the MRI scans (Table 1.84). The external obliques were projected at a 45 degree caudal/anterior angle passing through the L<sub>4</sub> centroid through the origin plane, and the internal obliques were projected at a 45 degree caudal/posterior angle passing through the L<sub>4</sub> centroid through the origin plane. These angles were chosen based upon the angles used by Schultz et al. (1982) in their biomechanical model of the trunk.

Model 5 was the same as Model 4, except that the origin and insertion plane vector locations were both derived from the MRI scans from Part 1 (Table 1.83 for the insertions and Table 1.84 for the origins).

Model 6 utilized the same inputs as Model 5 except for the vector locations for the internal and external oblique muscles (Table 1.86). In the sagittal plane, the external obliques were projected at a 45 degree caudal/anterior angle passing through the L<sub>4</sub> centroid through the insertion and origin plane, and the internal obliques were projected at a 45 degree caudal/posterior angle passing through the L<sub>4</sub> centroid through the insertion and origin plane.

Model 7 was the same as Model 6, however, the external obliques vector locations at the insertion and origin were based upon the observations from the MRI (Table 1.84), and not projected at a 45 degree angle.

Model 8 utilized PCSAs which were corrected for the fiber orientation for each of the muscles, using the regression equations shown in Table 2.6. The vector locations for the latissimus dorsi, erector spinae and rectus abdominis were all derived from the MRI scans for the insertion plane (Table 1.83) and origin plane (Table 1.84). The internal oblique was projected at

a 45 degree caudal/posterior angle (Table 1.86), and the external oblique vector locations were derived from the reported fiber angles of the muscle (Table 1.87 for the insertion and Table 1.88 for the origin).

Model 9 was the same as Model 8 for the PCSAs (Table 2.6) and vector locations for the latissimus dorsi, erector spinae and rectus abdominis (derived from MRI scans), however, both the external and internal oblique vector locations at the insertion (Table 1.87) and origin level (Table 1.88) were derived from reported fiber angles for these muscles.

Finally, Model 10 utilized the regression equations in Table 2.6 to predict the PCSAs, the vector locations for the latissimus dorsi and rectus abdominis were derived from the MRI scans (Table 1.83 for the insertion and Table 1.84 for the origin level), and the erector spinae, external oblique and internal oblique vector locations were developed by projecting the vectors through the insertion and origin planes utilizing the reported fiber angles for each of these muscles (Table 1.87 for the insertion and Table 1.88 for the origin).

Table 2.5. Male biomechanical model inputs.

Model Number	Muscle Group	Muscle Vector Locations		PCSA
		Origin	Insertion	
1	Lat Dorsi	Original Male Model	Original Male Model	Original Male Model
	Er Sp			
	Rect Abd			
	Ext Obl			
	Int Obl			
2	Lat Dorsi	Original Male Model	Original Male Model	Male BMI and Xyphoid Process Tables 1.53 to 1.57
	Er Sp			
	Rect Abd			
	Ext Obl			
	Int Obl			
3	Lat Dorsi	MRI Derived Table 1.84	Original Male Model	Male BMI and Xyphoid Process Tables 1.53 to 1.57
	Er Sp			
	Rect Abd			
	Ext Obl			
	Int Obl			
4	Lat Dorsi	MRI Derived Table 1.84	Original Male Model	Male BMI and Xyphoid Process Tables 1.53 to 1.57
	Er Sp	MRI Derived Table 1.84		
	Rect Abd	MRI Derived Table 1.84		
	Ext Obl	45° Angle Table 1.86		
	Int Obl	-45° Angle Table 1.86		
5	Lat Dorsi	MRI Derived Table 1.84	MRI Derived Table 1.83	Male BMI and Xyphoid Process Tables 1.53 to 1.57
	Er Sp			
	Rect Abd			
	Ext Obl			
	Int Obl			
6	Lat Dorsi	MRI Derived Table 1.84	MRI Derived Table 1.83	Male BMI and Xyphoid Process Tables 1.53 to 1.57
	Er Sp	MRI Derived Table 1.84	MRI Derived Table 1.83	
	Rect Abd	MRI Derived Table 1.84	MRI Derived Table 1.83	
	Ext Obl	45° Angle Table 1.86	45° Angle Table 1.85	
	Int Obl	-45° Angle Table 1.86	-45° Angle Table 1.85	
7	Lat Dorsi	MRI Derived Table 1.84	MRI Derived Table 1.83	Male BMI and Xyphoid Process Tables 1.53 to 1.57
	Er Sp	MRI Derived Table 1.84	MRI Derived Table 1.83	
	Rect Abd	MRI Derived Table 1.84	MRI Derived Table 1.83	
	Ext Obl	MRI Derived Table 1.84	MRI Derived Table 1.83	
	Int Obl	-45° Angle Table 1.86	-45° Angle Table 1.85	
8	Lat Dorsi	MRI Derived Table 1.84	MRI Derived Table 1.83	Fiber Corrected PCSA Table 2.6
	Er Sp	MRI Derived Table 1.84	MRI Derived Table 1.83	
	Rect Abd	MRI Derived Table 1.84	MRI Derived Table 1.83	
	Ext Obl	Fiber Derived Table 1.88	Fiber Derived Table 1.87	
	Int Obl	-45° Angle Table 1.86	-45° Angle Table 1.85	
9	Lat Dorsi	MRI Derived Table 1.84	MRI Derived Table 1.83	Fiber Corrected PCSA Table 2.6
	Er Sp	MRI Derived Table 1.84	MRI Derived Table 1.83	
	Rect Abd	MRI Derived Table 1.84	MRI Derived Table 1.83	
	Ext Obl	Fiber Derived Table 1.88	Fiber Derived Table 1.87	
	Int Obl	Fiber Derived Table 1.88	Fiber Derived Table 1.87	
10	Lat Dorsi	MRI Derived Table 1.84	MRI Derived Table 1.83	Fiber Corrected PCSA Table 2.6
	Er Sp	Fiber Derived Table 1.88	Fiber Derived Table 1.87	
	Rect Abd	MRI Derived Table 1.84	MRI Derived Table 1.83	
	Ext Obl	Fiber Derived Table 1.88	Fiber Derived Table 1.87	
	Int Obl	Fiber Derived Table 1.88	Fiber Derived Table 1.87	

Table 2.6. Regression equations predicting the male physiological cross-sectional area from external anthropometric measures.

Muscle	Independent Variable	Regression Equation	R <sup>2</sup>
R. Lat Dorsi	HTWT	$7.43 + 0.101HTWT$	0.508
L. Lat Dorsi	HTWT	$3.7 + 0.111HTWT$	0.425
R. Erector Spinae	HTDWT	$50.7 - 11.04HTDWT$	0.533
L. Erector Spinae	HTDWT	$53.65 - 12.34HTDWT$	0.624
R. Rectus Abd.	HTDWT	$23.84 - 6.6HTDWT$	0.595
L. Rectus Abd.	HTDWT	$24.44 - 6.87HTDWT$	0.634
R. External Obl.	TDTWXP	$2.32 + 0.011TDTWXP$	0.375
L. External Obl.	TDTWXP	$0.315 + 0.014TDTWXP$	0.466
R. Internal Obl.	Weight	$1.01 + 0.116Weight$	0.505
L. Internal Obl.	Weight	$-0.233 + 0.125Weight$	0.579

HTWT = height (m) × weight (kg);

HTDWT = height (cm) ÷ weight (kg);

TDTWXP = trunk depth (cm) × trunk width (cm) measured at the xyphoid process;

Weight = subject weight (kg).

### ***Evaluation of Model Performance***

To determine the validity of the new length-strength and force-velocity modulation factors, the performance of each of the ten models was examined by comparing the predicted and measured moment profiles quantitatively by means of a statistical squared correlation ( $r^2$ ), the average absolute error (AAE) of the comparison, along with the existence of a physiologically valid muscle gain. The value of the  $r^2$  indicates how well the measured and predicted sagittal moment variability coincide. The AAE indicates the average magnitude of the difference between the predicted and measured sagittal moments. For gain values to be physiologically valid, the predicted gain values must lie between 30 and 90 N-cm<sup>-2</sup> (McGill et al, 1988; Reid and Costigan, 1987; Weis-Fogh and Alexander, 1977). Thus, a high  $r^2$  value, combined with low AAEs and physiologically valid gain values implies that the inputs into the model accounts for the variability of the lifting moment.

## ***Statistical Analysis***

The objectives of the research of Part 2 were to 1) investigate how the muscles responsible for spinal loading respond to different conditions such as velocity and weight of lift, and 2) document how the biomechanical models with different parameters behave under these different conditions. Therefore, the normalized muscle activity as a function of the different conditions were documented, as well as the magnitudes and changes of the biomechanical performance parameters (i.e., gain,  $r^2$ , and AAE) as a function of the different inputs.

First, descriptive statistics on all the dependent variables, consisting of the mean and standard deviation were first determined, for both the PSS and free-dynamic portions of this study. Next, the normalized EMG data were analyzed to assess the effects of different task parameters on the resulting normalized EMG values, again for both the PSS and free-dynamic portions of the study. Multivariate Analysis of Variance (MANOVA) and ANOVA techniques were used to assess the effects of the task parameters, using a repeated measures approach since multiple observations were taken from the same subjects. The dependent variable consisted of the normalized EMG value from each of the ten trunk muscles at the time of the maximum sagittal moment during each of the lifting exertions. Post-hoc tests included Tukey pair-wise comparisons. Significance was judged relative to an  $\alpha$  value of 0.05.

## **Results**

### ***Mean Normalized Muscle Activity***

The descriptive statistics for the female mean (s.d.) measured sagittal moment and normalized muscle activity for lifting trials performed in the PSS and Free Dynamic lifting trials are shown in Tables 2.7 and 2.8, respectively. Generally, the greatest muscle activity across all velocities and weights occurred in the trunk extensor muscles, with the erector spinae muscles resulting in the largest normalized muscle activity (between 39% and 52% for PSS trials and between 45% and 57% for Free Dynamic trials), with smaller levels of activity present in the internal obliques (between 21% and 29% for PSS trials and between 23% and 29% for Free Dynamic trials). Although the latissimus dorsi changed very little as a function of velocity, larger increases occurred as a function of weight for both PSS and Free Dynamic trials. The sagittal moment remained relatively constant across all velocity conditions, however, it increased

as a function of the weight condition. For both lifting modes, the MANOVA indicated a non-significant velocity by weight interaction on the collective normalized EMG activity (Table 2.9), with an additional non-significant effect of velocity on the normalized EMG for the free-dynamic lifting mode. Generally, the 30 lb weight condition resulted in significantly greater normalized activity for all muscles except the left rectus abdominis. The erector spinae, external obliques and internal obliques demonstrated differences in normalized EMG as a function of the velocity, where post-hoc tests indicated that the 60 deg/s condition usually had greater EMG than the 30 deg/s and 15 deg/s conditions, and the 15 and 30 deg/s conditions were not significantly different from each other.

Descriptive statistics for the male mean (s.d.) measured sagittal moment and normalized muscle activity for lifting trials performed in the PSS and Free Dynamic lifting trials are shown in Tables 2.9 and 2.10, respectively. Similar to the females, the greatest muscle activity across all velocities and weights occurred in the trunk extensor muscles, with the erector spinae muscles resulting in the largest normalized muscle activity (between 47% and 58% for PSS trials and between 43% and 58% for Free Dynamic trials), with smaller levels of activity present in the internal obliques (between 28% and 34% for PSS trials and between 26% and 36% for Free Dynamic trials). The sagittal moment remained relatively constant across all velocity conditions, however, it increased as a function of the weight condition. For both lifting modes, the MANOVA indicated that the main effects of velocity and weight had a significant affect on the collective normalized EMG activity across all ten trunk muscles (Table 2.12). The individual ANOVAs indicated that for the trials in the pelvic support structure, only the right rectus abdominis and right external oblique did not vary as a function of the weight, and for the free-dynamic lifts, only the right and left sides of the rectus abdominis did not vary as a function of the weight. For the velocity condition, generally the normalized EMG activity of the rectus abdominis and external obliques were not affected by the different levels of trunk velocity, as well as the latissimus dorsi not affect for the trials in the pelvic support structure. Post-hoc tests indicated that where significant effects were present, the normalized EMG activity for the 15 deg/s and 30 deg/s were not significantly different from each other. Similarly, the normalized EMG for the 45 deg/s and 60 deg/s were not significantly different from each other for all muscles except for the right internal oblique during the free-dynamic mode.

Table 2.7. Descriptive results for the mean (s.d.) normalized female muscle activity (percent of maximum muscle activity) occurring at the maximum moment, and maximum sagittal moment (Nm) as a function of velocity and weight, for lifting trials performed in the Pelvic Support Structure.

Variable	Velocity (deg/s)				Weight (lbs)	
	15	30	45	60	15	30
Sagittal Moment (Nm)	94.5 (16.7)	96.2 (17.7)	98.6 (16.5)	99.6 (17.9)	87.8 (14.0)	106.6 (14.9)
RLAT	0.09 (0.07)	0.09 (0.09)	0.09 (0.07)	0.10 (0.10)	0.08 (0.06)	0.11 (0.10)
LLAT	0.10 (0.10)	0.11 (0.11)	0.10 (0.08)	0.12 (0.11)	0.09 (0.08)	0.13 (0.12)
RES	0.40 (0.17)	0.43 (0.18)	0.45 (0.22)	0.52 (0.25)	0.39 (0.16)	0.51 (0.23)
LES	0.40 (0.18)	0.43 (0.18)	0.46 (0.24)	0.50 (0.24)	0.39 (0.18)	0.51 (0.23)
RABD	0.06 (0.04)	0.07 (0.05)	0.07 (0.05)	0.07 (0.04)	0.07 (0.04)	0.07 (0.04)
LABD	0.07 (0.05)	0.07 (0.05)	0.07 (0.05)	0.07 (0.05)	0.07 (0.05)	0.07 (0.05)
REOB	0.06 (0.04)	0.07 (0.04)	0.07 (0.04)	0.07 (0.04)	0.07 (0.04)	0.07 (0.04)
LEOB	0.06 (0.03)	0.06 (0.03)	0.06 (0.03)	0.07 (0.04)	0.06 (0.03)	0.06 (0.03)
RIOB	0.22 (0.12)	0.23 (0.14)	0.25 (0.15)	0.29 (0.19)	0.21 (0.12)	0.28 (0.17)
LIOB	0.21 (0.10)	0.23 (0.13)	0.24 (0.13)	0.29 (0.18)	0.21 (0.11)	0.28 (0.16)

Table 2.8. Descriptive results for the mean (s.d.) normalized female muscle activity (percent of maximum muscle activity) occurring at the maximum moment, and maximum sagittal moment (Nm) as a function of velocity and weight, for lifting trials performed in Free Dynamic mode.

Variable	Velocity (deg/s)				Weight (lbs)	
	15	30	45	60	15	30
Sagittal Moment (Nm)	81.2 (23.7)	81.3 (25.0)	83.5 (23.0)	84.3 (25.4)	72.7 (20.0)	92.5 (24.0)
RLAT	0.13 (0.19)	0.15 (0.20)	0.14 (0.14)	0.15 (0.21)	0.11 (0.12)	0.17 (0.24)
LLAT	0.14 (0.20)	0.13 (0.18)	0.15 (0.15)	0.15 (0.15)	0.11 (0.13)	0.17 (0.20)
RES	0.45 (0.35)	0.50 (0.36)	0.45 (0.36)	0.57 (0.40)	0.45 (0.34)	0.54 (0.39)
LES	0.44 (0.29)	0.49 (0.32)	0.47 (0.35)	0.55 (0.32)	0.45 (0.30)	0.53 (0.33)
RABD	0.05 (0.04)	0.06 (0.05)	0.06 (0.04)	0.06 (0.06)	0.06 (0.05)	0.06 (0.04)
LABD	0.06 (0.03)	0.06 (0.04)	0.06 (0.03)	0.06 (0.04)	0.06 (0.04)	0.06 (0.04)
REOB	0.06 (0.04)	0.06 (0.05)	0.06 (0.05)	0.07 (0.07)	0.06 (0.04)	0.07 (0.06)
LEOB	0.06 (0.05)	0.06 (0.06)	0.06 (0.06)	0.07 (0.07)	0.06 (0.05)	0.07 (0.07)
RIOB	0.24 (0.20)	0.25 (0.19)	0.24 (0.19)	0.32 (0.26)	0.23 (0.20)	0.29 (0.23)
LIOB	0.25 (0.22)	0.28 (0.23)	0.27 (0.25)	0.33 (0.26)	0.25 (0.21)	0.32 (0.27)

Table 2.9. MANOVA and ANOVA p-values for normalized EMG for female lifting trials in the Pelvic Support Structure and Free Dynamic mode. Significant effects are indicated by shaded cells ( $p \leq 0.05$ ).

MANOVA	Pelvic Support Structure			Free Dynamic		
	Velocity (Vel)	Weight	Vel × Weight	Velocity (Vel)	Weight	Vel × Weight
		0.0021	0.0001	0.4748	0.3202	0.0028
ANOVA						
Muscle						
RLAT	0.0942	0.0001			0.0024	
LLAT	0.5673	0.0001			0.0001	
RES	0.0001	0.0001			0.0017	
LES	0.0001	0.0001			0.0006	
RABD	0.2601	0.5321			0.6349	
LABD	0.4168	0.0072			0.0028	
REOB	0.0073	0.0108			0.0082	
LEOB	0.0259	0.0173			0.0005	
RIOB	0.0001	0.0001			0.0001	
LIOB	0.0001	0.0001			0.0001	

Table 2.10. Descriptive results for the mean (s.d.) normalized male muscle activity (percent of maximum muscle activity) occurring at the maximum moment, and maximum sagittal moment (Nm) as a function of velocity and weight, for lifting trials performed in the Pelvic Support Structure.

Variable	Velocity (deg/s)				Weight (lbs)	
	15	30	45	60	15	30
Sagittal Moment (Nm)	111.2 (21.1)	117.2 (36.3)	116.9 (20.3)	118.7 (25.5)	106.5 (27.7)	125.5 (21.6)
RLAT	0.08 (0.12)	0.08 (0.12)	0.08 (0.14)	0.08 (0.06)	0.07 (0.12)	0.09 (0.13)
LLAT	0.08 (0.12)	0.08 (0.12)	0.09 (0.14)	0.07 (0.05)	0.08 (0.12)	0.09 (0.13)
RES	0.48 (0.27)	0.51 (0.28)	0.56 (0.32)	0.58 (0.27)	0.47 (0.27)	0.58 (0.32)
LES	0.47 (0.29)	0.50 (0.31)	0.55 (0.31)	0.55 (0.25)	0.47 (0.29)	0.57 (0.33)
RABD	0.08 (0.13)	0.08 (0.12)	0.08 (0.14)	0.07 (0.05)	0.08 (0.12)	0.08 (0.14)
LABD	0.07 (0.13)	0.07 (0.14)	0.08 (0.14)	0.07 (0.06)	0.07 (0.13)	0.08 (0.14)
REOB	0.08 (0.14)	0.09 (0.16)	0.08 (0.14)	0.05 (0.02)	0.08 (0.14)	0.09 (0.15)
LEOB	0.07 (0.14)	0.07 (0.14)	0.08 (0.15)	0.05 (0.03)	0.07 (0.14)	0.07 (0.14)
RIOB	0.28 (0.17)	0.30 (0.19)	0.33 (0.22)	0.36 (0.22)	0.28 (0.18)	0.34 (0.22)
LIOB	0.29 (0.16)	0.31 (0.18)	0.35 (0.20)	0.35 (0.19)	0.30 (0.17)	0.36 (0.20)

Table 2.11. Descriptive results for the mean (s.d.) normalized male muscle activity (percent of maximum muscle activity) occurring at the maximum moment, and maximum sagittal moment (Nm) as a function of velocity and weight, for lifting trials performed in the Free Dynamic mode.

Variable	Velocity (deg/s)				Weight (lbs)	
	15	30	45	60	15	30
Sagittal Moment (Nm)	97.8 (28.5)	94.6 (27.3)	97.3 (22.5)	99.4 (24.4)	87.0 (24.0)	107.5 (23.2)
RLAT	0.07 (0.04)	0.06 (0.04)	0.07 (0.04)	0.08 (0.06)	0.06 (0.04)	0.08 (0.05)
LLAT	0.07 (0.05)	0.07 (0.04)	0.07 (0.04)	0.07 (0.04)	0.06 (0.04)	0.08 (0.05)
RES	0.43 (0.26)	0.45 (0.26)	0.53 (0.29)	0.58 (0.27)	0.46 (0.26)	0.54 (0.28)
LES	0.43 (0.24)	0.45 (0.26)	0.51 (0.26)	0.55 (0.25)	0.45 (0.24)	0.52 (0.26)
RABD	0.06 (0.05)	0.07 (0.05)	0.07 (0.05)	0.07 (0.05)	0.06 (0.05)	0.07 (0.05)
LABD	0.07 (0.06)	0.08 (0.08)	0.07 (0.07)	0.07 (0.06)	0.07 (0.06)	0.07 (0.07)
REOB	0.04 (0.02)	0.04 (0.02)	0.04 (0.02)	0.05 (0.02)	0.04 (0.02)	0.05 (0.02)
LEOB	0.05 (0.03)	0.05 (0.03)	0.05 (0.03)	0.05 (0.03)	0.05 (0.02)	0.05 (0.03)
RIOB	0.26 (0.16)	0.29 (0.18)	0.32 (0.18)	0.36 (0.22)	0.28 (0.17)	0.34 (0.20)
LIOB	0.27 (0.17)	0.30 (0.20)	0.33 (0.20)	0.35 (0.19)	0.29 (0.18)	0.33 (0.20)

Table 2.12. MANOVA and ANOVA p-values for normalized EMG for male lifting trials in the Pelvic Support Structure and Free Dynamic mode. Significant effects are indicated by shaded cells ( $p \leq 0.05$ ).

MANOVA	Pelvic Support Structure			Free Dynamic		
	Velocity (Vel)	Weight	Vel × Weight	Velocity (Vel)	Weight	Vel × Weight
		0.0039	0.0001	0.2522	0.0001	0.0001
ANOVA						
Muscle						
RLAT	0.8637	0.0022		0.0196	0.0001	
LLAT	0.5588	0.0001		0.7618	0.0001	
RES	0.0002	0.0001		0.0001	0.0001	
LES	0.0001	0.0001		0.0001	0.0001	
RABD	0.7582	0.0842		0.0620	0.0552	
LABD	0.3558	0.0483		0.2734	0.4114	
REOB	0.5441	0.1615		0.0058	0.0009	
LEOB	0.1077	0.0105		0.1713	0.0017	
RIOB	0.0007	0.0001		0.0001	0.0001	
LIOB	0.0001	0.0001		0.0001	0.0001	

### ***Model Parameters***

The model performance results from systematic analysis of the inputs into the force and moment equations (Eq. 2.1 and 2.2) for the prediction of the sagittal moment for each of the ten female models are shown in Table 2.13 and for males in Table 2.14. The use of only the dynamic lifting trials resulted in better model parameters (lower gains and higher  $r^2$ 's) than when using both the static and dynamic trials. This is expected since the static exertions do not induce a *change* in the moment, which is what is described by the  $r^2$  statistic.

For females, all ten models resulted in acceptable model performance parameters (Table 2.13). For the PSS trials, all ten models resulted in very acceptable mean  $r^2$ 's ranging from 0.89 (Model 3) to 0.93 (Model 1), had physiologically acceptable mean muscle gain values, ranging from 34.7 N/cm<sup>2</sup> (Model 1) to 59.6 N/cm<sup>2</sup> (Model 9), and the AAEs were acceptable with mean values ranging from 5.7 Nm (Models 9 and 10) to 6.43 Nm (Model 1). When applying the input parameters (e.g., length-strength and force-velocity modulations, PCSAs, vector locations) from each specific model to the data from the Free Dynamic lifting trials, the mean gain and  $r^2$  across all models decreased by 2.2% and 7.6%, respectively. However, the mean AAE across all models increased by 49.6%.

Similar to the female models, all ten male models also resulted in acceptable model performance parameters (Table 2.14). For the PSS trials, all ten models resulted in very acceptable mean  $r^2$ 's ranging from 0.93 (Models 3 and 4) to 0.95 (Models 1 and 10), had physiologically acceptable mean muscle gain values, ranging from 32.0 N/cm<sup>2</sup> (Model 1) to 56.6 N/cm<sup>2</sup> (Model 3), and the AAEs were acceptable with mean values ranging from 6.73 Nm (Model 8) to 10.31 Nm (Model 2). When the input parameters (e.g., length-strength and force-velocity modulations, PCSAs, vector locations) from each specific model were applied to the Free Dynamic lifting trials, a modest decrease resulted for the mean gain (2.2%) and mean  $r^2$  (3.2%). The mean AAE, however, increased from 8.21 Nm to 13.41 Nm, representing a mean increase of 57.8%.

### ***Female Model Selection***

All female models investigated resulted in acceptable model performance parameters, however, some models performed better than others. Generally, all models performed the same regarding the mean and median  $r^2$ 's. Models 1 through 3 had mean gains between 30 and 40

N/cm<sup>2</sup>, with AAEs ranging from 6.0 to 6.4 Nm. Models 5 through 9 had higher mean gains (between 50 and 60 N/cm<sup>2</sup>), with lower AAEs (between 5.5 and 5.8 Nm). Model 10 had a mid-range mean gain compared to the other models (47.0 N/cm<sup>2</sup>), with the lowest AAE (5.7 Nm). Model 10 also incorporates the muscle vector locations consistent with the anatomical muscle fiber orientation, and uses the external anthropometric measures which best predict the PCSAs (Table 2.4). Therefore, Model 10 was selected as the “Female Model” for further study in Parts 3 and 4.

As shown in Figure 2.3, the distribution of the  $r^2$ s shows both a high mean and median for Model 10. Figure 2.4 shows the distribution of the estimated muscle gains from the lifting trials in the PSS. The Model 10 length-strength and force-velocity modulation factors determined from the PSS lifting trials were applied to the data from the Free Dynamic lifting trials (Table 2.15). This resulted in a slightly lower mean gain (44.4 N-cm<sup>-2</sup>), and still respectable mean and median  $r^2$  values (0.84 and 0.90, respectively). The distribution of the  $r^2$ 's from the trials in the free dynamic mode is shown in Figure 2.5, and the distribution of the estimated muscle gains from the free dynamic lifting trials is shown in Figure 2.6.

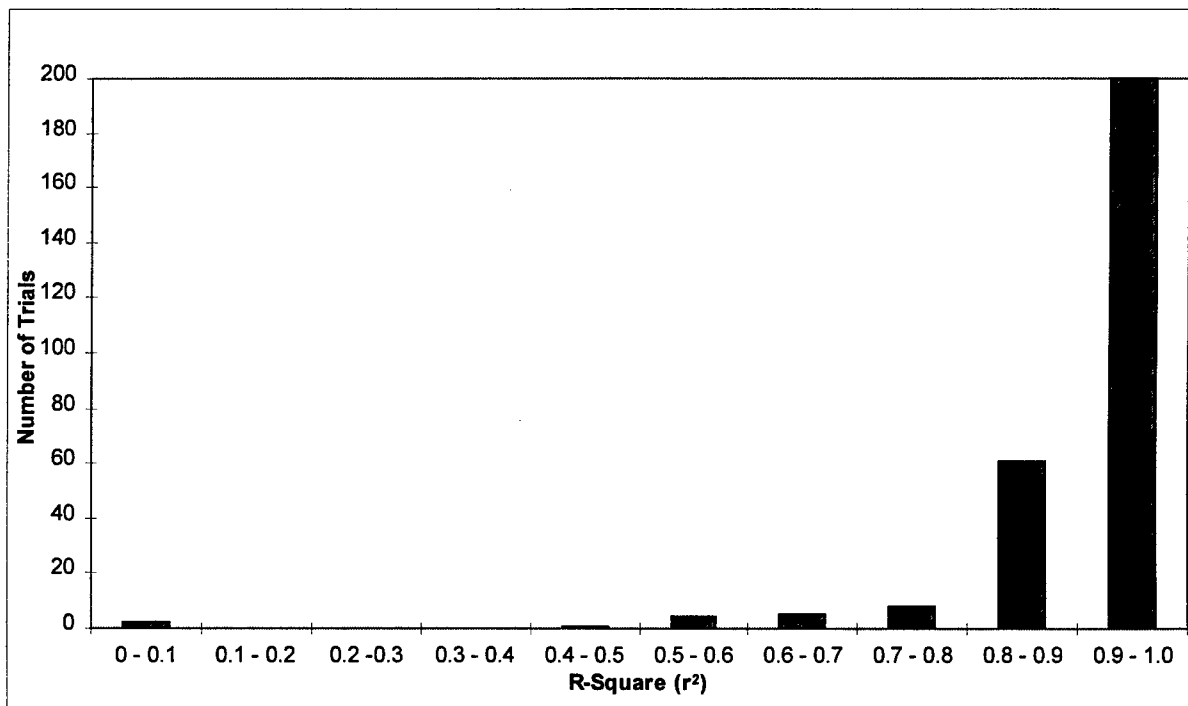


Figure 2.3. Distribution of the  $r^2$ s for the performance of Female Model 10, resulting from lifting trials in the Pelvic Support Structure.

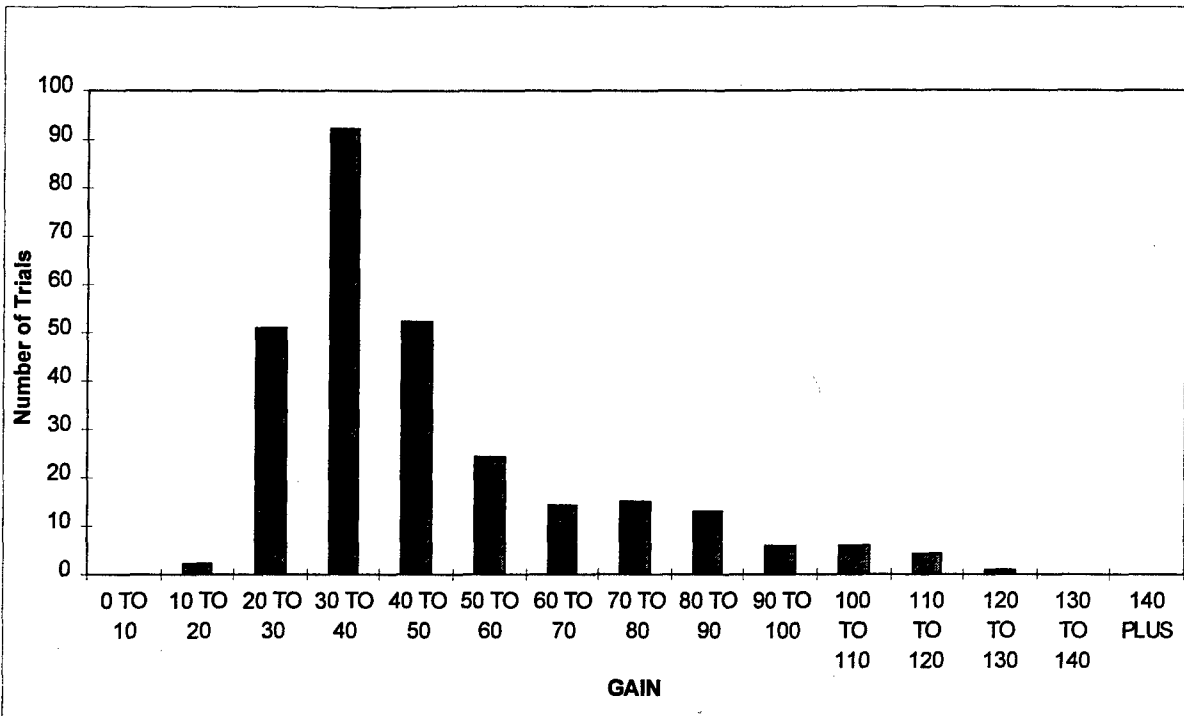


Figure 2.4. Distribution of the estimated muscle gains for the performance of Female Model 10, resulting from lifting trials in the Pelvic Support Structure.

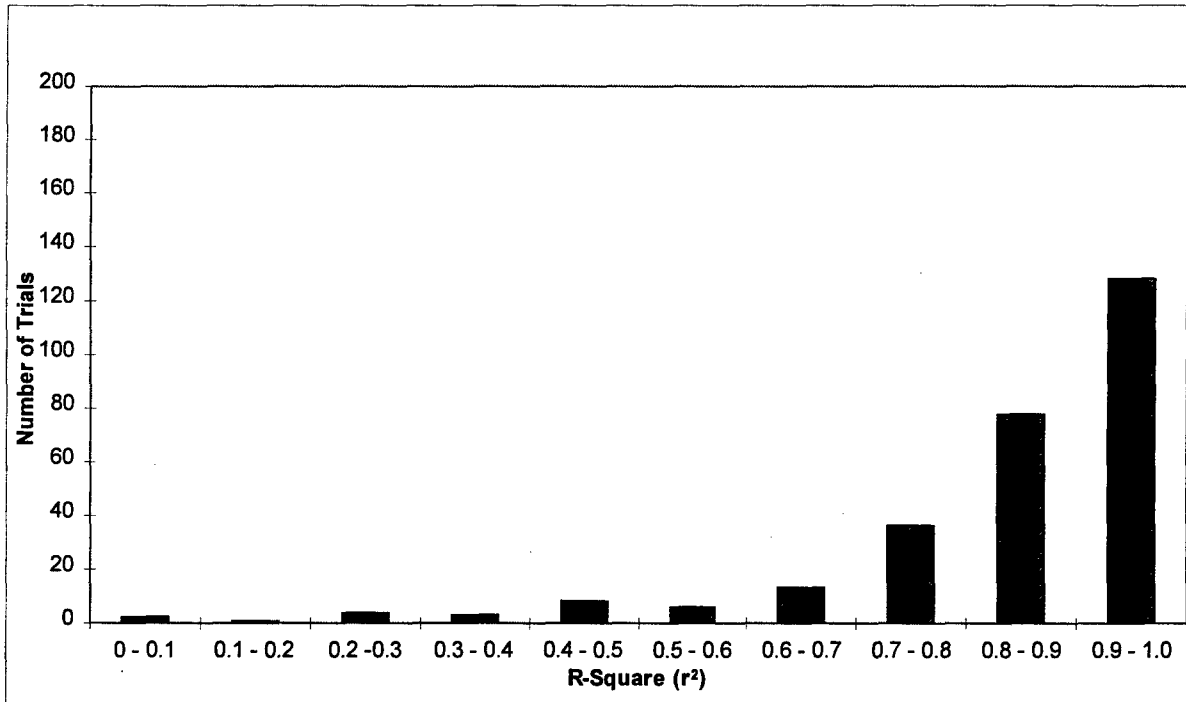


Figure 2.5. Distribution of the  $r^2$ s for the performance of Female Model 10, when the length-strength and force-velocity modulation factors derived from trials in the Pelvic Support Structure were applied to the lifting trials performed in the free-dynamic conditions.

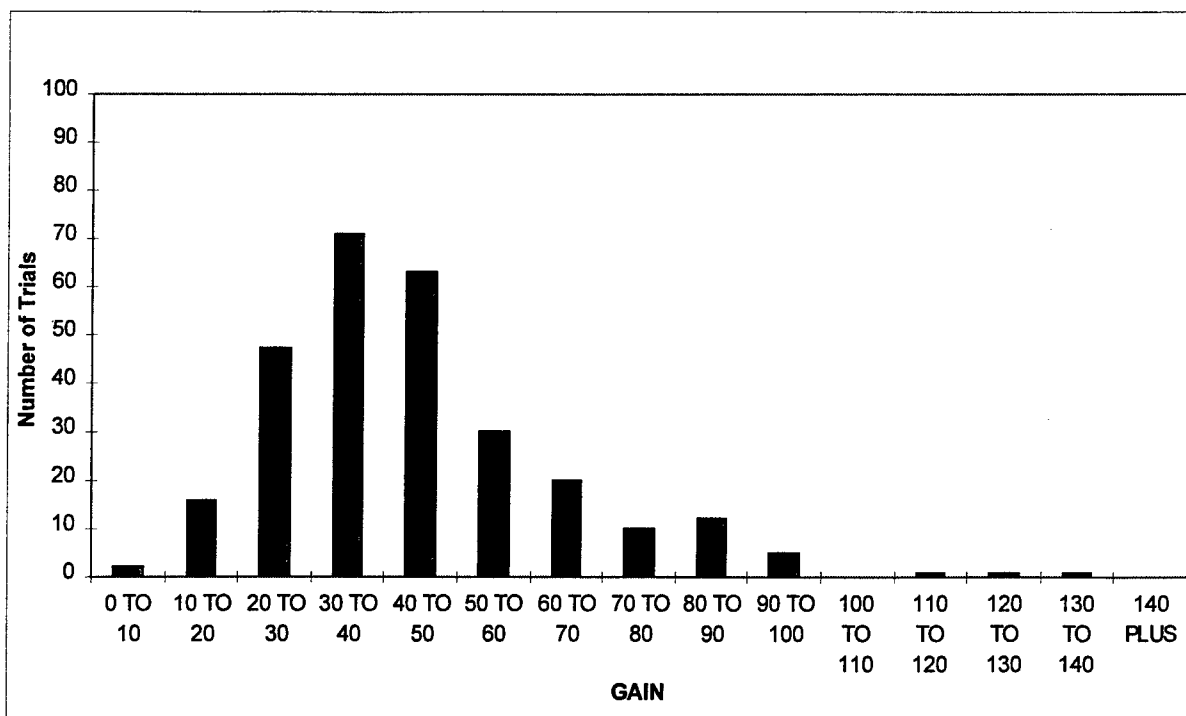


Figure 2.6. Distribution of the estimated muscle gains for the performance of Female Model 10, when the length-strength and force-velocity modulation factors derived from trials in the Pelvic Support Structure were applied to the lifting trials performed in the free-dynamic conditions.

### *Male Model Selection*

All male models investigated resulted in generally acceptable model performance parameters, however, some models performed better than others. Utilizing model inputs based solely from MRI observations (muscle vector locations, Tables 1.83 and 1.84), Model 5 resulted in an increase in the mean gain from the original male model, Model 1 (from 32.0 N/cm<sup>2</sup> to 43.7 N/cm<sup>2</sup>) and a decrease in the AAE (9.85 Nm to 6.89 Nm), and no real change in  $r^2$ . However, utilizing muscle fiber angles from the literature to determine the muscle force vector directions for the external oblique, internal oblique and erector spinae, and using external anthropometric measures which best predicted the male PCSA (Table 2.6), an anatomically oriented biomechanical model resulted with excellent performance parameters (Model 10). Therefore, Model 10 was selected as the “Male Model” for further study in Parts 3 and 4.

As shown in Figure 2.7, the distribution of the  $r^2$ s shows both a high mean and median for Model 10. Figure 2.8 shows the distribution of the estimated muscle gains from the lifting trials in the PSS. The Model 10 length-strength and force-velocity modulation factors determined from the PSS lifting trials were applied to the data from the Free Dynamic lifting trials (Table 2.16). This resulted in a virtually unchanged mean gain (33.8 N/cm<sup>2</sup>), and still highly acceptable mean and median  $r^2$  values (0.91 and 0.95, respectively). The distribution of the  $r^2$ 's from the trials in the free dynamic mode is shown in Figure 2.9, and the distribution of the estimated muscle gains from the free dynamic lifting trials is shown in Figure 2.10.

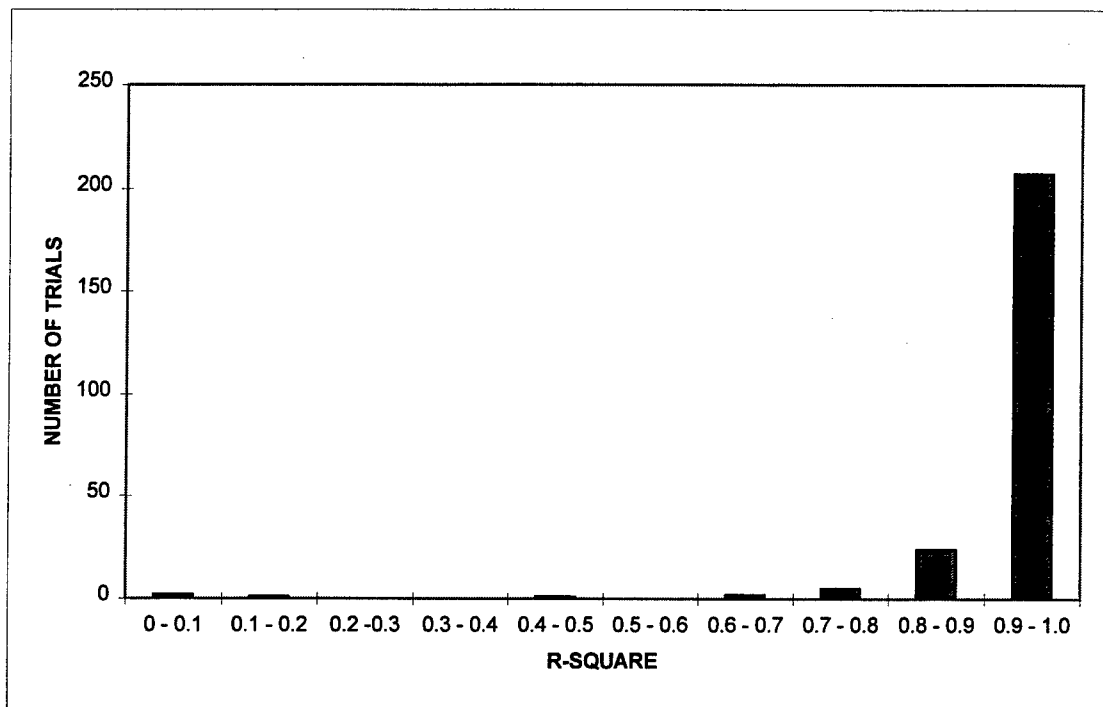


Figure 2.7. Distribution of the  $r^2$ s for the performance of Male Model 10, resulting from lifting trials in the Pelvic Support Structure.

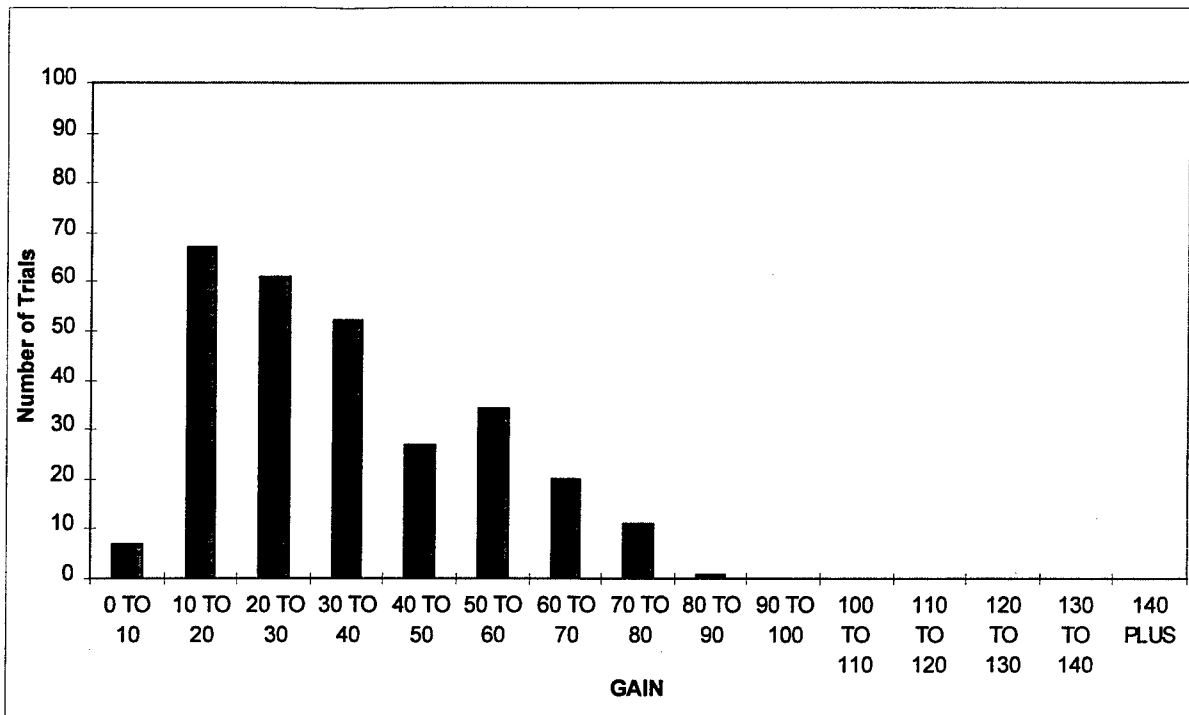


Figure 2.8. Distribution of the estimated muscle gains for the performance of Male Model 10, resulting from lifting trials in the Pelvic Support Structure.

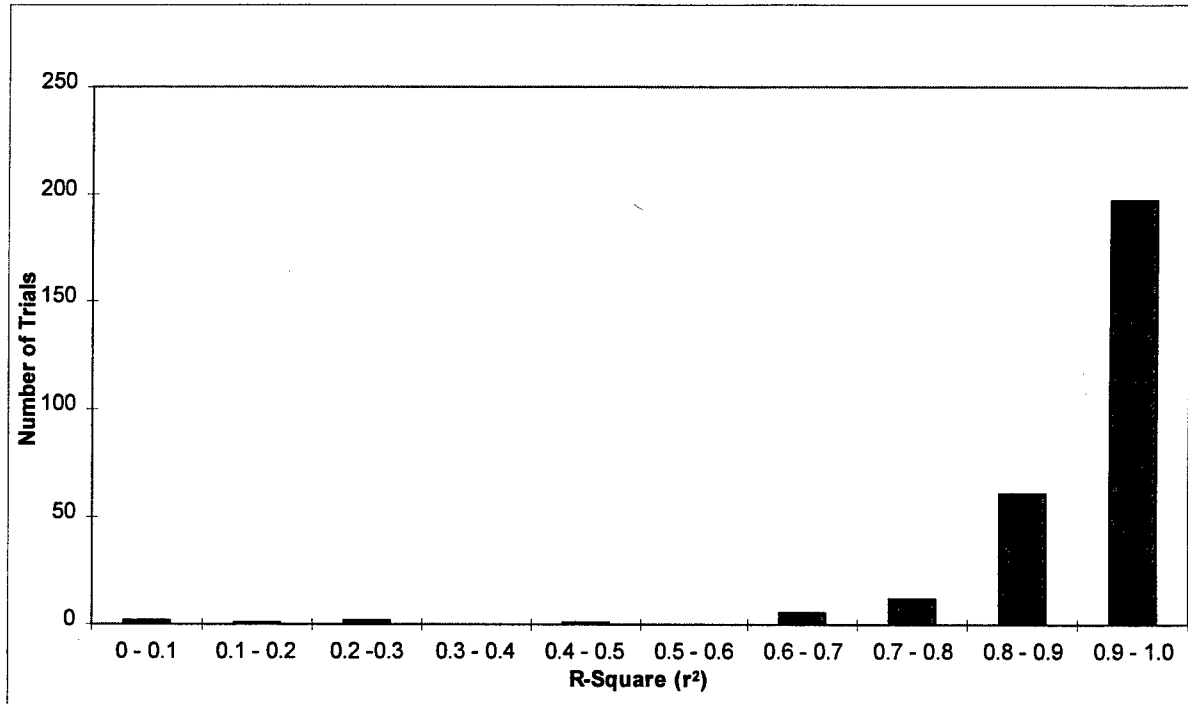


Figure 2.9. Distribution of the  $r^2$ s for the performance of Male Model 10, when the length-strength and force-velocity modulation factors derived from trials in the Pelvic Support Structure were applied to the lifting trials performed in the free-dynamic conditions.

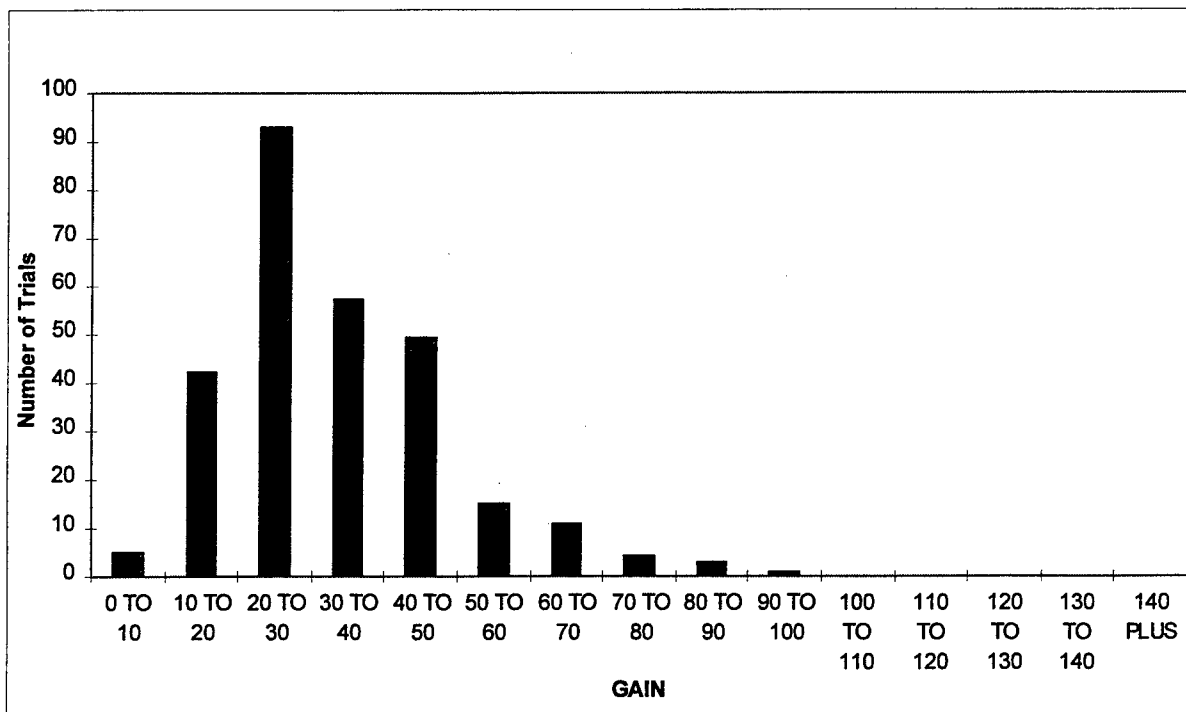


Figure 2.10. Distribution of the estimated muscle gains for the performance of Male Model 10, when the length-strength and force-velocity modulation factors derived from trials in the Pelvic Support Structure were applied to the lifting trials performed in the free-dynamic conditions.

### ***Modulation Factors***

The final female muscle length-strength and force-velocity modulation factors from Female Model 10 are shown below, where equation 2.5 is the female length-strength modulation factor, and equation 2.6 is the female force-velocity modulation factor:

$$f(\text{Length}_j) = -6.06 + 21.93 \times \text{Length}_j - 24.49 \times \text{Length}_j^2 + 9.6 \times \text{Length}_j^3 \quad (\text{Eq. 2.5})$$

$$f(\text{Vel}_j) = 1.039 + 0.126 \times \text{Velocity}_j \quad (\text{Eq. 2.6}).$$

For comparison purposes, the male muscle length-strength and force-velocity modulation factors determined by Granata and Marras (1993) are shown below in Equations 2.7 and 2.8, respectively:

$$f(\text{Length}_j) = -3.25 + 10.2 \times \text{Length}_j - 10.4 \times \text{Length}_j^2 + 4.59 \times \text{Length}_j^3 \quad (\text{Eq. 2.7})$$

$$f(\text{Vel}_j) = 0.4e^{(\text{Vel}_j/0.38)} + 0.76 \quad (\text{Eq. 2.8}).$$

Additionally, the male muscle length-strength and force-velocity modulation factors from Male Model 10 using the trunk muscle geometry from Part 1 (i.e., predicted PCSA, muscle vector locations) are shown below in Equations 2.9 and 2.10:

$$f(\text{Length}_j) = -13.74 + 44.88 \times \text{Length}_j - 47.62 \times \text{Length}_j^2 + 17.49 \times \text{Length}_j^3 \quad (\text{Eq. 2.9})$$

$$f(\text{Vel}_j) = 1.017 - 0.014 \times \text{Velocity}_j \quad (\text{Eq. 2.10})$$

As shown in Figure 2.11, the regression line of the female length-strength modulation factor (equation 2.5) is plotted against the male length-strength modulation factor from equation 2.7 (Granata and Marras, 1993), and also against the male length-strength modulation factor determined from the male MRI data from Part 1 (equation 2.9). The general shape of the three curves are very similar. As shown in Figure 2.12, the female force-velocity modulation factor regression equation (equation 2.6) is plotted against the male force-velocity modulation factor from equation 2.8 (Granata and Marras, 1993) and also against the force-velocity modulation factor for males developed using trunk geometry inputs determined in Part 1 (equation 2.10). The female moment ratio is smaller than the male moment ratio, with this difference increasing as the normalized velocity increases. These two curves developed in this study are different in slope and shape, however, from the male force-velocity modulation factor developed by previous researchers (Granata and Marras, 1993). At every normalized velocity point, the original male model had a force-velocity moment ratio that was less than either the male and female moment ratio, with this difference increasing as the normalized velocity increases.

Table 2.13. Female model results for lifting trials in the pelvic support structure and free dynamic lifting trials as a function of each of the ten models, with different combinations of inputs for the cross-sectional areas, length-strength and force-velocity modulation factors, and vector locations.

Model	Statistic	Pelvic Support Structure			Free Dynamic		
		Gain	$r^2$	AAE	Gain	$r^2$	AAE
1	Mean	34.7	0.93	6.43	35.1	0.87	10.88
	s.d.	14.4	0.08	4.08	20.3	0.15	7.17
	Median	30.8	0.95	5.40	32.1	0.92	9.40
2	Mean	38.1	0.91	6.10	38.2	0.85	9.23
	s.d.	16.7	0.10	3.65	22.4	0.17	6.48
	Median	33.3	0.94	5.20	35.1	0.90	7.40
3	Mean	38.7	0.89	5.96	38.4	0.81	7.68
	s.d.	17.0	0.15	3.64	18.1	0.20	5.91
	Median	34.4	0.93	4.80	33.7	0.89	6.00
4	Mean	46.9	0.91	6.19	46.5	0.84	8.59
	s.d.	18.1	0.11	3.71	21.9	0.17	6.51
	Median	41.6	0.94	5.35	41.1	0.90	6.90
5	Mean	52.8	0.91	5.82	52.5	0.84	8.69
	s.d.	20.3	0.12	3.56	23.5	0.17	6.42
	Median	47.8	0.94	4.80	48.1	0.89	6.90
6	Mean	52.0	0.91	5.83	51.8	0.84	8.89
	s.d.	20.2	0.12	3.62	24.0	0.16	6.65
	Median	47.2	0.94	4.70	46.9	0.90	7.15
7	Mean	50.4	0.90	5.52	48.5	0.84	8.18
	s.d.	20.6	0.12	3.36	21.7	0.17	6.15
	Median	44.4	0.94	4.60	44.3	0.90	6.30
8	Mean	59.4	0.91	5.71	55.4	0.84	8.82
	s.d.	28.4	0.12	3.40	23.6	0.16	6.31
	Median	49.9	0.94	4.85	52.1	0.90	7.20
9	Mean	59.6	0.91	5.70	56.8	0.84	8.58
	s.d.	27.9	0.12	3.43	26.2	0.17	6.23
	Median	50.7	0.94	4.75	51.8	0.89	6.90
10	Mean	47.0	0.92	5.70	44.4	0.84	8.70
	s.d.	21.9	0.10	3.43	20.2	0.17	6.24
	Median	39.7	0.94	5.00	40.2	0.90	7.30

Table 2.14. Male model results for lifting trials in the pelvic support structure and free dynamic lifting trials as a function of each of the ten models, with different combinations of inputs for the cross-sectional areas, length-strength and force-velocity modulation factors, and vector locations.

Model	Statistic	Pelvic Support Structure			Free Dynamic		
		Gain	$r^2$	AAE	Gain	$r^2$	AAE
1	Mean	32.0	0.95	9.85	29.8	0.92	14.96
	s.d.	19.8	0.06	11.51	18.0	0.10	16.49
	Median	26.6	0.97	6.40	24.5	0.95	10.55
2	Mean	35.6	0.94	10.31	33.1	0.92	14.80
	s.d.	21.8	0.08	11.39	18.6	0.10	15.72
	Median	29.9	0.97	6.90	27.0	0.95	10.70
3	Mean	56.6	0.93	7.08	56.2	0.90	11.06
	s.d.	27.0	0.10	4.59	27.0	0.12	9.19
	Median	51.9	0.96	6.00	49.6	0.94	8.00
4	Mean	50.7	0.93	7.16	49.3	0.90	10.39
	s.d.	24.1	0.10	5.45	23.6	0.12	8.58
	Median	47.0	0.96	5.80	43.9	0.93	7.75
5	Mean	43.7	0.94	6.89	43.6	0.91	11.65
	s.d.	21.7	0.09	4.37	20.9	0.11	9.45
	Median	39.5	0.97	5.95	38.5	0.94	8.40
6	Mean	40.6	0.94	7.12	40.1	0.91	11.19
	s.d.	20.2	0.09	5.02	19.2	0.11	9.27
	Median	36.6	0.97	5.90	36.2	0.94	7.85
7	Mean	39.6	0.94	6.78	39.2	0.91	10.92
	s.d.	19.8	0.09	4.18	18.8	0.11	9.10
	Median	35.8	0.96	5.80	35.4	0.94	7.70
8	Mean	40.0	0.94	6.73	41.1	0.91	10.97
	s.d.	18.8	0.09	4.06	19.4	0.11	9.11
	Median	36.1	0.96	5.80	36.9	0.94	7.75
9	Mean	45.8	0.94	7.08	45.1	0.91	11.89
	s.d.	23.5	0.09	4.59	20.9	0.11	9.65
	Median	40.8	0.97	5.85	40.5	0.94	8.55
10	Mean	34.8	0.95	8.21	33.8	0.91	13.41
	s.d.	17.8	0.08	5.99	15.8	0.10	11.06
	Median	30.9	0.97	6.35	30.0	0.95	10.00

Table 2.15. Female model performance results from Model 10 (see Table 2.3 for model inputs), compared to the model performance results when applied to trials from the free-dynamic lifting exertions.

Model	Statistic	Pelvic Support Structure			Free Dynamic		
		Gain	$r^2$	AAE	Gain	$r^2$	AAE
10	Mean	47.0	0.92	5.70	44.4	0.84	8.70
	s.d.	21.9	0.10	3.43	20.2	0.17	6.24
	Median	39.7	0.94	5.00	40.2	0.90	7.30

Table 2.16. Male model performance results from Model 10 (see Table 2.5 for model inputs), compared to the model performance results when applied to trials from the free-dynamic lifting exertions.

Model	Statistic	Pelvic Support Structure			Free Dynamic		
		Gain	$r^2$	AAE	Gain	$r^2$	AAE
10	Mean	34.8	0.95	8.21	33.8	0.91	13.41
	s.d.	17.8	0.08	5.99	15.8	0.10	11.06
	Median	30.9	0.97	6.35	30.0	0.95	10.00

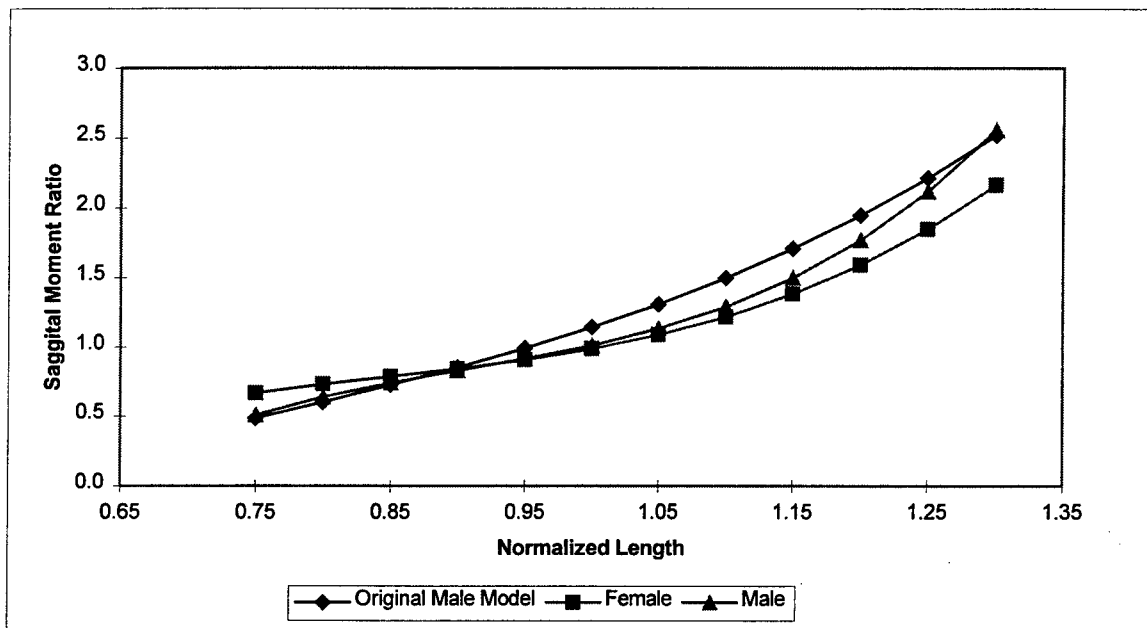


Figure 2.11. Female Model 10 length-strength versus Male Model 10 length-strength modulation factor comparison.

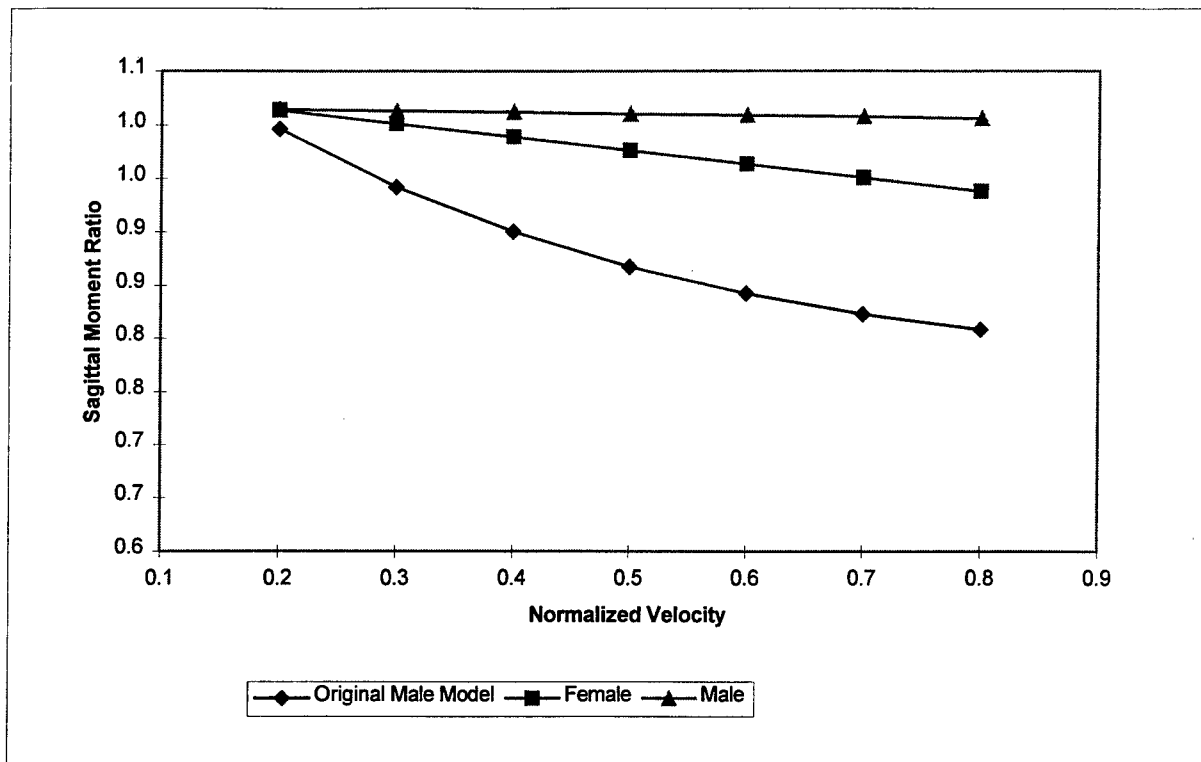


Figure 2.12 Female Model 10 force-velocity versus Male Model 10 force-velocity modulation factor comparison.

## Discussion

The results described in this research on female muscle length-strength and force-velocity relationships have not previously been reported by other researchers. Thus, there are no other female datasets available for comparison purposes. The length-strength modulation factor for the females (Figure 2.11) appears to follow very closely the shape of the length-strength relationship found by other researchers (Marras and Sommerich, 1991b; Granata and Marras 1993; Davis et al. 1998), as well as the male biomechanical model (Granata and Marras, 1993) modified to include the PCSAs and vector locations determined from Part 1 (Male Model 10). However, this study did result in different shapes for the force-velocity modulation factors from previously published research. As shown in Figure 2.12, the female force-velocity modulation curve demonstrated a slightly greater negative slope than the male force-velocity curve derived in this study. However, these two curves are different from that determined on males from previous literature (Granata and Marras, 1993). These differences may be indicative of more realistic and more accurate trunk muscle geometry used as inputs into the models, including the

PCSAs and the muscle vector locations and directions between the origin and insertion. The development of these modulation factors for the females followed previously used methods, including restricting the data to a sagittal flexion range to ensure that the active loading structures as well as limiting the lifting trials to sagittally symmetric exertions, and modeling the erector spinae muscle only. The decision to model only the erector spinae muscle appears valid, as the descriptive results for the normalized muscle activity revealed that this muscle group was by far the most active at all velocities and weights examined.

The systematic approach used to develop the length-strength and force-velocity modulation factors allowed a systematic evaluation of the contribution of different inputs into the biomechanical model, through examination of the model performance parameters of  $r^2$ s, muscle gains, and the average absolute error (AAE) between the predicted and measured moments. The improvement of the biomechanical model performance of the female model (Female Model 10) over the original male model (Female Model 1) was accentuated when utilizing the female specific physiological cross-sectional area equations as well as the female length-strength and force-velocity modulation factors. The mean and median muscle gain were in the physiologically valid range (47.0 N-cm<sup>-2</sup> and 39.7 N-cm<sup>-2</sup>, respectively), predictability of the sagittal moment remained acceptable with high  $r^2$ s (mean and median  $r^2$  of 0.92 and 0.94, respectively), and the average absolute error between the predicted and measured sagittal moment remained low.

Although the original research proposal called for the development of the length-strength and force-velocity modulation factors solely from free-dynamic lifting exertions, these trials resulted in unacceptable model performance parameters. Thus, it was decided to develop these modulation factors from trials where the hips were secured, and apply the resulting model to the free-dynamic data. The model performance parameters from the free-dynamic trials changed very little when the model based on data from the PSS trials were applied. The mean muscle gain decreased by 2.2% for both females and males, the mean  $r^2$  decreased to still respectable values of 0.84 and 0.91 for females and males, respectively, and the AAE increased to 8.7 Nm and 13.4 Nm for females and males, respectively. These results for free dynamic lifting represent an improvement from similar trials performed by previous researchers, where free-dynamic exertions by males modeled by Granata and Marras (1995) resulted in a mean muscle gain of 64.9 N/cm<sup>2</sup>, mean  $r^2$  of 0.81, and an AAE of 17.5 N-m for sagittally symmetric exertions.

Thus, the biomechanical models for both females and males represent an improvement in model performance when compared to prior biomechanical models evaluating similar lifting trials.

### ***Limitations***

A few limitations do exist at this point in the research. First, the lifting exertions that were modeled consisted of only sagittally symmetric exertions, and the relationship between spinal loading and muscle activity may be different in asymmetric conditions. These relationships, however, will be investigated in Part 3 of this, during a validation phase.

Decreases in the model performance parameters occurred when applying the length-strength and force-velocity modulation factors to the lifting trials performed in the free-dynamic mode. Specifically, for the selected model (Model 10 for both males and females), the mean absolute error increased from 5.7 Nm to 8.7 Nm for females, and from 8.2 Nm to 13.4 Nm for males. This may be a function of allowing the pelvis and hips to rotate and further changing the length-strength and force-velocity relationships in the free-dynamic mode, and thus changing the mechanics of the lifting and resulting EMG values. This very subject is currently being investigated in our lab, to determine the influence of allowing the hips and pelvis to rotate during lifting activities.

### **Conclusions**

The use of female trunk muscle physiological cross-sectional areas and the derived female muscle length-strength and force-velocity relationships, when applied to the existing male EMG-assisted biomechanical model, resulted in an increase in performance over the male only biomechanical model. This included high  $r^2$ 's between the predicted and measured moment, physiologically valid muscle gain values, and small magnitudes of error between the predicted and measured moment. The original procedure used to collect the data, however, had to be adjusted to reduce the variability in the length-strength and force-velocity modulations resulting from allowing the hips and pelvis to rotate during the lifting exertions. Thus, the lifting trials performed with the pelvis constrained resulted in very good model performance, and when applied to the trials collected during the free dynamic conditions still resulted in acceptable model performance parameters.

## **Part 3: Implementation and Validation of the EMG-assisted Model for Female Subjects.**

### **Introduction**

Much of the manual material handling activities (e.g., lifting) are not performed in a sagittally symmetric posture, but must be performed with trunk asymmetry involved. Thus, motions such as twisting or lateral side bending most likely are involved to some degree in most lifting activities. The biomechanical model parameters determined in Part 2 were developed under sagittally symmetric lifting exertions. The goal of Part 3 was to use the parameters developed for the females and apply to asymmetric lifting exertions, and adjust the model such that the model performs well under sagittally symmetric exertions as well as asymmetric exertions.

### **Background and Objectives**

The Biodynamics Laboratory EMG-assisted model, which predicts the three-dimensional spinal loading experienced by subjects during manual handling tasks currently has only been validated for males. The results of Part 1 and Part 2 indicate that females differ from males with respect to muscle anthropometry (e.g., muscle physiological cross-sectional areas as a function of external anthropometry, and muscle lines of action), as well as muscle length-strength and force-velocity relationships. These differences undoubtedly will have an affect on the accuracy of the spinal loads predicted by the EMG-assisted biomechanical model. Thus, the objectives of Part 3 include 1) utilizing the model parameters derived from Part 1 and Part 2 and implement these into the current form of the EMG-assisted biomechanical model, and 2) validation of the female-specific EMG-assisted biomechanical model for sagittally-symmetric and asymmetric lifting exertions.

### **Administrative Note**

In the accepted research proposal, weight conditions of 15, 50 and 80 lbs were to be used for female as well as male subjects. However, it became clear that we would be unable to find females capable of lifting 80 lbs up to a height of 102 cm above the floor. According to Snook and Ciriello (1991), for task parameters similar to those in this study, less than 10% of the female population is capable of lifting 50 lbs from knuckle to shoulder level, with even less capable of

lifting 80 lbs to this level. Thus, to eliminate the possibility of injury to female subjects, the experimental design was modified to still allow three weight levels, including 15, 30, and 50 lbs. Although we thought this weight range was more realistic for the capabilities of the female population, especially for the number of repetitions required by our experimental design for this study, only 23 of the 40 female subjects could lift the 50 lb loads to a height of 102 cm above the floor. Thus the analysis of the biomechanical model performance parameters in Part 3 as well as the predicted spinal loading in Part 4 includes all the subjects that could complete all the experimental conditions, as well as the female subjects who could not lift the 50 lbs.

## **Methods**

### *Experimental Design*

The subjects performed free-standing lifts representative of select military material handling tasks, using different weights, different starting and destination heights, as well as asymmetric exertions.

The independent variables are intended to simulate a range of realistic military material handling conditions as specified in the MOS Physical Task list (U.S. Army Infantry School), and to assess model sensitivity and applicability for female subjects. The independent variables include gender, weight of lift (15, 30, and 50 lbs), degree of asymmetry for the starting position of the lift (0 and 60 degrees), and lift condition (floor to waist, floor to 102 cm, knee to waist, and knee to 102 cm above the floor). Each combination of the task independent variable was performed twice by each subject. This repeated measures design resulted in 48 experimental trials per subject, thus permitting sensitivity analysis of those material handling factors that might influence model performance, as well as identifying gender differences in model performance as a function of the other independent variables. The presentation order of the experimental conditions were randomized and subjects were allowed at least two minute rest (Caldwell et al. 1974) or as much time as needed between trials to minimize the risk of fatigue and carryover effects on the results.

The dependent variables consisted of several model measures of performance. For a model to be considered robust and accurate it must, 1) accurately represent the changes in trunk and spine loading over time and, 2) accurately estimate the magnitude of the trunk loading during the lift. The squared correlation ( $r^2$ ) between the measured and predicted trunk moments

will serve as an indicator of the model ability to accurately assess the changes in trunk loading. Measured versus predicted magnitudes of the load imposed upon the trunk were assessed by examining the average absolute error (AAE) between the two measures. In addition, predicted muscle gains were used as a measure of the physiologic validity.

### ***Subjects***

The subjects consisted of 40 females and 20 males, all of generally observed military age. Male subjects were recruited to permit comparison and calibration of model performance and results with female subjects. Subject anthropometric measures are shown in Table 3.1.

Table 3.1 Anthropometric measurements (mean and s.d.) from female and male subjects.

Anthropometric Variable	Females	Males
Age (yrs)	23.5 (5.6)	23.8 (3.6)
Standing Height (cm)	165.2 (6.5)	177.0 (8.9)
Weight (kg)	60.1 (7.6)	73.9 (13.6)
Trunk Width at Iliac Crest (cm)	26.5 (2.2)	28.2 (2.8)
Trunk Depth at Iliac Crest (cm)	18.0 (2.1)	20.1 (2.6)
Trunk Width at Xyphoid Process (cm)	26.6 (1.8)	30.2 (1.9)
Trunk Depth at Xyphoid Process (cm)	19.1 (2.1)	20.7 (2.8)
Body Mass Index (kg/m <sup>2</sup> )	22.0 (2.0)	23.6 (3.8)

### ***Equipment***

The equipment used in this part has been previously described in Part 2. Specifically, subjects stood on a force plate (not moving their feet), and performed the lifts from ankle and knee heights to destinations of waist height and 102 cm above the floor. The forces and moments measured by the force plate were rotated and translated to the estimated position of the L<sub>5</sub>/S<sub>1</sub> through the use of a sacral location orientation monitor (SLOM) and a pelvic orientation monitor (Fathallah et al., 1997). The subjects trunk three-dimensional position, velocity, and acceleration were measured by an LMM (Marras et al, 1992), and trunk muscle activity was

measured through electromyography, placed over right and left sides of five trunk muscle groups (Mirka and Marras, 1993).

All data signals were collected simultaneously through customized Windows™ based software developed in-house. The signals were collected at 100 Hz and recorded on a 486 computer and stored for later analysis.

### ***Experimental Procedure***

Upon the subjects arrival to the testing laboratory, the subjects read and signed a consent form. Female subjects took a pregnancy test to determine their pregnancy status. None of the female subjects tested positive on the pregnancy test, and were permitted to continue with the study. Anthropometric data and demographic information were recorded next. Surface electrodes for the EMG were then applied over each of ten trunk muscles, while skin impedance's were kept below 500 k $\Omega$ . Maximum voluntary contractions (MVCs) for each of the trunk muscles were obtained, with the subjects performing MVCs for trunk extension and flexion static exertions, as well as right and left twisting and right and left lateral bending, all against a constant resistance. All resulting trunk muscle EMG data obtained from the experimental trials were then normalized to the maximum EMG activity obtained during these six directional MVCs. Following the MVCs, an LMM was placed on the subject's back, and the subject was attached to the SLOM as they stood upon the force plate. Each of the 48 experimental trials were then presented to the subject in a randomized order. The subjects were allowed to lift the load from the starting position to the destination using a free-style lift, however, they were instructed to keep their feet stationary on the force plate during the lifting exertion.

### ***Data Analyses***

Female biomechanical Model 10 developed in Part 2 were used in this part of the study. The normalized EMG signals, trunk position and velocity data from the LMM, and the predicted physiological cross-sectional muscle areas and vector locations from Part 1 were input into the biomechanical model to predict the forces and moments imposed upon the L<sub>5</sub>/S<sub>1</sub> joint. Experimental data collected from the male subjects was input into the EMG-assisted biomechanical model validated for males (Granata and Marras, 1993) which was updated to include the predictions of the physiological cross-sectional areas and vector locations determined

from the males in Part 1 (male model 10). The model performance parameters from the male biomechanical model were used for comparison purposes to those from the female model.

Model performance was assessed by examining the predictability, accuracy, and validity of model performance parameters. Time dependent predicted trunk moments were compared with the measured trunk moment via an  $r^2$  statistic. An  $r^2$  value of 0.80 or above across all trials indicates the model is working well. The accuracy of the model prediction was assessed by examining the absolute error between the measured and predicted moment, as a function of the measured moment, averaged continuously over the duration of the exertion. Thus, the average absolute error was expressed as a percent of the maximum measured moment in the sagittal plane. The model was considered acceptable in accuracy if the average absolute error was no greater than 20% of the measured moment in the sagittal plane. Predicted muscle gains were also examined to assure physiological feasibility. To be considered valid, the predicted muscle gains must fall between 30 N/cm<sup>2</sup> and 90 N/cm<sup>2</sup> (McGill et al, 1988; Reid and Costigan, 1987; Weis-Fogh and Alexander, 1977).

### ***Statistical Analysis***

Descriptive statistics describing the central tendency (mean and median) and the variability of the model performance parameters were first performed. The data were further described by determining the percent of trials where the  $r^2$  was above 0.80, collapsed over all conditions, as well as a function of the experimental conditions. The muscle gain was also described by determining the percent of trials with gains in the physiological range (30 N/cm<sup>2</sup> to 90 N/cm<sup>2</sup>), collapsed across all experimental conditions, as well as a function of the experimental conditions.

Analysis of Variance (ANOVA) procedures were used to test the significance of the model performance parameters (i.e.,  $r^2$ , gain, and AAE) as a function of the independent variables. The statistical analysis consisted of a mixed four-way repeated measures ANOVA, with one between factor (gender) and three repeated factors (weight, asymmetry and lift condition). Significant gender effects in model performance parameters were examined by testing the two-way interactions between gender and the other independent variables (i.e., weight, asymmetry and lift condition). Significant differences will indicate different levels of model performance between the conditions and can be used as a model sensitivity measure.

Tukey post-hoc procedures were used to understand the nature of these differences for the main effects using a family-wise Type I error rate of  $\alpha=0.05$ . To identify where the gender differences existed for significant gender interactions, post-hoc evaluations consisting of *t*-tests were used while adjusting the Type I error rate using a Bonferroni adjustment (Keppel 1991).

## Results

The Analysis of Variance on the biomechanical model performance parameters indicated that model performance varied significantly as a function of the experimental conditions (Table 3.2). The muscle gain varied as a function of gender for the lifting condition and weight of the lift, and also as a function of asymmetry independent of gender. Post-hoc tests revealed that males had a significantly higher gain for the 50 lb weight condition (7.5 N/cm<sup>2</sup> higher than females) (Figure 3.1). Males exhibited greater gain for the lift condition starting at the knee and ending at the waist (6.5 N/cm<sup>2</sup> higher than females) (Figure 3.2). Asymmetric lifts resulted in a small but significant increase in the gain over sagittally symmetric lifts (44.8 N/cm<sup>2</sup> to 47.3 N/cm<sup>2</sup>), independent of gender.

The squared correlation coefficient ( $r^2$ ) was also influenced statistically by differences in the experimental conditions, although the magnitudes of the differences were quite small. As shown in Table 3.2, gender differences existed as a function of the weight of the load, with post-hoc tests indicating that males had a greater  $r^2$  than females for both the 30 lb and 50 lb weight conditions, although these differences were rather small (Figure 3.3).

The ANOVA results also found that the prediction error for the sagittal moment was only affected by the asymmetry of the starting point of the lift, with the zero degree condition resulting in an average error of 8.6% error and the 60 degree average error increasing slightly to 9.8%.

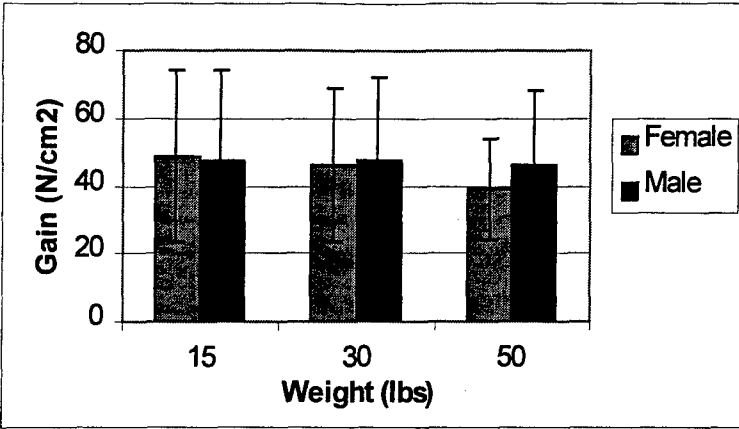


Figure 3.1. Mean muscle gain as a function of gender and weight.

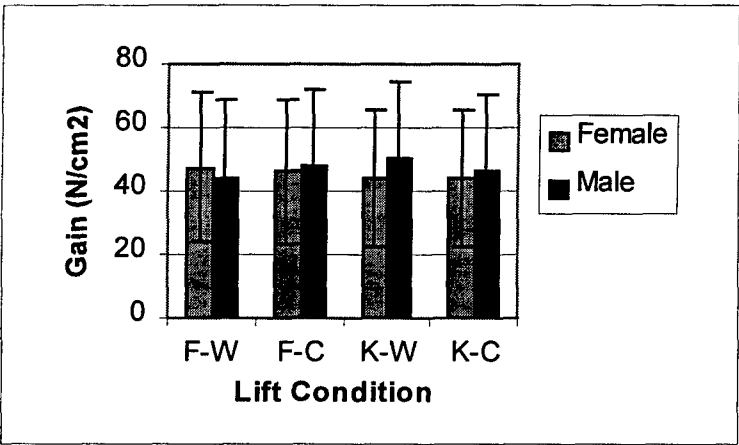


Figure 3.2. Mean muscle gain as a function of gender and lift condition.

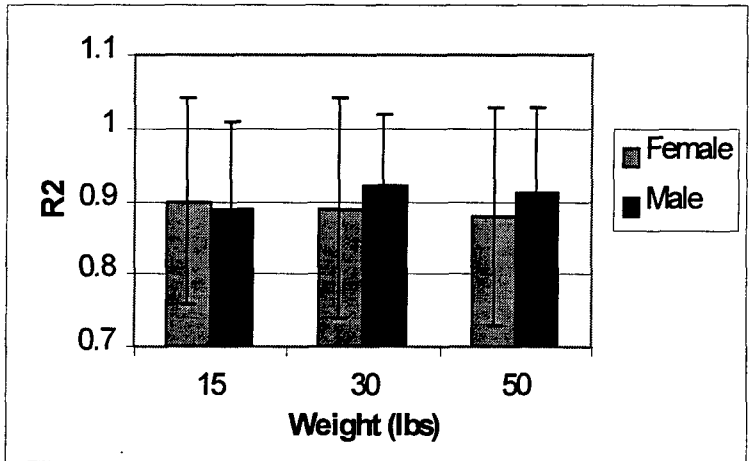


Figure 3.3. Squared correlation ( $r^2$ ) as a function of gender and weight.

Table 3.2 Analysis of Variance p-values on the EMG biomechanical model performance parameters as a function of the independent variables for both males and females. Shaded cells represent significant effects at  $p \leq 0.05$ .

Independent Variable	Model Performance Parameter		
	Gain	$r^2$	AAE/Moment
Gender (G)	0.7611	0.2842	0.2891
Weight (W)	0.0002	0.2994	0.2176
Asymmetry (A)	0.0003	0.2278	0.0329
Lift Condition (C)	0.1122	0.3307	0.7450
G × W	0.0133	0.0043	0.1085
G × A	0.9626	0.3651	0.8731
G × C	0.0001	0.6368	0.9894

The distribution of  $r^2$  for both genders can be examined as a function of the different experimental conditions, as shown in Table 3.6. Both females and males exhibited mean  $r^2$ s above 0.80, with females ranging generally between 0.88 and 0.90 across all levels of the experimental conditions. The  $r^2$ s for males spanned a similar range (between 0.89 and 0.92) across all levels of the experimental conditions. The median  $r^2$  across the different levels of the experimental conditions were generally between 0.93 and 0.95 for females, and between 0.93 and 0.97 for males, indicating a slightly skewed distribution of the  $r^2$ s. Overall, 86.1% of the female trials resulted in  $r^2$ s greater than 0.80 where between 83.7% and 87.9% of the female trials resulted in  $r^2$ s greater than 0.80 across the different experimental conditions (Table 3.6). For males, 87.4% of all trials resulted in  $r^2$ s greater than 0.80, where between 82.3% to 91.3% of the trials across the different experimental conditions resulting in  $r^2$ s greater than 0.80. Thus, across all experimental conditions, close to 90% of the trials resulted in  $r^2$ s greater than 0.80. Collectively, the distribution of the  $r^2$  values indicates acceptable response to changes of the sagittal moment for both male and female biomechanical models.

The distribution parameters for the gain for both genders as a function of the experimental conditions are shown in Table 3.7. Overall, the gains between male and female were similar in magnitude (mean gains of 45.3 and 47.3 N-cm<sup>-2</sup> for females and males, respectively). The percent of trials with gains within the physiologic range (30 to 90 N-cm<sup>-2</sup>) was slightly higher for females (74.1%) than males (70.2%). The mean and median gains for

both genders were similar, indicating a slightly skewed distribution, with the magnitudes falling within the estimated physiologic range. Thus, the majority of the trials resulted in valid predicted muscle gains.

Finally, the error in prediction of the lifting moment as compared to the measured sagittal moment was within an acceptable range for both males and females. The overall AAE as a percent of the measured moment in the sagittal plane for females was 10% for females and 8% for males. Thus, the AAE was well within the 20% boundary of an acceptable model prediction error.

Table 3.3 Overall biomechanical model performance parameters for males and females, collapsed across all experimental conditions.

Statistical Measure	Females			Males		
	Gain (N-cm <sup>-2</sup> )	r <sup>2</sup>	AAE/Moment	Gain (N-cm <sup>-2</sup> )	r <sup>2</sup>	AAE/Moment
Mean	45.3	0.89	0.10	47.3	0.91	0.08
s.d.	22.4	0.14	0.07	24.3	0.11	0.05
median	41.6	0.94	0.09	41.1	0.95	0.07

Table 3.4 Descriptive statistics (mean and standard deviation) for the muscle gain,  $r^2$  and AAE (as a percent of measured moment) model performance parameters for the female biomechanical model.

Variable	Weight (lbs)			Asymmetry (deg)	Lift Condition*				
	15	30	50		F - W	F - C	K - W	K - C	
Gain (N/cm <sup>2</sup> )	48.8 (25.1)	46.1 (22.7)	38.9 (15.1)	44.1 (21.5)	46.6 (23.3)	47.5 (23.6)	46.1 (23.0)	43.8 (21.5)	43.9 (21.4)
$r^2$	0.90 (0.14)	0.89 (0.15)	0.88 (0.15)	0.88 (0.16)	0.90 (0.13)	0.89 (0.14)	0.88 (0.16)	0.90 (0.14)	0.89 (0.14)
AAE/Moment	0.10 (0.08)	0.10 (0.06)	0.10 (0.06)	0.09 (0.08)	0.11 (0.06)	0.10 (0.08)	0.10 (0.07)	0.10 (0.07)	0.10 (0.07)

\* F-W = Floor to Waist;

F-C = Floor to Chest (102 cm above the floor);

K-W = Knee to Waist;

K-C = Knee to Chest (102 cm above the floor);

Table 3.5 Descriptive statistics (mean and standard deviation) for the muscle gain,  $r^2$  and AAE (as a percent of measured moment) model performance parameters for the male biomechanical model.

Variable	Weight (lbs)			Asymmetry (deg)	Lift Condition*				
	15	30	50		F - W	F - C	K - W	K - C	
Gain (N/cm <sup>2</sup> )	47.7 (26.3)	47.7 (24.7)	46.4 (21.7)	46.0 (23.1)	48.5 (25.4)	44.4 (24.3)	48.0 (24.0)	50.3 (24.4)	46.4 (24.3)
$r^2$	0.89 (0.12)	0.92 (0.10)	0.91 (0.12)	0.91 (0.11)	0.91 (0.12)	0.92 (0.11)	0.90 (0.12)	0.90 (0.10)	0.91 (0.12)
AAE/Moment	0.09 (0.05)	0.08 (0.05)	0.09 (0.05)	0.08 (0.04)	0.09 (0.05)	0.09 (0.05)	0.09 (0.05)	0.08 (0.05)	0.08 (0.05)

\* F-W = Floor to Waist;

F-C = Floor to Chest (102 cm above the floor);

K-W = Knee to Waist;

K-C = Knee to Chest (102 cm above the floor);

Table 3.6 Model  $r^2$  descriptive statistics for male and female biomechanical models as a function of the independent variables.

Independent Variable	Female			Male			
	Mean	Median	% $r^2 \geq 0.80$	Mean	Median	% $r^2 \geq 0.80$	
Weight (lbs)	15	0.90	0.95	87.8	0.89	0.93	82.3
	30	0.89	0.93	85.1	0.92	0.95	91.3
	50	0.88	0.93	85.0	0.91	0.96	88.1
Asymmetry (deg)	0	0.88	0.93	85.2	0.91	0.94	89.0
	60	0.90	0.94	86.9	0.91	0.96	85.8
Lifting Condition*	F - W	0.89	0.94	87.8	0.92	0.97	86.6
	F - C	0.88	0.93	83.7	0.90	0.94	88.3
	K - W	0.90	0.94	87.9	0.90	0.94	88.3
	K - C	0.89	0.94	84.8	0.91	0.95	86.3
Overall Results	0.89	0.94	86.1	0.91	0.95	87.4	

\* F-W = Floor to Waist;

F-C = Floor to Chest (102 cm above the floor);

K-W = Knee to Waist;

K-C = Knee to Chest (102 cm above the floor);

Table 3.7 Model muscle gain descriptive statistics for male and female biomechanical models as a function of the independent variables.

Independent Variable	Female			Male			
	Mean	Median	Percent 30≤Gain≤90	Mean	Median	Percent 30≤Gain≤90	
Weight (lbs)	15	48.8	43.3	72.5	47.7	41.8	70.1
	30	46.1	41.5	74.7	47.7	40.9	71.8
	50	38.9	37.4	75.2	46.4	40.9	66.9
Asymmetry (deg)	0	44.1	40.9	74.5	46.0	40.9	68.8
	60	46.6	42.3	73.7	48.5	41.2	71.6
Lifting Condition*	F - W	47.5	42.9	69.5	44.4	38.4	73.3
	F - C	46.1	42.0	72.5	48.0	42.4	66.8
	K - W	43.8	40.1	76.6	50.3	45.9	70.0
	K - C	43.9	41.6	77.9	46.4	38.9	70.2
Overall Results	45.3	41.6	74.1	47.3	41.1	70.2	

\* F-W = Floor to Waist;

F-C = Floor to Chest (102 cm above the floor);

K-W = Knee to Waist;

K-C = Knee to Chest (102 cm above the floor);

## Discussion

Collectively, these findings indicate that the female model (Model 10 from Part 2) utilizing inputs from the MRI results from Part 1 and the length-strength and force-velocity modulation factors developed in Part 2 resulted in an acceptable model based on the magnitudes and distribution of the biomechanical model performance parameters. The majority of the trials resulted in acceptable  $r^2$ s (86.1% greater than  $r^2=0.80$  with a mean of 0.89 and median of 0.94), with physiologically valid gains (mean gain of 45.3 N/cm<sup>2</sup>) and a low mean error magnitude of prediction of the sagittal moment (10.0% error).

The model performance parameters from the female biomechanical model compare favorably with the model performance parameters from a male biomechanical model (Granata and Marras, 1993), which was updated using the results of male PCSA and vector locations from Part 1 of this study (male model 10). The significant difference between the  $r^2$ s as a function of gender and weight of the load was no greater than 3%, which represents a very small biological effect. Muscle gain also showed a significant gender effect with the weight of the lift, where the largest difference was 7.5 N/cm<sup>2</sup> at the 50 lb condition. This represents a 19.3% larger gain for males over females at this weight. Similarly, for the lift condition, male muscle gain was greatest for the knuckle to waist condition, representing a 12.9% increase in gain compared to the females. This increase may be reflective of a multitude of differences between males and females, including differences in muscle size, fiber type composition of the extensor muscles, differences attributed to the length-strength and force-velocity modulation factors, as well as real differences in the force producing capability of the muscles. Thus, while a significant difference exists for muscle gain between genders as a function of weight, there may be many factors contributing to this difference, and more research is needed to identify the true effect.

Results of this validation effort compare favorably with the results of the biomechanical model performance parameters resulting from Part 2 of this study. The overall model performance parameters during this validation phase were consistent with those observed in Part 2, determined during the development of the length-strength and force-velocity modulation factors. The model, developed from sagittally symmetric controlled velocity lifts in Part 2 resulted in a mean  $r^2$  of 0.92, with the mean gain of 47.0 N-cm<sup>-2</sup> for the data derived with the hips secured, and mean  $r^2$  and gain of 0.84 and 44.4 N-cm<sup>-2</sup>, respectively, when applied to the

data from sagittally symmetric controlled velocity lifts performed under free dynamic conditions. The mean  $r^2$  and gain from Part 3 were 0.89 and 45.3 N-cm<sup>-2</sup>.

The model performance parameters for both female and male models represent an improvement compared with other EMG-assisted biomechanical models validated under similar experimental conditions. Granata and Marras (1995) found an average gain for free-dynamic exertions of 64.9 N-cm<sup>-2</sup> for sagittally symmetric lifts, with mean  $r^2$ s of 0.82, and percent error prediction less than 15%. Additionally, 86.1% of the female trials resulted in  $r^2$ s above 80%, and 87.4% of the male experimental trials had  $r^2$ s greater than 80%. Thus, the results for both male and female biomechanical models developed in Part 2 and Part 3, which utilizes trunk geometry data determined from MRI scans from Part 1, as compared to previously validated models, resulted in predictions which were better able to predict changes in the measured moment (e.g., higher  $r^2$ s), had lower but still valid gain values, and resulted in less prediction error.

### ***Limitations***

Although the biomechanical models which have been developed up to this point have resulted in very acceptable model performance, the model is only capable of assessing active trunk forces and is not sensitive to passive loading of the spine. While it is possible that some MMH activities do involve extreme trunk flexion (greater than 45 degrees sagittal flexion) which then rely increasingly on passive structures of the low back, surveillance studies have demonstrated that trunk flexion in excess of 45 degrees account for less than 5% of industrial MMH lifts (Marras et al. 1993, 1995). Thus, neglecting passive spine loading does not present a large problem.

### **Conclusions**

The resulting female EMG-assisted biomechanical model, which used trunk geometry inputs developed in Part 1, and the length-strength and force-velocity modulation factors derived in Part 2 has resulted in very acceptable model performance parameters. The high mean and median  $r^2$ s, low error of prediction for the measured moment, combined with physiologically valid muscle gains indicates that the biomechanical model is a valid model for the prediction of female spinal loading during free-dynamic three-dimensional lifting exertions.

## **Part 4: Assess Biomechanical Loads on the Female Spine During Military MMH**

### **Introduction**

Biomechanical risk of injury to the low back can be assessed using estimates of spinal loading derived from validated biomechanical models and comparing these estimates to tolerance limits of the soft tissues of interest. Thus, assessing risk of low back injury to female army personnel during military MMH would be assessed by predicting the shear forces and compression forces on the L<sub>5</sub>/S<sub>1</sub> intervertebral joint, and comparing these resulting values with intervertebral disc tolerance data as a function of age and gender.

### **Background and Objectives**

Damage to the soft tissues of the lower back can occur when the magnitude of loading on the soft tissues increases to levels above the threshold level of the tissue (McGill 1997; NIOSH 1981). According to NIOSH (1981), microfractures of the vertebral endplates would be expected in 50% of the working population at compression values of 6400 N. Increases in the magnitudes of biomechanical variables such as awkward postures of the trunk (asymmetry) and increases in the weight of the load lifted have been shown to result in increases of spinal loading as predicted by dynamic male biomechanical models (Marras and Sommerich 1991a,b; Granata and Marras 1993; Mirka and Marras 1993; Marras and Granata 1995, 1997; Granata and Marras 1995). These studies are further supported by cadaveric research (Adams and Hutton 1983; Adams et al. 1993; Adams et al. 1994) that have shown the initiation of failures to the intervertebral disc segments occurred under increases in magnitude and repetitive exposure to similar types of loading (e.g., increases in bending moments, compression forces).

Past research has indicated that females possess lower tolerance levels to compression force for the intervertebral discs than males (Jager et al. 1991). Thus, when males and females are exposed to the same material handling conditions, females may be closer to the spinal tolerance levels than males, which may indicate an increased risk of injury. However, spinal loading for females has not been investigated to date, as female specific biomechanical models have not been developed. Thus, it is currently unknown what levels of spinal loading occur

during MMH tasks, and how the loading compares to spinal loading experienced by males performing the same MMH tasks.

The objectives of Part 4, therefore, are threefold: 1) examine the spinal loads experienced by females as a function of specific MMH tasks by using the female biomechanical model developed and validated in the previous parts of this study; 2) compare the female loads to those experienced by males performing the same MMH tasks; and 3) compare the spinal loading to tolerance data as a function of gender and the experimental MMH lifting task conditions.

## **Methods**

### ***Subjects***

The subjects for this part consisted of the same subjects which participated in Part 3. Thus, all anthropometric characteristics for the 35 female and 35 male subjects can be found in Table 3.1 in Part 3 of this report.

### ***Experimental Design***

Since the data for this part were collected to complete Part 3, the experimental design is identical to that described in Part, except for the dependent variables.

The independent variables include gender, weight of lift (15, 30, and 50 lbs), degree of asymmetry for the starting position of the lift (0 and 60 degrees), and lift condition (floor to waist, floor to 102 cm, knee to waist, and knee to 102 cm above the floor). The 102 cm destination height corresponds to the bed height of a 2.5 ton military truck. Each combination of the task independent variable was performed twice by each subject. This repeated measures design resulted in 48 experimental trials per subject, thus permitting sensitivity analysis of those material handling factors that influence spinal loading, as well as any gender differences in spinal loading as a function of the experimental conditions. The presentation order of the experimental conditions were randomized and subjects were allowed at least two minute rest (Caldwell et al. 1974) or as much time as needed between trials to minimize the risk of fatigue and carryover effects on the results.

The dependent variables included the maximum externally measured moments (in the sagittal, coronal, transverse plane, as well as the resultant moment) and spinal loading. Spinal

loading variables included the mean and average shear forces in the sagittal and coronal plane and the compression force.

### ***Equipment***

Inputs into the EMG-assisted biomechanical model for evaluation of material handling activities includes estimates of trunk position and motion, external measures of the sagittal plane lifting moment, and monitoring of muscle activity via EMG. All equipment used to collect the data, including the LMM, EMG electrodes, force plate, pelvic orientation monitor, and sacral location orientation monitor, as well as signal processing and conditioning have been previously described in Part 2, and also apply to this Part 4 of this study.

### ***Data Analyses***

The female data from the normalized EMG, trunk velocity from the LMM, sagittal moment measured by the force plate were input into female Model 10 from Part 3 to determine the gain for each of the female subjects. Male lifting trial data were input into Model 10 from Part 3. Spinal loading forces in each of the three planes (i.e., lateral shear, anterior/posterior shear, and compression force) for each gender was estimated by summing the directional muscle forces determined from each of the muscles by using *Eq 2.1*, and the predicted sagittal moment was determined using *Eq 2.2*.

$$\text{Force}_j = \text{Gain} \times (\text{EMG}_t / \text{EMG}_{\text{max}}) \times \text{PCSA}_j \times f(\text{Vel}) \times f(\text{Length}) \quad (\text{Eq } 2.1)$$

$$M_{x\text{-pred}} = \sum r_j \times \text{Force}_j \quad (\text{Eq } 2.2)$$

where:

Force<sub>j</sub> = tensile force for muscle j;

Gain = physiological muscle stress (N/cm<sup>2</sup>);

EMG<sub>t</sub> = integrated EMG from the lifting exertion;

EMG<sub>max</sub> = integrated EMG from MVCs;

PCSA<sub>j</sub> = physiological cross-sectional area of muscle j;

f(Vel) = the muscle force-velocity modulation factor;

f(Length) = the muscle length-strength modulation factor;

M<sub>x-pred</sub> = predicted sagittal trunk moment during the lifting exertion;

r<sub>j</sub> = moment-arm for muscle j.

Mean and maximum lifting moments about each of the three planes were determined from measurements from the force plate.

Spinal compression tolerance limits were calculated as a function of age and gender using the following regression equations from Jager et al. (1991):

$$\text{Male Tolerance (kN)} = 10.53 - 0.974(\text{age/decade}) \quad \text{Eq. 4.1}$$

$$\text{Female Tolerance (kN)} = 7.03 - 0.591(\text{age/decade}) \quad \text{Eq. 4.2}$$

where:

Tolerance = compressive strength of the intervertebral disc in kN;  
age/decade = age of the individual in decades of life.

The predicted compression force for each trial was divided by the predicted tolerance to obtain a spinal compression tolerance ratio for each trial for each subject.

### ***Statistical Analyses***

Initially, descriptive statistics (mean and standard deviation) were generated, describing the maximum lifting moments, spinal forces, and compression tolerance ratio as a function of each of gender and the other experimental conditions. Analysis of Variance (ANOVA) procedures were used to test the significance of the spinal loading variables as a function of the experimental conditions. The statistical analysis consisted of a mixed four-way repeated measures ANOVA, with one between factor (gender) and three repeated factors (weight, asymmetry and lift condition). Trials which had an  $r^2$  greater than 0.8 and sagittal moment prediction error of 10% or less were included in the analyses in this section. Significant gender effects for spinal loading were examined by testing the two-way interactions between gender and the other independent variables (i.e., weight, asymmetry and lift condition). Significant differences will indicate different levels of spinal loading due to gender, when both genders were exposed to the same external loading conditions. Tukey post-hoc procedures were used to understand the nature of these differences for the main effects using a family-wise Type I error rate of  $\alpha=0.05$ . To identify where the gender differences existed for significant gender interactions, post-hoc evaluations consisting of  $t$ -tests were used while adjusting the Type I error rate using a Bonferroni adjustment (Keppel 1991).

### **Results**

Descriptive results for the measured lifting moments and predicted spinal loading as a function of gender and the experimental conditions are shown in Table 4.1. The results of the

ANOVA for measured moments and predicted spinal loading are shown in Table 4.2. The weight of the load had the largest impact on spinal loading, as there were significant effects on the moment in the sagittal, coronal and transverse plane, as well as the resultant moment, in addition to significant effects on shear forces (coronal and sagittal plane) and compression force. Post-hoc Tukey multiple comparisons indicated that for every significant main effect, each of the three weights were significantly different from each other, with the 15 lb condition resulting in the lowest spinal loading magnitude and the 50 lb condition resulting in the highest spinal loading magnitude. The asymmetry condition for the starting lift position also had a significant affect on all measures of spinal loading (measured moments and predicted spinal forces). Post-hoc comparisons indicated that for each of the significant effects, the 60 degree asymmetric starting position resulted in higher lifting moments and shear and compression forces than when the starting position was sagittally symmetric.

Table 4.2 Analysis of Variance p-value results on spinal loading as a function of the experimental conditions.

Independent Variable	Moment (Nm)				Spinal Load (N)		
	Sagittal Plane	Coronal Plane	Transverse Plane	Resultant	Lateral Shear	A/P Shear	Compression
Gender (G)	0.0268	0.0437	0.2932	0.0141	0.8783	0.5085	0.3476
Lift Condition (C)	0.1839	0.1484	0.4063	0.1864	0.3650	0.4019	0.8617
Weight (W)	0.0001	0.0001	0.0001	0.0001	0.0001	0.0001	0.0001
Asymmetry (A)	0.0001	0.0001	0.0001	0.0001	0.0001	0.0012	0.0001
G × C	0.0027	0.0031	0.0536	0.0145	0.5892	0.0715	0.1561
G × W	0.0264	0.0489	0.1859	0.0300	0.9283	0.8196	0.0496
G × A	0.1151	0.0183	0.2378	0.6262	0.9454	0.7576	0.7166

Spinal loading varied significantly as a function of gender and weight of the load for the compression force and the sagittal, coronal and resultant moment. For the significant moments, males demonstrated larger moments than females for every weight level. For the compression force, the males had significantly greater compression force at only the 50 lb condition (Figure 4.1).

The externally measured moments also varied as a function of gender and lift condition. Post-hoc tests indicated that males had larger peak sagittal and resultant moment than females for

every lift condition, and also for the lateral moment, except when lifting from the floor to the waist level.

The lateral moment varied significantly as a function of starting asymmetry of the lift and gender, with males resulting in greater peak lateral moments than females at both levels of asymmetry, although the difference between the genders was much greater at the 60 degree asymmetry than the sagittally symmetric lifts (zero degrees).

Descriptive statistics on the spinal compression tolerance ratio as a function of gender and the experimental conditions are shown in Table 4.3. Descriptively, for every level of every experimental condition, females exhibited higher compression tolerance ratios than males.

Analysis of Variance on the spinal compression tolerance ratio (Table 4.4) indicated that gender differences were present collapsed across all experimental conditions, with females having a mean tolerance ratio of 0.75, and males exhibiting a mean tolerance ratio of 0.54 (see Figure 4.2). No other gender differences were present.

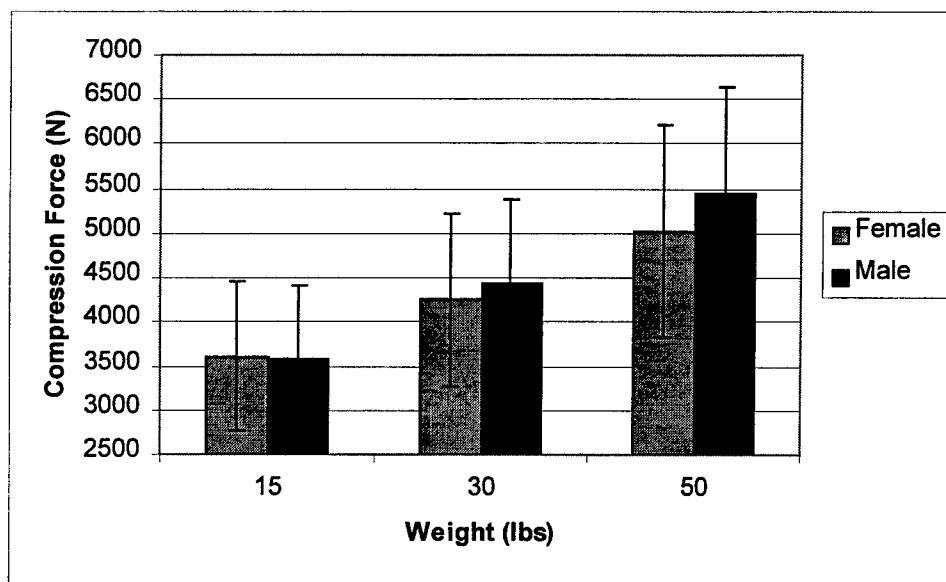


Figure 4.1 Mean compression force (N) on the  $L_5/S_1$  intervertebral disc as a function of gender and weight.

Table 4.1 Descriptive statistics (mean (s.d.)) from biomechanical model results for both male and female as a function of the experimental conditions.

Independent Variables	Moment (Nm)						Spinal Loading (N)							
	Sagittal Plane		Coronal Plane		Transverse Plane		Resultant		Lateral Shear		A/P Shear		Compression	
	Female	Male	Female	Male	Female	Male	Female	Male	Female	Male	Female	Male	Female	Male
Weight (lbs)	15	124.2 (26.6)	135.9 (37.8)	55.5 (26.9)	66.8 (27.3)	28.0 (18.4)	21.6 (14.0)	141.7 (30.9)	155.6 (39.2)	195.1 (179.0)	183.7 (169.7)	607.7 (158.4)	563.9 (115.4)	3606.8 (843.1)
	30	147.1 (31.2)	166.8 (38.5)	58.6 (24.5)	74.1 (33.2)	29.3 (18.0)	25.7 (16.5)	163.3 (34.0)	187.5 (40.7)	193.3 (176.9)	221.4 (189.7)	684.6 (219.8)	659.7 (196.3)	4246.1 (955.3)
	50	169.7 (36.3)	202.1 (47.3)	68.0 (30.3)	79.7 (34.7)	38.2 (23.3)	27.3 (21.5)	189.6 (41.1)	222.1 (50.0)	236.7 (204.5)	272.5 (246.1)	743.4 (325.8)	754.1 (243.5)	5025.8 (1176.4)
Asymmetry (deg)	0	137.9 (32.5)	165.2 (49.8)	54.7 (23.5)	62.3 (28.2)	27.7 (16.9)	19.1 (16.2)	153.2 (34.7)	180.7 (49.2)	143.0 (107.6)	153.9 (107.9)	649.4 (228.4)	638.3 (187.8)	3994.9 (1019.4)
	60	151.1 (37.9)	170.8 (47.5)	65.7 (30.3)	85.9 (32.1)	34.9 (22.4)	31.3 (16.9)	171.5 (42.3)	196.2 (51.1)	276.9 (227.0)	304.5 (254.4)	693.8 (246.9)	680.7 (222.8)	4431.2 (1321.9)
Lift Condition*	F-W	147.0 (37.5)	162.1 (55.0)	61.6 (29.4)	67.0 (29.8)	30.6 (17.8)	23.4 (21.7)	164.8 (41.8)	180.3 (56.4)	205.5 (185.1)	198.4 (178.5)	684.6 (244.2)	611.6 (178.1)	4296.5 (1302.4)
	F-C	144.6 (33.0)	169.9 (46.4)	60.8 (26.0)	73.6 (30.1)	29.8 (19.7)	23.9 (14.4)	162.3 (35.8)	189.6 (46.4)	198.3 (182.9)	240.5 (205.1)	681.4 (238.3)	664.4 (200.2)	4143.7 (1266.8)
	K-W	140.8 (35.2)	175.3 (45.5)	59.9 (28.1)	78.2 (35.0)	33.2 (21.8)	25.5 (15.1)	159.5 (39.8)	196.6 (48.5)	195.0 (179.3)	229.4 (208.5)	654.3 (243.0)	689.2 (203.5)	4097.0 (1083.0)
	K-C	143.6 (36.7)	163.7 (47.3)	56.6 (25.6)	74.7 (33.2)	30.4 (20.3)	26.6 (18.6)	159.8 (40.1)	185.1 (50.1)	220.9 (195.3)	230.9 (226.3)	659.0 (225.2)	665.0 (231.5)	4245.5 (1158.4)

\* F - W = Floor to Waist;  
 F - C = Floor to Chest;  
 K - W = Knee to Waist;  
 K - C = Knee to Chest.

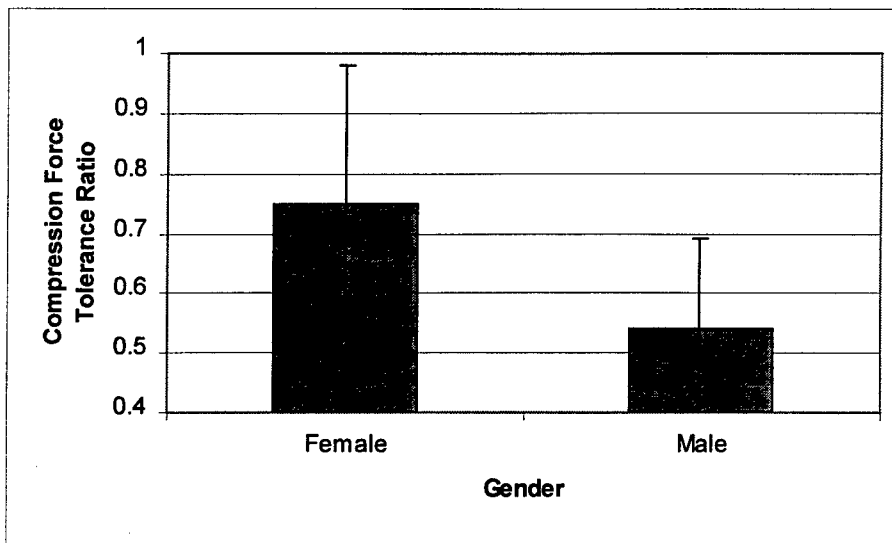


Figure 4.2 Compression force tolerance ratio for the L<sub>5</sub>/S<sub>1</sub> intervertebral disc as a function of gender.

Table 4.3. Compression tolerance ratio for females and males as a function of the experimental conditions. The ratio's were determined by dividing the predicted compression force by the predicted disc compression force tolerance using equations from Jager et al. (1991).

<i>Independent Variables</i>		Compression Tolerance Ratio	
		Female	Male
Weight (lbs)	15	0.64 (0.16)	0.43 (0.11)
	30	0.76 (0.19)	0.54 (0.12)
	50	0.91 (0.28)	0.66 (0.15)
Asymmetry (deg)	0	0.71 (0.20)	0.52 (0.14)
	60	0.79 (0.25)	0.57 (0.16)
Lift Condition	F-W	0.77 (0.28)	0.52 (0.17)
	F-C	0.73 (0.19)	0.55 (0.15)
	K-W	0.73 (0.21)	0.60 (0.19)
	K-C	0.76 (0.23)	0.53 (0.16)

Table 4.4 Analysis of Variance p-value results on Spinal Compression Tolerance Ratio for males and females.

Independent Variable	Compression Tolerance Ratio
Gender (G)	0.0001
Weight (W)	0.0001
Asymmetry (A)	0.0001
Lift Condition (C)	0.8953
G × W	0.4281
G × A	0.1598
G × C	0.1594

## Discussion

The results presented in this Part of the study represent the first of its kind for assessment of spinal loading of females utilizing a female specific biomechanical model. Thus, there are no other datasets for which to compare the pattern of spinal loading predicted from this study.

The magnitudes of the spinal loading for females and males approached levels that may represent high risk for LBD from spinal compression. Lifting loads as low as 15 lbs resulted in compression forces of 3607 N and 3578 N for females and males, respectively. NIOSH (1981) states that above compression forces of 3400 N, microfractures in the vertebral endplates will begin to appear in some individuals. When subjects in this study lifted 50 lbs, mean maximum compression forces were 5026 N and 5454 N for females and males, respectively. NIOSH has estimated that at compression forces above 6400 N, most individuals will start to have microfractures of the vertebral endplates. Thus, the compression levels predicted from lifting these weights indicates that there would be an elevated level of risk of damage to the endplates. Most interesting about these results is the lack of a gender difference in compression force as a function of any of the independent variables, except for the 50 lb weight condition. This indicates that females and males experience similar loading magnitudes for identical task parameters. However, when considering the tolerance to compression, females expressed a significantly greater tolerance ratio (0.75) than the males (0.54) across all weights, lift conditions and starting lift asymmetry. Thus, females were closer to the tolerance limit than males for the same tasks, indicating a higher risk for LBD for females than males when performing the same tasks.

Although the magnitudes of the A/P shear forces are similar between males and females for the same task conditions, if one assumes that females have a lower tolerance to shear forces on the intervertebral disc, similar to that for compression forces, females would be at a greater risk of LBD than males for similar task conditions.

## **Conclusions**

This part of the study provides the results from the first of its kind assessment of spinal loading of females utilizing a female specific biomechanical model. Although females and males experienced similar compression and A/P shear forces on the L<sub>5</sub>/S<sub>1</sub> intervertebral disc for the same task conditions, females were found to be at an elevated risk for LBD when the compression loading was expressed as a percent of the predicted spinal tolerance.

## **Part 5: Evaluate High Risk Military MMH Tasks**

### **Introduction**

Females are now performing manual materials handling tasks that once were exclusively performed by males. Thus, it is necessary to be able to evaluate the risk of injury to the low back for several reasons. First, we expect differences in the magnitude and pattern of spinal loading as males and females differ in anthropometry. Secondly, the spinal tolerances have been shown to be different between males and females, which suggests that injury to the low back would occur at different spinal loads for females than that for males. Finally, the low back injury rates, although dependent upon age, differ between the genders for individuals performing similar tasks.

### **Background and Objectives**

The OSU EMG-assisted biomechanical model has been updated for anatomical characteristics including gender specific force producing trunk muscle areas (Part 1), gender specific muscle vector coefficients which determine the sagittal plane and coronal plane moment-arms at the model origin and insertion levels, and gender specific muscle length-strength and force-velocity relationships (Part 2). As demonstrated in Part 3 and Part 4 of this study, the new anatomical inputs have been shown to result in very acceptable predictability, with high  $R^2$ 's for the prediction of the sagittal plane lifting moment, low sagittal plane lifting moment prediction error, and physiologically realistic muscle gain values.

The gender specific EMG-specific model as utilized in the model performance validation (Part 3) and the investigation of predicted spinal loading during the model validation (Part 4) was performed with the subjects standing on a force plate. When subjects perform experimental MMH tasks while standing on a force plate, they must remain stationary on the force plate by not moving their feet. This is typically not a realistic way of performing MMH tasks, as much of the time, material handlers are able to move their feet during the task.

Once the EMG-assisted biomechanical model has been validated, as it was in Part 3 and Part 4, the force plate, pelvic orientation monitor, and sacral location orientation monitor (SLOM) are no longer necessary for the performance and predictive power of the model. Thus,

the EMG-assisted biomechanical model can be used in an “open loop” configuration for the evaluation of free-dynamic MMH tasks that allow subjects to move their feet and legs in a realistic manner.

The objective of this final part of this research, therefore, is to utilize the gender specific EMG-assisted biomechanical model as an evaluation tool to assess a simulated realistic military manual material handling task performed by military women and men.

## Methods

### *Subjects*

The subjects for this demonstration part of the EMG-assisted model consisted of two females and two males. The subject anthropometric measurements are shown in Table 5.1.

Table 5.1 Anthropometric measurements (mean and s.d.) from female and male subjects.

Anthropometric Variable	Females	Males
Age (yrs)	19.5 (0.7)	23.5 (2.1)
Standing Height (cm)	161.5 (3.5)	175.7 (5.8)
Weight (kg)	59.0 (1.3)	73.7 (8.0)
Trunk Width at Iliac Crest (cm)	29.6 (1.4)	28.2 (0.3)
Trunk Depth at Iliac Crest (cm)	19.4 (2.3)	19.8 (1.7)
Trunk Width at Xyphoid Process (cm)	26.5 (2.8)	31.1 (1.8)
Trunk Depth at Xyphoid Process (cm)	19.4 (0.4)	21.1 (0.1)
Body Mass Index (kg/m <sup>2</sup> )	22.6 (0.5)	23.8 (1.0)

### *Experimental Task*

The experimental task for this demonstration consisted of a laboratory simulated lifting task, simulating a one- and two-person lift of product to a height corresponding to the bed height of a 2.5 ton military truck.

The independent variables included number of people lifting, gender, and the lifting condition. The number of people lifting included one and two person lifts. The one-person lift consisted of lifting a 35 lb box in each of the three lifting conditions (described below), with the handles placed 45 cm apart. The two-person lifts consisted of lifting 70 lbs on a structure with handles also 45 cm apart, with the two lifters facing each other 95 cm apart. The subjects for the one- and two-person lifts performed three different lifting conditions:

- 1) Sagittal-to-Sagittal – The origin of the lift was 52 cm from the floor directly in front of the subject in the sagittal plane. The destination was 102 cm from the floor, also directly in front of the subject in the sagittal plane.
- 2) Sagittal-to-Asymmetric – The origin of the lift was 52 cm from the floor directly in front of the body. The destination was 102 cm above the floor, 36 cm to the right side of the subject.
- 3) Asymmetric-to-Asymmetric – The origin of the lift was 52 cm from the floor, 36 cm to the left of the subject. The destination was 102 cm above the floor and 36 cm to the right of the subject.

The dependent variables in this demonstration consisted of the predicted spinal loading on the L<sub>5</sub>/S<sub>1</sub> intervertebral disc (lateral and anterior/posterior shear force, and compression force), and the compression tolerance ratio.

### ***Equipment***

All equipment used to collect the data during the calibration exertions (described below) and the experimental trials, including the LMM EMG electrodes, force plate, pelvic orientation monitor, and sacral location orientation monitor, as well as signal processing and conditioning have been previously described in Part 2, and apply to this part of the study.

### ***Experimental Procedure***

Upon arrival to the testing laboratory, the subjects read and signed a consent form. Anthropometric data were recorded next. Surface electrodes for the EMG were then applied over each of ten trunk muscles, while skin impedance's were kept below 500 kΩ. Maximum voluntary contractions (MVCs) for each of the trunk muscles were obtained, with the subjects performing MVCs for trunk extension and flexion static exertions, as well as right and left twisting and right and left lateral bending, all against a constant resistance. All resulting trunk

muscle EMG data obtained from the experimental trials were then normalized to the maximum EMG activity obtained during these six directional MVCs.

When using the EMG-assisted biomechanical model in an “open loop” configuration for the experimental task (i.e., no force plate, SLOM and POM), it is necessary to determine the subject-specific muscle gain prior to the experimental tasks, via a set of five calibration exertions. The calibration exertions consisted of lifting a box from knee height to elbow height, while recording the trunk motion with the LMM, the external forces and moments with the force plate, muscle activity from EMG electrodes, and the pelvic orientation and lumbosacral joint position using the POM and SLOM, respectively. The measured forces and moments were translated and rotated from the center of the force plate to the L<sub>5</sub>/S<sub>1</sub> position (Fathallah et al. 1997). The predicted internal moments at the L<sub>5</sub>/S<sub>1</sub> were then adjusted to equal the external moments through the use of the predicted muscle gain. This gain factor was then input into Eq 2.1 to estimate the muscle forces and internal moments for the experimental tasks, which allowed the subjects to move without being restricted to a force plate.

### **Data Analysis**

The subject specific gain, the normalized trunk muscle EMG and trunk motion data from the LMM for each of the experimental task trials for the females were input into the female biomechanical model (Model 10 as described in Part 2 and Part 3). Likewise, the subject specific gain, the normalized trunk muscle EMG and trunk motion data from the males were input into the male specific biomechanical model (Model 10 as described in Part 2 and Part 3). Spinal loading forces at L<sub>5</sub>/S<sub>1</sub> in each of the three planes (i.e., lateral shear, anterior/posterior shear, and compression force) for each gender was estimated by summing the directional muscle forces determined from each of the muscles by using Eq 2.1, and the predicted sagittal moment was determined using Eq 2.2.

$$\text{Force}_j = \text{Gain} \times (\text{EMG}_t / \text{EMG}_{\text{max}}) \times \text{PCSA}_j \times f(\text{Vel}) \times f(\text{Length}) \quad (\text{Eq } 2.1)$$

$$M_{x\text{-pred}} = \sum r_j \times \text{Force}_j \quad (\text{Eq } 2.2)$$

where:

Force<sub>j</sub> = tensile force for muscle j;

Gain = physiological muscle stress (N/cm<sup>2</sup>);

EMG<sub>t</sub> = integrated EMG from the lifting exertion;

EMG<sub>max</sub> = integrated EMG from MVCs;

PCSA<sub>j</sub> = physiological cross-sectional area of muscle j;

$f(\text{Vel})$  = the muscle force-velocity modulation factor;  
 $f(\text{Length})$  = the muscle length-strength modulation factor;  
 $M_{x\text{-pred}}$  = predicted sagittal trunk moment during the lifting exertion;  
 $r_j$  = moment-arm for muscle  $j$ .

Spinal compression tolerance limits were calculated as a function of age and gender using the following regression equations from Jager et al. (1991):

$$\text{Male Tolerance (kN)} = 10.53 - 0.974(\text{age/decade}) \quad \text{Eq. 4.1}$$

$$\text{Female Tolerance (kN)} = 7.03 - 0.591(\text{age/decade}) \quad \text{Eq. 4.2}$$

where:

Tolerance = compressive strength of the intervertebral disc in kN;  
age/decade = age of the individual in decades of life.

The predicted  $L_5/S_1$  compression force for each trial was then divided by the predicted compression tolerance to obtain a spinal compression tolerance ratio for each trial for each subject.

## Results

The predicted spinal loading for both females and males for the one-person lifts for all three lifting conditions are shown in Table 5.2. Similarly, the predicted spinal loading for females and males for the two-person lifts for all three lifting conditions are shown in Table 5.3. A comparison between female and male predicted lateral and A/P shear forces are graphically shown in Figures 5.1 and 5.2, respectively. Generally, when lifting the load in a sagittal-to-sagittal manner, as well as a sagittal-to-asymmetric manner, the predicted lateral and A/P shear loading experienced by females and males were very similar. However, when lifting from asymmetric-to-asymmetric points, the males experienced much higher lateral and A/P shear forces than females. When performing a two-person lift, Figure 5.3 shows that both females and males experienced similar lateral shear forces for each of the three lift conditions, and only the males experienced any real decrease in predicted lateral shear force, during the asymmetric-to-asymmetric lifting condition. When considering the predicted A/P shear force, there does not appear to be any real difference in the magnitude when one-person lifts 35 lbs (Figure 5.2) from when two-people lift 70 lbs (Figure 5.4), for all three lifting conditions involved in this demonstration.

The predicted  $L_5/S_1$  compression force as a function of gender and lift condition for the one-person lifts is shown in Figure 5.5. This figure indicates that the predicted compression force for females is about 150 N higher than that experienced by males for the sagittal-to-sagittal and sagittal-to-asymmetric lifting conditions. However, when lifting asymmetric-to-asymmetric, the males predicted  $L_5/S_1$  compression force increased by over 1200 N over the first two lifting conditions, yet the female predicted  $L_5/S_1$  compression force remained about the same as the previous two lifting conditions.

When considering the impact of gender and age specific spinal compression tolerance, a different scenario emerges. Although the females experienced similar  $L_5/S_1$  compression forces as males when performing the sagittal-to-sagittal and sagittal-to-asymmetric experimental tasks for both the one-person and two-person lifts, the impact of females having a lower tolerance to compression force resulted in the compression force tolerance ratio being much higher than the males for these two tasks. For the asymmetric-to-asymmetric task, which resulted in higher compression force for males, the female compression tolerance ratio was slightly higher than the males for the one-person (Figure 5.6) and two-person lifts (Figure 5.8).

The impact of having two people lift twice the weight as one person was much greater for the compression force than the shear forces. The predicted compression forces and compression force tolerance ratio were both lower when two people were lifting than when one person was lifting, for both females and males (Tables 5.2 and 5.3, and Figures 5.5 through 5.8) for the sagittal-to-sagittal and sagittal to asymmetric lifting condition. However, there was very little decrease in compression force and the tolerance ratio when going from a one-person (Figure 5.5 and 5.6) to a two-person lifting scheme (Figure 5.7 and 5.8) for the asymmetric-to-asymmetric lifting condition for both females and males.

Table 5.2. Predicted spinal loading for one-person lifts for male female and male subjects as a function of lift condition.

Lift Condition	Gender	Predicted Spinal Loads			Percent Compression Tolerance
		Lateral Shear Force	A/P Shear Force	Compression Force	
Sagittal to Sagittal	Female	85.9 (25.9)	361.7 (75.9)	3300.6 (262.3)	0.56 (0.04)
	Male	118.4 (92.9)	421.1 (61.9)	3151.0 (678.8)	0.38 (0.07)
Sagittal to Asymmetric	Female	171.0 (78.8)	423.7 (100.1)	3227.8 (377.3)	0.55 (0.06)
	Male	144.5 (42.9)	507.6 (134.8)	2973.0 (319.2)	0.36 (0.03)
Asymmetric to Asymmetric	Female	272.0 (79.9)	406.6 (72.9)	3264.7 (452.8)	0.56 (0.08)
	Male	378.3 (283.8)	849.8 (429.5)	4370.8 (1105.5)	0.53 (0.12)

Table 5.3. Predicted spinal loading for two-person lifts for male female and male subjects as a function of lift condition.

Lift Condition	Gender	Predicted Spinal Loads			Percent Compression Tolerance
		Lateral Shear Force	A/P Shear Force	Compression Force	
Sagittal to Sagittal	Female	104.2 (67.7)	422.2 (31.1)	2395.8 (233.8)	0.41 (0.04)
	Male	103.5 (34.7)	366.4 (27.3)	2409.8 (213.5)	0.29 (0.03)
Sagittal to Asymmetric	Female	133.9 (44.5)	411.1 (27.1)	2775.5 (245.1)	0.47 (0.04)
	Male	120.3 (25.0)	533.0 (75.1)	2569.7 (287.1)	0.31 (0.03)
Asymmetric to Asymmetric	Female	274.6 (143.0)	449.0 (81.1)	3185.4 (1007.1)	0.54 (0.17)
	Male	273.8 (229.4)	782.0 (302.9)	3974.8 (1686.3)	0.48 (0.19)

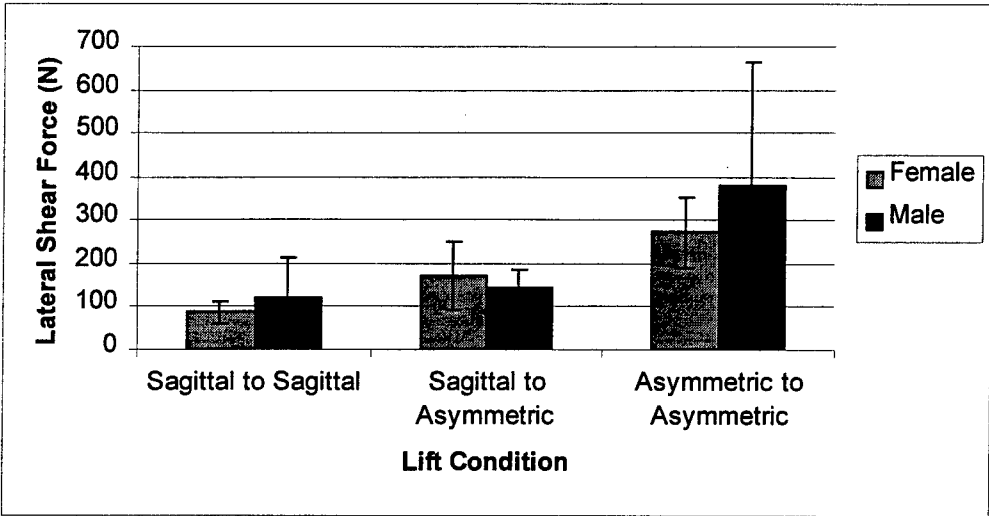


Figure 5.1. Predicted mean L<sub>5</sub>/S<sub>1</sub> lateral shear force as a function of gender and lift condition for one-person lifts.

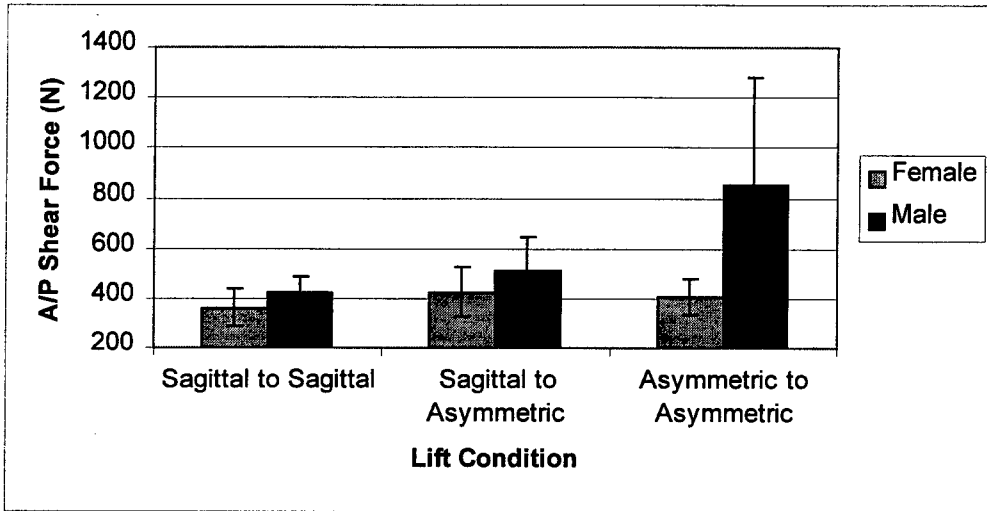


Figure 5.2. Predicted mean L<sub>5</sub>/S<sub>1</sub> anterior/posterior (A/P) shear force as a function of gender and lift condition for one-person lifts.

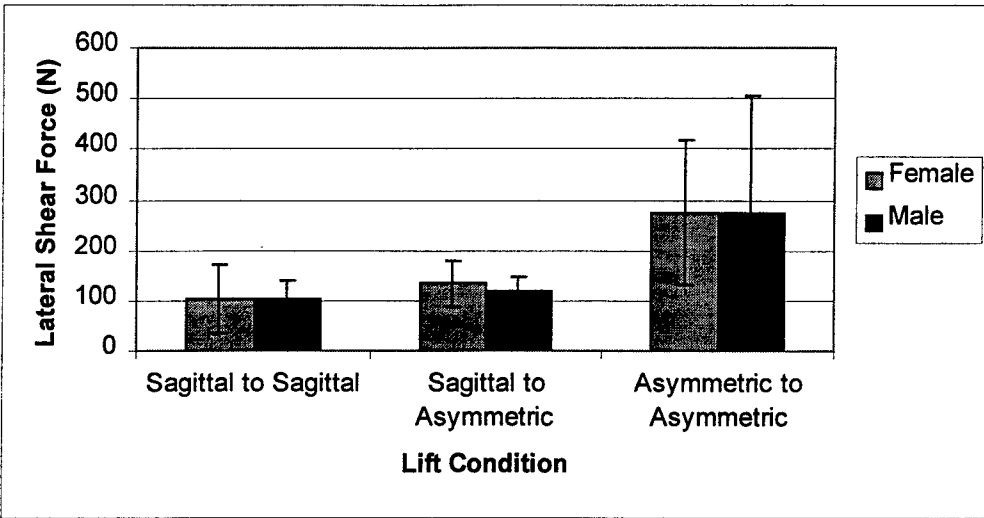


Figure 5.3. Predicted mean L<sub>5</sub>/S<sub>1</sub> lateral shear force as a function of gender and lift condition for two-person lifts.

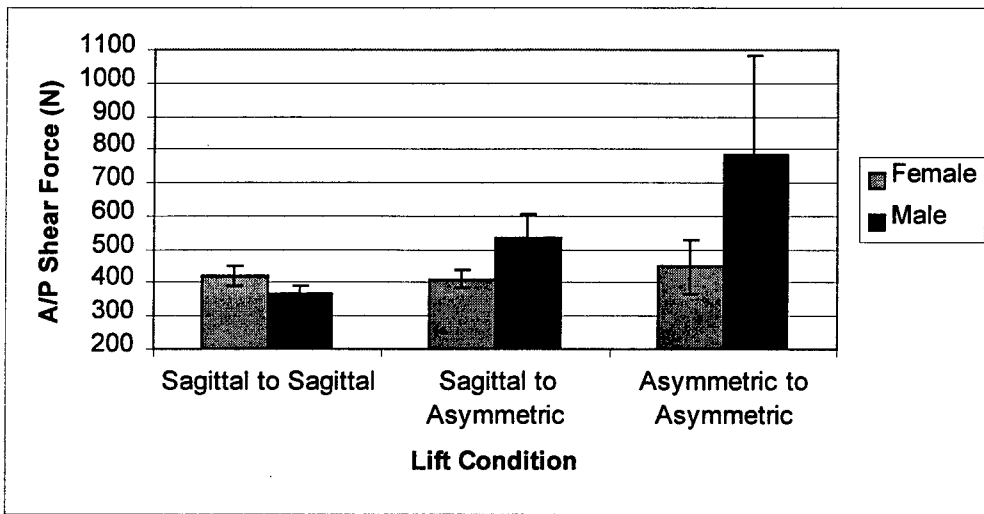


Figure 5.4. Predicted mean L<sub>5</sub>/S<sub>1</sub> anterior/posterior (A/P) shear force as a function of gender and lift condition for two-person lifts.

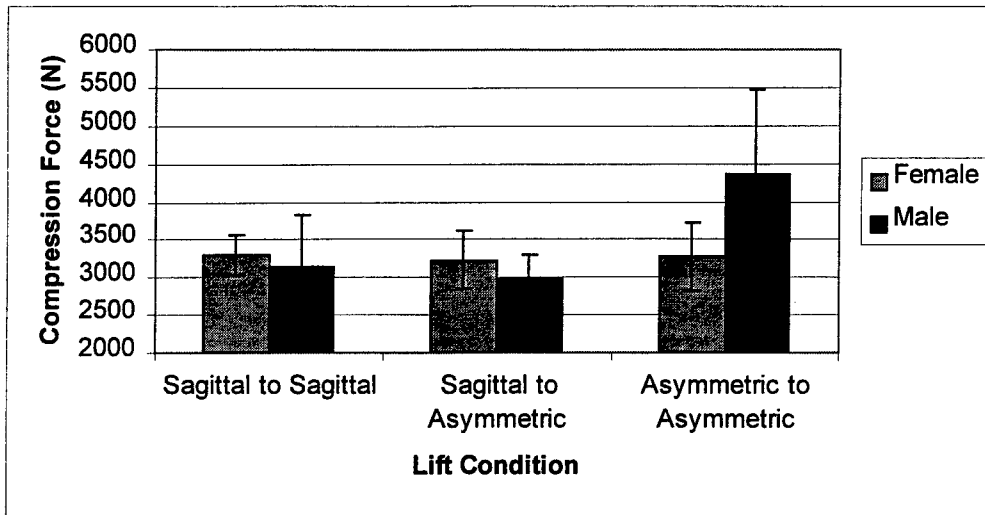


Figure 5.5. Predicted mean L<sub>5</sub>/S<sub>1</sub> compression force as a function of gender and lift condition for one-person lifts.

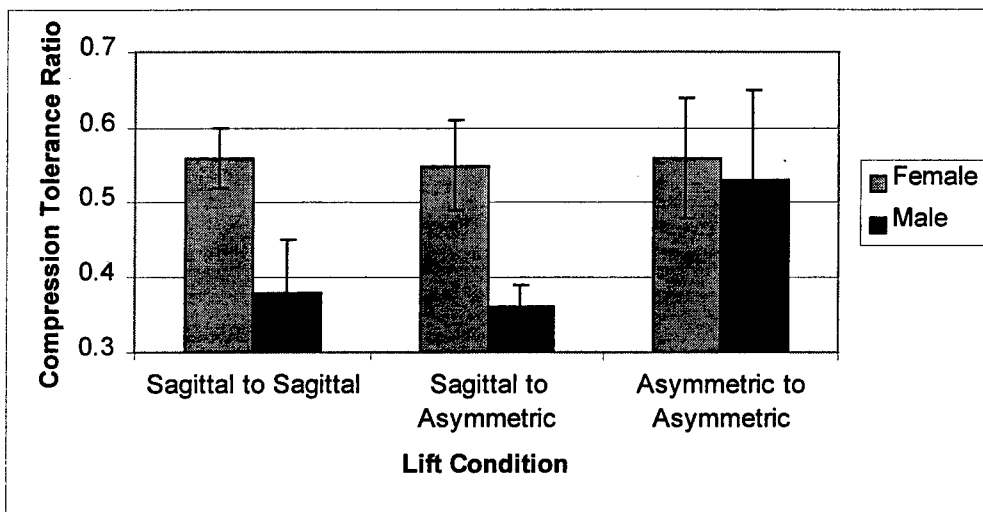


Figure 5.6. Predicted mean L<sub>5</sub>/S<sub>1</sub> compression force tolerance ratio as a function of gender and lift condition for one-person lifts.

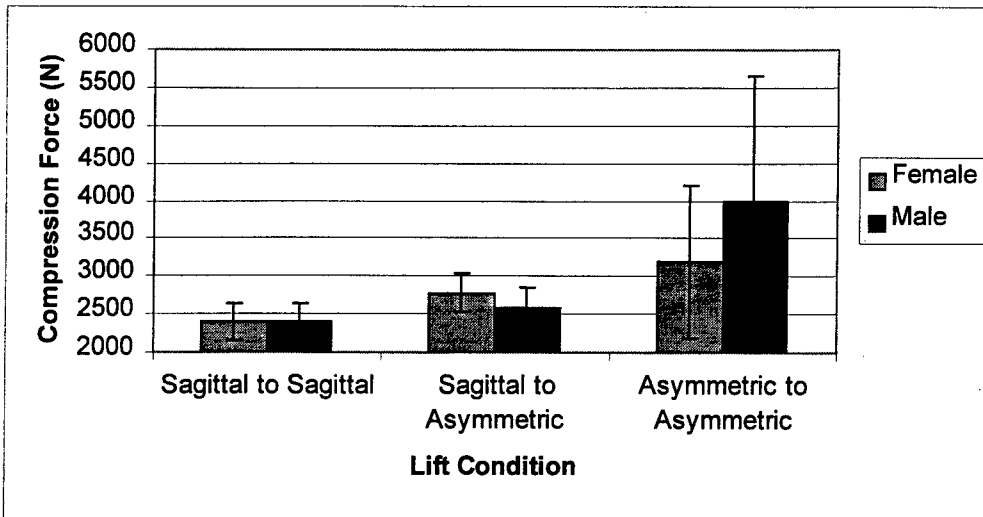


Figure 5.7. Predicted mean L<sub>5</sub>/S<sub>1</sub> compression force as a function of gender and lift condition for two-person lifts.

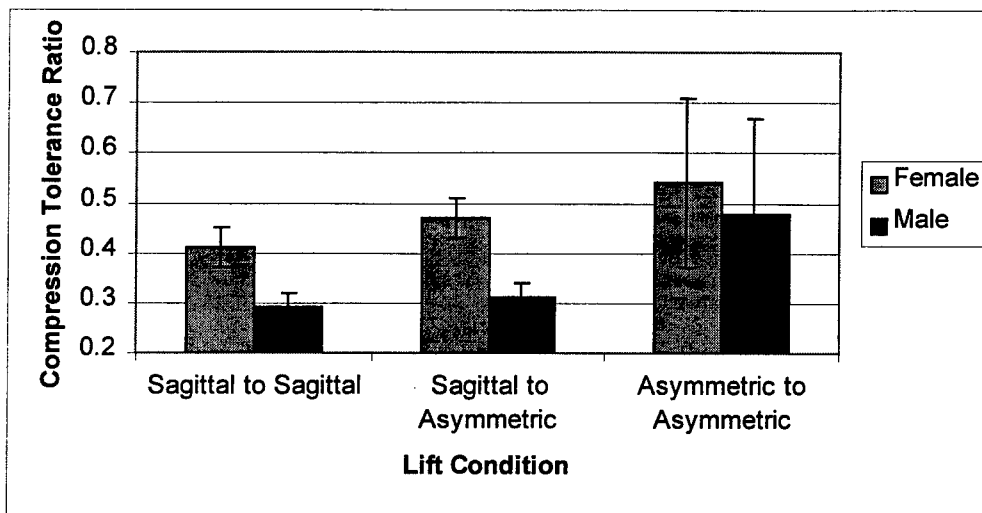


Figure 5.8. Predicted mean L<sub>5</sub>/S<sub>1</sub> compression force tolerance ratio as a function of gender and lift condition for two-person lifts.

## Discussion

This final part of the study demonstrated that the gender specific EMG-assisted biomechanical model developed in this research is able to be used for the evaluation of the spinal loading experienced in individuals during the performance of manual materials handling tasks.

The simulated military lifting task chosen to demonstrate the utility of the EMG-assisted biomechanical model consisted of three lifting conditions, ranging from sagittally symmetric lifts at the origin and destination, to completely asymmetric at both the origin to the destination of the

lift. The resulting predicted spinal loading observed in each of the lifting conditions was consistent with the external configuration of the task (e.g., sagittally symmetric vs. asymmetric lifting). For example, consistent with prior biomechanical studies (Marras and Granata 1995), higher lateral shear forces were predicted for the asymmetric-to-asymmetric lifting condition, which had more lateral trunk motion, than the sagittal-to-sagittal or sagittal to asymmetric lifting condition. Progressively higher L<sub>5</sub>/S<sub>1</sub> compression forces were predicted as the lifting conditions became more asymmetric, from sagittal-to-sagittal to asymmetric-to-asymmetric. This is expected as one would experience higher degrees of trunk muscle coactivation, which has been shown to result in higher spinal compression forces (Granata and Marras 1995). Thus, the resulting spinal loading predictions were consistent with the design of the task.

Although females and males performed the same lifting conditions during this demonstration, apparent gender differences in predicted spinal loading as a function of lift condition were found. These differences in predicted spinal loading are consistent with the differences in muscle anatomy found in the first part of this study, and incorporated into the biomechanical model. For example, the erector spinae have a shorter relative moment-arm in sagittal plane at the origin for males than females, thus, contributes more to compression for a given load, and contributes less anterior shear resistance than females. The orientation of the muscles, combined with a larger upper body torso mass may contribute to the higher A/P shear forces experienced by the males for the asymmetric-to-asymmetric lifting condition. Thus, the gender specific models predict differences in the pattern and magnitude of spinal loading consistent with the gender differences found in trunk geometry, which impact the risk of injury for a similar task performed by males and females.

Quite interesting is the fact that both genders experienced similar magnitudes of loading for many of the same conditions, consistent with the findings in Part 4 of this study. For example, the lateral shear forces for females and males were very similar for all three lifting conditions (Figures 5.1 and 5.3). Similarly, the compression forces were similar between females and males for the sagittal-to-sagittal and sagittal-to-asymmetric lifting condition (Figures 5.5 and 5.7). However, one needs to consider the differences in the tolerance of the intervertebral disc to the compression force to gain better insight to the risk of injury from spinal loading resulting from material handling tasks. Thus, as shown in Figures 5.6 and 5.8, the males experienced a compression tolerance ratio of about 35% for the sagittal-to-sagittal and sagittal-to-

asymmetric. However, the female compression force tolerance ratio was much higher, approaching 60% of their predicted tolerance. Thus, although the females experienced similar internal magnitudes of spinal loading when performing the same task, the lower intervertebral disc tolerance places the females at an elevated level of risk of injury to the low back.

## **Conclusions**

This part of the study has demonstrated that the EMG-assisted biomechanical model which accounts for gender anthropometric and anatomical differences can be used to evaluate the biomechanical loading experienced by individuals performing a manual materials handling task. Utilization of this model can provide insight into the loading experienced by individuals, as well as accounting for differences in the magnitude and pattern of loading resulting from gender anatomical differences, or differences in the performance of the same task. Finally, accounting for differences in predicted tolerances to the intervertebral disc, the predictions of the spinal loading provide additional insight to the risk of injury to the low back as compared to the predicted loading.

## KEY RESEARCH ACCOMPLISHMENTS

- Demonstrated that gender differences exist for the physiological cross-sectional area (PCSA) and moment-arms of the major spine loading trunk muscles. Males exhibited, on average, 69% larger trunk muscle PCSA than females. Males had 14.2% and 17.5% larger moment-arms in the coronal and sagittal plane, respectively, than females.
- Established significant predictions of PCSA of trunk muscles for males and females not previously found in prior research, utilizing external anthropometric measures.
- Demonstrated that prediction of several trunk muscle PCSAs from external anthropometry is gender specific, and relies on different anthropometric variables; thus, males and females must be considered different for purposes of biomechanical model inputs.
- Derived gender specific muscle length-strength and force-velocity relationships.
- Developed and validated a female specific EMG-assisted biomechanical model of the torso for prediction of spinal loading utilizing anatomical inputs derived from MRI and *in vivo* testing of muscle activity.
- Concluded that utilizing male and female specific EMG-assisted biomechanical models, females experience similar spinal loading magnitudes (shear and compression forces ) for identical tasks, except when lifting higher weights.
- Demonstrated that females may be at higher risk for LBD than males for similar manual materials handling tasks. Although females and males experienced similar magnitudes of spinal loading for similar tasks, females tend to exhibit lower tolerance for compression force for the intervertebral discs, which for similar spinal loads would be closer to their injury threshold.
- The gender specific EMG-assisted biomechanical model was shown to be capable of evaluating males and females performing a military manual material handling task (e.g., lifting loads to the bed of a truck), and allowing an assessment on risk of injury to the low back for each gender.

## REPORTABLE OUTCOMES

### Manuscripts, abstracts, presentations:

Marras WS, Jorgensen MJ, Granata KP and Wiand JW. Size and prediction of female and male trunk muscle geometry derived from MRI. *Clinical Biomechanics* 2000; (in press).

Jorgensen MJ, Marras WS, Granata KP and Wiand JW. MRI derived moment-arms of the female and male spine loading muscles. *Clinical Biomechanics* 2001;(in press).

Marras WS, Davis KG, and Jorgensen MJ. Biomechanical differences between males and females during symmetric and asymmetric lifting. *Spine* 2000; (in review).

Jorgensen MJ, Marras WS and Granata KP. Quantification and prediction of male and female spine loading muscles, *The Human Factors and Ergonomics Society 44<sup>th</sup> Annual Meeting*, 2000.

Marras WS, Davis KG and Jorgensen MJ. Assessment of anatomical representations of the trunk muscles in EMG-assisted spinal load models, *The Human Factors and Ergonomics Society 44<sup>th</sup> Annual Meeting*, 2000.

Marras WS, Jorgensen MJ, Granata KP and Wiand B. Predictions of trunk muscle cross-sectional areas for males and females. Poster presented at the *International Society for the Study of the Lumbar Spine*, 1999.

### Funding applied for based on work supported by this award:

The Ohio Bureau of Workers Compensation, 1999, The Control of Occupationally-Related Secondary Low Back Injuries.

The U.S. National Institute for Occupational Safety and Health, 2000, Spine Loading and Muscle Overexertion during Repetitive Lifting.

## **CONCLUSION**

Utilizing the female specific trunk muscle anatomy and the derived muscle length/strength and force/velocity relationships, we are now able to biomechanically model the female torso and quantify spinal loading during military manual materials handling tasks.

## REFERENCES

1. Adams, M.A. and Hutton, W.C. The effect of fatigue on the lumbar intervertebral disc. *J Bone Joint Surg* 1983; 65-B:199-203.
2. Adams, M.A., McNally, D.S., Wagstaff, J., and Goodship, A.E. Abnormal stress concentration in lumbar intervertebral discs following damage to the vertebral bodies: A cause of disc failure? *European Spine Journal* 1993; 1:214-221.
3. Adams, M.A., Green, T.P. and Dolan, P. The strength in anterior bending of lumbar intervertebral discs. *Spine* 1994; 19:2197-2203.
4. Army Safety Center Annual Report (1992).
5. Army Times, Aug. 8, 1994, 13-15.
6. Bigland, B. and Lippold, O.C.L. The relation between force, velocity and integrated electrical activity in human muscle. *J Physiology* 1954; 123:214-224.
7. Bogduk N, Johnson G and Spalding D. The morphology and biomechanics of latissimus dorsi. *Clinical Biomechanics* 1998; 13:377-385.
8. Caldwell LS, Chaffin DB, Dukes-Dobos FN, Kroemer KHE, Laubach LL, Snook SH and Wasserman DE. A proposed standard procedure for static muscle strength testing. *Am Ind Hyg Assoc J* 1974; 35:201-206.
9. Chaffin, D.B., Redfern, M.S., Erig, M. and Goldstein, S.A. Lumbar muscle size and locations from CT scans of 96 women of age 40 to 63 years, *Clinical Biomechanics* 1990; 5:9-16.
10. Cooper, R.D., Hollis, S. and Jayson, M.I.V. Gender variation of human spinal and paraspinal structures, *Clinical Biomechanics* 1992; 7:120-124.
11. Davis, K.G., Marras, W.S. and Waters, T.R. Evaluation of the spinal loading during lowering and lifting, *Clinical Biomechanics* 1998; 13:141-152.
12. Dumas GA, Poulin MJ, Roy B, Gagnon M and Jovanovic M. Orientation and moment arms of some trunk muscles. *Spine* 1991; 16:293-303.
13. Fathallah, F.A., Marras, W.S., Parnianpour, M. and Granata, K.P. A method for measuring external spine loads during unconstrained free-dynamic lifting, *J Biomechanics* 1997; 30:975-978.
14. Granata, K.P. (1993), An EMG-assisted model of biomechanical trunk loading during free-dynamic lifting, *Unpublished Ph.D. Dissertation*, The Ohio State University, Columbus, OH.
15. Granata, K.P. and Marras, W.S. An EMG-assisted model of loads on the lumbar spine during asymmetric trunk extensions. *J Biomechanics* 1993; 26:1429-1438.
16. Granata and Marras WS. The influence of trunk muscle coactivity on dynamic spinal loads, *Spine* 1995; 20:913-919.
17. Granata, K.P. and Marras, W.S. An EMG-assisted model of trunk loading during free-dynamic lifting. *J Biomechanics* 1995; 28:1309-1317.
18. Granata, K.P., Marras, W.S. and Fathallah, F.A. A method for measuring external trunk loads during dynamic lifting exertions. *J Biomechanics* 1995; 29:1219-1222.
19. Hill, A.V. The head of shortening and the dynamic constants of muscle, *Proceedings of the Royal Society of Biology* 1938; 126:136-195.
20. Jager, M., Luttmann, A. and Laurig, W. Lumbar load during one-handed bricklaying, *Int J Ind Ergon* 1991; 8:261-277.

21. Jones B.H., Bovee, M.W., Harris, J.M. and Cowan, D.N. Intrinsic risk factors for exercise-related injuries among male and female Army trainees, *Am J Sports Med* 1988; 21:705-710.
22. Keppel G. Design and Analysis – A Researchers Handbook, 3<sup>rd</sup> edition. Prentice Hall, Inc. Englewood Cliffs, NJ, 1991.
23. Kirking, B.C., (1997), An assessment of muscle, passive, and connective tissue forces acting at L<sub>5</sub>/S<sub>1</sub>, during lifting, *Unpublished Masters Thesis*, The Ohio State University, Columbus, OH.
24. Komi, P.M. Measurement of the force-velocity relationship in human muscle under concentric and eccentric contractions, *Medicine and Sport* 1973; 8:224-229.
25. Kumar, S., Moment arms of spinal musculature determined from CT scans, *Clinical Biomechanics* 1988; 3:137-144.
26. Macintosh JE and Bogduk N, The attachments of the lumbar erector spinae. *Spine* 1991; 16:783-792.
27. Marras, W.S. and Sommerich, C.M. A three-dimensional motion model of loads on the lumbar spine: I. Model structure, *Human Factors* 1991a; 33:123-137.
28. Marras, W.S. and Sommerich, C.M. A three-dimensional motion model of loads on the lumbar spine: II. Model validation, *Human Factors* 1991b; 33:139-149.
29. Marras, W.S., Fathallah, F.A., Miller, R.J., Davis, S.W. and Mirka, G.A. Accuracy of a three-dimensional lumbar motion monitor for recording dynamic trunk motion characteristics. *Int J Ind Erg* 1992; 9:75-87.
30. Marras, W.S., Lavender, S.A., Leurgans, S.E., Rajulu, S.L., Allread, W.G., Fathallah, F.A. and Ferguson, S.A. The role of dynamic three-dimensional trunk motion in occupationally-related low back disorders, *Spine* 1993; 18:617-628.
31. Marras, W.S., Lavendar, S.A., Leurgans, S.E., Fathallah, F.A., Ferguson, S.A., Allread, W.G., and Rajulu, S.L. Biomechanical risk factors for occupationally related low back disorders, *Ergonomics* 1995; 38:337-410.
32. Marras, W.S. and Granata, K.P. A biomechanical assessment and model of axial twisting in the thoracolumbar spine. *Spine* 1995; 20:1440-1451.
33. Marras, W.S. and Granata, K.P. Spine loading during trunk lateral bending motions. *J Biomechanics* 1997a; 30:697-703.
34. Marras, W.S. and Granata, K.P. The development of an EMG-Assisted model to assess spine loading during whole-body free-dynamic lifting. *J Electromyogr Kinesiol* 1997b; 4:259-268.
35. McGill, S.M. and Norman, R.W. Partitioning of the L<sub>4</sub>/L<sub>5</sub> dynamic moment into disc, ligamentous, and muscular components during lifting. *Spine* 1986; 11:666-678.
36. McGill SM, Patt N and Norman RW. Measurements of the trunk musculature of active males using CT scan radiography: Implications for force and moment generating capacity about the L<sub>4</sub>/L<sub>5</sub> joint. *J Biomechanics* 1988; 21:329-341.
37. McGill SM and Hoodless K, Measured and modelled static and dynamic axial trunk torsion during twisting in males and females. *J Biomedical Engineering* 1990; 12:403-409.
38. McGill SM, Santiguada L and Stevens J. Measurement of the trunk musculature from T<sub>5</sub> to L<sub>5</sub> using MRI scans of 15 young males corrected for muscle fiber orientation. *Clinical Biomechanics* 1993; 8:171-178.
39. McGill SM. The biomechanics of low back injury: Implications on current practice in industry and the clinic. *J Biomechanics* 1997; 30:465-475.

40. Mirka, G.A. and Marras, W.S. A stochastic model of trunk muscle coactivation during trunk bending. *Spine* 1993; 18:1396-1409.
41. Narici M. Human skeletal muscle architecture studied in vivo by non-invasive imaging techniques: functional significance and applications. *J Electromyogr Kinesiol* 1999; 9:97-103.
42. National Institute for Occupational Safety and Health, (1981), *Work Practices Guide for Manual Lifting*, NIOSH Technical Report DHHS(NIOSH) Publication No. 81-122.
43. Neter, J., Wasserman, W., and Kutner, M.H., (1985), *Applied Linear Statistical Models*, 2nd Edition, Richard D. Irwin, Inc., Homewood IL.
44. Paton ME and Brown JMM, Functional differentiation within latissimus dorsi. *Electromyogr Clin Neurophysiol* 1995; 35:301-309.
45. Pheasant, S., (1988), *Bodyspace: Anthropometry, Ergonomics and Design*, Taylor & Francis, N.Y.
46. Raschke, U. and Chaffin, D.B. Support for a linear length-tension relation of the torso extensor muscles: an investigation of the length and velocity EMG-force relationships. *J Biomechanics* 1996; 29:1597-1604.
47. Reid, J.G. and Costigan, P.A. Trunk muscle balance and muscular force. *Spine* 1987; 12:783-786.
48. Reid JG, Costigan PA and Comrie W. Prediction of trunk muscle areas and moment arms by use of anthropometric measures. *Spine* 1987; 12:273-275.
49. Schultz AB and Andersson GBJ. Analysis of loads on the lumbar spine. *Spine* 1981; 6:76-82.
50. Schultz AB, Andersson GBJ, Haderspeck K, Ortengren R, Nordin M and Bjork R, Analysis and measurement of lumbar trunk loads in tasks involving bends and twists. *J Biomechanics* 1982; 15:669-675.
51. Sharp M.A and Vogel J.A, (1992), Maximal lifting strength in military personnel, *Adv Ind Ergon Safety IV*, Proceedings of the Annual Int'l. Ind. Ergon. Safety Conference, Denver CO., S. Kumar ed., Taylor & Francis, Washington, D.C.
52. Sharp M.A. (1994), Physical fitness, physical training and occupational performance of men and women in the U.S. Army: A review of literature, *U.S. Army Research Institute of Environmental Medicine*, Natick, MA.
53. Snook SH and Ciriello VM. The design of manual handling tasks: revised tables of maximum acceptable weights and forces. *Ergonomics* 1991; 34:1197-1213.
54. Tischauer, E.R., (1978), *The Biomechanical Basis of Ergonomics: Anatomy Applied to the Design of Work Situations*, John Wiley & Sons, N.Y.
55. Tracy MF, Bigson MJ, Szypryt EP, Rutheford A and Corlett EN. The geometry of the lumbar spine determined by magnetic resonance imaging. *Spine* 1989; 14:186-193.
56. Weis-Fogh, T. and Alexander, R.M. The sustained power output from striated muscle. *Scale Effects in Animal Locomotion* 1977, pp. 511-525. Academic Press, London.
57. Wilkie, D.R. The relation between force and velocity in human muscle. *J Physiology* 1950; 110:249-280.
58. Wood S, Pearsall DJ, Ross R and Reid JG. Trunk muscle parameters determined from MRI for lean to obese males. *Clinical Biomechanics* 1996; 11:139-144.

## **Personnel Receiving Pay from this Research Effort**

William S. Marras  
Kevin P. Granata  
Michael J. Jorgensen  
Kermit Davis  
Anthony Maronitis  
Duprane Pedaci Young  
Karen Keefer Lewis  
Kevin Stockton  
William Marstellar  
Vedat Suvag  
Danielle Waters  
Alia Hussein  
Candi McCain  
Pat Bertsche  
Katie McQuaid



DEPARTMENT OF THE ARMY  
US ARMY MEDICAL RESEARCH AND MATERIEL COMMAND  
504 SCOTT STREET  
FORT DETRICK, MARYLAND 21702-5012

REPLY TO  
ATTENTION OF:

MCMR-RMI-S (70-1y)

1 JUN 2001

MEMORANDUM FOR Administrator, Defense Technical Information  
Center (DTIC-OCA), 8725 John J. Kingman Road, Fort Belvoir,  
VA 22060-6218

SUBJECT: Request Change in Distribution Statement

1. The U.S. Army Medical Research and Materiel Command has reexamined the need for the limitation assigned to technical reports. Request the limited distribution statement for reports on the enclosed list be changed to "Approved for public release; distribution unlimited." These reports should be released to the National Technical Information Service.

2. Point of contact for this request is Ms. Judy Pawlus at DSN 343-7322 or by e-mail at [judy.pawlus@det.amedd.army.mil](mailto:judy.pawlus@det.amedd.army.mil).

FOR THE COMMANDER:

A handwritten signature in black ink, appearing to read "Phyllis M. Rinehart", is written over the typed name and title.

PHYLLIS M. RINEHART  
Deputy Chief of Staff for  
Information Management

Encl

Reports to be changed to "Approved for public release;  
distribution unlimited"

<u>Grant Number</u>	<u>Accession Document Number</u>
DAMD17-94-J-4147	ADB221256
DAMD17-93-C-3098	ADB231640
DAMD17-94-J-4203	ADB221482
DAMD17-94-J-4245	ADB219584
DAMD17-94-J-4245	ADB233368
DAMD17-94-J-4191	ADB259074
DAMD17-94-J-4191	ADB248915
DAMD17-94-J-4191	ADB235877
DAMD17-94-J-4191	ADB222463
DAMD17-94-J-4271	ADB219183
DAMD17-94-J-4271	ADB233330
DAMD17-94-J-4271	ADB246547
DAMD17-94-J-4271	ADB258564
DAMD17-94-J-4251	ADB225344
DAMD17-94-J-4251	ADB234439
DAMD17-94-J-4251	ADB248851
DAMD17-94-J-4251	ADB259028
<del>DAMD17-94-J-4499</del>	<del>ADB221883</del>
DAMD17-94-J-4499	ADB233109
DAMD17-94-J-4499	ADB247447
DAMD17-94-J-4499	ADB258779
DAMD17-94-J-4437	ADB258772
DAMD17-94-J-4437	ADB249591
DAMD17-94-J-4437	ADB233377
DAMD17-94-J-4437	ADB221789
DAMD17-96-1-6092	ADB231798
DAMD17-96-1-6092	ADB239339
DAMD17-96-1-6092	ADB253632
DAMD17-96-1-6092	ADB261420
DAMD17-95-C-5078	ADB232058
DAMD17-95-C-5078	ADB232057
DAMD17-95-C-5078	ADB242387
DAMD17-95-C-5078	ADB253038
DAMD17-95-C-5078	ADB261561
DAMD17-94-J-4433	ADB221274
DAMD17-94-J-4433	ADB236087
DAMD17-94-J-4433	ADB254499
DAMD17-94-J-4413	ADB232293
DAMD17-94-J-4413	ADB240900